IMPACT OF LIVER FLUKE (*Fasciola hepatica*) MEDIATED IMMUNOMODULATION ON THE HOST'S IMMUNE RESPONSE TO BACTERIAL INFECTION

Thesis submitted in accordance with the requirements of the University of Liverpool for the degree of Doctor in Philosophy

Shamsul Bahrin Gulam Ali

201143008

May 2021

UNIVERSITY OF LIVERPOOL

AUTHOR'S DECLARATION

I declare that this thesis is a presentation of my original work and has been composed solely by myself. This work has not previously been presented or submitted, in whole or in part, in any previous application for a degree. All sources are acknowledged as References. This research was carried out in the Department of Infection and Microbiomes (IC2 Building, Liverpool Science Park) and Department of Clinical Infection Microbiology and Immunology (Ronald Ross Building), Institute of Infection, Veterinary and Ecological Sciences (IVES), University of Liverpool.

Shamsul Bahrin Gulam Ali
May 2021

ABSTRACT

The helminth parasite *Fasciola hepatica* (liver fluke) causes fasciolosis in mammals. It causes significant economic loss to the agricultural industry, primarily affecting cattle and sheep. It is also a zoonotic disease affecting humans worldwide. *Streptococcus pneumoniae*, a commensal bacterium of humans, is asymptomatically carried in the nasopharynx of healthy individuals. However, if the bacterium escapes from its natural niche to other anatomical loci, it can cause pneumonia, middle ear infection or a range of disseminated infections collectively termed invasive pneumococcal disease. The pneumococcus is a global killer, especially in children under 5 years old and in the elderly.

F. hepatica is known to release excretory/secretory (FhES) and tegumental coat (FhTEG) molecules that drive Th2 and regulatory responses with concomitant suppression of protective Th1/Th17 immune responses. These are associated with the switching of macrophage (MΦ) phenotypes from classically activated (M1/CAMΦ) to alternatively activated (M2/AAMΦ). Helminth-bacterial co-infections have been reported to result in harmful consequences, due to the effects of the helminth on host immune responses. Previous studies have demonstrated that hosts, co-infected with liver fluke and bacterial respiratory pathogens, such as *Bordetella pertussis* and *Mycobacterium bovis,* fail to clear these bacterial infections, which require Th1 or Th17 immune responses. Recent findings in animal models have shown that chronic helminth infections may have implications for vaccine efficacy against *Streptococcus pneumoniae*. The aim of this project was to investigate the impact of *F. hepatica* on pneumococcal infection utilising FhES antigens to emulate *F. hepatica–S. pneumoniae* co-infection.

Chapter 3 describes the modulation of the immortalised murine macrophage cell line, J774.2, in response to *F. hepatica* antigens and different bacterial stimulants (*Mycobacterium bovis* sonicate extract (MbSE) and different *S. pneumoniae* D39 preparations). Macrophage activity was assessed by measuring nitric oxide (NO) (CAMΦ marker) and arginase (AAMΦ marker) levels in cell culture supernatants and cell lysates. Significant down-modulation of NO was observed in both FhES+ and FhTEG+MbSE co-exposed cultures compared to MbSE alone, suggesting the J774.2 phenotype was modulated towards AAMΦ. Co-exposure to FhES+MbSE augmented arginase production further supporting the evidence of AAMΦ polarisation caused by *F. hepatica.* Neither *F. hepatica* antigen alone affected arginase production in J774.2 MΦs. Whilst live Ply-deficient mutant D39Δply and wild type D39 failed to induce NO production, culture supernatant derived from D39 (D39SN) alone induced significant levels of NO. Significantly up-modulated NO production was detected in FhES+D39SN co-exposed cultures suggesting CAMΦ activation.

Data presented in Chapter 4 demonstrates the capacity of FhES to modulate the immune response to live D39 using *ex vivo* murine BMDMΦs. Co-exposed outbred CD1 BMDMΦs had a mixed CAMΦ and AAMΦ phenotype. BMDMΦs derived from BALB/c mice, co-exposed to FhES and D39 infection, showed evidence of CAMΦ activation, supported by up-modulation of pro-inflammatory cytokines and chemokines. In contrast, C57BL/6 BMDMΦs showed evidence of AAMΦ activation during co-exposure. In older BALB/c mice there was evidence of declining CAMΦ function in D39 infection.

In Chapter 5, the effect of FhES on *S. pneumoniae* nasopharyngeal carriage was investigated using an *in vivo* CD1 mouse model. Counts of viable bacteria in the nasopharynx and lungs were determined, cytokines were quantified and immune cell populations were analysed. Exposure to FhES antigens promoted a favourable environment for nasopharyngeal colonisation with D39 in the co-exposed animals. Lower levels of TGF-β1 production were observed in D39 alone infected mice compared to FhES treated and co-exposed mice. The involvement of AAMΦ in the co-exposed mice was supported by the recruitment of mannose receptor (MR) expressing populations of MΦ and monocytes. The nasopharynx was the focal point of immune responses to pneumococcal carriage compared to the lungs, indicated by the apparent influx of innate and adaptive immune cells.

Chapter 6 describes gene expression in *ex vivo* BALB/c BMDMΦ in response to *F. hepatica*-pneumococcus co-exposure. The combination of both fluke and D39 stimulants up-regulated Th1 associated genes. The pathogen response gene *IL-1β* induce CAMΦ activation likely resulted from *NLRP3* inflammasome activation, possibly mediated by Ply released by D39 and cathepsins in FhES. Toll-like receptor gene *TLR2* but not *TLR4* and *TLR7* genes were activated in the co-exposed BALB/c BMDMΦs. Down-regulation of *CCL6, CXCL14* and *TGF-β1* in co-exposed cultures could alter the immune response in the real co-infection scenario in human hosts.

Overall, this study provides a valuable insight into the potential of *F. hepatica*-pneumococcus interaction to subvert immune system responses. The results presented here demonstrated the capacity of *F. hepatica* ES antigens to modulate immune responses to pneumococcal infection, although the differences observed in different models systems suggests host factors including age and genetics play a role in determining how this modulation manifests. The findings suggest that an active *F. hepatica* infection in the liver may impact on pneumococcal survival and dissemination in the human host, a topic to be comprehensively addressed in future studies.

ACKNOWLEDGEMENTS

First and foremost, I would like to thank my supervisors Professor Diana Williams, Dr. Daniel Neill and Professor Aras Kadioglu for their valuable supervision, support and guidance. I also thank my sponsor, the Ministry of Higher Education (Malaysia) and Universiti Teknologi MARA (UiTM) for the opportunity given to pursue my doctoral studies in the UK.

I want to express my sincere thanks to:

- Veterinary Parasitology group members (Jane, John, Alison, Nicola, Tess, Stefan and Bethan), Bacterial Pathogenesis group members (Hind, Laura J, Mary, Shadia, Game, Murielle, Mansoor, Becca, Rong, Alice, Laura T, Jenny, Hajar, Eleri and Stavros) and MEGALab group members (Hasan, Angharad, Harrison, Malak, Adrienne, Reene and Dilem) for their friendship and encouragement during my study.
- iC2 technicians (Catherine, Cathy, Jenny, Jenna, Paul and Becky) and Ronald Ross (RR) technicians (Emma, Erwan, Wess, Nahida, Trevor) for their assistance in the lab
- iC2-RR staff and friends: Debby, Robin, Ben, Lesley, Lance, Ahmed, Janine, Jill, Hannah, Samia, Ghada, Khalid, Adam, Amir, Sondus, Nada, Mai etc. To others, I cannot list all names here, but you are always on my mind. Thank you for your encouragement, friendship and support.

I greatly thank my beloved parents (Gulam Ali and Lailan Karim), Che Ayu (my auntie who was a second mother to me) and my family members (V, Khairani, Buck, Jaja, Emmy, Ghouse, Hamid and Saira) for their love and moral support when I was miles away from home. It would have been difficult to make my Ph.D. journey this far without their encouragement. Thank you to my lovely wife Nisa for standing by my side when times get hard and listening to all my Ph.D. stories (including reminding the chapters' datelines!). Good friends and neighbours I have met in this beautiful city of Liverpool (Auntie Raja, Shada-Hewi, Anne, Faisal, Fahad, Hina, Atuk Mat Noor, Md Noor-Fariza, Ahmad, Tony, Lee, Paul, Karen, Syeikh Zane, Fuad and Nazrith), thank you for all your love, support and prayers. Finally, to Mrs. Farah Raaz and Semina and their families – thanks for welcoming Nisa and me into your family! All your love and words of encouragement will always stay with us.

DEDICATION

This thesis is dedicated to:

- *Omar Latif (my uncle who was a second father to me), Abdul Jamal and Aishah Abdullah (father- and mother-in-law) and my beloved son Shazwan Shah who sadly passed away before I completed this work.*
- *Nisa and my daughter Shafazrun Nahar – thanks for your love and support.*
- *My nephews and nieces Najwan, Hadfina, Syafi, Nuqman, Hakimi, Sofia and Ariq.*
- *Ms. Julie and Mr. Jimie*

TABLE OF CONTENTS

LIST OF TABLES

LIST OF FIGURES

LIST OF ABBREVIATIONS

^{o}C	Degree Celsius
µg	Microgram
µl	Microlitre
AAMΦ	Alternative activated macrophage
ADCC	Antibody-dependent cell-mediated cytotoxic
AMΦ	Alveolar macrophage
ANOVA	Analysis of Variance
APC	Allophycocyanin
APC	Antigen presenting cell
APS	Ammonium persulphate
Arg/ Arg-1	Arginase
BAB	Blood agar base
BCG	Bacillus Calmette Guerin
BMDM	Bone marrow-derived macrophage
bTB	Bovine tuberculosis
BOMA	Bovine monocyte/ macrophage
CAMΦ	Classical activated macrophage
CAP	Cathelicidin antimicrobial peptides
CD	Cluster of differentiation
CDC	Centers for Disease Control and Prevention
CFU	Colony forming unit
CLR	C-type lectin receptor
CL	Cathepsin
CXCL1/ KC	Chemokine ligand 1/ Keratinocytes-derived chemokine
CXCL2/ MIP-2	Chemokine ligand 2/ Macrophage Inflammatory Protein 2

DCs	Dendritic cells
DEGs	Differentially expressed genes
dH_2O	Distilled water
DMEM	Dulbecco's Modified Eagle Medium
DMSO	Dimethyl sulphoxide
D-PBS	Dulbecco's phosphate buffer saline
D39	Serotype 2 pneumococcal strain
D39Δply	Serotype 2 pneumococcal strain pneumolysin-deficient mutant
D39Δply-SD	Serotype 2 pneumococcal strain pneumolysin-deficient mutant sodium deoxycholate treated
D39Δply-HK	Serotype 2 pneumococcal strain pneumolysin-deficient mutant heat killed
D39SN	Serotype 2 pneumococcal strain culture supernatant
e.g.	*exempli-gratia* (for example)
ELISA	Enzyme-linked immunosorbent assay
EndoT-EB	EndoTrap equilibration buffer
EndoT-RB	EndoTrap regeneration buffer
ES	Excretory/ secretory antigen
FABP	Fatty acid binding protein
Facs	Fluorescence activated cell sorting
Fc	Fragment crystallisable region
FDR	False Discovery Rate
FhES	*Fasciola hepatica* (fluke) excretory/ secretory antigen
FhHDM-1	*Fasciola hepatica* helminth defence molecule-1
FhSOM	*Fasciola hepatica* (fluke) somatic antigen
FhTEG	*Fasciola hepatica* (fluke) tegmental antigen
Fizz1	Resistin-like molecule alpha1
FMO	Fluorescence minus one

FOV	Field of Variants
FOXP3	forkhead box P3
G	Gauge
GSA	Gene Set Analysis
GST	Glutathione S transferase
Hb	Haemoglobin
HCl	Hydrochloric acid
HEPES	4-(2-hydroxyethyl)-1-piperazineethanesulfonic acid
HRP	Horse radish peroxidase
H_2SO_4	Sulphuric acid
IFN	Interferon
IFN-ɣ	Interferon gamma
Ig	Immunoglobulin
IL	Interleukin
IN	Intranasally
iNOS	Inducible nitric oxide synthase
IPD	Invasive pneumococcal disease
ISF	Isonitrosopriopherone
J774	Monocyte/ macrophage cell line
KEGG	Kyoto Encyclopaedia of Genes and Genomes
KO	Knockout
LFH	Liver fluke homogenate
LPS	Lipopolysaccharides
MΦ	Macrophage
mA	Milliampere
MbSE	*Mycobacterium bovis* sonicate extract (MbSE)
M-CFU	Macrophage-colony forming unit

MCSF	Macrophage colony stimulating factor
MIP	Macrophage inflammatory protein
mM	Millimolar
MMR	Macrophage mannose receptor
MR	Mannose receptor
mRNA	Messenger ribonucleic acid
MSD	Meso Scale Discovery
NaOH	Natrium hydroxide
NED	N-1-napthylethylenediamine dihydrochloride
NEJ	Newly excysted juvenile
NK	Natural killer cell
NLRP3	pyrin domain-containing protein 3 inflammasome
NO	Nitric oxide
NOS	Nitric oxide synthase
NP	Nasopharynx
NTD	Neglected tropical disease
PAMPs	Pathogen-associated molecular patterns
PBMC	Peripheral blood mononuclear cell
PBS	Phosphate buffer saline
PCA	Principle component analysis
PCV	Pneumococcal conjugate vaccine
PDL	Programme death ligand
PLN-A	Pneumolysin deficient
Ply	Pneumolysin
Prx	Peroxiredoxin
PRRs	Pattern recognition receptors
P/S	Penicillin/ Streptomycin

RANTES	Regulated upon activation normal T cell expressed and secreted (CCL5)
RLF	Reporter Library File
rpm	revolutions per minute
RPMI	Roswell Park Memorial Institute medium
RSV	Respiratory syncytial virus
SCCIT	Single comparative cervical intradermal tuberculin
SDS-PAGE	Sodium dodecyl sulphate polyacrylamide gel electrophoresis
SEM	Standard error of the mean
SN	Supernatant
TEMED	Tetramethylethylenediamine
TGF-β	Transforming growth factor beta
Th	T helper cell
Th1	T helper 1
Th2	T helper 2
THB	Todd-Hewitt Broth
TLRs	Toll-like receptors
TNF-α	Tumour necrosis factor alpha
TPx	thioredoxin peroxidase
Treg	T regulatory cell
Tris-HCl	Trizma hydrochloride
UK	United Kingdom
V/ V	Volume/ volume %
V	Volt
WHO	World Health Organisation
WT	Wild-type
Ym1	Chitinase-like protein

Chapter 1

Introduction

CHAPTER 1

Introduction

1.1 General introduction

The pathogens of animals and humans are ubiquitous, which is why all mammalian hosts are in constant danger of infection. To cause an infection and survive in their host, bacteria, fungi, parasites and viruses have evolved a wide range of mechanisms to manipulate or modulate the immune response of the host. The host-organism relationship is called symbiosis (living together) and can be further categorised into phoresis, commensalism, mutualism and parasitism. In parasitism, the parasite either harms its hosts or in some sense lives at the expense of the host.

The interaction between host and parasite determines the outcome of the infection. Host susceptibility, infection duration, transmission risks and clinical symptoms are altered in host-parasite interactions (Vaumourin *et al.*, 2015). In countries with poor hygienic conditions, a lack of sanitation and health care facilitates the transmission and spread of helminths like *Ascaris lumbricoides*, *Schistosoma spp*., hookworms and protozoa like *Entamoeba histolytica* (Lechner *et al*., 2013). Helminths or parasitic worms (macroparasites) secrete molecules that alter the mammalian cells' signalling pathways that are critical for their survival, potentially exacerbating an infection. To date, a number of secreted immunoregulatory helminth molecules have been identified and investigated to understand how these parasites communicate effectively with the host organism (McSorley and Maizels, 2012; McSorley *et al*., 2013; Dalton *et al*., 2013; Harnett, 2014; Nutman, 2015; Bashi *et al*., 2015; Shepherd *et al*., 2015; Maizels and McSorley, 2016; Smallwood *et al.*, 2017; Maizels *et al*., 2018; Zakeri *et al.*, 2018; Gazzinelli-Guimaraes and Nutman, 2018).

Excretory/ secretory (ES) molecules from the common liver fluke *Fasciola hepatica* are known to modulate innate and adaptive immunity (Donnelly *et al*., 2008; Flynn *et al*., 2010). *F. hepatica* promotes a polarised switch in the phenotype of host immune responses towards a T helper (Th)2/ regulatory phenotype, like many other helminth parasites, with suppression of Th1/ Th17 immune responses that are normally protective to bystander microbial infections (Vukman *et al.*, 2013a). *F. hepatica* often results in chronic infection, with the parasite surviving in the host for extended periods of time despite the magnitude of the host's immune response (Clery *et al.*, 1996). This process is associated with the switching of macrophage phenotypes from classically activated (CAMΦ/ M1) to alternatively activated (AAMΦ/ M2). Isolated adherent peritoneal exudate macrophage cells from mice infected with metacercariae - the infective stage of *F. hepatica* - were found to express markers of alternative activation, namely arginase (Arg-1), chitinase-like protein, Ym1 (Chil3) and resistin-like molecule alpha1 (Fizz1) (Donnelly *et al.*, 2005). On the other hand, the production of nitric oxide (NO; a marker for classical activation) was down-modulated in macrophage cells exposed to *F. hepatica* products, indicating the ability of fluke molecules alone or in *Mycobacterium bovis* co-infection cultures to suppress classical activation of macrophage (Flynn *et al.*, 2007a; Flynn and Mulcahy, 2008a; Golden *et al.*, 2010; Figueroa-Santiago and Espino, 2014; Garza-Cuartero *et al.*, 2016; Garcia-Campos *et al.*, 2019).

Bacterial pathogens are also capable of invading and interacting with the host cells. Bacterial colonisation can be achieved by their virulence factors, which allow adaptation to the specific environment of their host niche and to promote transmission to another host. *M. bovis* and *Streptococcus pneumoniae* (*S. pneumoniae*; the pneumococcus) are respiratory bacteria responsible for bovine tuberculosis (bTB), principally in cattle, and pneumonia and invasive disease in humans, respectively. bTB is an uncontrolled, chronic disease that is important to both animal production and welfare and also of public health concern (Howell *et al.*, 2019a). *S. pneumoniae* is the leading cause of infectious disease deaths in children under 5 years old globally (Subramanian *et al.*, 2018). Pneumococcus can migrate from its natural niche in the human nasopharynx to cause pneumonia and invasive pneumococcal diseases (IPD), including sepsis and meningitis

(LeMessurier *et al*., 2013). *S. pneumoniae* releases the pneumococcal pore-forming toxin known as pneumolysin (Ply) (Gilbert *et al.*, 1999; Tilley *et al.*, 2005; Mitchell and Mitchell, 2010) that has been identified as a key virulence factor contributing to high morbidity and mortality rates in invasive disease (Jacques *et al.*, 2020).

Infection with helminth parasites causes damage to host tissues, resulting in the release of danger signals that induce recruitment of various cells, including innate immune cells such as macrophages (MΦ), dendritic cells (DCs), eosinophils, basophils, and mast cells (Motran *et al.*, 2018). Studies have shown that macrophage-mediated phagocytosis is an essential part of host immune defence against *S. pneumoniae* (Jonsson *et al.*, 1985) and *in vitro* infection of human macrophages with pneumococcus results in delayed onset of apoptotic cell death (Dockrell *et al.*, 2001).

Multiparasitism infections are ubiquitous in nature. Parasites, both macro- and microparasites, pose a pervasive danger to their hosts. Macroparasites include parasitic helminths, such as cestodes (tapeworms), trematodes (flukes) and nematodes, as well as parasitic arthropods, including parasitoids, and ectoparasites, such as lice, ticks, fleas, and biting flies that might act as a vector of microparasites. Microparasites are small relative to their hosts and include fungi, viruses and bacteria. Whilst macroparasites typically cause chronic and persistent infections, many microparasites can induce acute fatality. Within the same host, co-infecting pathogens also alter the host response, which can have effects on disease transmission and progression and on diagnostic test accuracy (Mabbott, 2018). Recognised as masters of immune regulation, helminths have the ability to alter pathology and the course of infection in the same host by bystander immunoregulation (Brady *et al*., 1999; Maizels *et al*., 2004; Vukman *et al*., 2013a; Gazzinelli-Guimaraes and Nutman, 2018). The effects of helminth bystander immunoregulation on concurrent bacterial and viral infections in the same host is of widespread interest.

A helminth-bacterial co-infection research milestone was published by Brady *et al.* (1999), who demonstrated the first evidence of delayed bacterial clearance from the lungs of *F. hepatica-Bordetella pertussis* co-infected BALB/c mice. In ruminants, calves and cattle co-infected with *F. hepatica* and *M. bovis* showed the alteration of single comparative cervical intradermal tuberculin (SCCIT) test responses used for *F. hepatica* diagnosis (Flynn *et al.*, 2007b) and changes in the immune response to virulent bTB infection (Flynn *et al.*, 2009). Claridge *et al.* (2012) reported reduced sensitivity of the SCCIT test to detect bTB in calves experimentally-infected with *F. hepatica*. Howell *et al.* (2017) published an article showing that *F. hepatica* might increase the risk of *Escherichia coli* 0.157 shedding in British cattle.

F. hepatica is a major livestock pathogen which also causes serious disease in humans, especially in rural areas where people are in close contact with animals. Liver fluke infections are usually chronic in cattle and are associated with changes in the host immune response caused by fluke immunomodulatory products that can alter the activity of immune cells. These effects may potentially impair the host's ability to suppress fluke infection but may have bystander effects on the host response to other types of infection.

In this thesis, I have investigated how *F. hepatica* antigens might affect the ability of mammalian hosts to control and eliminate respiratory bacterial infections. In particular, I have focused on macrophages, cells that play key roles in defence against both fluke and bacteria. The immunomodulatory effects of fluke antigens on macrophage responses to *M. bovis* and *S. pneumoniae* were investigated *in vitro*. An *in vivo* murine model was established to observe the effect of *F. hepatica* excretory/ secretory (FhES) products on pneumococcal nasopharyngeal carriage density, signalling proteins and immune cell populations. Finally, to understand the molecular basis of this effect, I determined transcriptomic changes using targeted NanoString gene expression profiling in *ex vivo* macrophages that were infected with *S. pneumoniae* in the presence of liver fluke products.

1.2 The biology of *Fasciola hepatica*

F. hepatica is an important zoonotic agent that has been reclassified by the World Health Organisation (WHO) as a re-emerging and highly neglected tropical disease (NTD) in human populations (Sabourin *et al.*, 2018); it has a global distribution and causes major economic losses and health problems in livestock (Skuce and Zadoks, 2013; Cwiklinski *et al.*, 2016; Beesley *et al.*, 2017a; Mazeri *et al.*, 2017). Together with its sister species, *Fasciola gigantica*, they are responsible for a food-borne zoonosis known as fasciolosis. Fasciolosis is the world's most common foodborne trematode infection (Fürst *et al*., 2012). Whilst the temperate fluke *F. hepatica* is found worldwide, *F. gigantica*, the tropical fluke, is found in tropical areas of Asia and Africa (Anuracpreeda *et al.*, 2011; Cwiklinski *et al.*, 2016).

Both species are known to infect humans, although they are primarily parasites of ruminants. In the UK, sheep and cattle are commonly associated with liver fluke infection (Williams and Hodgkinson, 2017). Adult flukes have been isolated from the livers of registered horses in the UK (Howell *et al.*, 2019b). However, a recent study has shown that oral challenge with fluke metacercariae failed to establish an infection in experimentally infected horses (Quigley *et al.*, 2020). A wide variety of wild animals (e.g. deer, rabbits, hare, boars, beavers and otters) have also been identified to be infected by *F. hepatica* (Robinson and Dalton, 2009).

The ingestion of the infective metacercariae that lies dormant in cysts on vegetation is vital for the infection. The pathology associated with *F. hepatica* infection is determined by the stage of the parasite and the number of flukes present in the final host. The first stage occurs in the liver parenchyma during which juvenile flukes migrate and are associated with liver damage and severe haemorrhage. Destruction of the bile ducts and the biliary mucosa can be seen in the second stage, due to the haematophagic activity of the adult flukes and by their cuticular spines (Taylor *et al.*, 2016).

In sheep, the disease is characterised by three distinct clinical phases related to parasite migration. Acute fasciolosis is far more common in sheep than in cattle and occurs 2-6 weeks after ingestion of vegetation contaminated with large numbers of encysted metacercariae. Affected animals are lethargic, with pale mucous membrane (anaemia), dyspnoea, ascites and sudden death during autumn and early winter in the UK (Taylor *et al.*, 2016). Acute fasciolosis may predispose to secondary bacterial infection with *Clostridium novyi* type B or D, resulting in clostridial necrotic hepatitis ('Black disease') which causes sudden death in unvaccinated sheep (Sargison and Scott, 2011; Taylor *et al.*, 2016).

Subacute fasciolosis in sheep occurs 6-10 weeks after ingestion of approximately 500-1500 metacercariae over a longer period of time, and also appears in the late autumn and winter. Although it is not so rapidly fatal as the acute phase, the affected sheep suffer from severe haemorrhagic anaemia with hypoalbuminaemia. Some adult flukes will have matured and reside in the bile ducts and cholangitis is common. But some juvenile flukes are still migrating through the liver parenchyma causing liver enlargement with numerous necrotic and visible haemorrhagic tracts on the surface and in the parenchyma. Clinical signs, such as rapid loss of coordination, reduced appetite, enlarged and palpable liver, submandibular oedema ('bottle-jaw') or ascites can be seen 1-2 weeks prior to death. At this point, eggs can be found in faeces (Taylor *et al.*, 2016).

Chronic fasciolosis, seen mainly in late winter/ early spring, develops once mature adult worms establish within the biliary ducts after 4-5 months from the ingestion of small numbers of metacercariae (200-500), with typical clinical signs including progressive loss of coordination and weakness, lowered appetite, anaemia, 'bottle-jaw' and ascites (Taylor *et al.*, 2016).

The pathogenesis of fasciolosis varies depending on the number of metacercariae ingested, the time over which the metacercariae are ingested, the fluke developmental stages in the liver and the host species involved. As cattle appear to show less severe clinical signs of the disease compared to small ruminants, higher metacercariae challenge are required to cause all three forms of clinical

fasciolosis. This can be attributed to the large liver size in cattle, and a more fibrous texture in the liver than in other animals (Mitchell, 2002). Therefore, fasciolosis in cattle is manly a subclinical or chronic disease associated with the hepatic damage and blood loss caused by the liver fluke (Kaplan, 2001).

Infection with *F. hepatica* results in decreased milk yield (Charlier *et al.*, 2007; Mezo *et al.*, 2011; Charlier *et al.*, 2012; Howell *et al.*, 2015). Increased inter-calving interval was also previously reported in Flemish dairy herds (Charlier *et al.*, 2007), but others did not find evidence to link *F. hepatica* infection and fertility parameters in dairy cattle (Charlier *et al.*, 2012; Howell *et al.*, 2015; Köstenberger *et al.*, 2017).

There is no substantial evidence of protective immunity in ruminants to *F. hepatica* infections (Molina-Hernández *et al.*, 2015). The absence of protective immunity has been reported in all ages of cattle, while chronically infected cattle remain susceptible to experimental superinfection (Clery *et al*., 1996). The risk of infection increases with age, suggesting that immunity does not prevent re-establishment of a new infection (Khan *et al.*, 2013). Some early reports suggested that, unlike sheep, cattle might develop partial immunity with age, but this is thought to be related to the fibrous reaction to migration of fluke through the liver rather than a protective immune response (Andrews, 1999). Up to now, most of the vaccine candidates were first isolated from adult fluke ES native proteins, including cathepsin L (CL) proteases (a well-known immunomodulatory family of enzymes), glutathione S transferase (GST) and fatty acid binding protein (FABP), all of which have induced significant protection in sheep and cattle (Toet *et al.*, 2014). Several studies have demonstrated that vaccination with CL proteinases (L1 and L2) and fluke haemoglobin (Hb) is able to induce protective immunity in cattle (Dalton *et al.*, 1996; Mulcahy *et al.*, 1999; Mulcahy and Dalton, 2001).

Traditionally, fasciolosis is considered a livestock disease, but it has gained attention as an important emerging zoonotic disease in humans (Mas-Coma, 2005; Robinson and Dalton, 2009). Transmission risk includes human and livestock migration, climate change and man-made modifications of the environment (Afshan *et al.*, 2014). As accidental hosts, humans become infected by drinking

contaminated water or eating water plants that grow in animal-raising areas (Preza *et al.*, 2019). An assessment of the current scenario of human fasciolosis worldwide concluded that the infection sources include foods, water and combination of both (Mas-Coma *et al.*, 2018). Recent advances in human activities such as irrigation systems, building, livestock management, the use of unsafe water and raw vegetable consumption have contributed to the re-emergence of human fasciolosis in certain countries (Sabourin *et al.*, 2018). A few weeks after the infection, humans experience an acute febrile syndrome characterised by fever, eosinophilia and hepatosplenomegaly due to the juvenile fluke migration through the liver, followed by a chronic-latent stage which may last for years or decades (Dietrich *et al.*, 2015).

A review by Nyindo and Lukambagire (2015) estimated the real number of cases could be between 35 and 72 million people, with more than 180 million people at risk of infection, mainly people living in poverty, mostly children, without adequate sanitation and in close contact with livestock (Sabourin *et al.*, 2018). Human fasciolosis is now increasingly reported from Europe, the Americas and Oceania, where only *F. hepatica* is transmitted, whilst infections caused by the two *Fasciola* species overlap in Africa and Asia (WHO, 2020). The growing demand for animal-derived food products to sustain global population growth, shows that fasciolosis is one of the major One Health problems. However, less attention has been invested to look into the direct impact on human health of *Fasciola* infections (Piedrafita *et al.*, 2010). To date, triclabendazole is the only effective treatment available for human infections (Gandhi *et al.*, 2019) and immunological analysis of infection has been confined to animal studies and can only assume that the immune response to *Fasciola* infections is similar in humans (Cwiklinski *et al*., 2016).

Human fasciolosis is now considered to be relevant in travel medicine, as travellers have been involved in human infection reports, where the imported cases were from Europe, Asia, Africa and America. These include tourists, migrants and refugees that are travelling in the same or neighbouring countries or from one continent to another (Ashrafi *et al.*, 2014).

1.3 The life cycle of *Fasciola hepatica*

As a hermaphrodite, self- and cross- fertilisation occurs, although cross-fertilisation is more common (Beesley *et al*., 2017b). Unembryonated eggs are shed and transported with bile via the common bile duct into the intestine and passed in the faeces. When in contact with an aquatic environment, the eggs become embryonated with miracidium that upon release will invade the intermediate host. The indirect life cycle of *F. hepatica* involves lymnaeid snail intermediate hosts, with *Galba truncatula* being the dominant species in Europe (Beesley *et al.*, 2017a), that can be found in moist, especially smooth and firm, clay soils (Knubben-Schweizer and Torgerson, 2015).

Each egg produces a single, motile but short-lived (within 24 hours) miracidium which must find its way to penetrate the snail host through their mantle, tentacles or foot (Préveraud-Sindou and Rondelaud, 1995; Graczyk and Fried, 1999). Within the snail, asexual replication occurs from sporocyst giving rise to rediae and finally cercariae that are shed from the snail and encyst as metacercariae on aquatic vegetation (or pastures), and may remain infectious for several months, depending on conditions (Graczyk and Fried, 1999; Andrews, 1999). The animal definitive hosts become infected by ingesting metacercariae-contaminated pasture or other plants. Following this, the metacercariae excyst in the duodenum where the immature worm (newly excysted juvenile, NEJ) continues to penetrate through the intestinal wall and migrate to the liver parenchyma and into biliary ducts, where they will mature into egg laying adults and the cycle continues. Juvenile fluke are 1.0-2.0mm in length and lancet-like at the time of entry into the liver. Adults of *F. hepatica* are sexually mature in the bile ducts and can be seen as leaf-shaped (around 25-35 mm in length and 10mm in width), grey-brown in colour with conical anterior end marked by distinct shoulders and a visible ventral sucker (Figure 1.1). The tegument is covered with spines that projected backwards (Taylor *et al.*, 2016). The *F. hepatica* life cycle is shown in Figure 1.2.

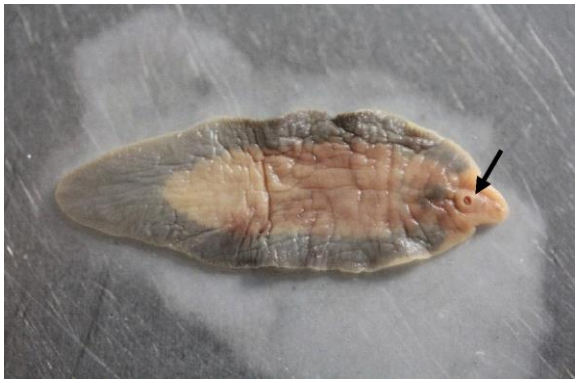

Figure 1.1: Adult *F. hepatica* isolated from the liver of an infected sheep. Arrow shows ventral sucker (provided by Dr. John Graham Brown)

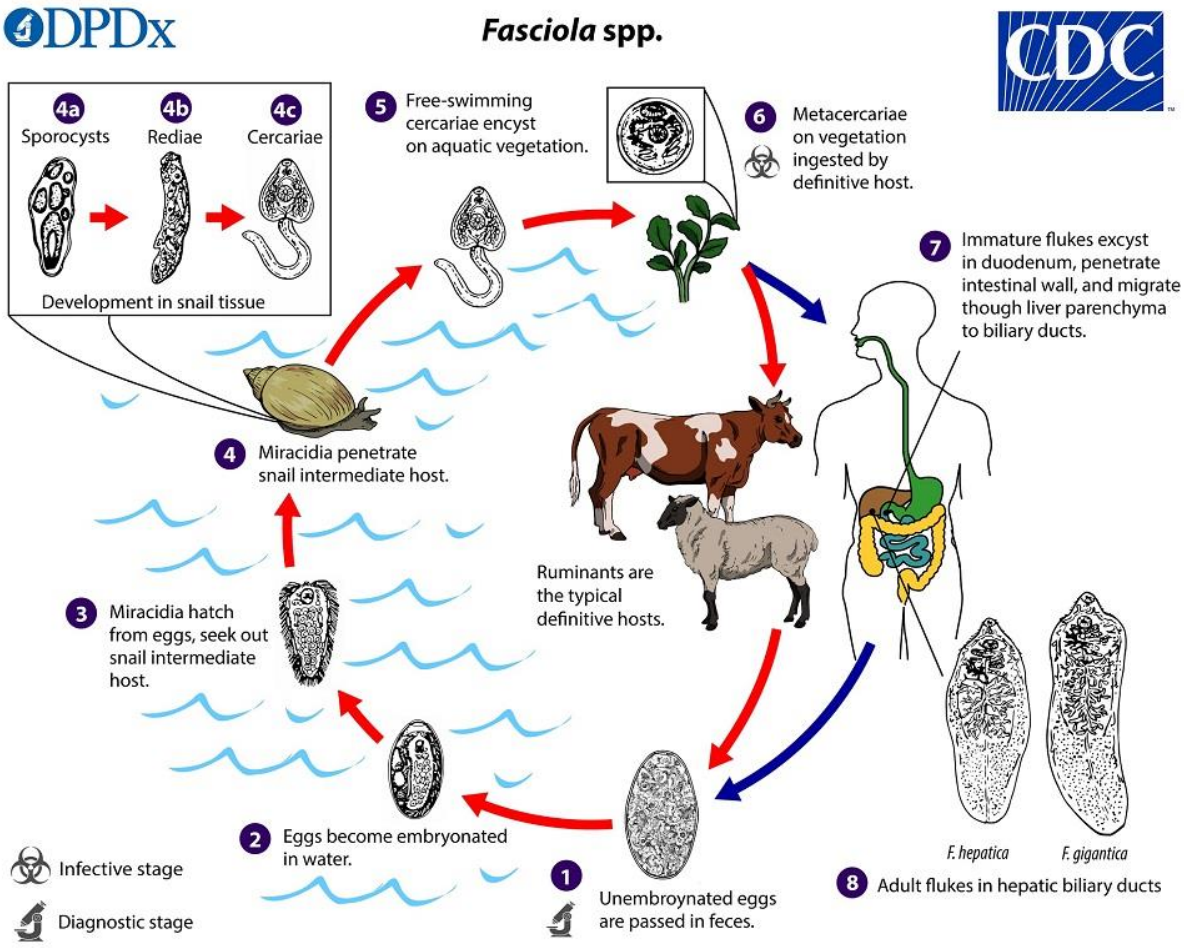

Figure 1.2: **Life cycle of *F. hepatica* (Centres for Disease Control and Prevention (CDC) Laboratory Identification of Parasites of Public Health, http://www.cdc.gov/dpdx/fascioliasis/index.html).** The life cycle of liver fluke is a complex two-stage life cycle which involves development of the parasite within the intermediate (mud snail; *Galba truncatula*) and definitive host (human and other mammals).

1.4 Overview of the immune system

Human body surfaces are covered by epithelium, which provides a physical barrier to infectious agents. If these are compromised, host innate and adaptive immune systems fight to expel the pathogens. Whilst the innate immune system acts quickly and employs a non-specific defence mechanism to expel invaders, the specific acquired immune system is slower acting but highy adaptable. Innate immune cells including macrophages (MΦ), mast cells and dendritic cells (DCs), recognise conserved structures on pathogens, termed pathogen-associated molecular patterns (PAMPs) through pattern recognition receptors (PRRs), of which the family of Toll-like receptors (TLRs) are well described (Mogensen, 2009). Acquired immune responses are separated into two arms of defence, namely, B-cell-mediated or humoral immunity and T-cell-mediated or cellular immunity.

Inflammation, a major component of the body's defence mechanism, is a physiological process typically initiated by endogenous factors in response to tissue damage (tissue necrosis or bone fracture) and exogenous factors such as immunological (hypersensitivity reactions) or biological (infections) injuries. Inflammation induces signaling molecules, including cytokines, that mediate and regulate the inflammatory response. Activated macrophages produce pro-inflammatory cytokines such as interleukin (IL) -6, IL-1β and tumour necrosis factor-alpha (TNF-α). The involvement of TNF-α, IL-6 and IL-1β characterise the early phase of the innate immune response that also includes monocytes, macrophages, NK cells and lymphocytes (Kurt *et al*., 2007; Turner *et al.*, 2014; Chen *et al.*, 2018; Bennett *et al.*, 2018). On the other hand, anti-inflammatory cytokines which include IL-4, IL-10 and transforming growth factor (TGF)-β act in concert to control pro-inflammatory responses (Zhang and An, 2007). Known as a key immunoregulator during infection with micro-and macroparasite, IL-10 ameliorates excessive Th1 and $CD8^+$ cell responses that, left unchecked, can cause severe immunopathology (Couper *et al*., 2008).

The adaptive immune response involves specific $CD4^+$ T helper cells (Th), $CD8^+$ cytotoxic T cells, B lymphocytes (B cells) and T regulatory (Treg) lymphocytes, that play a crucial role in host defence and immunoregulation (Hirahara *et al.*, 2011). Th cells can be divided into three main types, based on their cytokine-secretion phenotype and function, i.e. Th1, Th2 and Th17 (Kaiko *et al*., 2008). Th1 cells secrete interferon (IFN) -ɣ, IL-2 and TNF-α, which promote effective killing of both extracellular and intracellular pathogens, including bacteria and viruses that grow in macrophages (Romagnani, 2000; O'Neill *et al*., 2000; Kidd, 2003). In contrast, Th2 cells produce a number of cytokines including IL-4, IL-5, IL-6 and IL-10 which promote a type 2 response (O'Neill *et al*., 2000) and play a central role against extracellular macroparasites, such as helminths (Makepeace *et al*., 2012; Muraille *et al*., 2014) and promote tissue repair (Muraille *et al*., 2014). IL-10 was initially described as a Th2 cytokine; however it is now clear that IL-10 is also made by Th1 cells and various types of Treg cells (Mishra *et al*., 2014). $CD4^+$Treg cells are characterised by expression of the forkhead box P3 (FOXP3) transcription factor and high levels of CD25 (Anthony *et al*., 2007). Th17 cells are protective against extracellular bacteria (Makepeace *et al*., 2012). Expression of the transcription factor FOXP3, along with TGF-β and IL-2, leads to differentiation of Treg cells, which down-regulate many types of immune responses (Anthony *et al*., 2007).

1.5 Macrophage-Pathogen Interactions

Macrophages (MΦ) are immune cells that induce, suppress or modulate both innate and adaptive immune responses. Being one of the professional antigen-presenting cells (APCs), macrophages help to present foreign antigens to Th cells. On the other hand, DCs and B cells also belong to the APCs where the interaction between APCs and T cells link innate and adaptive immune responses. Mirroring Th1-Th2 polarisation, macrophage can be classified as classically activated/ type 1 macrophages (CAMΦ/ M1) and alternatively activated/ type 2 macrophages (AAMΦ/ M2) (Roszer, 2015). CAMΦ and AAMΦ macrophages promote type 1 and type 2 T helper lymphocytes, Th1 and Th2 respectively (Mills, 2012). The polarisation of both CAMΦ or AAMΦ are driven by microbial infection or innate danger signals, without the influence of adaptive immune cells (Rath *et al*., 2014).

Whilst CAMΦ can rapidly kill and expel pathogens and are thus the primary host defence, AAMΦ routinely repair and maintain tissue integrity (Mills and Ley, 2014; Mills, 2015; Martinez and Gordon, 2014). During infection (or inflammation-associated disease), activated macrophages can migrate to inflammation sites where they encounter pathogens, engulf and lyse them, a process which is accomplished by an increased production of toxic oxygen species and induction of inducible nitric oxide synthase (iNOS) to produce nitric oxide (NO). iNOS (marker for M1 or CAMΦ) and Arg-1 (marker for M2 or AAMΦ) catalyse the consumption of L-arginine in activated macrophages and are associated with the classical or alternative pathways, respectively (Munder *et al*., 1988). These two enzymes, associated with the M1 pro-inflammatory killer type response and the M2 anti-inflammatory repair type response, are used to characterise the two macrophage phenotypes (Yang and Ming, 2014).

Whether arginine metabolism proceeds via iNOS or Arg-1 has important functional consequences. In CAMΦ, NO is produced from L-arginine by iNOS (MacMicking *et al*., 1997) that is induced by inflammatory cytokines such as TNF-α, IFN-ɣ and IL-12 (Modolell *et al*., 1995). In AAMΦ, arginase metabolises L-arginine to L-ornithine and urea and is induced mainly by Th2 cytokines and anti-inflammatory agents by down-regulation of NO synthesis (Munder, 2009; Pesce *et al*., 2009). Parasites, fungal cells, immune complexes, complement, apoptotic cells, macrophage colony stimulating factor (MCSF), IL-4, IL-13 and TGF-β are all associated with AAMΦ activation (Murray *et al*., 2014; Roszer, 2015; Viola *et al*., 2019). In contrast, intracellular pathogens, bacterial cell wall components (e.g. lipopolysaccharides (LPS), a cell wall component of Gram negative bacteria), lipoproteins, IFN-ɣ and TNF-α induce CAMΦ activation, characterised by pro-inflammatory cytokine secretion and production of nitric oxide (NO), resulting in an effective pathogen killing mechanism (Benoit *et al*., 2008; Murray *et al*., 2014; Martinez and Gordon, 2014).

In parasitic infections, type 1 cytokine pro-inflammatory IFN-ɣ induced-CAMΦ produce NO to control protozoan infections. In contrast, type 2 cytokines (anti-inflammatory IL-4 and IL-13) antagonise CAMΦ, up-regulate Arg-1 expression and

thereby induce the AAMΦ that can be seen in helminth infections (Stempin *et al*., 2010). An AAMΦ profile with expression of Fizz1 and Ym1 was observed in *Taenia crassiceps*-induced macrophages (Terrazas *et al*., 2005) and *F. hepatica* metacercariae infection in mice (Donnelly *et al*., 2005). Whilst in the murine model, Fizz1 and Ym1 are commonly used AAMΦ markers (Nair *et al*., 2005), chitinase activity is used as marker of alternative activation in ruminant hosts (Flynn *et al*., 2007a).

In bacterial infections, whilst CAMΦ polarisation was associated with gastrointestinal infections (e.g. typhoid fever and *Helicobacter pylori* gastritis) and active tuberculosis, AAMΦ polarisation was observed in lepromatous leprosy, Whipple's disease and localised infections (keratitis, chronic rhinosinusitis) (Mège *et al*., 2011). *Brucella* and *Mycobacterium* are reported to have evolved mechanisms that interfere with CAMΦ polarisation (Dornand *et al*., 2002; Miller *et al*., 2004). In addition, genes encoding cytokines such as TNF-α, IL-6, IL-12 and IL-1β are demonstrated to be up-regulated in CAMΦ polarisation following bacterial infections in human and mouse macrophages (Benoit *et al*., 2008).

Macrophages contribute to the host response to pneumococcal infection, as they initially recognise the bacteria and subsequently modulate the inflammatory response (Knapp *et al*., 2003). Others have reported that *S. pneumoniae*-infected macrophages mediate bactericidal activity, which is a prerequisite for bacterial clearance and resolution of inflammation (Dockrell *et al*., 2001; Dockrell *et al*., 2003; Bewley *et al*., 2011). Pneumococcal killing was decreased and the cell death programme shifted from apoptosis to necrosis due to NO inhibition by an iNOS inhibitor (Marriott *et al*., 2004).

1.6 C-type lectin receptor (CLR), the mannose receptor (MR, CD206)

C-type lectin receptors (CLRs) are soluble and membrane-bound proteins that share the carbohydrate recognition domain required for binding to carbohydrate structures of endogenous self-molecules as well as specific pathogens and pathogen-derived ligands (Drickamer, 1992; Weis *et al*., 1998). Among the CLRs,

the mannose receptor (MR, CD206) is primarily expressed on human and mouse MΦ and DCs (Martinez-Pomares, 2012; van Die and Cummings, 2017) and is involved in pathogen recognition (Gazi and Martinez-Pomares, 2009) and antigen presentation (Taylor *et al*., 2005). Another CLR, Dectin-1 is normally expressed on monocytes, MΦ, DCs, neutrophils and subset of splenic T cells (Taylor *et al.*, 2002).

MR plays a role in pathogen clearance by recognising and binding mannose and fucose residues on the surface of microorganisms. It plays a role in both innate and adaptive immune responses (Schlesinger *et al*., 1978). MR is an AAMΦ phenotype marker (Gordon and Martinez-Pomares, 2017) and a phagocytic receptor (Kang *et al*., 2005). In the context of MR and immune surveillance, the MR is able to interact with a wide range of microorganisms or microbial products, including recognition of the capsular polysaccharide of *S. pneumoniae* (Zamze *et al*., 2002). More recently, the *Streptococcus pneumoniae* toxin pneumolysin was observed to bind to MR and induce down-regulated inflammation, enhancing pneumococcal survival in the airways (Subramanian *et al*., 2018).

Several studies highlighted the role of CLRs in mediating the immune regulation induced by helminth-derived gycoconjugates (Everts *et al*., 2012; Klaver *et al*., 2013). In a study investigating the helminth-macrophage MR binding capacity, deSchoolmeester *et al*. (2009) reported that *Trichuris muris (T. muris)* ES contains MR-binding activity but infection of MR knockout mice expel the parasites with the same kinetics as wild-type animals suggesting that MR is not critically involved in the generation of the immune response to *T. muris.* MR and Dectin 1 ligands (Mannan and Laminarin, respectively) inhibited AAMΦ induction in mouse peritoneal macrophages, indicating the participation of CLRs in responses to *F. hepatica* ES products (Guasconi *et al*., 2011). MR expression was enhanced in *F. hepatica* tegumental antigen stimulated DCs, which are critical for DC-$CD4^+$ T cell communication (Aldridge and O'Neill, 2016).

1.7 Immunity to helminth infection

Helminths are multicellular metazoan organisms with complex multistage life cycles that involve several hosts (Macdonald *et al*., 2002) or direct lifecycles with only one host. They are known for their ability to modulate the host immune responses for their survival (Hewitson *et al.*, 2009). Helminths are long-lived and commonly establish chronic infections resulting in anaemia, malnutrition, growth impairment, cognitive deficiencies and immunopathology in their hosts (Inclan-Rico and Siracusa, 2018). The protective immune response to some helminths is well characterised, with Th2/ Treg immune response that leads to the expression of IL-4, IL-5, IL-9 and IL-13, an increase in immunoglobulin E (IgE) and mast cells, eosinophils, basophils and the recruitment and expansion of AAMΦ that are essential for the control of parasitic infections (Maizels *et al*., 2004; Wills-Karp and Finkelman, 2011; van Panhuys *et al*., 2011; Rosenberg *et al*., 2013; Maizels and McSorley, 2016).

1.8 *Fasciola hepatica* antigens

Studies on the immunoregulatory effects of *F. hepatica* secreted molecules have described the involvement of many types of innate immune cells such as MΦ, DCs and mast cells (Donnelly *et al*., 2005; Flynn *et al*., 2007a; Cervi *et al*., 2009; Guasconi *et al*., 2012; Vukman *et al*., 2013a; Adams *et al*., 2014; Lund *et al*., 2014; Rodríguez *et al*., 2017; Figueroa-Santiago and Espino, 2017). There are three types of *F. hepatica*-derived antigens commonly used in experimental studies: the excretory/ secretory products (FhES), the tegumental coat antigen (FhTEG) and the whole liver fluke homogenate (LFH, also known as somatic antigen; FhSOM).

F. hepatica excretory/ secretory products (FhES), the most intensively studied group of molecules, can be easily isolated from the media where *F. hepatica* is maintained. FhES originate from the parasite gut, the contents of which are regularly expelled into the local environment (Adams *et al.*, 2014). FhES major components include CL1 and CL2 enzymes, which are involved in parasite migration, acquisition of host nutrients and modulation of immune response (Dalton

and Mulcahy, 2001; Collins *et al.*, 2004; Jedlina *et al.*, 2011; Figueroa-Santiago and Espino, 2017). CL1 prevents parasite death by cleaving host immunoglobulin, thus preventing antibody-dependent cell-mediated cytotoxic (ADCC) killing of fluke by host immune cells (Carmona *et al*., 1993).

Several anti-oxidant enzymes are found in FhES, (i) peroxiredoxin (Prx), has been reported to induce Th2 responses via AAMΦ (Donnelly *et al*., 2008) and (ii) thioredoxin peroxidase (TPx) induced the recruitment of AAMΦ to the peritoneal cavity of BALB/c mice (Donnelly *et al.*, 2005). Another FhES protein, *F. hepatica* helminth defence molecule-1 (FhHDM-1) mimics the mammalian host antimicrobial peptides (or defensins) where FhHDM-1-LPS binding prevents macrophage activation and induction of innate immune responses. FhHDM-1 exhibit similar biochemical and functional characteristics to human defence peptides (e.g. CAP18), thus FhHDM-1 could be a potential therapeutic agent in anti-sepsis treatment and prevention of inflammation (Robinson *et al.*, 2011). Others have reported that FhHDM-1 promotes the AAMΦ phenotype and partially activates DCs (Dalton *et al*., 2013; Robinson *et al*., 2011; Robinson *et al*., 2013). Recently, FhHDM-1has been shown to impair NLRP3 inflammasome activation in macrophages, which prevents IL-1β production and protective Th1 immune responses (Alvarado *et al*., 2017). Whilst *F. hepatica* Prx drives Th2 immune response, FhHDM-1, cathepsin L1, fatty acid-binding protein (FABP), kunitz-type molecule and Sigma class glutathione (GST) indirectly promote Th2 responses by suppressing the development of Th1/ Th17-associated inflammation (Dowling *et al*., 2010; Donnelly *et al*., 2010; Robinson *et al*., 2011; Martin *et al*., 2016).

F. hepatica tegumental (FhTEG) antigen is shed every 2-3 hours as the parasite migrates through the host tissue. FhTEG is a mixture of rich glycoprotein, sourced from the pathogen's glycocalyx coat (Savage *et al.*, 2013). It has multiple functions, such as absorption of exogenous nutrients, synthesis, osmoregulation and protection against host enzymes and bile *(*Adams *et al.*, 2014). During the interaction with immune cells, the surface tegument of *F. hepatica* contains immunomodulatory molecules that are capable of manipulating the host's immune response. FhTEG was able to inhibit the ability of mast cells to drive Th1 immune

responses (Vukman *et al*., 2013a) and indirectly induced a M2-like macrophage phenotype *in vivo* (Adams *et al*., 2014). FhTEG has also been shown to impair toll-like receptor (TLR) –driven immune responses in both DCs and mast cells, by suppressing TLR-induced cytokine secretion and costimulatory marker expression (Vukman *et al*., 2013b).

1.9 Immunology of *Fasciola hepatica* infections

While the definitive host's immune responses to *F. hepatica* is thought to be primarily Th2 biased, Th1 cells are also believed to be involved in the early stages of infection (Moreau and Chauvin, 2010) *. F. hepatica* infected animals exhibit Th2 type immune responses, characterised by eosinophilia, AAMΦ, elevated IgG1, IL-4, IL-5 and IL-13 production, and an absence of IFN-ɣ and IL-2 (Clery and Mulcahy, 1998; Mulcahy *et al*., 1998; O'Neill *et al*., 2000; Donnelly *et al*., 2008). Th1 responses are down-modulated during fluke infection (O'Neill *et al.*, 2000). As the chronic infection progresses, a regulatory environment becomes dominant, which is characterised by the suppression of parasite-specific Th1 and Th2 responses and activation of immunosuppressive cytokines IL-10 and TGF-β (O'Neill *et al.*, 2000; Flynn *et al*., 2007b; Flynn and Mulcahy, 2008b; Walsh *et al*., 2009; Haçariz *et al*., 2009; Dalton *et al*., 2013).

1.10 *Mycobacterium bovis* and bovine tuberculosis

Bovine tuberculosis (bTB) is caused by a slow growing intracellular bacterium *M. bovis* (Pollock and Neill, 2002). bTB is a chronic disease of cattle that is difficult to control (Howell *et al.*, 2019a) and a zoonotic pathogen worldwide (Muller *et al.*, 2013; Cosivi *et al*., 2016). Human transmission requires direct occupational exposure to infected animals such as the presence of a wound and inhalation of aerosols exhaled by infected animals (Vayr *et al*., 2018) or consumption of contaminated animal products (Pérez-Lago *et al.*, 2014). Zoonotic TB has become an endemic, albeit uncommon, disease in the UK population, due to the consumption of unpasteurised contaminated raw cow's milk (de La Rua-Domenech, 2006). Several studies have investigated the immunological effects of

M. bovis and *F. hepatica* co-infection in animals. A reduced diagnostic sensitivity of the SICCT test used to diagnose *M. bovis* (Claridge *et al*., 2012), altered responsiveness (Flynn *et al*., 2009) and down-regulation of *M .bovis*-BCG-specific immune responses (Flynn and Mulcahy, 2008a) have all been described in co-infected animals.

1.11 *Streptococcus pneumoniae*, the pneumococcus

Streptococcus pneumoniae is a Gram-positive bacterium that is known to cause a variety of diseases in humans ranging from minor middle ear infections (otitis media) to severe invasive infections such as community-acquired pneumonia, meningitis and septicaemia (del Mar García-Suárez *et al*., 2004). It was discovered by Pasteur and Sternberg in 1881 in human saliva (Watson *et al*., 1993). *S. pneumoniae* is a common coloniser of the upper respiratory tract, specifically the nasopharynx of humans, including healthy children (Bogaert *et al.*, 2004) where it occurs asymptomatically as a commensal (Kadioglu *et al*., 2008). However, it is also a major cause of disease in children and elderly people with weak immune systems (Jeong *et al*., 2015). Invasive pneumococcal disease (IPD) is defined as isolation of *S. pneumoniae* from a normally sterile body site such as blood, cerebrospinal fluid (CSF), joint, pleural, or pericardial fluid (Rose *et al*., 2014).

In 2017, the WHO included the pneumococcus as one of 12 priority pathogens causing continuous high burden of disease and a rising rate of antibiotic resistance (Weiser *et al*., 2018). A carrier with colonised pneumococci can shed *S. pneumoniae* in nasal secretions and transmit the bacterium beyond its niche along the nasal epithelium which can lead to IPD (Weiser *et al*., 2018).

1.12 The biology of *Streptococcus pneumoniae*

S*. pneumoniae* is a commensal bacteria that resides on the mucosal surface of the nasopharynx of humans (Rayner *et al.*, 1995). Pneumoccocci are highly adapted commensals, and their main reservoirs on the mucosal surface of the upper airways of carriers enable the transmission from person to person through droplets or aerosols (Weiser *et al*., 2018). Colonisation leads to airway inflammation marked by suppurative rhinitis and increased secretion of mucus (Lemon *et al.*, 2015). Pneumococci enter the nasal cavity during colonisation and adhere to the nasopharyngeal epithelial cells.

Pneumococcal colonisation is common in children, with carriage rate peaking around 2-3 years of age and decreasing to less than 10% in the adult population (Henriques-Normark and Tuomanen, 2013). As the carriage rates decline with age, duration of carriage is also found to be longer in younger than older children (Högberg *et al*., 2007). Colonisation is mostly asymptomatic, but it can progress to respiratory or systemic disease (Bogaert *et al*., 2004). Pneumococcal nasopharyngeal carriage is a prerequisite for both transmission to other individuals and invasive disease in the carrier (Neill *et al.*, 2014). Risk of IPD correlates with the carriage rates (Bogaert *et al*., 2004; Hausdorff *et al*., 2005). Experimental studies of human carriage confirmed that colonisation increases nasal, lung and serum antibody levels (McCool *et al*., 2002; Wright *et al.*, 2012; Wright *et al*., 2013)

The carriage duration can vary significantly between serotypes. Serotypes 6B, 9V, 14, 19F and 23F are commonly found in children (Henriques-Normark and Tuomanen, 2013). Whilst serotype 1 is rarely found causing asymptomatic nasopharyngeal carriage, serotype 6B can colonise for over 19 weeks (Sleeman *et al*., 2006; Ritchie *et al*., 2012). Capsular polysaccharide serotyping helps in tracking the global and local spread of pneumococci. The capsule is critical to *S. pneumoniae* survival and acts as a shield from the host immune system (Geno *et al*., 2015). Currently 100 serotypes were identified on the basis of their polysaccharide capsule (Ganaie *et al*., 2020) and these serotypes are correlated with nasopharyngeal colonisation (Koppe *et al.*, 2012; Geno *et al*., 2017; Lees *et*

al., 2017; Weiser *et al*., 2018). The capsular polysaccharides are essential in bacterial physiology and determining the host immune response (Lees *et al*., 2017), and different serotypes have different clearance and acquisition rates (Auranen *et al*., 2010; Hill *et al*., 2010: Abdullahi *et al.*, 2012). Nasopharynx immune responses are altered during long–term pneumococcal carriage, marked by high levels of TGF-β and Treg cells, reduced neutrophil infiltration and increased AAMΦ activation (Neill *et al*., 2014).

Depending on the pneumococcal serotype and host's immune status, bacteria either remain as colonisers, spread further into organs such as ears or lungs, or breach the mucosal layer into the blood stream. Meningitis can develop if the bacteria are able to cross the blood brain barrier (Henriques-Normark and Tuomanen, 2013). The risk of pneumococcal disease is also increased by smoking and exposure to air pollution (Almirall *et al.*, 1999; Mortimer *et al*., 2012). E-cigarette vapour exposure potentially increases the risk of pneumococcal infection by enhancing pneumococcal adherence to airways epithelial cells (Miyashita *et al*., 2018). High temperature exposure or dust inhalation promote progression of asymptomatic pneumococcal nasopharyngeal carriage to pneumonia and invasive disease (Jusot *et al*., 2017). A recent study by Shears *et al*. (2019) demonstrated that diesel exhaust particle exposure increases susceptibility to IPD in mice.

1.13 Pneumolysin (Ply) virulence factor

One of the major virulence factors of *S. pneumoniae* is pneumolysin (Ply), which is the cause of many disease manifestations associated with IPD (Alhamdi *et al.*, 2015; Shenoy *et al*., 2017). Ply is a bacterial pore-forming toxin that belongs to the family of cholesterol-dependent cytolysins (Harvey *et al*., 2014). Ply separates tight junctions between epithelial cells and promotes human mononuclear phagocyte activation and release of TNF-α and IL-1β (Houldsworth *et al*., 1994). Wild-type pneumococci expressing Ply promote successful colonisation of the nasopharynx, compared to the Ply-deficient mutant PLN-A (Kadioglu *et al*., 2002). Similarly, Ply-deficient mutant pneumococci attach less well to respiratory epithelial cells (Rubins *et al*., 1998).

Increased invasiveness of serotype 1 is related to the amount of Ply produced and released (Jacques *et al*., 2020). Recently, sequence type (ST)615 pneumococcal serotype 1 has been found to be hypervirulent, relative to ST306 serotype 1. ST615 causes invasive pneumonia in a mouse model and harbours the expression of two haemolytic variants of Ply. (Panagiotou *et al*., 2020). Mannose receptor on mouse alveolar macrophages and dendritic cells act as a Ply receptor which enables invasion of pneumococci, leading to anti-inflammatory responses and enhanced pneumococcal survival (Subramanian *et al*., 2018).

Ply induces nitric oxide (NO), which is released by macrophages via the pro-inflammatory interferon-γ (IFN-γ)-dependent pathway (Braun *et al*., 1999). Ply contributes to both NO production and apoptosis induction in macrophages (Marriott *et al*., 2004). Purified Ply and serotype 2 D39 pneumococci, but not the Ply-deficient PLN-A strain, induce the anti-inflammatory immune modulatory cytokine TGFβ1 from lungs and nasopharyngeal epithelial cells (Neill *et al*., 2014).

1.14 Immunity to *Streptococcus pneumoniae*

Protection against pneumococcal infections is mediated by activation of the classical pathway of complement, by antibody and complement-dependent opsonisation and by opsonin-dependent phagocytosis (Brown *et al.*, 2002). NO is required for macrophage-mediated killing of *S. pneumoniae* (Marriott *et al*., 2007). Ply and the pneumococcal cell wall stimulates MΦ NO production that leads to antimicrobial killing (Marriott *et al*., 2004; Standish and Weiser, 2009). Ply is able to stimulate TNF-α and IL-1β production from human monocytes, and NO, IL-6 and cyclooxygenase 2 production from MΦ (Houldsworth *et al*., 1994; Braun *et al*., 1999). Activation of MΦ NLRP3 inflammasome by Ply induces caspase-1 activation and the IL-1β secretion that lead to protective immunity to *S. pneumoniae* (McNeela *et al*., 2010; Fang *et al*., 2011).

Alveolar MΦ play a significant role in eliminating pneumococci from the lung during subclinical infection (Dockrell *et al.*, 2003). Splenic and liver macrophage subsets are also essential for *S. pneumoniae* clearance from the systemic circulation

(Gerlini *et al*., 2014) . Some evidence suggests the involvement of regulatory immune responses during S*. pneumoniae* infections. Pneumococcal carriage is maintained without inducing damaging host inflammation by the actions of TGF-β and Treg cells (Neill *et al*., 2014). Tregs secrete IL-10, and Tregs in nasal associated lymphoid tissue may contribute to the persistence of pneumococcus in children (Zhang *et al*., 2011). The adaptive response to nasopharyngeal colonisation by *S. penumoniae* involves the acquisition of anti-capsular (Zhang *et al*., 2006a; Weinberger *et al*., 2008) and anti-protein antibodies (McCool and Weiser, 2004; Zhang *et al.*, 2006b) and cellular CD4+ T cell cellular immune responses (Mureithi *et al.*, 2009).

1.15 *Fasciola hepatica* and bacterial co-infection

Several studies have documented the impacts of *F. hepatica-M. bovis* co-infection on the host's immune system that result in a reduction in the diagnostic sensitivity tests for bovine tuberculosis in cattle (Flynn *et al*., 2007a; Flynn *et al*., 2009; Claridge *et al*., 2012). Co-infection with *F. hepatica* may have an impact on the shedding of *Escherichia coli* O157 in cattle destined for the human food chain (Howell *et al*., 2017). *F. hepatica* infection reduced *B. pertussis*-specific IFN-ɣ production in co-infected mice (O'Neill *et al*., 2001) and Th2 responses induced by *F. hepatica* infection can exert a bystander suppression of protective Th1-responses against *B. pertussis* (Brady *et al.*, 1999). Previous studies have demonstrated the susceptibility of cattle to oral or intravenous exposure to *Salmonella* Dublin infection (Aitken *et al*., 1976; Aitken *et al*., 1978; Hall *et al*., 1981). Thus *F. hepatica* appears to exert a profound effect on the host immune response, which has consequences for the immune system's ability to contain bacterial co-infections. That has particular importance for pathogenic infections such as *S. pneumoniae*.

1.16 *Streptococcus pneumoniae* and helminth co-infection

In recent years, there has been an increasing interest in the impairment of bacterial disease vaccination programmes in countries with endemic helminth infections. Pneumococcal conjugate vaccine (PCV) hyporesponsiveness was linked with growth stunting, but previous parasitic exposure did not appear to impair the ability of children (4- to 7-years old) to respond to PCV (Singer *et al*., 2017). Ineffective *S. pneumoniae* opsonisation by alveolar MΦ was observed from the antibodies taken from *Taenia crassiceps*-infected, vaccinated mice, and there was no protection against pneumococcal challenge when cells were adoptively transferred into naïve mice (Apiwattanakul *et al*., 2014a). These mice also had increased susceptibility to pneumococcal pneumonia and high mortality compared to helminth-negative vaccinated mice (Apiwattanakul *et al*., 2014a). Chronically *Taenia crassiceps*-infected mice were predisposed to fatal pneumococcal pneumonia when challenged with *S. pneumoniae* type 3 strain A66.1 (causes primary pneumonia without bacteraemia) and type 2 strain D39 (causes pneumonia with secondary bacteraemia and sepsis), respectively (Apiwattanakul *et al*., 2014b). *H. polygyrus* infected mice recapitulated the fatal outcome when challenged with strain A66.1 but the effect was reversible when mice were treated with an anthelmintic. Both of these chronic helminth infection models predisposed mice to bacterial outgrowth in lungs, resulting in pneumonia and death (Apiwattanakul *et al*., 2014b). There could be a potential for widespread co-infection of *F. hepatica* and pneumococcus in humans in parts of the world, such as South America and South-East Asia, where both are endemic.

1.17 Thesis aims

The general aim of this thesis was to investigate the mechanisms underlying the interaction between two common, highly pathogenic organisms; a helminth parasite, *F. hepatica* and the bacterium *S. pneumoniae*. Considerable work has been done on understanding the basic immune responses in hosts infected with a single organism, but the impact of *F. hepatica* mediated immunomodulation on the host's immune response to *S. pneumoniae* infection is unknown. The specific objectives are:

1. To investigate the modulation of the macrophage J774.2 cell line exposed to *F. hepatica* antigens and two respiratory bacteria (Chapter 3).
2. To investigate the capacity of *F. hepatica* ES antigens to modulate the immune response to *S. pneumoniae* using murine bone marrow-derived macrophages (BMDMΦs) (Chapter 4).
3. To investigate the effect of *F. hepatica* ES antigens in *Streptococcus pneumoniae* serotype 2 D39 nasopharyngeal carriage in the mouse model (Chapter 5).
4. To analyse the gene expression in *F. hepatica*-pneumococcus co-exposed murine macrophages (Chapter 6).

Chapter 2

Materials and Methods

CHAPTER 2

Materials and Methods

2.1 Parasitology

2.1.1 *Fasciola hepatica* (liver fluke) collection from animal livers

Fluke-infected livers from slaughtered animals (cattle or sheep) were collected from a local abattoir near Liverpool and transported to the Diagnostic Laboratory, University of Liverpool at room temperature. The liver was inspected for the presence of *F. hepatica,* where adult parasites were isolated from the bile ducts.

2.1.2 Preparation of *F. hepatica* antigens

As reported elsewhere (Guasconi *et al*., 2012; Guasconi *et al*., 2015; Lund *et al*., 2014; McNeilly and Nisbet, 2014; Ravida *et al.*, 2016; Toet *et al*., 2014; Vukman *et al.*, 2013a, b; Moxon *et al*., 2010; Falcón *et al*., 2014), there are three groups of antigens derived from *F. hepatica*: the excretory/ secretory products (FhES), the tegumental coat antigen (FhTEG) and somatic antigen (FhSOM). In this study, I have focused on FhES (*in vitro*, *in vivo* and *ex vivo* studies) and FhTEG (*in vitro*). All antigens were prepared under aseptic conditions using sterile reagents.

2.1.2.1 *F. hepatica* excretory/ secretory antigen (FhES)

Using atraumatic forceps, adult flukes were harvested from the bile ducts and placed in 1ml RPMI (Sigma-Aldrich, UK) with 25µg/ml gentamicin (Sigma-Aldrich, UK) in sterile 24-well tissue culture plates (VWR, Radnor UK). The flukes were then incubated at 37^{o}C for 2 hours to purge caecal contents and eggs. After incubation, any dead or damaged parasites were discarded. Each remaining individual parasite was then washed three times in copious volumes of warm Dulbecco's Phosphate Buffer Saline (D-PBS) (Sigma-Aldrich, UK). Ten flukes were placed in RPMI with 25µg/ml gentamicin in 25cm^2 tissue culture flasks (Corning, UK) and

incubated overnight at 37ºC with 5%CO_2. The following day, media containing E/S products were aspirated using disposable pipettes and centrifuged at 4000xg for 3 minutes to separate out eggs and other solid debris. Finally, the products were filter sterilised using Sartorius™ Minisart™ syringe filters (pore size 0.2µm) (Sartorius, Germany) and aliquoted into sterile tubes and stored at -80ºC.

2.1.2.2 *F. hepatica* tegumental coat antigen (FhTEG)

The remaining fluke from above (Section 2.1.2.1) were removed, washed three times in copious volumes of D-PBS and transferred to a 75cm^2 tissue culture flask (Corning, UK) containing D-PBS with 1% Nonidet (N) P-40 (BDH Chemicals, UK) at a volume of 1ml per fluke. The flask was then placed on ice and rocked gently for 1 hour, after which the supernatant containing tegument antigen was harvested. To remove the NP-40 detergent from the solution, Pierce® Detergent Removal spin columns (Thermo Scientific, UK) were used according to manufacturer's instructions (Thermo Scientific user guide_2164.3_87779: 4ml, 5 columns, for 500-1000µl samples).

In brief, the bottom closure of the columns and caps were removed and loosened, respectively. The columns were placed in 15ml falcon tubes and centrifuged at 1000xg for 2 minutes to remove the storage solution. Then, 4ml of wash/ equilibration buffer (D-PBS) was added to each column and centrifuged as before. This step was repeated for two additional times. Next, the columns were placed in new collection (falcon) tubes and FhTEG containing 1% NP-40 solution was applied slowly by pipetting to the top of the compact resin bed within the column and incubated for 2 minutes at room temperature and centrifuged as before to collect the NP-40 free FhTEG. These final detergent free samples were filter sterilised as before and aliquoted into sterile tubes and stored at -80ºC before use.

2.1.2.3 *F. hepatica* somatic antigen (FhSOM)

Tegument depleted fluke in Section 2.1.2.2 were washed three times in copious volumes of D-PBS and snap-frozen overnight at -80^{o}C. The following day, fluke were removed from the freezer and homogenised in a small volume of D-PBS with a sterile pestle and mortar. The fluke homogenate was then transferred to a 50ml falcon tube and diluted to a concentration of 0.5ml/ fluke and left to stand overnight at 4^{o}C. The resulting supernatant was pipetted off and centrifuged at 12,000xg for 30 minutes at 4^{o}C to remove dense particulate. The final supernatant was then filter sterilised, aliquoted and stored at -80^{o}C. In this study, FhSOM antigen was only used for protein separation analysis using sodium dodecyl sulphate polyacrylamide gel electrophoresis (SDS-PAGE) whilst FhES and FhTEG were used for further experiments (*in vitro* and *in vivo*).

2.1.3 Sodium dodecyl sulphate polyacrylamide gel electrophoresis (SDS-PAGE) analysis of *Fasciola hepatica* products

SDS-PAGE was performed based on previously established methods (Laemelli, 1970) using a vertical mini gel electrophoresis system (Mini-PROTEAN® Tetra Vertical Electrophoresis Cell, Bio-Rad, UK). A 12% acrylamide resolving gel and 4% stacking gel were prepared (Table 2.1) and all preparations for the solutions used are given in Table 2.2.

Table 2.1: Gel for SDS-PAGE

12% resolving gel		4% stacking gel	
Reagent	**Volume (ml)**	**Reagent**	**Volume (ml)**
30% acrylamide	4.0	40% acrylamide	0.650
Resolving gel buffer (1.5M Tris-HCl, pH 8.8)	2.5	Resolving gel buffer (0.5M Tris-HCl, pH 6.8)	1.25
10% SDS	0.05	10% SDS	0.05
dH_2O	3.4	dH_2O	3.0
10% APS	0.075	10% APS	0.025
TEMED	0.0075	TEMED	0.005

Acrylamide available from Severn Biotech, UK
Tris-HCl : Trizma hydrochloride (Sigma-Aldrich, UK)
SDS : sodium dodecyl sulphate polyacrylamide (Sigma-Aldrich, UK)
dH_2O : distilled water
APS : ammonium persulphate (Sigma-Aldrich, UK)
TEMED : tetramethylethylenediamine (Bio-Rad, UK)

Table 2.2: Buffers and solutions for SDS-PAGE

Buffer	Reagent	Amount
Resolving gel buffer (1.5M Tris-HCl, pH 8.8)	Tris-HCl dH_2O	18.15 g 100 ml
Stacking gel buffer (1.0M Tris-HCl, pH 6.8)	Tris-HCl dH_2O	6.05 g 100 ml
10% SDS	SDS dH_2O	10.0 g 100 ml
10% APS	APS dH_2O	1.0 g 10.0ml
Tris-glycine running buffer	Tris-HCl Glycine 10% SDS dH_2O	7.55 g 47.0 g 25 ml 500ml
Laemmli buffer, pH 6.8 (ready to use) (Sigma-Aldrich, UK)	SDS Glycerol 2% mercaptoethanol Bromphenol blue Tris-HCL	4 % 20 % 10 % 0.004 % 0.125M

Glycine available from Sigma-Aldrich, UK

In a clean eppendorf tube, neat and diluted samples were heated to 100^{o}C for 10 minutes using a heat block. The denatured proteins were then centrifuged for 1 minute at medium speed. 10µl of samples and protein ladder (New England BioLabs®, UK) were carefully loaded into the wells and allowed to run at 200 V, 60 mA (per gel) for 40 minutes or until the front dye reaches the bottom of the gel. Once electrophoresis was finished, the gel was removed from the plates, placed in a plastic tray and rinsed under running tap water. The gel was then heated in a microwave for 1 minute with medium power level and rinsed as before. The heat and rinse steps were repeated for 3 times before being stained with PageBlue stain (Thermo Scientific, UK). Next, the gel was heated again in a microwave for ≈ 1 minute (or stopped at any sign of boiling) and left on a rocker for 5-10 minutes. Finally, the gel was de-stained under running water until the blue stain had disappeared. Protein bands were visualised using BioRad Chemidoch Touch Imaging System and processed using Image Lab Software Version 5.2.1 (http://www.bio-rad.com/en-uk/sku/soft-lit-170-9690-ilspc-image-lab-software-version-5-2-1-pc).

2.1.4 Protein determination (Coomassie Plus™ (Bradford) assay)

Protein concentrations for all prepared fluke antigens were calculated using the Coomassie Plus™ (Bradford) assay following standardised microplate protocol as per manufacturer's protocols (Thermo Scientific user guide_0229.8_23236: Microplate Protocol_working range: 1-25µg/ml). Reference standards of bovine serum albumin (BSA) (Thermo Scientific, UK) were diluted in distilled water to give a standard curve of protein concentrations ranging from 2.5-25µg/ml following the manufacturer's protocols (Appendix A1). Samples were serially diluted in distilled water to 1:100 or 1:500. In duplicate, 150µl of each standard and diluted samples were pipetted into Immulon 2HB flat-bottomed 96-wells (Thermo Scientific, UK). Next, 150µl of Coomassie Plus Reagent (Sigma Aldrich, UK) was added to each standard and sample dilution using a multichannel pipette, and carefully mixed. For the most consistent results, the plate was incubated for 10 minutes at room temperature before absorbance was measured at 595nm on a Tecan Infinite® F50 plate reader supported with Magellan software. Finally, protein concentrations for

all antigens were calculated by reference to a standard curve (absorbance obtained from a series of standard protein (BSA) dilutions).

2.1.5 Endotoxin quantitation assay

F. hepatica antigens (FhES and FhTEG) and *Mycobacterium bovis* sonicate extract (MbSE) (see Section 2.2.1) intended for use in tissue culture were checked for Gram negative bacterial endotoxin (lipopolysaccharides, LPS) using Pierce® Limulus Amebocyte Lysate (LAL) Chromogenic Endotoxin Quantitation kit (Thermo Scientific, UK) (Thermo Scientific user guide_2445.3_88282: Microplate Assay Procedure). Endotoxin standard stock solutions were prepared following the manufacturer's instructions (Appendix A2). The microplate was heated for 10 minutes at 37ºC. Samples were serially diluted in endotoxin-free water (provided with the kit) to 1:10 or 1:100. In duplicate, 50µl of each standard and diluted samples were dispensed carefully into an appropriate microplate well, covered with a lid and incubated for 5 minutes at 37ºC. Next, 50µl of LAL was added to each well, covered with a lid, with gentle shaking for 10 seconds and incubated for 10 minutes at 37ºC.

Consistent pipetting order and rate of reagent addition were ensured from well-to-well and row-to-row. After exactly 10 minutes, 100µl of substrate solution was added to each well with consistent pipetting speed as before, covered with a lid and incubated at 37ºC for 6 minutes. To stop the reaction, 50µl of stop reagent (25% acetic acid) was added at the same pipetting speed. The plate was placed on a plate mixer for 10 seconds before absorbance was measured at 405-410nm using Tecan Infinite® F50 plate reader and final endotoxin concentrations for FhES, FhTEG and MbSE were calculated.

2.1.6 Endotoxin removal

Only FhES antigens were detected to have more endotoxin than the assay's detection limit (>1.0 EU/ml). Endotoxin in FhES preparation was removed using EndoTrap®red 5/1 chromatography resin kit (Hyglos GmBH, Germany) following continuous (column mode) chromatography protocol. Briefly, the top cap of the prepacked column was removed first before the bottom cap and the storage solution was allowed to drain from the column. To activate the column, 3 ml of regeneration buffer (EndoT-RB) was pipetted immediately into the column (to avoid the resin drying out) and left to drain off completely. This activation step was repeated once more before 3 ml of equilibration buffer (EndoT-EB) was added.

Next, the sample was added (in EndoT-EB) to the column and the eluates were collected immediately into sterile 15 ml Falcon tubes. As soon as the sample was completely absorbed into the column, an additional 1 ml of EndoT-EB was pipetted to elute the entire sample. For regeneration of the column, 3 ml of EndoT-RB was applied, drained off and repeated two times before adding another 1 ml of EndoT-RB supplemented with 0.02% sodium azide (or 20% ethanol as storage buffer with reduced storage time) and stored at 2-8^{o}C. The whole process was performed in a cold room to maintain the sample integrity and each sample fraction collected was tested again for endotoxin level separately as the substances passed through the column at different rates. The protein determination was calculated again for each sample after endotoxin removal.

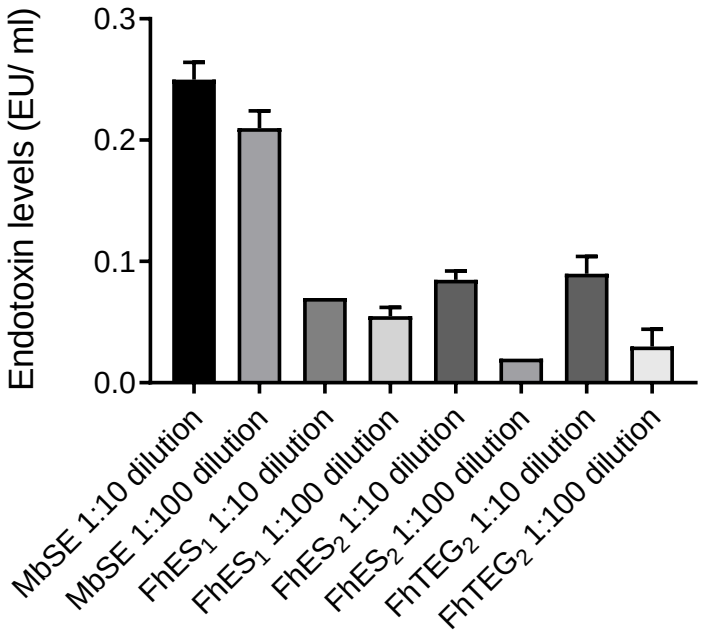

Figure 2.1: Endotoxin levels of fluke antigens and MbSE quantified using LAL assay. Lipopolysaccharide (LPS) levels in all tested antigens were below the standard endotoxin limit (<1.0 EU/ml; recommended by the manufacturer). The $FhES_1$ and $_2$ bars shown, are following removal of endotoxins.

Prior to *in vitro* stimulation, fluke antigens and MbSE were tested for endotoxin levels. This is important because LPS can affect the activation of macrophages. The endotoxin level in $FhES_1$ and $_2$ products were detected at 2.58 EU/ml and 1.89 EU/ml, respectively which is higher than the limit of 1.0 EU/ml. The contaminating endotoxins were then removed using the EndoTrap chromatography resin kit and re-tested again. From Figure 2.1, all the antigens had negligible endotoxin contamination.

2.2 Bacteriology

2.2.1 Bacteria species

Two respiratory bacterial species were used in this study. First, sonicate extract preparation of *Mycobacterium bovis* (MbSE) that was kindly provided by Dr. Lyanne McCallan (Veterinary Sciences Division, Agri-Food and Biosciences Institute (AFBI), Belfast) and second, laboratory serotype 2 strain D39 (live wild-type (WT) culture) and pneumolysin (Ply)-deficient mutant D39Δ6ply (live, heat- and detergent-inactivated) of *Streptococcus pneumoniae* were used.

2.2.2 Culture and cryopreservation media

2.2.2.1 Blood agar base (BAB) plates + 5% v/v horse blood

16 grams of BAB medium (Sigma-Aldrich, UK) was added to 400ml of distilled water and autoclaved at 15psi (103kPa) for 30 minutes. The same pressure and time apply to all autoclaving processes involved in this study. After autoclaving, the media were cooled to ~56^{o}C, 20ml of Sterile Defibrinated Horse Blood (Sigma-Aldrich, UK) (5% v/v) was added and gently mixed. For *S. pneumoniae* isolation and growth in *in vivo* experiments, 2µg/ml of gentamicin (Sigma-Aldrich, UK) was added with the horse blood (as above) and gently mixed. The medium was then poured into sterile petri dishes (90mm) and left to dry overnight at room temperature. On the next day, the plates were stored inverted at 4^{o}C for up to 14 days.

2.2.2.2 Brain heart infusion (BHI) broth

14.8 grams of BHI medium (Sigma-Aldrich, UK) was added to 400ml of distilled water and autoclaved. Following autoclaving, the ‘straw’ coloured medium was stored at room temperature for up to 4 weeks.

2.2.2.3 BHI Serum broth

BHI broth was prepared and autoclaved as above (Section 2.2.2.2). Next, 20ml of Foetal Bovine Serum (FBS) (Sigma-Aldrich, UK) was added to 80ml of BHI medium (a mixture of 80% v/v medium and 20% v/v serum). The BHI serum broth was prepared fresh for each use.

2.2.2.4 Cryopreservation media

A freezing media was prepared to cryopreserve cells from isolated murine tissue (in Section 2.10.2) using the ratios 75% RPMI medium (Sigma-Aldrich, UK), 15% FBS (Sigma-Aldrich, UK) and 10% dimethyl sulphoxide (DMSO) (Sigma-Aldrich, UK).

2.2.3 Preparing stocks of pneumococci

Laboratory bead collections of both pneumococcal strains mentioned in Section 2.2.1 were streaked onto BAB culture plates with an optochin antibiotic disk (Oxoid) placed on a site of inoculation. The plates were then incubated overnight at 37^{o}C with 5% CO_2. Following overnight incubation, the plates were checked for a zone of bacterial growth inhibition around the antibiotic disk to indicate the susceptibility of pneumococci to optochin. This is to ensure only pneumococci are present.

Then, a full sweep of colonies was inoculated into 10ml of BHI broth in a sterile universal tube. The inoculum was then incubated statically for 16-18 hours at 37^{o}C with 5% CO_2 until OD_{500} 1.4-1.6 was reached. On the next day, when the broth culture reached the desired OD, the tube was centrifuged at 1500xg for 15 minutes. The supernatant was removed and the remaining pellet re-suspended in 1ml BHI serum broth. 700µl of the re-suspended pellet was then added to 10ml of warm BHI serum and incubated statically at 37^{o}C with 5% CO_2 for 5 hours until OD_{500} ≥1.2 was reached. Finally, serum broth containing pneumococci was divided into 500µl single-use aliquots in sterile cryotubes and kept at -80^{o}C. The bacterial viability was determined by a Miles and Misra count (described in Section 2.2.4).

In brief, after 24 hours the aliquots were thawed, centrifuged at 12,000xg for 2 minutes, re-suspended and serially diluted in sterile PBS and cultured onto the BAB culture plate. Viability was reported as colony-forming unit per ml (CFU/ml) of pneumococci.

2.2.3.1 D39Δ6ply heat-killed pneumococci (D39Δ6ply-HK)

After the serum broth containing D39Δ6ply pneumococci had reached OD_{500} ≥1.2, the tube was placed in the water bath heated to 60^{o}C for 45 minutes. To ensure that all bacteria were killed, a loop full of inoculum was streaked onto the BAB culture plate and incubated overnight at 37^{o}C with 5% CO_2. No growth on the plate was taken to indicate successful killing of bacteria. A volume of 500µl of D39Δ6ply-HK was added per well for infection of J774.2 macrophages.

2.2.3.2 D39Δ6ply sodium deoxycholate–treated pneumococci (D39Δ6ply-SD)

D39Δ6ply pneumococci were allowed to grow overnight in 10ml BHI broth to a late exponential phase (OD_{500}>1.0) and the inoculum was centrifuged on the next day as before (Section 2.2.3). This time, the pellet was re-suspended in 1ml sterile PBS and 10µl of a 10% stock solution of sodium deoxycholate was added and incubated for 10 minutes. One hundred microliter (100µl) of D39Δ6ply-SD was added per well for infection of J774.2 macrophages. As above (Section 2.2.3.1), a loop full of the solution was streaked onto the BAB culture plate and incubated overnight to confirm no viable bacteria in the preparation.

2.2.3.3 D39 culture supernatant (D39SN)

Frozen vials of D39 culture supernatant (D39SN) were kindly provided by Dr. Rong Xu/ Dr. Qibo Zhang (University of Liverpool). In brief, a sweep of D39 colonies was inoculated into Todd-Hewitt Broth (THB; added with 0.5% w/v yeast extract and 10% v/v FBS) and incubated at 37^{o}C overnight. Following overnight incubation, 5 ml of culture was added into 50ml of THB in a large tissue culture flask and

incubated for several hours until the culture reached OD_{600} 0.5 and placed in the cold room to stop the bacterial growth. On the next day, the culture was centrifuged at 3000xg for 30 minutes and the supernatant was filtered through 0.45µm followed by 0.2µm syringe filters and placed in the cold room overnight. Following this, the supernatant was centrifuged using Vivaspin centrifugal concentrator at 3000xg for 30 minutes at 4^{o}C. Finally, the concentrated supernatant was aliquoted into 100µl single-use sterile cryotubes and stored at -80^{o}C until assay. For the *in vitro* assay, a volume of 5µl of D39SN (containing supernatant derived from approximately 10^5 CFU) was added per well for stimulation of J774.2 macrophages.

In summary, different pneumococcal preparations and experimental models used in this study are given below (Table 2.3).

Table 2.3: Different pneumococcal preparations used in the study

Pneumococcal preparation	Experimental model
Live D39 (wild-type; WT)	*in vitro* *ex vivo* *in vivo*
Live D39Δ6ply	*in vitro*
D39Δ6ply-HK	*in vitro*
D39Δ6ply-SD	*in vitro*
D39 SN	*in vitro*

2.2.4 Miles and Misra method for viable count determination of bacteria

In this study, the Miles and Misra technique was used to determine the number of colony forming unit (CFU). Using a sterile 96-well round-bottom plate (Greiner Bio-One GmBH, Germany), 20µl of a sample (e.g. stock solution in Section 2.2.3 or animal tissue homogenates in Section 2.10.2) was added to 180µl of sterile PBS and serially diluted 10^1-10^6. BAB + gentamicin culture plates were divided into six sections, and 60µl (3 drops x 20µl) of each dilution was plated onto each corresponding sector and incubated overnight at 37^{o}C with 5%CO_2. The following day, visible sections in 20-200 CFU were counted and the CFU/ml were calculated as follow:

To calculate the numbers of CFU in infection dose:

CFU/ml = average number of colonies in sector x dilution factor x (1000/60)

2.3 Cell culture

2.3.1 Macrophage cell line culture (J774.2)

For *in vitro* study, J774.2 cell line derived from mouse (BALB/c) monocyte/ macrophage was used. The cells were grown in Dulbecco's Modified Eagle Medium (DMEM) (Sigma-Aldrich, UK) supplemented with 10% heat-inactivated FBS and 1% Penicillin/ Streptomycin (Pen/ Strep or P/S) (Sigma-Aldrich, UK). In brief, a cryovial containing frozen cells was brought up from liquid nitrogen storage and immediately thawed in a water bath at 37^{o}C by gentle swirling. In a sterile hood, the cell pellet was decanted into 10ml warm DMEM media in 50ml Falcon tube and centrifuged at 300xg for 5 minutes to remove DMSO.

Aseptically, the supernatant was then removed and the pellet was re-suspended in 1 ml warm DMEM and transferred to 75cm^2 tissue culture flask (Corning, UK) containing pre-warmed 9ml medium. The cells were incubated at 37^{o}C with 5%CO_2 and culture medium was changed every three days. The cells were sub-cultured for at least 2 to 3 passages before they were used.

When the confluency reached about 70-80%, the J774.2 cells were washed by replacing the old media with fresh warm medium and the cells were gently detached using a cell scraper (Corning, UK). Viable cells were counted using a haemocytometer (Neubauer) chamber and the trypan blue (Thermo Scientific, UK) exclusion method and re-suspended in fresh DMEM medium at desired final concentrations before stimulation/ infection (see Table 2.5). All cell cultures used in this chapter were confirmed to be *Mycoplasma* negative before use, by PCR *Mycoplasma* Test Kit I/C (PromoCell, Germany).

2.3.2 Generation of murine bone marrow-derived macrophages (BMDMΦ)

For *ex vivo* studies, mice were humanely culled by CO_2 asphyxiation followed by cervical dislocation. Euthanised mice were rinsed with 70% ethanol and tibias and femurs were immediately dissected from both hind limbs and transported to the lab in 2% FBS in PBS on ice. Aseptically, under a cell culture hood, the bones were sterilised with 3 washes of 70% ethanol in a petri dish and placed in ice-cold DMEM complete media (DMEM supplemented with 10%FBS and 1% P/S). Any additional muscle or connective tissue attached to the bones was removed using sterile scissors, forceps and Kimwipes. Using a scalpel, the proximal and distal epiphyses were cut to expose the bone marrow cavity.

Bone marrow cells were flushed out using a 10ml syringe (Terumo, UK) loaded with 10 ml cold D-PBS (without calcium and magnesium chloride, Sigma-Aldrich, UK) with a 26G ½" needle and filtered by 70µm cell strainer (Corning, UK) until the bone cavity turned white/ pale. The strainer was washed with 5ml of cold D-PBS and the filtered suspension was mixed by pipetting before centrifugation at 300xg for 10 minutes. The supernatant was removed, and the cells re-suspended in 10 ml cold DMEM complete media and centrifuged again at the same speed and time. The cell pellet was then re-suspended in the same volume of DMEM medium and viable cells were counted. The cell count was adjusted to $1x10^6$ cells/ml and dispensed into sterile 60mm x 15mm tissue culture dishes (Corning, UK). The medium was supplemented with M-CSF (20ng/ml, Bio-Rad, UK).

Cultures were maintained at 37ºC 5%CO_2 and the medium was replaced on days 3 and 6. On day 7, attached differentiated macrophages were gently removed by scraping, centrifuged at 300xg for 5 minutes to remove antibiotics and plated for use in the assay. Table 2.4 summarises the mouse strains for *ex vivo* experiments and functional assays used in this thesis.

Table 2.4: Mouse strains used in *ex vivo* murine BMDMΦ assays

Mouse strain	Age	Supplier	Functional Assay
CD-1	6-7 weeks	Charles River, UK	NO – M1 type MΦ Arg – M2 type MΦ
C57BL/6	6-7 weeks	Charles River, UK	NO – M1 type MΦ Arg – M2 type MΦ
BALB/c	6-7 weeks	Charles River, UK	NO – M1 type MΦ Arg – M2 type MΦ Digital multiplexed gene expression (NanoString nCouter system)
	15 weeks	Charles River, UK	NO – M1 type MΦ Arg – M2 type MΦ

NO : nitric oxide M1 : type 1 (classically activated) macrophage (MΦ)
Arg : arginase M2 : type 2 (alternative activated) macrophage (MΦ)
Only female mice were used for BMDMΦ isolation and differentiation

2.4 *F. hepatica* antigen and bacterial stimulation of J774.2 and bone marrow-derived macrophages

Prior to fluke antigen (FhES and FhTEG) and bacterial stimulation (MbSE and different pneumococcal preparations), J774.2 cell suspensions were seeded (see Section 2.3.1) at a final concentration of $1x10^6$ cells/ml and were then added to 24-well tissue culture plate, allowed to adhere overnight and then media was removed the next day. After three washes with 200µl D-PBS, fresh warm media with no antibiotics was added before introducing the stimulants at the indicated concentrations. For co-exposure cultures, the same concentration of fluke antigens and different bacteria preparations were added together in the same culture well.

J774.2 cells infected with live WT D39 (D39 alone and co-exposure cultures) were initially incubated for 2 hours and the cells were rinsed with sterile D-PBS to remove unbound bacteria. Any extracellular bacteria were killed by adding medium supplemented with Penicillin G (1mg/ml, Sigma-Aldrich, UK) for 1 hour. Following this, the medium was removed and the cells were washed repeatedly with non-antibiotic media before adding 1ml of fresh medium with no antibiotics but with added fluke antigens where indicated. For control cultures, sterile D-PBS was added. Gram negative bacteria lipopolysaccharide (LPS) from *E. coli* strain 111:B4 (Sigma-Aldrich, UK) and recombinant mouse interleukin 4 (IL-4) (carrier free) (BioLegend, UK) were used as positive controls for nitric oxide (M1 macrophage marker) and arginase (M2 macrophage marker) respectively. All cultures were incubated at 37^{o}C 5%CO_2 for 24, 48 and 72 hours.

In a 96-well flat-bottom plate, 5x10^5 BMDMΦs were cultured in DMEM 10% FBS with no antibiotics, overnight and the medium was changed the next day. Sterile D-PBS (control culture), *F. hepatica* ES (FhES) antigen and live D39 were added at the same volume, concentration and CFU, respectively and incubated at 37^{o}C with 5% CO_2 for 24 and 48 hours. Extracellular D39 in BMDMΦs culture were killed following the protocol described above. LPS and IL-4 were used as M1 and M2 macrophage positive controls as before.

J774.2 and BMDMΦ supernatants and cell lysates were collected from each well at each time point for nitric oxide (NO) and arginase assays (Section 2.8 and 2.9) and stored at -80^{o}C. All concentrations of stimulants and controls used in this assay were previously optimised to give consistent reproducible results after 24, 48 or 72 hours stimulation. All stimulants and their concentrations are shown in Table 2.5. Supernatants were also analysed for cell signalling proteins using a multiplex cytokine ELISA assay (see Section 2.10.3.1).

Table 2.5: Concentration of stimulants exposed/ infected on J774.2 and bone marrow-derived macrophages

Stimulant	Concentration optimised/ Inoculum dose	Cell type
***F. hepatica* antigens**		
FhES (excretory/ secretory)	5µg/ml	J774.2, *BMDMΦ
FhTEG (tegumental)	5µg/ml	J774.2
***T. muris* antigen**		
TmES (excretory/ secretory)	5µg/ml	J774.2
M. bovis		
MbSE (sonicate extract)	5µg/ml	J774.2
Serotype 2 strain D39 *S. pneumoniae*		
a) Ply-deficient mutant D39Δply-HK		
b) Ply-deficient mutant D39Δply-SD	500µl (Section 2.2.3.1)	J774.2
c) #Ply-deficient mutant D39Δply (live)	100µl (Section 2.2.3.2)	J774.2
d) #Wild-type D39 (live)	10µl of $1x10^5$ CFU (Section 2.2.3)	J774.2
e) D39 supernatant (D39 SN)	10µl of $1x10^5$ CFU (Section 2.2.3)	J774.2, *BMDMΦ
	5µl (approximately 10^5 CFU) (Section 2.2.3.3)	J774.2
Positive controls		
LPS (M1/ CAMΦ)	5µg/ml	J774.2, BMDMΦ
IL-4 (M2/ AAMΦ)	20ng/ml	J774.2, BMDMΦ

#the dose concentration for both live bacteria in c) and d) are $1x10^7$ CFU/ml

*same inoculum concentration of FhES and D39 were used in BMDMΦ culture for NanoString nCounter experiment (see Section 2.11)

2.5 *Trichuris* (*T*) *muris* excretory/ secretory (TmES) antigen

Another helminth excretory/ secretory product was used in this study, to enable comparison with the production of NO and arginase elicited by fluke antigens in J774.2 macrophages. *Trichuris muris* (a nematode parasite of mice) E/S antigen (TmES; 5µg/ml) (kindly provided by Alice Law, University of Liverpool) was added to the same J774.2 cell seeding density and maintained for 72 hours. Further experiments using low passage cells number primed with IL-4 were also completed using TmES.

2.6 Priming of J774.2 cells with interleukin 4 (IL-4)

To investigate the effect of different passage number on cell response, low and high passage number of J774.2 cells were primed with IL-4 (20ng/ml, BioLegend, UK) before FhES and TmES stimulation and evaluation of arginase production. Cells were primed with IL-4 and incubated for 24 to 48 hours. At each timepoint, the old medium was replaced with fresh medium containing parasite antigens and arginase levels were assayed from the cell lysates. Table 2.6 summarises the J774.2 priming experiment at different passage cell numbers.

Table 2.6: IL-4 primed J774.2 macrophages at different passage numbers

Passage number (P)	Time point (hour)	Stimulants
F. hepatica		
P28 (H)	48	FhES and FhTEG
P7 (L)	24 and 48	FhES and FhTEG
T. muris		
P5 (L)	24 and 48	TmES

Low (L) : between 3-10 passages
High (H) : more than 10 passages

2.7 Macrophage mannose receptor (MMR) (CD206) expression

In a 6 well tissue culture plate (VWR, Radnor UK), $1x10^6$ cells/ml of J774.2 macrophages were stimulated with IL-4 (20ng/ml) and incubated for 24, 48 and 72 hours. At each time point, J774.2 macrophages were detached by scraping, spun at 300xg for 5 minutes at 4^{o}C, plated into a 96-well round-bottom plate and washed twice with flow cytometry buffer (fluorescence-activated cell sorting (Facs) buffer) which consisted of PBS and 2% FBS, before being incubated with a purified anti-mouse CD16/CD32 antibody (TruStain fcX™ Clone 93, BioLegend, UK). This treatment blocked for non-antigen specific binding of immunoglobulin to the Fc receptors. The antibody was used at 1:200 dilution and cells incubated for 30 minutes at room temperature. Cells were washed with Facs buffer and the cells were incubated with conjugated APC anti-mouse CD206 (MMR) (Clone C068C2, BioLegend, UK) at 1:400 dilution. A 1:400 dilution of purified isotype control antibody (Rat IgG2a, $_{K}$ Clone RTK2758, BioLegend, UK) was used as the negative control. The plate was incubated in dark for 30 minutes at room temperature. After that, cells were washed twice and re-suspended in 300µl of Facs buffer and transferred into a round-bottom polystyrene tube. The samples were analysed using a BD FACSCalibur™ flow cytometer (BD Biosciences) and data were analysed by FlowJo™10.5.3 software (TreeStar).

2.8 Nitric oxide (NO) measurement

After incubation, supernatants from J774.2 or BMDMΦ cells were collected, centrifuged at maximum speed for two minutes to remove cells and tested using a commercially available Griess reagent system (Promega, UK). Following the manufacturer's protocol, the nitrite standard reference curve was prepared by diluting the provided 0.1M Nitrite Standard (1:1000) in DMEM medium. In triplicate, 50µl of DMEM was dispensed to wells of a 96-well flat-bottom plate (Immulon 2HB) in rows B-H. A 100µl volume of the 100µM nitrite solution was added to the 3 wells in row A. Immediately, six serial twofold dilutions (50µl/ well) were made on the plate to generate the Nitrite Standard reference curve (100, 50, 25, 12.5, 6.25, 3.13 and 1.56µM), discarding 50µl from the final set of wells. No nitrite solution was

added to the last set of wells (0µM). To measure the NO in the test samples, 50µl of the supernatants were added in duplicate. Following this, 50µl of sulfanilamide solution was added to the standard and sample wells and the plate was incubated for 10 min in the dark at room temperature. Finally, 50µl of N-1-napthylethylenediamine dihydrochloride (NED) solution was added and the plate incubated as before. Readings were taken at 540 nm with Tecan Infinite® F50 plate reader and NO concentration was determined by comparison with the standard curve (Appendix A3).

2.9 Arginase activity assay

The assay protocol was adapted from Flynn *et al*., 2007b. After the collection of cell culture supernatants (Section 2.8), lysis of the macrophages from the same culture well was accomplished by vigorous pipetting, addition of 1ml of 1% Triton X-100 in PBS and incubation on a rocking platform for 20 min. Following this, 50µl of lysate or beef liver homogenate obtained from the same local abattoir (1:200 dilution; positive control) was added to 50µl of 10mM $MnCl_2$/ 50mM Tris–HCl buffer and incubated at 55^{o}C for 10 min using a heat block for enzyme activation. After incubation, 50µl of arginine substrate (Sigma-Aldrich, UK) was added to 50µl of the activated lysates. This mixture was incubated at 37^{o}C for 1 hour and then the reaction was stopped by addition of 400 µl of acid stop solution, comprising H_2SO_4 (96%), H_3PO_4 (85%), and H_2O in a ratio of 1:3:7. A urea standard curve was used to quantify the arginase concentration in each sample. Details are given in Appendix A4.

Colour was developed by adding 25µl of 9% isonitrosopriopherone (ISF) (Sigma-Aldrich, UK) into the sample and control tubes and heating to 103^{o}C for 45 min using a heat block. 200µl of the reaction mixture were added to wells of Immulon 2HB flat-bottomed 96-wells and the OD measured at 570 nm Tecan Infinite® F50 plate reader. One unit of enzyme activity was defined as the quantity of enzyme that results in the formation of 1 mmol urea/min. All preparations for the arginase assay reagents and chemicals are given in Table 2.7 and preparation of urea standard in Appendix A4.

Table 2.7: Reagents and chemicals used for arginase assay

Name	Reagent/ Chemical	Amount
1% Triton X-100	Triton X-100 PBS	500µl 50 ml
50mM Tris–HCl buffer (pH 7.5)	Tris-HCl dH2O	7.88 g 1000 ml
10mM MnCl2/ 50mM Tris–HCl	MnCl2 50mM Tris–HCl buffer	0.126 g 100 ml
0.5M Arginine substrate (pH 9.7)	L- Arginine dH2O	0.871 g 10 ml
9% ISF in absolute ethanol	ISF absolute ethanol	0.09 g 1 ml

Tris-HCl : Trizma hydrochloride (Sigma-Aldrich, UK)
98% $MnCL_2$: Manganese dichloride (Sigma-Aldrich, UK)
ISF : isonitrosopriopherone (Sigma-Aldrich, UK)
96% H_2SO_4 : sulphuric acid (VWR Chemicals, UK)
85% H_3PO_4 : phosphoric acid (VWR chemicals, UK)
L-Arginine : available from Sigma-Aldrich, UK
Triton X-100: available from Sigma-Aldrich, UK

2.10 Murine model of nasopharyngeal carriage of *S. pneumoniae*

Female CD-1 mice (Charles River, UK) aged between 6-7 weeks were used in this study. All animals were received and maintained in the Biomedical Services Unit (BSU), University of Liverpool and allowed to acclimatise for one week upon arrival. All mice were randomly grouped with five mice per group in individually ventilated GM500 micro-isolator cages (IVC) with food and water provided *ad libitum*. The experimental groups are shown in Table 2.8. All *in vivo* experiments were conducted following guidelines from the local animal welfare and ethical review board (AWERB) under the authority of the UK Home Office (project licence PPL: 40/ 3602, personal licence PIL: 169F907FD).

Table 2.8: Experimental groups of nasopharyngeal carriage in murine model

Group	Infection/ stimulation dose and time point (day)				
	Day 0	**Day 1 (n=5)**	**Day 2 (n=5)**	**Day 3 (n=5)**	**Day 4 (n=5)**
Control (PBS)	am: Dose with 20µl PBS pm: Dose with 10µl PBS	am: Dose with 20µl PBS pm: cull	am: cull	am: cull	am: cull
D39	am: Dose with 20µl PBS pm: Dose with 10^5 CFU D39 *S. pneumoniae* in 10µl PBS	am: Dose with 20µl PBS pm: cull	am: cull	am: cull	am: cull
FhES	am: Dose with FhES (20-50µg/ml in 20µl PBS) pm: Dose with 10µl PBS	am: Dose with FhES (20-50µg/ml in 20µl PBS) pm: cull	am: cull	am: cull	am: cull
FhES + D39	am: Dose with FhES (20-50µg/ml in 20µl PBS) pm: Dose with 10^5 CFU D39 *S. pneumoniae* in 10µl PBS	am - Dose with FhES (20-50µg/ml in 20µl PBS) pm: cull	am: cull	am: cull	am: cull

FhES antigen, D39 and PBS were intranasally (IN) administered into CD-1 mice
am : ante meridiem (before midday)
pm : post meridiem (after midday)

2.10.1 Dose preparation and intranasal infection/ stimulation

Previously prepared frozen aliquots of FhES antigen (see Section 2.1.2.1) and D39 stock (see Section 2.2.3) were thawed at room temperature. Aliquots of D39 stock with a predetermined CFU count (see Section 2.2.4) were centrifuged at 12,000xg for 2 minutes and the supernatant was removed and the remaining D39 cell pellet was re-suspended in sterile PBS. Thawed FhES aliquots were also diluted in sterile PBS to achieve the desired inoculum concentrations as shown in Table 2.9. Both inoculum preparations were introduced into the nostrils to establish nasopharyngeal carriage in mice.

Table 2.9: Dose preparation for nasopharyngeal carriage model

Infectious agent	Stock concentration	Inoculation volume (in sterile PBS)	Inoculum concentration
D39	$1x10^5$ CFU	10µl	$1x10^7$ CFU/ml
FhES	1592.0µg/ml	20µl	0.4-1.0µg in 20µl

Mice were placed in an induction chamber and anaesthesia was induced with 2.5% v/v isofluorane over oxygen with a delivery rate of 1.4-1.6 litres/ min until loss of righting reflex. Anaesthetised mice were intranasally administered either PBS, D39 or FhES, according to infection/ stimulation inoculum doses (see Table 2.9), using a pipette, on Day 0 and 1 (see Table 2.8). Both types of infectious inoculum and PBS were equally distributed between both nostrils in a drop-wise fashion. The dose and volume of *S. pneumoniae* administered ensures colonisation of the nasopharynx but does not induce lung infection (Neill *et al.*, 2014). At days 1, 2, 3 and 4 post-infection, mice were humanely culled using a Schedule 1 method and nasopharyngeal and lung tissues were taken for analysis of bacterial loads (CFU), levels of signalling proteins (cytokines and chemokines using ELISA) and immune cell populations, using flow cytometry. Figure 2.1 summarises an overview

schematic of the intranasal inoculation and further analysis in the nasopharyngeal carriage murine model.

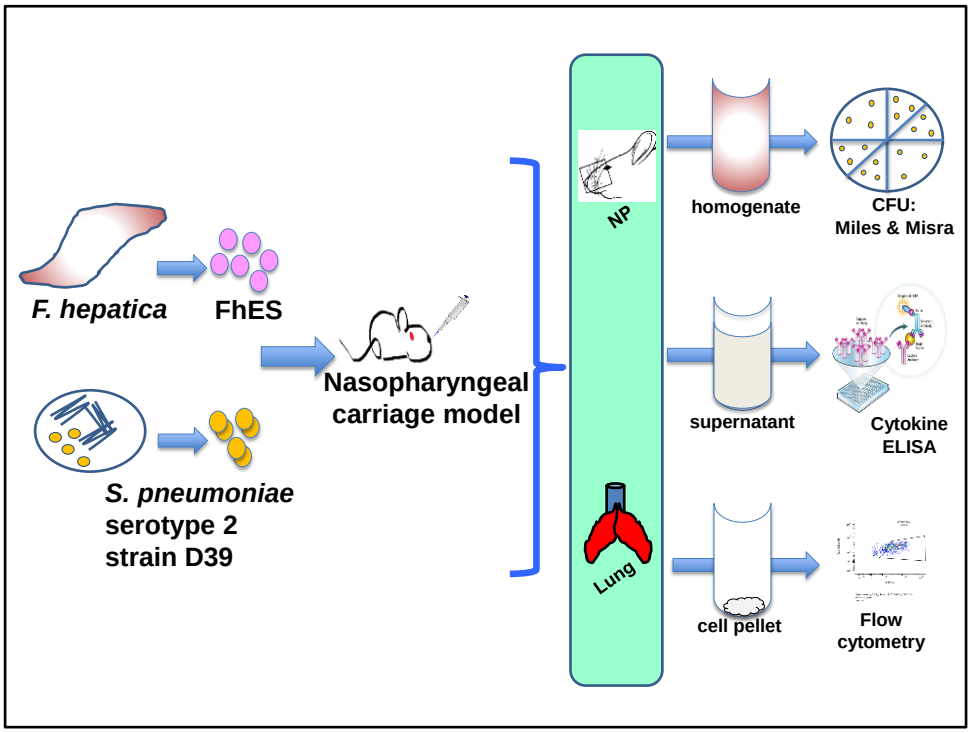

Figure 2.2: D39 nasopharyngeal carriage model in mice. The D39 pneumococcus and FhES antigen are inoculated to mice intranasally. Mice were culled at different time points and their nasopharynx and lung tissues were collected. Tissue homogenates were used to determine bacterial loads, before centrifugation. Supernatants from spun homogenates were subject to cytokine and chemokine analysis and cell pellets were analysed for immune cell populations.

2.10.2 Nasopharynx and lung tissue preparation for bacterial load, signalling protein and flow cytometry analysis

Death of animals was confirmed by cervical dislocation. On a clean dissection board and with aseptic technique, the nasopharynx and lung were harvested and placed in labelled bijou tubes containing 3mls of sterile PBS. Each tissue was mechanically homogenised using IKA™ T 10 disperser (Fisher Scientific, UK) for ~1 minute.

Following this, 20µl of the tissue homogenates were taken for CFU counts using Miles and Misra method (see Section 2.2.4). The remaining homogenates were then passed through a 40µm cell strainer (EASYstrainer™, Greiner Bio-One GmBH, Germany) and washed twice with 3ml of PBS to give a total volume of 6ml. Filtrates from both types of tissue were then centrifuged at 400xg for 5 minutes and the supernatant was aliquoted and stored at -80^{o}C prior to signalling proteins analysis.

The nasopharynx cell pellet was re-suspended in cryopreservation media (see Section 2.2.2.4), placed in a Mr. Frosty™ Freezing Container (Thermo Scientific, UK) for slow-freezing at -80^{o}C for future cell population analysis using flow cytometry. The lung cell pellet was re-suspended in 1:10 of 1x Red Blood Cell (RBC) lysis buffer (eBioscience™, Thermo Scientific, UK) to lyse the red blood cells and incubated for 5 minutes. The reaction was stopped with PBS before being centrifuged at 400xg for 5 minutes. The supernatant was discarded and the cell pellet was re-suspended in cryopreservation media and slow-frozen at -80^{o}C for flow cytometry analysis.

2.10.3 Signalling protein studies in nasopharynx by ELISA

From the bacterial load results (Figure 5.1), nasopharynx supernatants were analysed for cell signalling proteins using commercially available kits. All tested proteins from the nasopharynx alongside the previously collected J774.2 and BMDMΦ supernatants (see Section 2.4) were analysed in the same 96-well plate multiplex assays (MSD® U-PLEX (Mouse) Platform, Meso Scale Discovery, USA) (Section 2.10.3.1). For transforming growth factor-beta 1 (TGF-β1), nasopharynx supernatants were assayed using Mouse TGF-β1 DuoSet ELISA kit (DY1679-05, R&D Systems, USA).

2.10.3.1 Multiplex MSD® U-PLEX cytokine ELISA

Following the manufacturer's protocols, 200µl of each biotinylated capture antibody was added to 300µl of the assigned linker, mixed by vortexing and incubated at room temperature for 30 minutes. Next, 200µl of stop solution was added to the linker, vortexed and incubated as before. In a single 15ml centrifuge tube, 1800µl of stop solution was added with 600µl of each U-PLEX coupled antibody solution from each linker to bring the final volume to 6000µl (when combining fewer than 10 antibodies). The mixture was vortexed again.

Following this, 50µl of multiplex coating solution was added to each well (96-well SECTOR plate), sealed with adhesive seal and incubated at room temperature on a plate shaker for 1 hour. After incubation, the plate was aspirated and washed with at least 150µl/ well of 0.05% PBS Tween 20.

To prepare calibrator standard solutions, the vial of Calibrator 5 was reconstituted by adding 250µl of Diluent 41 in a polystyrene glass test tube to achieve a 5X concentrated stock. The concentrated stock was then diluted 5-fold. Next, the reconstituted calibrator was inverted at least 3 times and left to equilibrate for 15-30 minutes at room temperature and finally briefly vortexed.

The samples were thawed at room temperature and diluted in Diluent 41 at a ratio of 1:10. Into each well, 25µl of Diluent 41 was added before adding the same volume of the sample and prepared calibrator standard. The plate was sealed and incubated at room temperature with shaking for 1 hour. Following incubation, the plate was aspirated and washed as before. The detection antibody solution was prepared in a single 15ml centrifuge tube by adding 5580µl of Diluent 45 and 60µl of each 100X of each SULFO-TAG™ labelled anti species detection antibody to bring the final volume to 6000µl. 50µl of prepared detection antibody solution was added to each well, sealed with adhesive seal and incubated with shaking at room temperature for 1 hour. Then, the plate was aspirated and washed as before. Finally, 25ml of distilled water was added to 25ml of 2X Read Buffer T with surfactant and 150µl of this working solution was added to each well before the

absorbance was measured at 620nm using MSD Sector 6000 instrument and results were analysed with the MSD Discovery Workbench software, version 4.0. Kit components with selected cytokines are detailed in Table 2.10, standard reference curves are detailed in Appendix A5.

Table 2.10: Mouse MSD® U-PLEX pro and anti-inflammatory cytokines ELISA

Description	Biotinylated capture antibody	SULFO-TAG™ detection antibody
Pro-inflammatory	**Catalogue #**	
Interferon-γ (IFN-γ)	B22TT-2	D22TT-2
Interleukin - 1β (IL-1β)	B22TU-2	D22TU-2
Interleukin - 6 (IL-6)	B22TX-2	D22TX-2
Interleukin – 12p70 (IL-12p70)	B22UA-2	D22UA-2
Tumour necrosis factor-α (TNF- α)	B22UC-2	D22UC-2
Chemokine ligand 1 (CXCL1/ KC)	B22VW-2	D22VW-2
Anti-inflammatory		
Interleukin - 10 (IL-10)	B22TZ-2	D22TZ-2
Other components		
Calibrator 5	C0065-2	
U-PLEX Linker Set, 7-Assay (300µl)	Linker 1 E2226-2 Linker 2 E2227-2 Linker 3 E2228-2 Linker 4 E2229-2 Linker 8 E2233-2 Linker 9 E2234-2 Linker10 E2235-2	
U-PLEX 7-Assay, 96-well SECTOR plate	N05232A-1	
Read Buffer T (4x) with surfactant, 50ml	R92TC-3	
Stop Solution, 40ml	R50AO-1	
Diluent 41, 10ml	R50AH-1	
Diluent 45, 8ml	R50AI-3	

Kit Catalogue # : K15069L-1
Kit Lot # : 275783

2.10.3.2 Transforming growth factor-β1 (TGF-β1) cytokine ELISA

Mouse nasopharynx supernatants were assayed for transforming growth factor-β1 (TGF-β1) production (DY1679-05, R&D Systems, USA). In brief, the capture antibody was diluted to the working concentration in PBS without a carrier protein. Immediately, 100µl of the diluted capture antibody was coated into each well of a high binding 96-well flat-bottom microplate (Greiner Bio-One, GmBH, Germany),

sealed and incubated overnight at room temperature. Following incubation, the content was aspirated and washed three times with wash buffer (0.05% PBS Tween 20). After the last wash, any remaining wash buffer was removed by aspirating or by inverting the plate and blotting it against a clean paper towel. Next, the plate was blocked with 200µl of block buffer (reagent diluent containing BSA), sealed and incubated for 1 hour at room temperature. After incubation, the plate was aspirated/ washed as before.

The samples were thawed at room temperature and treated to activate latent TGF-β1 to immunoreactive TGF-β1. To 100µl of supernatant, 20µl of 1N HCl (R&D Systems, USA) was added, mixed well and incubated 10 minutes at room temperature. Then the acidified sample was neutralised by adding 1.2N NaOH/ 0.5M HEPES (R&D Systems, USA) and mixed well. Following this, 100µl of the activated nasopharynx supernatant and prepared standards in reagent diluent (see Appendix A6) were added into each well, sealed and incubated for two hours at room temperature, then aspirated/ washed as before. Then, 100µl of the detection antibody prepared in reagent diluent was added, sealed with a new adhesive strip and incubated for two hours at room temperature.

Following incubation, the plate was aspirated/ washed as before. A working dilution (40-fold dilution) of horseradish peroxidase (HRP) conjugated streptavidin in reagent diluent was added (100µl/ well), sealed and incubated in the dark for 20 minutes at room temperature, then aspirated/ washed as before. A 100µl volume of substrate solution (Colour reagent A and B) at a ratio of 1:1 was added and incubated in dark for 20 minutes. Finally, the reaction was stopped by adding 50µl of stop solution (2N sulphuric acid) before absorbance was measured at 450nm with wavelength correction using a BMG Omega plate reader. All details for each solution used are shown in Table 2.11.

Table 2.11: Antibodies and solutions for TGF-β1 ELISA

Reagent	Working Concentration/ dilution	Preparation
Mouse anti-TGF-β1 capture antibody	4.00 µg/ml	Reconstitute with 0.5ml of PBS
Biotinylated chicken anti-TGF-β1 detection antibody	75.0 ng/ml	Reconstitute with 1.0ml of RD
Recombinant Mouse TGF-β1 Standard	31.2-2000 pg/ml	Reconstitute with 0.5ml of RD
Streptavidin-HRP	40-fold dilution	Dilute with RD
RD (blocking buffer)	-	1% BSA in PBS
Colour reagent A (stabilised hydrogen peroxide) and Colour reagent B (stabilised tetramethylbenzidine)	1:1	-
Stop solution	2N sulphuric acid (H_2SO_4)	98.08 H_2SO_4 in 500ml water
Wash buffer	-	500µl Tween 20 in 1L PBS

RD : Reagent diluent

2.10.4 Immune cell population studies in nasopharynx and lung by flow cytometry

Nasopharynx and lung tissues were collected and processed as described in Section 2.10.2. For flow cytometry, all tissues were stored frozen at -80^{o}C and thawed before analysis. The staining and acquisition protocols applied in this section are similar to the CD206 staining on J774.2 cells in Section 2.7. The cell suspension was centrifuged at 300xg for 5 minutes at 4^{o}C, plated into a 96-well round-bottom plate and washed twice with Facs buffer. The supernatant was removed and the cell pellet was re-suspended in 1:200 of a purified anti-mouse CD16/CD32 antibody (TruStain fcX™ Clone 93, BioLegend, UK) and incubated for 30 minutes at room temperature as before.

Following this, cells were washed with Facs buffer and cell surface markers were labelled with antibodies or their respective isotype controls (listed in Table 2.12). The plate was incubated in the dark for 30 minutes at room temperature. After that, cells were washed twice and fixed in the dark for 30-45 minutes in a mixture of Fixation/ Permeabilisation Concentrate (Invitrogen™) and eBioscience™ Fixation/ Perm Diluent (ratio 1:3). Following fixation, cells were washed twice and re-suspended in 300µl of Facs buffer and transferred into a round-bottom polystyrene tube and stored at 4^{o}C until the assay was performed on the next day. The samples were acquired using a BD FACSCalibur™ flow cytometer (BD Biosciences) and data were analysed by FlowJo™10.5.3 software (TreeStar).

Table 2.12: Antibodies used for FACS analysis of different immune cell types

Target cell/ receptor	Antibodies/ Fluorochrome	Clone	Isotype control	Dilution
Monocytes/ Macrophages	CD45 FITC	30-F11		1/400
	F4/80 PB	BM8	Rat IgG2b, κ	1/300
	CD115 PerCP/ Cyanine 5.5	AFS98	Rat IgG2a, κ	1/400
Neutrophils	CD45 FITC	30-F11		1/400
	*Gr-1 PE Cyanine 7	RB6-8C5	Rat IgG2b, κ	1/600
	CD11b PE	M1/70	Rat IgG2b, κ	1/400
Mannose receptor	CD45 FITC	30-F11		1/400
	CD206 APC	C068C2	Rat IgG2a, κ	1/400
B cells	CD45 FITC	30-F11		1/400
	CD19 PB	6D5	Rat IgG2a, κ	1/300
T helper (Th) cells	CD45 FITC	30-F11		1/400
	CD3 APC	17A2	Rat IgG2b, κ	1/400
	CD4 PE	GK1.5	Rat IgG2b, κ	1/400
Natural killer (NK) cells	CD45 FITC	30-F11		1/400
	*NK1.1 PE Cyanine 7	PK136	Mouse IgG2a, κ	1/400
Mast cells/ Basophils/ Eosinophils	CD45 FITC	30-F11		1/400
	FcεRIα PerCP/ Cy 5.5	MAR-1	Armenian hamster IgG PerCP/ Cy5.5	1/400

FITC: Fluorescein Isothiocyanate; PB: Pacific Blue; PE: phycoerythrin; PerCP: peridinin chlorophyll-A protein; APC: allophycocyanin

All antibodies available from BioLegend, UK except for *Gr-1 and *NK1.1 available from eBioscience, UK.

2.11 Macrophage digital multiplexed gene expression analysis by NanoString nCounter system

Cultured macrophages derived from BALB/c mouse bone marrow (See Section 2.3.2) were treated with four different conditions (Table 2.13), lysed and hybridised and analysed for mRNA transcriptome using a Mouse Myeloid_v2 panel (NanoString® Technologies, Inc., USA) and quantified using the NanoString nCounter Digital Analyser.

Table 2.13: Experimental design for murine BMDMΦ gene expression analysis by NanoString nCounter

Group	Time point (hour)	
	4 hours (cell titration study)	6 hours (actual study)
	Cell concentration	
Control (PBS)	NP	30,000
D39	NP	30,000
FhES	NP	30,000
FhES + D39	15,000, 20,000, 25,000 and 30,000	30,000

NP : not performed

Differentiated murine macrophages were harvested on Day 7 by scraping and centrifuged at 300xg for 5 minutes to remove antibiotic. To determine optimum cell numbers per well for NanoString analysis, a preliminary cell titration was performed using four different cell concentrations, all stimulated with both FhES and D39.

In a 96-well flat-bottom plate, the four different concentrations of macrophages were plated in DMEM 10% FBS with no antibiotics, cultured overnight and the medium changed the next day. The standard inoculum dose of FhES (5µg/ml) and D39 ($1x10^5$ CFU) were then added (See Table 2.5) and the cells were incubated for four hours. From the preliminary mRNA results (without normalisation against the expression of the housekeeping genes), 30,000 macrophages/well was determined to be optimum and was used for the main experiment. Stimulants were added for 6 hours. For both multiplexed gene expression studies, extracellular D39

were not killed with Penicillin G, due to the short time scale for this experiment. Under the microscope, macrophages were observed, their cell morphology checked and any dead cultures were excluded. Three biological replicates per condition were selected for further analysis.

Following 6 hours incubation, the plate was centrifuged at 300xg for 5 minutes at 4^{o}C and the supernatant was carefully removed by aspiration. The supernatant was completely removed to prevent the remaining medium diluting the lysis buffer and resulting in incomplete cell lysis. The cell pellet in each well was disrupted by slow pipetting with 6µl of chaotrophic lysis buffer which consists of 1% β-mercaptoethanol (to improve RNase inactivation) in RNeasy Lysis Buffer @ QIAGEN Buffer RLT (QIAGEN, UK) (10µl of β-mercaptoethanol per 1ml Buffer RLT). The cell lysate was homogenised by vortexing for 1 minute and briefly centrifuged to recover all material to the bottom of the well before it was aliquoted into sterile tubes and stored at -80^{o}C.

Standard NanoString protocols were followed. Hybridisation reactions were performed at room temperature, in triplicate per condition, based on the 12 reactions per cartridge provided. Samples for each hybridisation were prepared by using no more than 1.5µl lysate added together with 3.5µl nuclease-free water to bring the final volume to 5µl. Reporter CodeSet and Capture ProbeSet (both Mouse Myeloid_v2) were thawed at room temperature, inverted several times and quickly centrifuged using microfuge. To create a Master Mix, 70µl of hybridisation buffer was added to the Reporter CodeSet tube, mixed by inversion and quickly centrifuged. Into each of the 12 strip tubes provided, 8µl of Master Mix was mixed together with 5µl of sample and 2µl of Capture ProbeSet to bring the final volume to 15µl. The tubes were capped, flicked with a finger to ensure complete mixing and finally briefly centrifuged before placed in a pre-heated Veriti™ 96-well thermal cycler at 65^{o}C for 20 hours (the cover temperature at 70^{o}C and sample temperature at 65^{o}C). Following hybridisation, samples were transferred and processed in the NanoString nCounter Prep Station following the manufacturer's protocol. In brief, the Prep Plate and cartridge were removed from the fridge and freezer, respectively, and left at room temperature for 20 minutes. Then, the Prep Plate was

centrifuged at 2000xg for 2 minutes. The lid of the Prep Plate was removed and together with the cartridge they were placed in the Prep Station and the run initiated. During the run, the excess probes were washed away and the target/ probe complexes were purified using magnetic beads. The purified target/ probe complexes were deposited in a cartridge, laid flat and immobilised for data collection. When the run completed, the cartridge was transferred to the NanoString nCounter Digital Analyser. The cartridge was scanned by the fluorescence imaging system and nucleic acids signals were digitally counted at the maximum sensitivity setting at 555 fields of variants (FOV). Data, captured in the Reporter Library File (RLF) were further extracted using nSolver 4.0 Analysis Software. Data were normalised using the housekeeping genes and normal data were log2-fold change transformed. Differential gene expression analysis, pathway analysis and heatmaps representing the probes expression across experimental groups were analysed, generated and clustered using nCounter Advanced Analysis (version 2.0.115), which makes use of the open source R statistical software. All kits and panels used in NanoString nCounter analysis are detailed in Table 2.14.

Table 2. 14: Kits and panels for NanoString nCounter analysis

Protocol	Kit/ Panel	Lot number
Master Mix preparation and hybridisation set up	nCounter XT CodeSet XT_PGX_MmV2_Myeloid: - Mouse Myeloid_v2 Reporter CodeSet - Mouse Myeloid_v2 Capture ProbeSet	 RC6794X1 CP6269X1
Prep Station and Digital count	Prep Plate	310119
	Cartridge #1 - cell titration study Cartridge #2 - actual study Cartridge #3 - actual study	31020839230 31020839247 31020839141

2.12 Statistical analysis

Data were statistically analysed using GraphPad Prism 8.0. Results are expressed as means ± standard error of the means (SEM). For *in vitro* and *ex vivo* culture (J774.2 and BMDMΦ) experiments, the levels shown are the mean of three tested cultures plus SEM. When multiple group comparisons were made, data were analysed with a one way Analysis of Variance (ANOVA) followed by a Tukey's or Dunnett's multiple comparison post-test. Bacterial loads determined in carriage density were analysed with a two way ANOVA followed by a Sidak's multiple comparisons test. The measurement of cytokines in the macrophage supernatant was performed for three wells per condition. Immune cell populations in the nasopharynx and lung were analysed using two-way ANOVA. In all tests, p-values <0.05 were deemed significant and ns denotes not significant. For gene expression studies, data were analysed for significant differences by two-tailed t-test on the log-transformed normalised data using nCounter Advanced Analysis.

Chapter 3

Modulation of macrophage phenotype following Fasciola hepatica and bacterial co-stimulation in the monocyte/macrophage cell line J774.2

CHAPTER 3

Modulation of macrophage phenotype following *Fasciola hepatica* and bacterial co-stimulation in the monocyte/ macrophage cell line J774.2

3.1 Introduction

Macrophages (MΦs) are innate immune cells characterised by phagocytic and high lysosomal activity and recognised for their role in development as well as in healthy and pathological states. MΦs commonly used as infection models include primary MΦs, such as human or animal monocyte-derived macrophages (MDMs), murine bone marrow-derived macrophages (BMDMs) or other *ex vivo* macrophages (e.g. alveolar, peritoneal MΦs), and cell lines, such as the human THP-1 or the murine J774 and RAW 264.7. Several macrophage models have been used to study the macrophage response to infections with *Fasciola hepatica* (Flynn *et al.*, 2007a; Haçariz *et al.*, 2011; LaCourse *et al.*, 2012; Donnelly *et al.*, 2005), *Mycobacterium bovis* (Talaue *et al.*, 2006; Trivedi *et al*., 2018), *F. hepatica-M. bovis* co-infection (Flynn *et al.*, 2007b; Garza-Cuartero *et al*., 2016), and *Streptococcus pneumoniae* (Braun *et al*., 1999; Harvey *et al.*, 2014; Preston *et al.*, 2019; Bewley *et al.*, 2014; Marriott *et al.*, 2006; Daigneault *et al.*, 2012). In this chapter, I have used the J774.2 cell line which is derived from monocyte/ macrophages of the BALB/c mouse.

F. hepatica infection drives Th2 and regulatory responses with suppression of Th-1 driven immune responses raised to bystander microbial infections (Brady *et al.*, 1999; O'Neill *et al.*, 2000). This is associated with induction of type 2, alternatively activated macrophages (M2/ AAMΦ). Injection of antioxidant thioredoxin peroxidase (TPx), a molecule that is actively secreted by *F. hepatica*, induced the recruitment of AAMΦ to the peritoneal cavity of BALB/c mice. Similarly, murine macrophage cell line RAW264.7 were also alternatively activated when induced with TPx, which resulted in the induction of arginase-1 (Arg1) and the secretion of high levels of IL-10 and prostaglandin E_2 (PGE_2) (Donnelly *et al*., 2005). AAMΦ were also observed by Flynn *et al*. (2007a) when ovine MOCL7 monocytes were

exposed to *F. hepatica* homogenate (LFH), excretory/ secretory (ES) products and recombinant peroxiredoxin (rPrx).

Several studies have reported calves co-infected with *F. hepatica* and *M. bovis* had altered immune responses compared to calves infected with *M. bovis* alone. It has been suggested that these results have implications for disease progression and diagnosis of bovine tuberculosis (BTB) (Flynn *et al.*, 2007b; Flynn *et al.*, 2009; Claridge e*t al.*, 2012; Garza-Cuartero *et al.*, 2016). *In vitro* stimulation of naïve blood-monocyte derived macrophages with *F. hepatica* excretory/ secretory (ES) and PPD-B (purified protein derivative B; derived from *M. bovis*) confirmed that ES products induced AAMΦ whilst PPD-B alone produced NO, indicative of classically activated macrophages (M1/ CAMΦ). Furthermore, the whole-blood lymphocytes from the co-infected calves that were re-stimulated with *M. bovis* antigen demonstrated altered expression of IL-4 and IFN-ɣ, where *F. hepatica* infection caused the antigen-specific IFN-ɣ response to shut down (Flynn *et al.*, 2007b).

Impairment of the protective Th1 immune response to bacteria by the development of Th2 responses driven by helminth infections have been reported for mice infected with *B. pertussis* and *F. hepatica* (O'Neill *et al*., 2000; O'Neill *et al*., 2001; Supali *et al*., 2010; Pathak *et al*., 2012). To the best of our knowledge, there are no published data so far on the impact of the *F. hepatica* mediated immunomodulation on the host's immune response to *S. pneumoniae* infection. This is an important knowledge gap, as *F. hepatica* infection of humans is increasingly common in parts of the world like Asia and Africa (Ashrafi *et al*., 2014; Mas-Coma *et al*., 2018) where pneumococcal disease is also prevalent (Hung *et al*., 2013; Kalata *et al*., 2019). Previous studies have demonstrated that *Taenia crassiceps* and *Heligmosomoides polygyrus* infected mice challenged with serotype 3 strain A66.1 pneumococcus had impaired responses to pneumococcal vaccine, whilst helminth-infected mice were also predisposed to pneumococcal pneumonia, following infection with serotype 2 strain D39 (Apiwattanakul *et al.* 2014a, b). The aim of this chapter is to define the polarisation of macrophages exposed to either *F. hepatica* antigens, *S. pneumoniae* or *M. bovis* and to investigate the effect of exposure to *F. hepatica* on the subsequent response to *S. pneumoniae* infection. *M. bovis* was included as an

additional comparator due to the well characterised effects of *F. hepatica-M. bovis* co-infection on macrophage phenotype.

3.2 Results

3.2.1 Determining the protein concentration and SDS-PAGE of *F. hepatica* products

Table 3.1 shows the protein concentrations for all three fluke antigen preparations quantified from the Bradford assay. Flukes were isolated from two batches of infected livers identified by subscripts$_1$ and $_2$. Batch 1 FhES$_1$, FhTEG$_1$ and FhSOM$_1$ were used for SDS-PAGE analysis and for optimising the NO and arginase assays.

Table 3. 1: Protein concentrations in fluke antigen preparations measured by Bradford assay

***F. hepatica* antigen**	**Protein concentration (µg/ml)**
FhES:	
• FhES$_1$	715.0
• FhES$_2$	1592.0
FhTEG:	
• FhTEG$_1$	2030.5
• FhTEG$_2$	8613.0
FhSOM:	
• FhSOM$_1$	9932.6

Initially, three different antigen concentrations were used in macrophage stimulation assays: 5, 10 and 20 µg/ml. J774.2 macrophages were exposed to fluke antigens and incubated at 37^{o}C 5%CO_2 for 24, 48 and 72 hours. Five µg/ml of both FhES and FhTEG ($_1$ and $_2$) gave the optimum results with a consistent and reproducible NO and arginase response (see Table 2.5). For all the subsequent assays, Batch 2 FhES$_2$ and FhTEG$_2$ were used and are referred to as FhES or FhTEG throughout this thesis. Neat and diluted fluke antigens were analysed by

SDS-PAGE. Neat $FhES_1$ products showed two prominent protein bands at approximately 24-26kDa; cathepsins CL1 and CL2 (Figure 3.1).

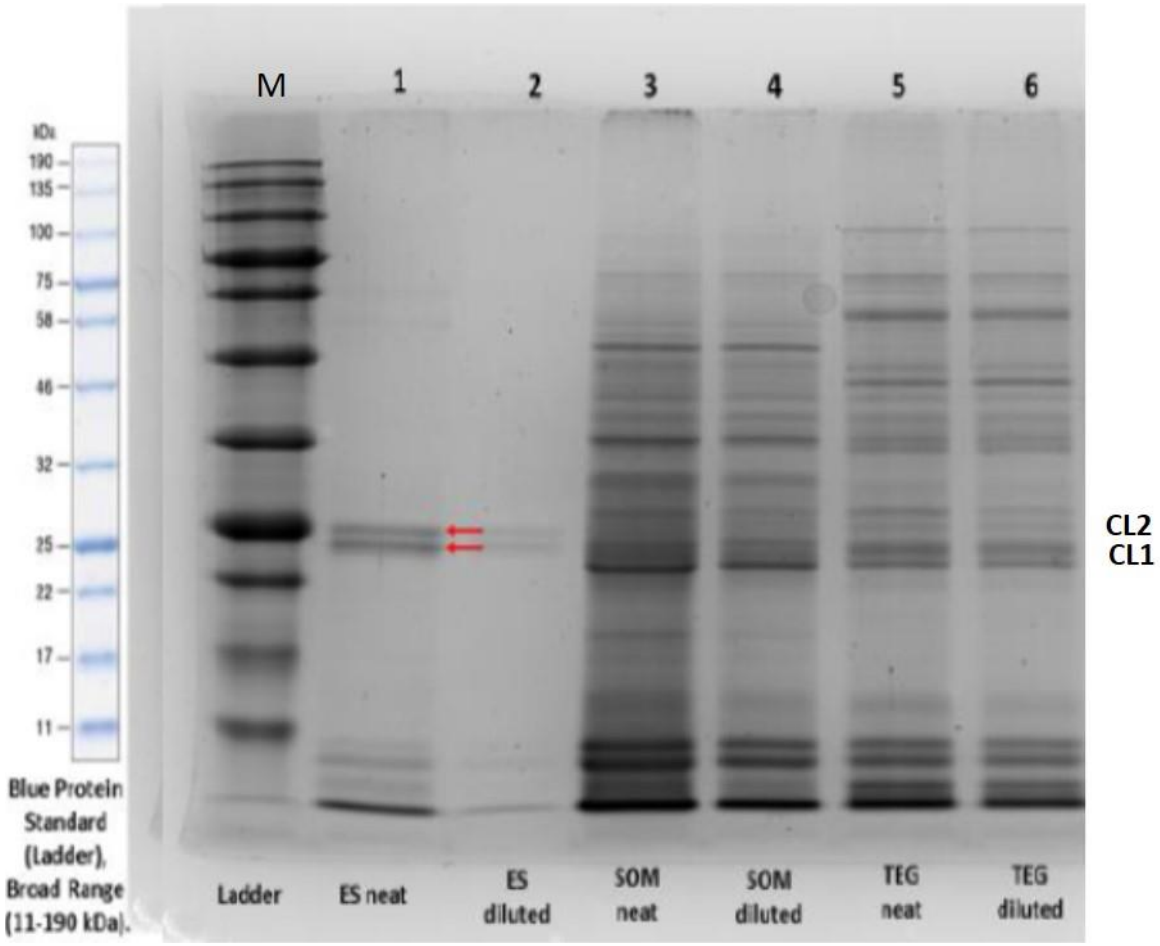

Figure 3.1: SDS-PAGE of *F. hepatica* products. The gel was run using batch 1 infected livers. Red arrows indicate position of major secreted cathepsin (C) L1 (approximately 24kDa) and CL2 (approximately 26kDa) in $FhES_1$ products (lane 1 and 2). Lane M, molecular size markers; lane 3 and 4: $FhSOM_1$; lane 5 and 6: $FhTEG_1$.

3.2.2 Fluke ES augments arginase production and suppresses NO production following MbSE treatment

To demonstrate that J774.2 NO and arginase responses were comparable to those identified in other macrophage models, I concomitantly stimulated the cells with 5µg/ml of LPS (M1 positive control) and 20ng/ml of IL-4 (M2 positive control). During the assay optimisation, I observed low levels of production of NO in the LPS stimulated cultures at 24 and 48 hours and maximum levels were detected at 72 hours whilst no difference in arginase production were observed at each time point. Figure 3.2 shows the results at 72 hours. The positive controls (LPS and IL4, respectively) produced NO and arginase that were significantly greater than the negative control (cells stimulated with PBS alone) after 72h (p<0.0001). No NO was detected in the PBS control *F. hepatica* ES or Teg antigens cultures. NO was significantly up-regulated in the MbSE culture compared to the PBS control (p<0.0001). NO was significantly down-modulated in both co-exposure cultures compared to MbSE alone (FhES + MbSE; p<0.0001; FhTEG + MbSE; p=0.0029; Figure 3.2a).

Fluke antigens alone failed to induce macrophage arginase production compared to PBS , but MbSE plus ES exposed cells showed significantly increased arginase production, whilst tegumental antigen co-exposed cultures produced significantly less arginase than macrophages exposed to *M. bovis* antigen alone (FhES + MbSE; p=0.0007; FhTEG + MbSE; p = 0.0049; Figure 3.2b).

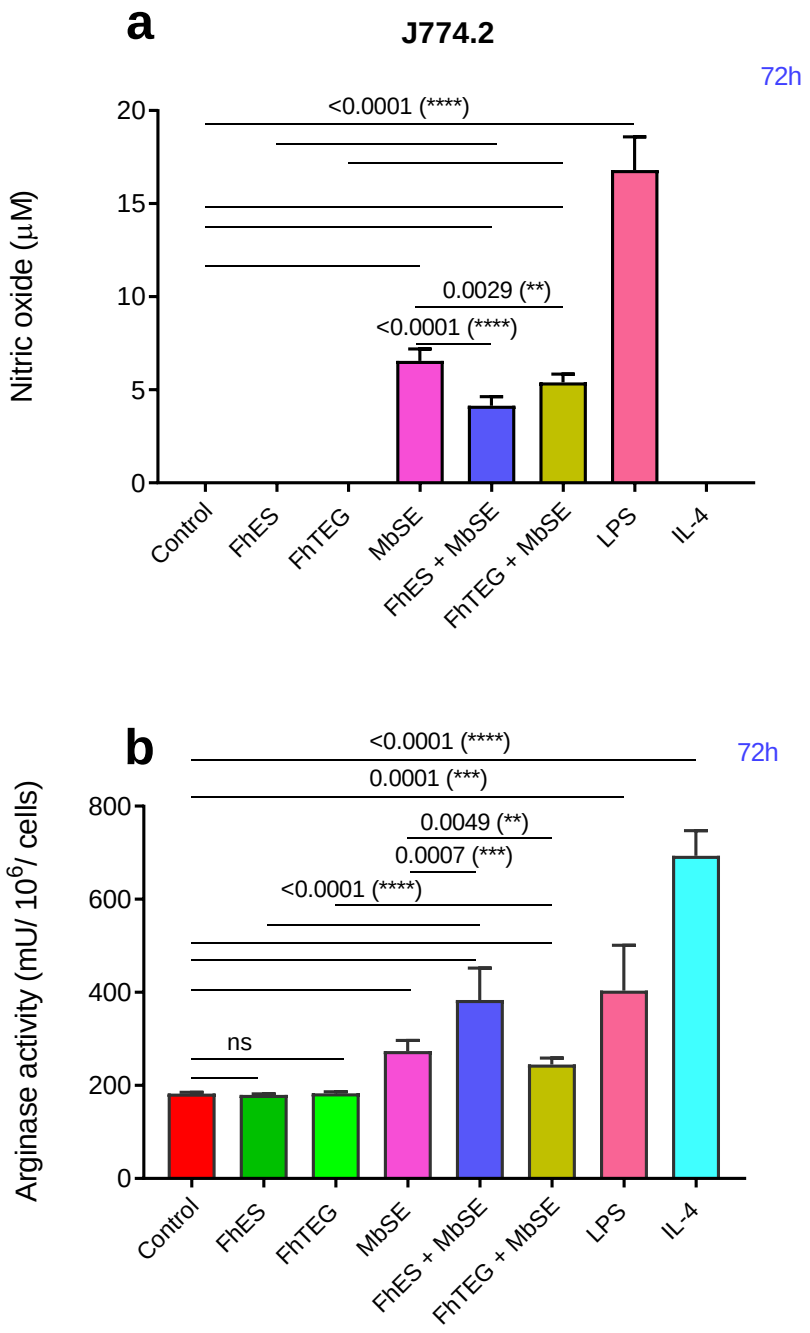

Figure 3.2: NO/ arginase production of J774.2 macrophages in fluke antigen and MbSE co-exposed cultures. Production of (a) nitric oxide (NO) and (b) arginase in J774.2 cells exposed to stimulants. Supernatants and lysates were analysed after 72h. The experiment was repeated three times and one representative experiment is shown. The levels shown are the mean of three tested cultures ± SEM. Asterisks indicate statistically significant differences analysed using one-way ANOVA followed by Tukey's multiple comparison post-test.

3.2.3 Exposure to live, heat- and detergent-inactivated Ply-deficient mutant D39Δply had no effect on NO production by J774.2 macrophages

This part of the study was first conducted in the Department of Infection Biology (iC2 Building), where live bacterial cultures were not permitted. Thus, heat-killed (HK) and sodium deoxycholate (SD) preparations of PLY-deficient mutant D39Δply were used. Ply-deficient bacteria were used to avoid artefactual outcomes resulting from Ply-induced cell death at high doses. J774.2 macrophage cells were exposed to killed bacteria for 24, 48 and 72 hours. I observed a lack of production of nitric oxide (NO) in supernatants from treated and control cultures for each time point (Figure 3.3). Experiments with live D39Δply were conducted in the Department of Clinical Infection, Microbiology and Immunology, where live cultures could be used. J774.2 cells were exposed to $1x10^7$ CFU/ ml and incubated as before. No NO production was detected (Figure 3.3). Macrophage cultures stimulated with 5µg/ml of LPS produced consistent levels of NO after 72h.

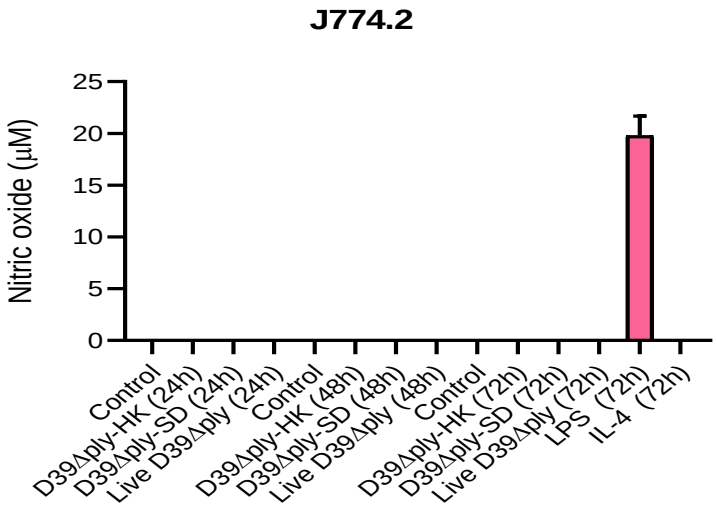

Figure 3.3: Lack of NO production by J774.2 macrophages following heat- and detergent- inactivated and live D39Δply pneumococcus exposure. Supernatants were analysed for NO production after 24, 48 and 72h. The experiment was repeated three times and one representative experiment is shown. The levels shown are the mean of three cultures ± SEM.

3.2.4 Effect of live wild-type (WT) D39 and co-exposure to FhES on the induction of NO

Since the Ply-deficient mutant D39Δply failed to elicit NO from J774.2 macrophages, I now tested wild-type (WT), virulent D39. Different bacteria inoculum concentrations (titration of 10^3-10^5 CFU/ml) were used to infect J774.2 cells and the supernatants were collected and analysed after 24, 48 and 72 hours. Low amounts of NO were produced from the cultures and the amount of NO detected was dose- and time-dependent (Figure 3.4a).

Since Ply is produced by the WT D39, I suspected that some macrophages were being killed by the toxin. The cultures were not treated with antibiotics meaning bacterial proliferation could potentially kill the macrophages. For the next experiment the bacterial inoculum was increased to $1x10^7$ CFU/ml and the macrophages were then co-exposed to 5µg/ml of FhES. Macrophage cultures that were infected with pneumococcus (WT D39 alone and co-exposed cultures) were treated with 1mg/ml of Penicillin G for one hour to kill extracellular bacteria before adding the FhES (see Section 2.4).

Figure 3.4b compares the levels of NO in WT D39 alone and when co-exposed to FhES. NO was significantly increased in co-exposed cultures compared to cells exposed to WT D39 alone at 24 (p<0.0001) and 48 hours (p<0.003). Low levels of NO were detected, which is consistent with the results from J774.2 cells treated with10^3-10^5 of CFU/ml of live WT D39 (Figure 3.4a). However, no significant differences in NO secretion were observed at 72 hours. Macrophage cultures stimulated with positive control of 5µg/ml LPS produced consistent levels of NO after 72h (15 µM).

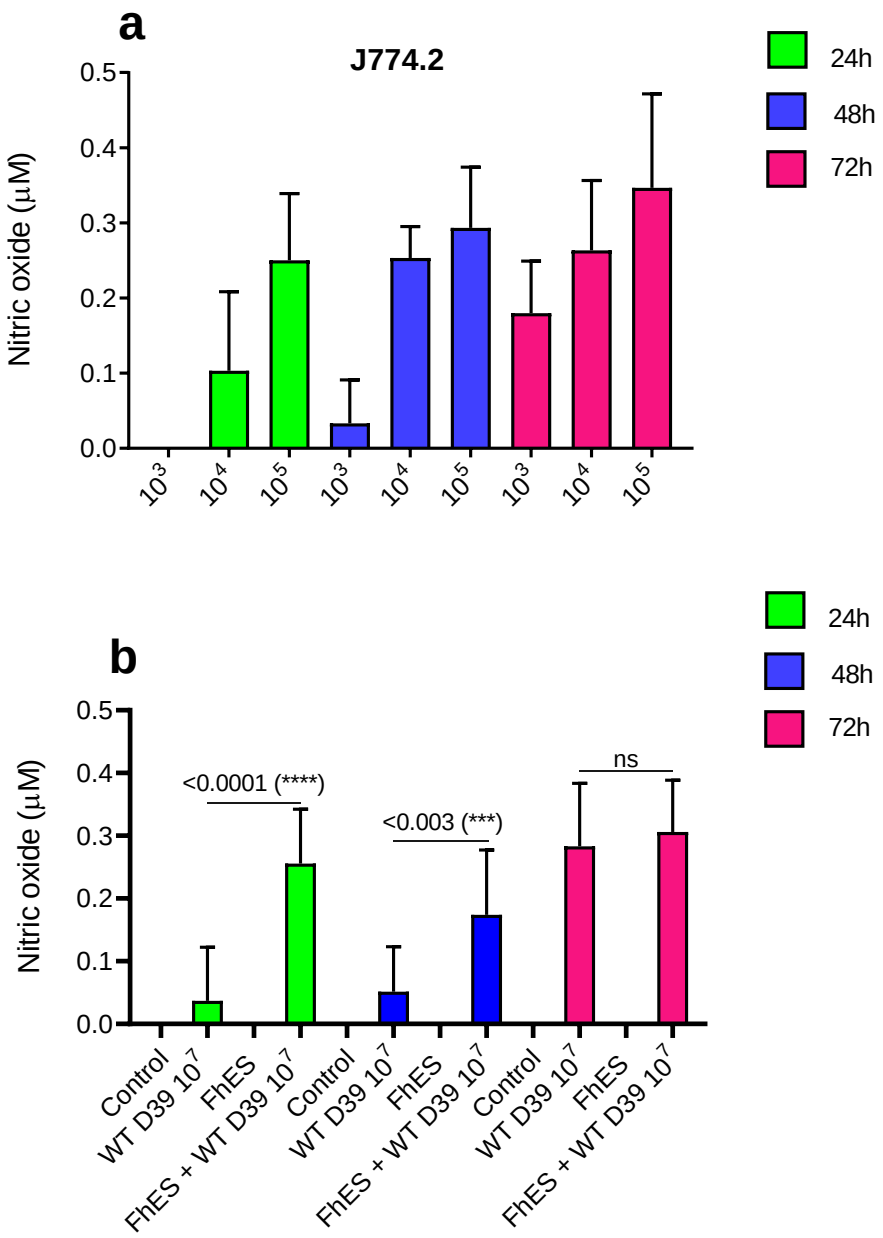

Figure 3.4: Trace amounts of NO produced by J774.2 cells infected with live wild-type D39 and co-exposed to FhES products. Supernatants from (a) 10^3-10^5 of WT D39 titration and (b) $1x10^7$ CFU/ml of WT D39 and co-exposed cultures were analysed for NO production after 24, 48 and 72h. The experiment was repeated three times and one representative experiment is shown. The levels shown are the mean of three tested cultures ± SEM. Asterisks indicate statistically significant differences analysed using one-way ANOVA followed by Tukey's multiple comparison post-test.

3.2.5 The co-exposure using FhES and culture supernatant of D39 (D39SN) promotes J774.2 macrophages to M1 type/ classical activation phenotype (CAMΦ)

I observed a lack of NO production from J774.2 macrophages following treatment with live, heat- and detergent-inactivated PLY-deficient mutant D39Δply *S. pneumoniae*. Low amounts of NO were detected when J774.2 macrophages were infected with live WT D39 at different concentrations of CFUs (10^3-10^5 CFU/ml), and that response was dose- and time-dependent. Our findings also demonstrate that FhES and WT D39 co-exposed macrophage cultures produced significantly higher NO levels than WT D39 alone at 24 and 48 hours when the bacteria concentration was increased to $1x10^7$ CFU/ml.

I continued the investigation on NO production in J774.2 macrophages following treatment with D39 culture supernatant (D39SN). A volume of 5µl of D39SN was added to each well of J774.2 macrophages and incubated for 24, 48 and 72h hours. Figure 3.5a compares the levels of NO produced by J774.2 macrophages in D39SN alone and when co-exposed to FhES. After 48 hours, no significant difference was observed with D39SN alone compared the PBS control but the NO levels were significantly increased from cells treated with D39SN alone after 72 hours (p<0.0001). NO levels from co-exposed macrophages were significantly up-regulated compared to D39SN alone at 48 and 72 hours (p<0.0001) suggesting the modulation to CAMΦ phenotype in FhES+D39SN treated cells. There were no significant differences observed in the arginase production for each time point (Figure 3.5b).

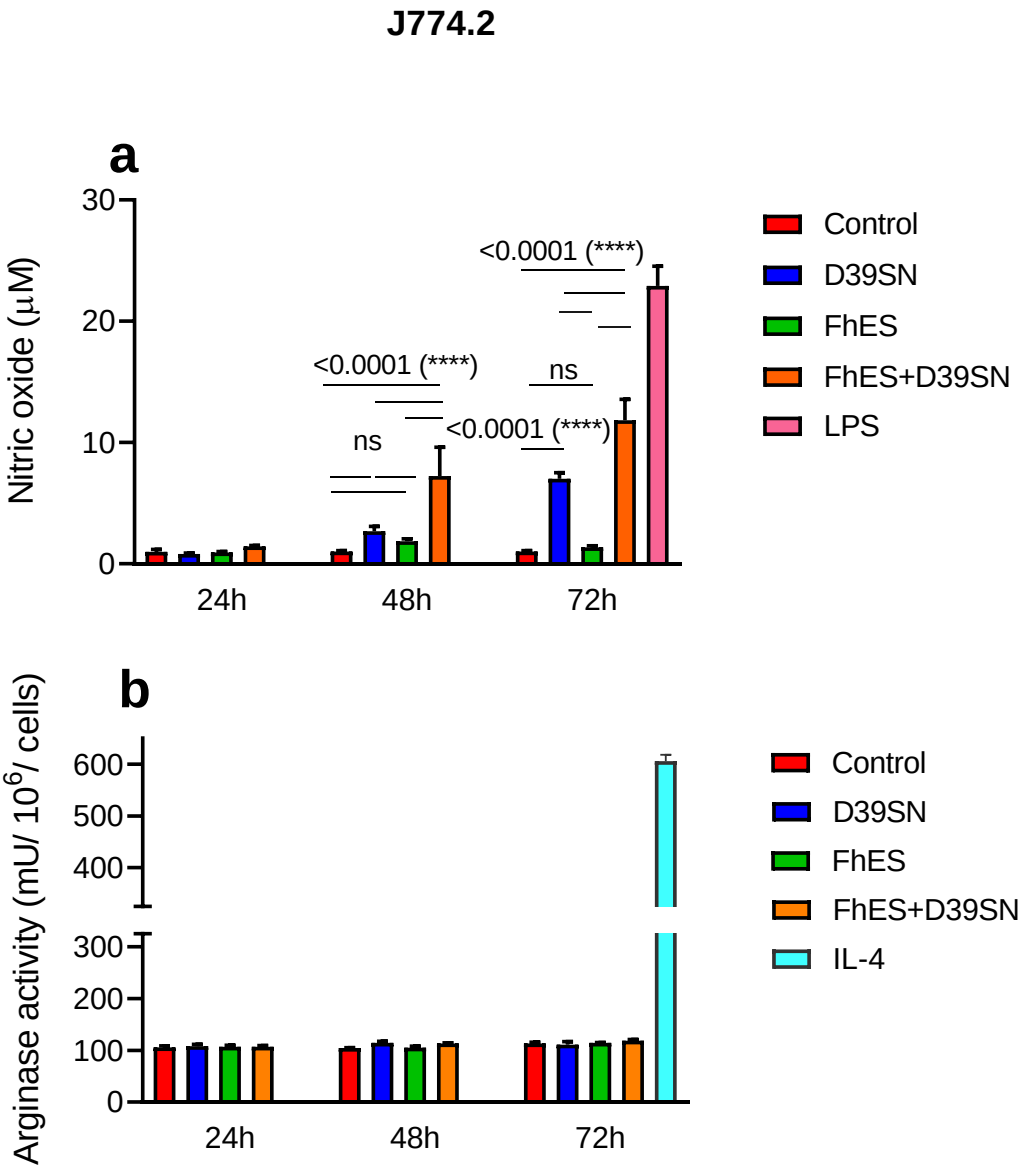

Figure 3.5: M1/ CAMΦ phenotype of J774.2 macrophages in FhES+D39SN co-exposed cultures. Supernatants and lysates were analysed for (a) NO and (b) arginase levels after 24, 48 and 72h. The experiment was repeated three times and one representative experiment is shown. The levels shown are the mean of three tested cultures ± SEM. Asterisks indicate statistically significant differences analysed using one-way ANOVA followed by Tukey's multiple comparison post-test.

3.2.6 ES from another helminth shows similar patterns of NO and arginase secretion

As FhES and FhTEG did not stimulate arginase production greater than levels observed in PBS stimulated J774.2 cells (Figure 3.2b), the ability of J774.2 cells to produce arginase was further investigated. Excretory-secretory products from the murine nematode parasite, *Trichuris muris* (TmES) at the concentration of 5µg/ml was used to treat J774.2 cells and the supernatants were assayed for NO after 72 hours. Figure 3.6a shows that PBS control and TmES treated cultures did not produce NO and the arginase levels were not significantly different from those observed in cultures stimulated with PBS alone (Figure 3.6b). These results are similar to those found following treatment with *F. hepatica* antigens (Figure 3.2).

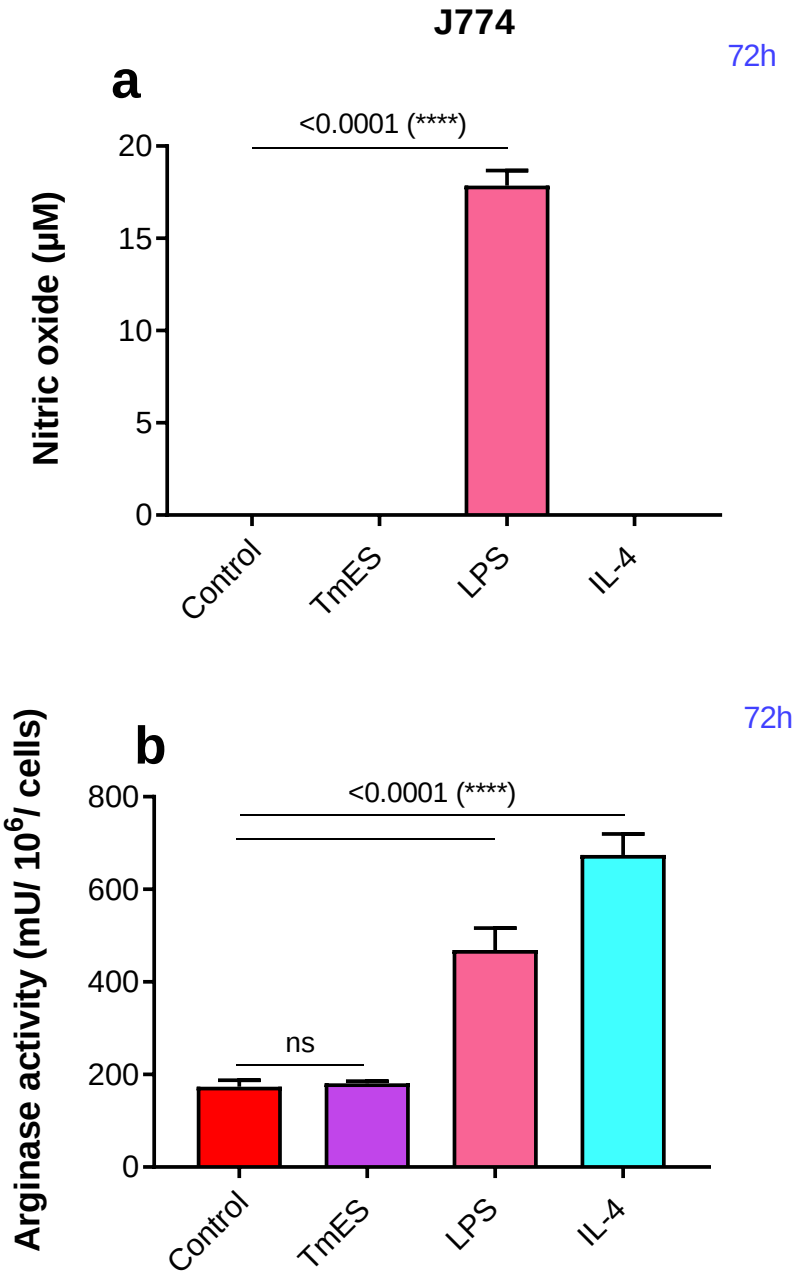

Figure 3.6: NO and arginase production following stimulation with *Trichuris muris* ES (TmES) after 72h. Levels of (a) NO and (b) arginase in TmES stimulated J774.2 macrophage cultures. The experiment was repeated two times and one representative experiment is shown. The levels shown are the mean of three cultures ± SEM. Asterisks indicate statistically significant differences analysed using one-way ANOVA followed by Dunnett's multiple comparison post-test.

3.2.7 Enhanced arginase production in IL-4 primed low passage number J774.2 cells, exposed to helminth antigens

To investigate whether cell priming could enhance arginase production, I incubated J774.2 macrophages with Th2 cytokine IL-4 (20ng/ml) before adding the *F. hepatica* antigens. For the first set of experiments, J774.2 cells at a high passage cell number (passage 28) were used and primed with IL-4 for 48 hours before being stimulated with different concentrations of FhES (5, 10 and 20µg/ml). Again, there were no significant differences in arginase secretion from primed and unprimed cells (Figure 3.7a)

The same experiment was repeated using a low passage cell number (passage 7) and both FhES and FhTEG were used. The levels of arginase were significantly higher in all IL-4 primed cells exposed to both *F. hepatica* antigens at 24 and 48 hours compared to unprimed cells ($p<0.0001$). Arginase levels were highest in cultures where J774.2 cells were primed for 48 hours and then treated with FhES or FhTEG ($p<0.0001$) (Figure 3.7b).

To confirm our findings on the priming effects of IL4 on J774.2 cells using TmES, I primed low passage cell number (passage 5) with the same concentration of IL-4 (20ng/ml). Five µg/ml of TmES was then used to treat primed and unprimed cells, and arginase levels were assayed after 72 hours. IL-4 primed cells exposed to TmES produced significantly higher arginase levels compared to unprimed cells and priming for 48 hours resulted in significantly higher arginase expression compared to 24 hours priming (Figure 3.8).

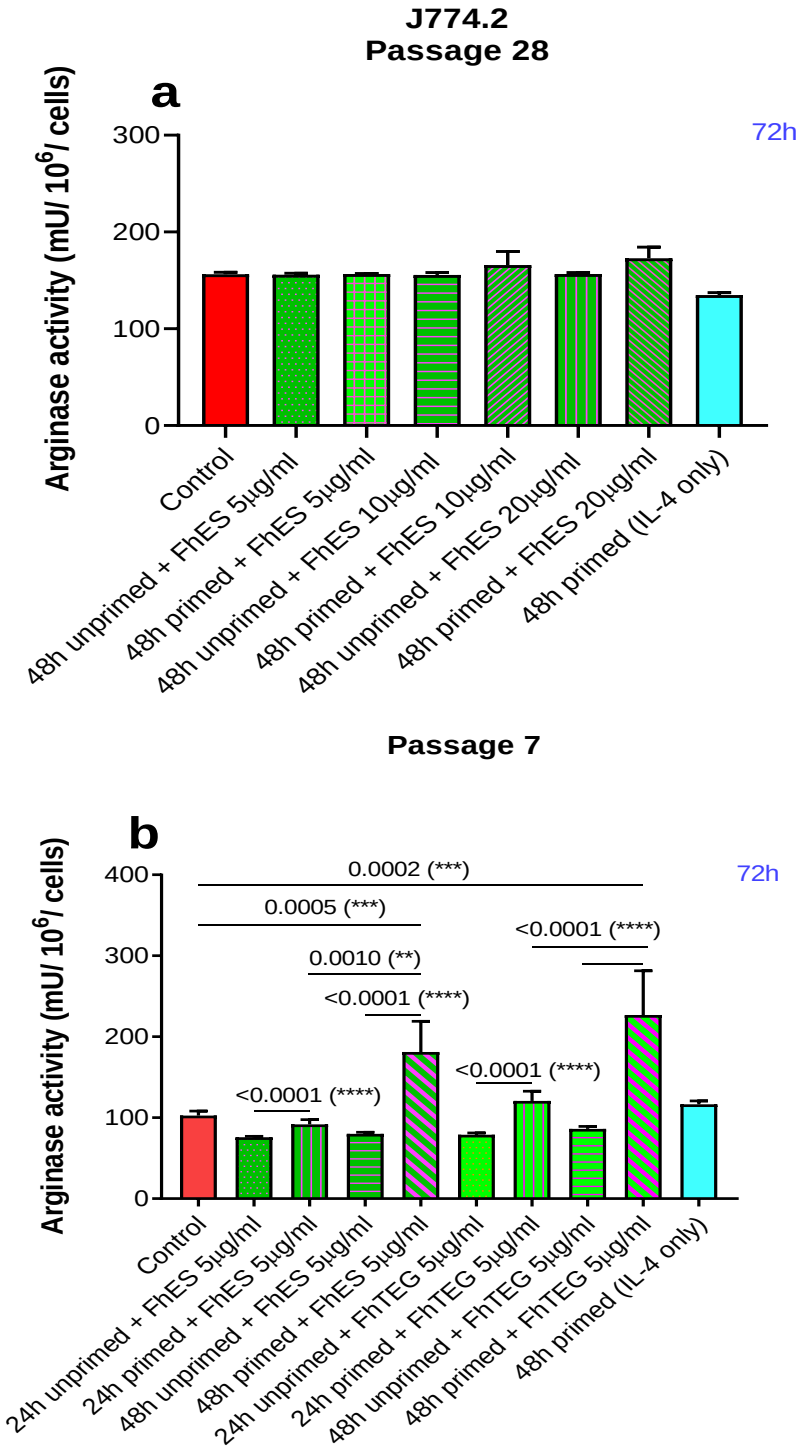

Figure 3.7: Arginase production in primed and unprimed of J774.2 cells exposed to *F. hepatica* antigens. Level of arginase in (a) high and (b) low passage number. Cell lysates were analysed after 72h and the levels shown are the mean of three tested cultures ± SEM. The experiment in (a) and (b) were repeated two and three times, respectively and one representative experiment is shown. Asterisks indicate statistically significant differences analysed using one-way ANOVA followed by Tukey's multiple comparison post-test.

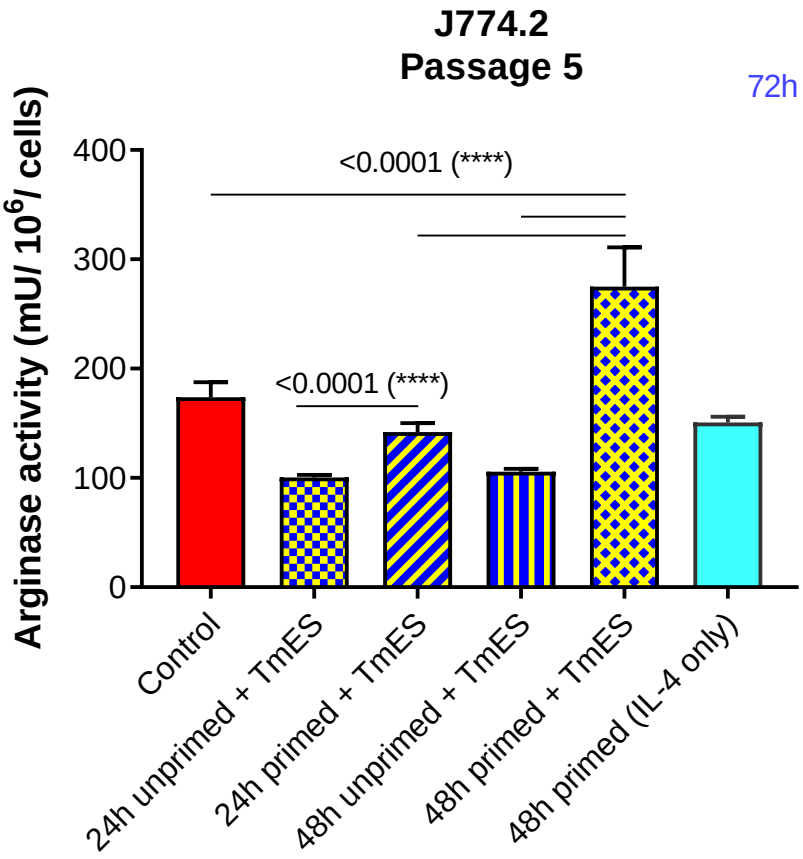

Figure 3.8: TmES exposed to primed and unprimed low passage number of J774.2 macrophages. Cell lysates were analysed for arginase levels after 72h. The experiment was repeated two times and one representative experiment is shown. The levels shown are the mean of three tested cultures ± SEM. Asterisks indicate statistically significant differences analysed using one-way ANOVA followed by Tukey's multiple comparison post-test.

3.2.8 IL-4 primed J774.2 cells do not express CD206

IL-4 priming on low passage J774.2 cells increased arginase levels due to helminth antigen induction. As macrophage mannose receptor (CD206) is an important marker for M2, alongside arginase, I asked if IL-4 primed J774.2 cells had increased CD206 expression. CD206 expression was evaluated by flow cytometry using passage 8 J774.2 cells primed with IL-4 (20ng/ml) for 24, 48 and 72 hours. Figure 3.9 shows that a low percentage of $CD206^+$ cells in IL-4 primed and unprimed J774.2 cells were detected. The highest percentage of $CD206^+$ cells (0.82%) was observed in primed cells at 48 hours. I concluded that priming J774.2 macrophages with IL-4 did not significantly increase CD206 expression compared to unprimed cells.

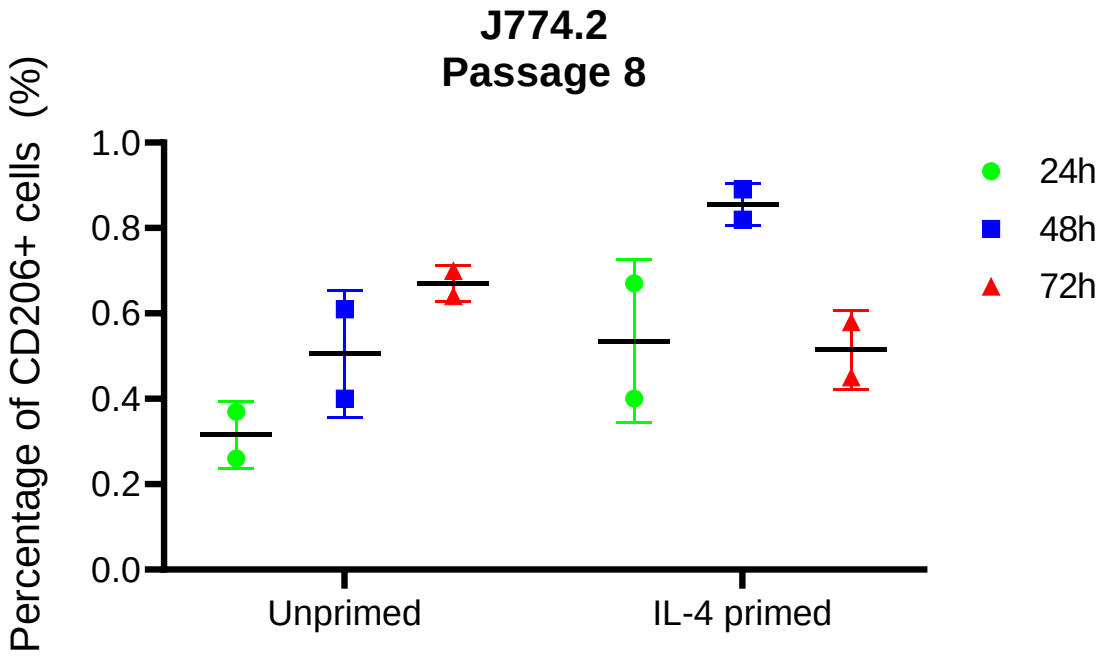

Figure 3.9: Low percentage of macrophage mannose receptor (CD206) expression in IL-4 primed J774.2 cells. Cells were primed with 20ng/ml of IL-4 for 24, 48 and 72 hours, stained with CD206 antibody and acquired using flow cytometry. An appropriate isotype control was included to define parameter gates. The levels shown are the mean of two experiments ± SEM.

3.2.9 Co-culture with FhES resulted in modest increases in IL-1β and CXCL1/KC compared to D39SN alone

Supernatants taken at 72hrs following exposure to either FhES, D39SN or both FhES and D39SN were analysed for presence of cytokines and chemokines. The NO expression from these cultures is shown in Figure 3.5a. Figure 3.10 shows the pro- and anti-inflammatory cytokines and chemokine assayed from three cultures for each protein using Multiplex MSD® U-PLEX. TNF-α production (Figure 3.10a) was significantly greater in D39SN alone (p=0.0066) and co-stimulated (FhES+D39SN; p=0.0013) cultures than PBS control. Production of TNF-α in D39SN cultures were significantly higher compared to FhES (p=0.0043). There was no significant difference between TNF-α levels in cultures from cells treated with D39SN alone and those treated with FhES and D39SN.

No IL-1β, IL-6, CXCL1/KC and IL-10 was detected in control cultures or those treated with FhES alone. These cytokines/ chemokines were all increased in J774.2 cells following exposure to D39SN. Co-culture with FHES induced a significant increase in IL-1β and CXCL1/KC expression. Anti-inflammatory IL-10 production was significantly higher in D39SN (p=0.0045) and FhES (p=0.0040) than in the unstimulated control. Co-exposed cultures produced significantly more IL-10 than control (p=0.0134) and FhES (p=0.0119) cultures. Only one FhES stimulated culture showed detectable IL-10.

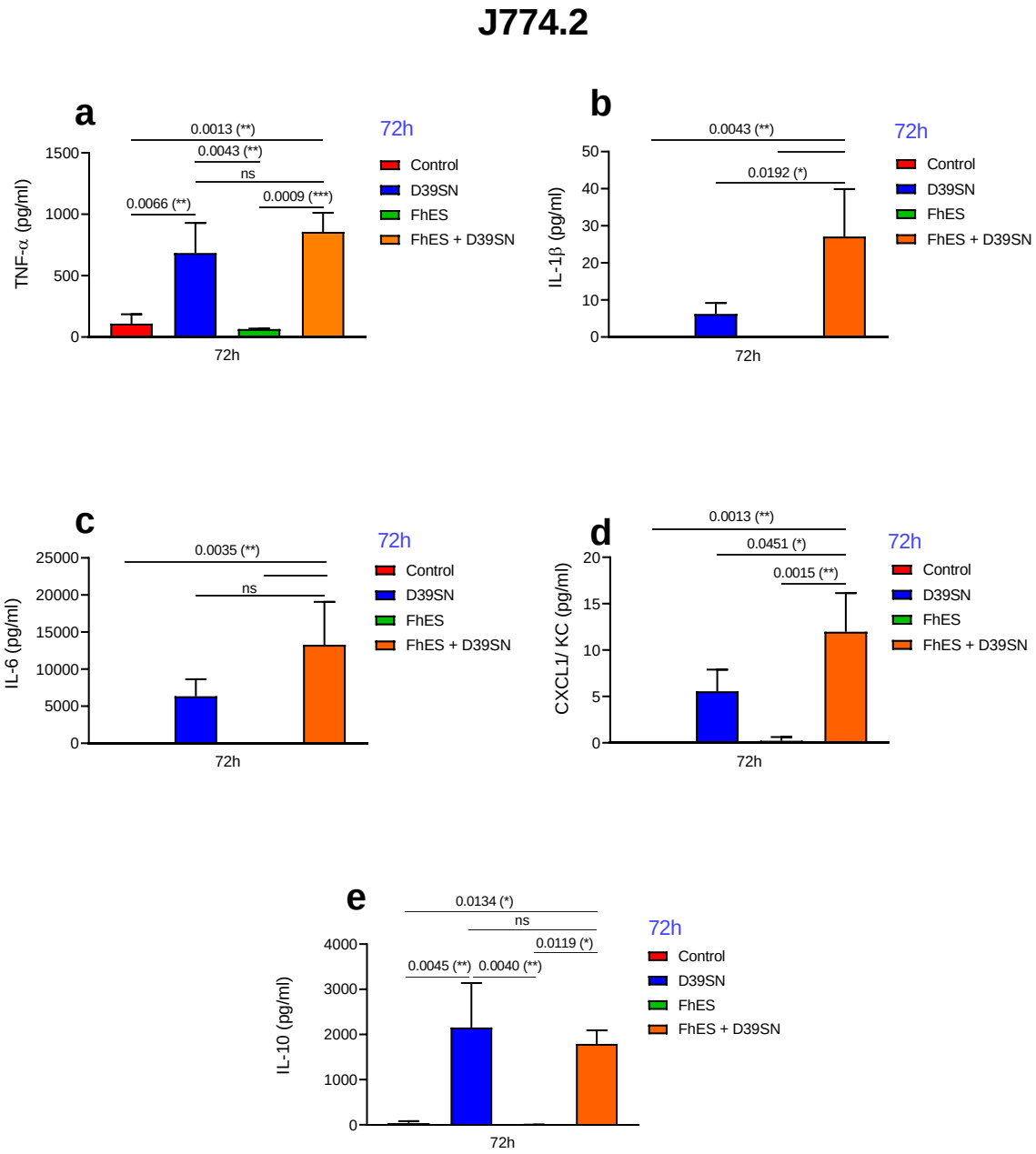

Figure 3.10: Cytokine and chemokine expression in J774.2 cells 72 hours after exposure to FhES *and* D39SN. Supernatants were analysed using Multiplex MSD® U-PLEX for (a-c) pro-inflammatory cytokines TNF-α, IL-1β and IL-6, (d) chemokine CXCL1/ KC and (e) anti-inflammatory IL-10. The levels shown are the mean of three assays ± SEM. Asterisks indicate statistically significant differences analysed using one-way ANOVA followed by Tukey's multiple comparison post-test.

Pro-inflammatory cytokines, IFN-ɣ and IL12p70 were measured in the same culture supernatants by ELISA using Multiplex MSD® U-PLEX. The results are shown in Table 3.2. No IFN-ɣ was detected in any cultures except one D39SN culture (Well 1; 0.60pg/ml). IL-12p70 production was detected in one well out of three in cells exposed to culture medium alone, FhES and one co-exposed well. No IL12p70 was detected in D39SN alone stimulated cultures.

Table 3. 2: Levels of IFN-ɣ and IL-12p70 in J774.2 macrophages in response to *F. hepatica* and D39SN

Group	Signalling protein (pg/ml)							
	IFN-ɣ				IL-12p70			
	Well 1	Well 2	Well 3	Mean	Well 1	Well 2	Well 3	Mean
Control	0.00	0.00	0.00	0.00	81.99	0.00	0.00	27.33±22.32
D39SN	0.60	0.00	0.00	0.2±0.16	0.00	0.00	0.00	0.00
FhES	0.00	0.00	0.00	0.00	34.25	0.00	0.00	11.42±9.32
FhES + D39SN	0.00	0.00	0.00	0.00	0.00	0.00	48.91	16.30±13.31

The values are mean ± SEM.

3.3 Discussion

This chapter investigated the modulation of the macrophage cell line J774.2 phenotype when exposed to *F. hepatica* antigens and two respiratory bacteria. *M. bovis* is an important zoonotic species known as the causative agent of bovine tuberculosis. Bovine tuberculosis accounts for a small proportion (0.5-7.2%) of all patients with a bacteriologically confirmed diagnosis of tuberculosis in industrialised countries, including the United Kingdom (de la Rua-Domenech, 2006), whilst *S. pneumoniae* (pneumococcus) is a major pathogen causing community-acquired infections such as otitis media, pneumonia, bacteraemia and meningitis.

Of all the fluke antigens prepared, I utilised the FhES (excretory/ secretory) products for all *in vitro*, *in vivo* and *ex vivo* infection/ co-exposure works reported in this thesis, whilst FhTEG was used only in MbSE co-exposure and IL-4 primed J774.2 macrophage experiments. In this chapter, I focussed on FhES antigens because of their highly immunogenic properties that have been reported to exert various immunomodulatory effects, such as alternative macrophage activation (Flynn *et al.*, 2007a; Flynn and Mulcahy, 2008a; Guasconi *et al.*, 2011; Guasconi *et al.*,2012; Guasconi *et al.*, 2015). Results showed that neither fluke antigen alone had an effect on arginase production in J774.2 cells, but that FhES augments arginase production and suppresses NO production following MbSE stimulation, as compared to FhTEG. During infection, these two major sources of antigens are in constant contact with immune cells and have been shown to elicit immune-modulatory effects (Hamilton *et al*., 2009; Vukman *et al.*, 2013a, b; Adams *et al*., 2014). SDS-PAGE analysis from $FhES_1$ demonstrated that cathepsin L1 and L2 were the major components of FhES, which is consistent with previous findings (O'Neill *et al*., 1998). Cathepsins are involved in several important functions, including tissue penetration, immune evasion and feeding (Dalton and Mulcahy, 2001). The immunomodulatory/ immunosuppressive effects of the secreted cathepsin L have been reported to block the development of protective Th1 responses in the host and help the progression of non-protective Th2 responses that favour parasite longevity (O'Neill *et al*., 2000; O'Neill *et al*., 2001). Cathepsin

L proteinase activity is expressed when the immature newly encysted juvenile (NEJ) migrates through the liver parenchyma and in adults that reside in the bile ducts (Carmona *et al.*,1993; Smith *et al.*, 1993). Cathepsin L3 and cathepsins B1, B2 and B3 have been recently isolated in both NEJ secretome and metacercariae somatic proteome that play important roles in the early stages of infection (Cancela *et al.*, 2008; Robinson *et al.*, 2009; Cancela *et al.*, 2010; Cwiklinski *et al.*, 2018).

The first experiments in this chapter sought to determine whether J774.2 macrophage phenotype was modulated following stimulation with either FhES alone, bacterial antigens alone or both FhES and bacterial antigens together. Nitric oxide (CAMΦ marker) in both FhES+ and FhTEG+MbSE co-exposed cultures was significantly down-modulated compared to MbSE alone suggesting that *F. hepatica* antigens prevented CAMΦ induction and modulated the phenotype towards AAMΦ phenotype. Significantly increased of arginase levels in FhES+MbSE co-exposed cultures further support the evidence of AAMΦ polarisation caused by *F. hepatica* in our study. These results are in agreement with Flynn *et al.* (2007b), where monocyte-derived macrophages from male Friesian calves co-infected with *F. hepatica* and *M. bovis* BCG (Bacillus Calmette Guerin) induced AAMΦ with lack of NO output. An increased arginase activity that correlated with the induction of Arg-1 gene expression was also observed in the lysates of RAW 264.7 macrophage cells treated with recombinant thioredoxin peroxidase (TPx), an antigen that is found in ES products. Similarly, it has been shown that helminth-induced AAMΦ have reduced IFN-ɣ and NO output (Donnelly *et al*., 2005). Stimulation of the ovine cell line MOCL7 *in vitro* with recombinant *F. hepatica* Prx, ES products and liver fluke homogenate (LFH) induced AAMΦ was marked by elevated arginase levels and minimal NO production. Chitinase-like proteins were also found in supernatants which is another marker of AAMΦ (Flynn *et al*., 2007a). Many helminth species have now been reported to modulate murine AAMΦ activity and function (Rolot and Dewals, 2018). Although I have shown that similar results were obtained with FhTEG+MbSE, I chose to focus on the immunomodulation effects of FhES in this thesis.

Macrophage J774 and RAW 264.7 cell lines have been used to study the effect of *F. hepatica* glutathione transferase (GST) family, Sigma class GST (highlighted as a vaccine candidate in parasitic flatworms) stimulation on the production of prostaglandin (PG) E2 and D2 (LaCourse *et al.*, 2012). To the best of our knowledge, there are no published data evaluating NO and arginase production by J774 (or J774.2) macrophage cells stimulated with *F. hepatica* antigens. The data presented here is the first investigation to assess the impact of *F. hepatica*-MbSE co-stimulation on J774.2 macrophages.

The second aim of this chapter was to investigate the responses of J774.2 macrophages following exposure to *F. hepatica* and pneumococcus. Pneumolysin (Ply) is a bacterial pore-forming toxin of the cholesterol-dependent cytolysin family and has been recognised as one of the key virulence factors of pneumococci. Braun *et al.* (1999) show that isogenic pneumolysin-negative mutant of *S. pneumoniae* (PLN-A) failed to elicit NO from murine RAW 264.7 macrophages compared to the wild-type (WT) strain D39. Building on these findings, I first investigated the effect of our laboratory serotype 2 pneumococcal strain, the Ply-deficient mutant D39Δply and WT D39 on NO production by J774.2 macrophages. The results showed that all types of mutant D39Δply preparations (live, heat- and detergent-inactivated) failed to induce NO secretion whilst low levels (<1.0 µM of nitrite) were detected in cultures following stimulation with WT D39. Braun *et al.* (1999) primed the RAW 264.7 cells with 0.3 to 0.5 ng of IFN-ɣ before infecting with live PLN-A, nevertheless, the NO was weak compared to the response induced by WT D39. I detected NO following stimulation of J774.2 cells following addition of WT D39 in the absence of pre-activation with IFN-ɣ, but levels may have been higher if I had used IFN-ɣ pre-treatment. Group B streptococci (GBS) was also found to induce NO production in J774A.1 clone in the presence of IFN-ɣ (Goodrum *et al*., 1994).

Next, I evaluated the NO and arginase production by J774.2 macrophages exposed to culture supernatant derived from serotype 2 pneumococci D39 (D39SN). NO production in FhES+D39SN co-exposed cultures was significantly up-regulated compared to D39SN alone, whilst arginase levels were not

significantly different in all treated cultures. These findings were unexpected, given that FhES is able to induce AAMΦ phenotype that is marked by the production of arginase and results in down-regulation of iNOS expression and NO synthesis in bovine monocyte-derived MΦ (Flynn *et al.*, 2007b), ovine MOCL7 monocytes (Flynn *et al.*, 2007a), murine RAW264.7 incubated with PI (fraction of *F. hepatica* excretory secretory products which contains TPx) and TPx (Donnelly *et al*., 2005) and, in the present study, when low passage number J774.2 macrophage cells were primed with IL-4 were exposed to FhES.

Since previous studies suggested that NO production was dependent on Ply (Braun *et al*., 1999; Bewley *et al*., 2014), our results may be explained if Ply was released via autolysis of pneumococci during D39SN preparation. Ply in the SN may have resulted in CAMΦ instead of AAMΦ phenotype. In support of this, others have detected Ply in bacterial supernatant through autolysis (Benton *et al*., 1997; Balachandran *et al.*, 2001; Martner *et al.*, 2008). Jusot *et al*. (2017) demonstrated that increased autolysis was associated with increased release of Ply into the culture medium.

Braun *et al.* (1999) showed that IFN-ɣ priming was essential to induce NO in WT D39 and that NO production was dependent on Ply. In contrast, our results using D39SN showed high levels of NO from J774.2 cells, even though the cells had not been pre-treated with IFN-ɣ. Whether Ply released via autolysis in the D39SN preparation is more potent, due to the concentrated D39SN samples prepared (supernatant was concentrated using Vivaspin concentrator), than the spontaneous autolysis of pneumococcus when reaching the stationary phase of growth (Martner *et al*., 2008, 2009) remains to be elucidated. It is likely that the amount of Ply present in these two different preparations of D39 could be different. Thus, future studies should consider investigating the amount of Ply produced in WT D39 and D39SN preparations, using ELISA.

I have previously shown that *F. hepatica* antigens alone failed to stimulate arginase levels greater than PBS stimulated J774.2 macrophage cells. To investigate this further, I used *T. muris* ES products (TmES) and after 72 hours of incubation,

supernatants and cell lysates were analysed for arginase and NO. The results obtained with TmES were very similar to those observed following stimulation with FhES. For both assays, the positive control, IL4 elicited high levels of arginase, indicating that the cells were functionally capable of secreting arginase. IL-4 induces macrophage arginase activity and results in polarisation to AAMΦ phenotype (Bronte *et al.*, 2003; Briken and Mosser, 2011; Hodgkinson *et al.*, 2017; Stempin *et al.*, 2010). IL4 was used to prime the J774.2 macrophage cells before adding the fluke and *T. muris* antigens. When re-stimulated with helminth antigens, only low passage cell numbers (between 3-10 passages) that were primed with IL-4 able to induce arginase production. In contrast high passage J774.2 cells (more than 10 passages), although primed with IL-4, did not secrete arginase levels greater than the unprimed cells or PBS controls. However, my results demonstrated that the positive control of IL-4 alone induced high arginase in J774.2 cells of high passage number, suggesting these cells lose responsiveness to helminth antigens rather than becoming functionally incapable of arginase production.

Cellular morphology is a simple and direct method to identify the health and condition of cells, and cell health begins to decline at higher passages (Kwist *et al*., 2016). Data from high passage cultures can produce variable data. Others have reported that the expression of genes encoding markers of uveal melanoma are severely reduced during cell passage from primary cell lines isolated from tumours (Mouriaux *et al*., 2016). In the investigation of the phenotypic and functional stability of RAW 264.7 macrophage cell line, Taciak *et al*. (2018) suggested that they should not be used after the passage 30 as it may influence the data reliability. In this study, I did not evaluate the J744.2 cell line for phenotype (expression of surface markers) or function (phagocytosis and NO production) between passages. However, from our experience, I recommend that future studies are restricted to using passage number 3-10 (low passage) to obtain consistent results. Cell line misidentification, genetic or phenotypic shift and *Mycoplasma* contamination are some of the problems which are frequently forgotten in research involving cell lines (Taciak *et al.*, 2018).

The third aim of this chapter was to investigate the ability of J774.2 macrophages to express CD206 in the presence of IL-4. CD206 or macrophage mannose receptor (MR) is a member of the C-type lectin family and is expressed on the surface of macrophages and immature dendritic cells (DCs) where it acts as pattern recognition receptor (PRR) (Paveley *et al*., 2011). IL-4 and IL-13 increase CD206 expression whilst IFN-ɣ and LPS decrease CD206 expression (Passos *et al*., 2017). CD206 is also a marker of AAMΦ, in addition to arginase. I investigated whether the J774.2 clone could express CD206 after stimulation with IL-4 at different time points but very low numbers of $CD206^+$ cells were observed. Others have shown that J774 cells express variable levels of CD206 (Fiani *et al*., 1998). Similarly J774 cells were reported to express low MR but levels could be induced with 5-azacytidine, and cells could be separated into different populations with a range of MR expression (Diment *et al*., 1987). High levels of MR were also displayed by the J774E clone that could be passaged whilst maintaining high MR expression (Stahl *et al*., 1980). The J774E clone was also reported by others to express high levels of MR (Fiani *et al*., 1998) and this clone has been used to study MR involvement during influenza virus invasion (Reading *et al*., 2000).

The J774.2 clone used in our studies clearly shows a different MR expression compared to the MR-positive murine J774E clone. Our results suggest that MR expression is absent in the J774.2 clone when stimulated with IL-4 where low $CD206^+$ cell expression was detected. Nevertheless, the J774.2 clone did express the macrophage activation phenotype-defining markers, NO and arginase, under various conditions. Although arginase and CD206 expression are both used as markers for AAMΦ, their pathways are not related during AAMΦ phenotype polarisation. To the best of our knowledge, there are no published data that describe the relationship between arginase induction and CD206 expression in the pathways that lead to AAMΦ in the context of specific immune responses.

The final aim of this chapter was to determine the effect of exposure of J774.2 cells to *F. hepatica* and pneumococcus antigens on cytokine secretion. The results presented here demonstrated that D39SN induced secretion of the pro-inflammatory cytokines, TNF-α, IL-1β and IL-6. The anti-inflammatory cytokine, IL-

10 was also detected, together with the chemokine CXCL1/ KC. Co-culture with D39SN and FhES had no effect on TNF- α, IL-6 or IL-10 secretion whereas small, but significant increases in IL-1β and CXCL1 were detected. IFN-ɣ and IL-12p70 were not detected either with D39SN alone or in D39SN plus FhES co-cultures.

It is known that CAMΦ macrophages are induced by either LPS or IFN-ɣ (Orecchioni *et al*., 2019). It has been reported that macrophages respond to IFN-ɣ in the surrounding milieu and are also potent IFN-ɣ-producing cells, via an autocrine pathway (Munder *et al*.,1998). In an infected host, when bacteria are phagocytosed, macrophage activity is increased by the secretion of cytokines by Th1 cells and NK cells, with IFN-ɣ being the most potent macrophage activator (Duque and Descoteaux, 2014).

Th1 cells drive CAMΦ polarisation not only via IFN-ɣ (Mège *et al*., 2011) but also IL-12, where the latter synergises with TNF and other pro-inflammatory cytokines in stimulating IFN-ɣ production (Orecchioni *et al*., 2019). IL-12 is a pro-inflammatory cytokine produced mainly by professional antigen-presenting cells (APCs), including DCs and monocytes/ macrophages (Trinchieri, 2003). Functionally, IL-12 activates NK cells and induces the differentiation of naïve CD4+ T lymphocytes to become IFN-ɣ producing Th1 effectors in cell-mediated immune responses to intracellular pathogens (Ma *et al*., 2015), where IFN-ɣ acts on APCs to augment IL-12 secretion in a positive feedback loop (Grohmann *et al*., 2001). During infection and tissue stress, activated mononuclear phagocytes (monocytes, macrophages, DCs) release 1L-12 which in turn activates Th1 cells to secrete IFN-ɣ that stimulates macrophages to activate antimicrobial effects (Hume, 2006; Gee *et al*., 2009; Murray and Wynn, 2011b). In the present study, J774.2 cells were cultured in the absence of other immune cell types, which may explain lack of IFN-ɣ and IL-12p70 levels in D39SN. Since IL-12 activates the IFN-ɣ secretion by Th1 cells (Yun *et al*., 2002) and their interrelationship is particularly complex where IFN-ɣ stimulation of macrophages is also needed for the production of bioactive IL-12 (de Groen *et al*., 2015), future studies should consider appropriate stimulation (e.g. IL-12) on J774.2 cells for IFN-ɣ induction or *vice versa* depending on the cytokine special interest to be studied.

Few studies have investigated TNF-α induction in J774 macrophage cells in the context of *S. pneumoniae* infection, although studies have been performed with other bacterial species. TNF-α was released from J774 macrophages following antibiotic-mediated killing of *S. pneumoniae* type 3 (A66.1) (Karlström *et al*., 2009). Although Ply is highly inflammatory, J774A.1 macrophages exposed to wildtype TIGR4 (*S. pneumoniae* serotype 4), growing as a biofilm, produced less TNF-α and CXCL2 than wildtype planktonic TIGR4 (Shenoy *et al.*, 2017). Inflammatory cytokines were secreted by various clones of J774 macrophages when stimulated with different types of bacteria. TNF-α, IL-6, IL-10 and IL-12 were released by J774.1 cells after exposure to strains of Lactobacilli (Morita *et al*., 2002). Culture supernatants of J774 macrophages infected with the human fungal pathogen, *Candida albicans* were observed to induce TNF-α and IL-10 (Sarazin *et al*., 2010). Jones *et al.*, 2005, reported the ability of J774.2 macrophages to induce NO and pro-inflammatory cytokines such as TNF-α, IL-6 and IL-1β when stimulated with *Staphylococcus epidermidis* products. It shows that bacterial products, including those of *S. pneumoniae*, can induce pro-inflammatory and anti-inflammatory/ regulatory cytokines, but, in this study, co-culture with FhES had no impact on the production of those cytokines other than those observed with CXCL1/ KC and IL-1β production. The elevated production of the CAMΦ-associated cytokines are consistent with the previous observation where D39SN up-regulates NO and co-culture with FhES increases the amount of NO produced.

I demonstrated a significant increase in NO in FhES+D39SN co-cultures, suggesting the modulation of CAMΦ phenotype, evidence supported by the detection of TNF-α, IL-6 and IL-1β. It is possible that Ply, present in the D39SN as the result of autolysis, is responsible for inducing those pro-inflammatory molecules. Our results are in agreement with previous studies where only bacteria expressing cytolytic Ply were capable of triggering IL-1β release from human macrophage-like cells (THP-1) (Harvey *et al*., 2014). It has been suggested that pneumolysin induces inflammation via the stimulation of TNF-α and IL-1β in human peripheral blood monocytes and a human monocyte cell line U937 (Houldsworth *et al*., 1994) and induced NO, IL-6 and cyclooxygenase 2 production from peritoneal macrophages (Braun *et al.*, 1999). Others have reported that pro-inflammatory

cytokines including IL-6, IL-12, IL-17 and IL-18 are important mediators in the innate response to pneumococci (Paterson and Orihuela, 2010) and their concentrations in serum are usually higher in pneumococcal pneumonia than in non-pneumococcal lung infection (Endeman *et al*., 2011). The release of Ply by autolysis does not involve any secretion signal (Canvin *et al*., 1995). This could further explain the limited induction of IL-1β, but not TNF-α and IL-6, production in the present study, if Ply is not actively secreted into D39SN and rates of autolysis were low. In the context of pneumococcal interaction with macrophages, resident alveolar macrophages (AMΦ) are the first cells that are likely to combat pneumococci in the early stages of lung infection and IL-6, IL-8 and TNF-α are known to be released by AMΦ in lung tissue (Hirst *et al*., 2004).

During infectious insults, chemokines (chemoattractant cytokines) are released by various cells, including macrophages and DCs, which in turn recruit effector cells to the infection site. I observed a significant increase in the neutrophil chemoattractant CXCL1/ KC (keratinocyte-derived chemokine; KC) in response to FhES + D39SN co-culture, compared to D39SN alone. This finding is contrary to previous studies by Su *et al*. (2014) which have demonstrated the down-regulation of CXCL1/ KC and another chemokine sensed by neutrophils, CXCL2/ MIP-2 (macrophage inflammatory protein-2) in *H. polygyrus* and *Salmonella typhimurium* co-infected mice. Gondorf *et al.* (2015) also reported significantly reduced TNF-α, IL-6, IL-1β, MPI-2β, CXCL1/ KC and CXCL2/ MIP-2 in mice co-infected with *Litomosoides sigmodontis* and *Escherichia coli*. *F. hepatica* tegument antigen-stimulated DCs were reported to induce CXCL2/ MIP-2 (Vukman *et al*., 2013c). Down-regulation of CXCL2 genes were observed in the comparison between bovine monocyte/ macrophage cell line (BOMA) stimulated with two *F. hepatica* strains (wild isolate; Fh-WildES and a laboratory isolate Weybridge; Fh-WeyES) (Bąska *et al*., 2019).

In pneumococcal infection, CXCL1 regulates neutrophil homeostasis after pulmonary bacterial pneumonia-induced sepsis, resulting in improved host survival (Paudel *et al*., 2019). Human monocyte-derived DCs stimulated with concentrated culture supernatant derived from D39, induced CXCL8 (IL-8), CCL2 and CCL5

(Domon *et al*., 2016). J774.1 macrophages do not produce CXCL1 in response to either biofilm or planktonic TIGR4 pneumococcus that are also marked by low TNF-α levels (Shenoy *et al.*, 2017). My findings show that D39SN elicited NO production that stimulates pro-inflammatory responses in the form of CXCL1/ KC, TNF-α and IL-1β production. Although the above-mentioned studies reported the suppression of CXCL1/ KC and IL-1β (Su *et al.*, 2014; Gondorf *et al.*, 2015) in the context of helminth-bacterial co-infection, co-culture with FhES induced modest changes in J774.2 macrophages in the present study. Further work should be undertaken to look whether concurrent *F. hepatica* product exposure may augment expression of IL-1β and those two major neutrophil chemoattractants.

Produced by innate immune cells, including macrophages, IL-1β is a potent pro-inflammatory cytokine inducing inflammatory responses in all tissues and organs (Piccioli and Rubartelli, 2013). IL-1β is also crucial to host-defence responses to injury and is required for protective immunity against *S. pneumoniae* (Kafka *et al.*, 2008; Lemon *et al*., 2015; LaRock and Nizet, 2015). Furthermore, the NLRP3 inflammasome, an essential mediator of host immune responses, via the activation of caspase-1, is required for Ply- and live *S. pneumoniae*-mediated enhancement of IL-1β and IL-18 that also leads to protective immunity against *S. pneumoniae* (McNeela *et al*., 2010; Fang *et al*., 2011). Increased levels of IL-1β in FhES+ D39SN co-cultures could be relevant to disease outcomes during pneumococcal-*F. hepatica* interaction, where increased IL-1β production may have the potential to aggravate tissue-damaging inflammatory responses or might providing enhanced protective immunity against *S. pneumoniae* in the co-infected hosts.

I observed high levels of IL-10 in the D39SN treated cultures and co-culture with FhES had no impact on IL-10 secretion. IL-10 is a regulatory cytokine that also has anti-inflammatory properties. Elevated levels of IL-10 in the nasopharynx homogenates of low- and high-density WT and pneumolysin-deficient (PLN-A) D39 colonised mice were reported by Neill *et al*., (2014). Furthermore, elevated levels of IL-10 were shown in the same study in human nasal washes from carriage-positive individuals after challenge with serotype 6B pneumococci. Enhanced production of IL-10 as well as several other cytokines (TNF-α, IL-6, IL-

12 and IL-23) by splenocytes, indicate that Ply can promote secretion of both pro- and anti-inflammatory cytokines (McNeela *et al*., 2010). IL-10 is produced by various types of cells, including monocytes, macrophages, Tregs, Th2 and other $CD4^+$ T cells (Couper *et al*., 2008; Mosser and Zhang, 2008; Kessler *et al*., 2017).

Surprisingly, IL-10 production was not detected following exposure to FhES. The finding is contrary to previous studies, where peritoneal macrophages from naïve mice produced high levels of IL-10 after stimulation with *F. hepatica* ES products (Guasconi *et al*., 2011) and infection of mice with *F. hepatica* resulted in both macrophages and DCs expressing high levels of IL-10 (Walsh *et al*., 2009). High IL-10 levels were reported in *in vitro* cultured peripheral blood mononuclear cells (PBMC) from calves chronically infected with *F. hepatica* (Flynn and Mulcahy, 2008b) and bovine monocyte-derived macrophages (MDM) stimulated with *F. hepatica* ES produced high levels of IL-10 (Flynn and Mulcahy, 2008a). RAW 264.7 macrophages stimulated with recombinant TPx showed evidence of polarisation to AAMΦ, characterised by high levels of IL-10 (Donnelly *et al.*, 2005) and recruitment of IL-10 expressing macrophages in both the peritoneal cavity and spleen were observed in mice infected with *F. hepatica* (Rodríguez *et al*., 2015). FhES at a concentration of 20µg/ml can directly induce Arg1 and IL-10 in RAW 264.7 macrophage population (Adams *et al*., 2014).

Our results, including those in the following chapters, suggest that different macrophage cell types, cell lines or *ex vivo* isolated primary cells, have different IL-10 responses in the presence of FhES products and the concentration of ES may also play a role in IL-10 induction. In the present study, I stimulated murine J774.2 macrophage cell line with 5 µg/ml FhES based on the optimal NO and arginase production in our titration studies. The same supernatants were used to assay IL-10 production. The lower concentration of ES used here could explain the lack of IL-10 production in FhES stimulated cultures. Bąska *et al*., 2017 observed differences in IL-10 levels in an LPS-activated bovine monocyte/ macrophage cell line using two different *F. hepatica* isolates (Fh-WildES and Fh-WeyES). Both FhWildES and FhWeyES dampened the release of IL-10 by bovine macrophages,

which indicated that various isolates can have different immunomodulatory abilities (Bąska *et al*., 2019).

It is well documented that co-infection with helminths suppresses immune responses to a wide range of bystander pathogens/ antigens and atopic, autoimmune and metabolic disorders (Brady *et al*., 1999; Vukman *et al*., 2013b; Maizels, 2016; Maizels and McSorley, 2016; Lucena *et al*., 2017; Gazzinelli-Guimaraes and Nutman, 2018). In the present study, I have shown CAMΦ phenotype was induced following FhES + D39SN co-culture. Previous studies have reported that co-infection with the Th2 inducing enteric nematode *H. polygyrus* in mice previously infected with Th1 inducing parasite, *Toxoplasma gondii* displayed polarisation toward a Th1 immune response with a lack of eosinophilia and reduced expression of Th2 effector molecule RELM-β (resistin-like molecule-β) in intestinal tissue (Ahmed *et al*., 2017). Miller *et al*. (2009) found that *T. gondii* was capable of suppressing the responses to *F. hepatica* infection, characterised by the suppression of the AAMΦ recruitment normally associated with helminth infection and the inability of splenocytes from *Toxoplasma-Fasciola* co-infected mice to produce Th2 cytokines. In addition, the expression of iNOS was observed from co-infected mice and from those infected with *T. gondii* alone and this pattern was observed whether *F. hepatica* was the first infecting organism or the second. In the present study, I observed AAMΦ phenotype in *F. hepatica-M. bovis* co-cultures and CAMΦ phenotype in FhES+ D39SN co-cultures, where I stimulated J774.2 cells with all the antigens simultaneously. The induction of CAMΦ phenotype and AAMΦ phenotype in co-exposure appears to depend on the specific pathogen's potency for regulating the immune response.

3.4 Conclusion

For this chapter of work, experiments were designed to study the modulation of J774.2 macrophages when co-cultured with *F. hepatica* and bacterial antigens. The results showed that J774.2 cells have the capacity to develop AAMΦ when co-exposed to *F. hepatica* antigens (FhES and FhTEG) with bacterial antigen MbSE but not fluke antigens alone. Secondly, the results demonstrated that J774.2 cells developed a CAMΦ phenotype when exposed to D39SN, which was maintained even in the presence of *F. hepatica* (FhES). It is possible that Ply, released into the culture medium during the autolysis of D39 cells, is responsible for maintaining the CAMΦ phenotype. The results are supported by detection of pro-inflammatory cytokines, released by J774.2 cells when cultured with D39SN with or without FhES, whilst the regulatory cytokine, IL-10 was down-modulated. I also showed that, on repeated passage, J774.2 macrophages lose the capacity to secrete arginase in response to fluke antigens. Finally, low CD206 expression by J774.2 was also observed, even following priming with IL4.

Whilst J744.2, an immortalised murine macrophage cell line, was a useful model of M1/M2 polarisation, because of its lack of ability to express a true M2 phenotype, in Chapter 4 I investigate if *F. hepatica* antigens have the capacity to modulate immune response to *S. pneumoniae* using bone marrow-derived macrophages (BMDM) from different strains of mice.

Chapter 4

Fasciola hepatica and Streptococcus pneumoniae interactions with murine bone marrow-derived macrophages

CHAPTER 4

Fasciola hepatica and *Streptococcus pneumoniae* interactions with murine bone marrow-derived macrophages

4.1 Introduction

The mononuclear phagocyte system comprises a family of cells including bone marrow progenitors, blood monocytes and tissue macrophages. Macrophages (MΦs) are resident sentinel cells in almost all tissues and the activation of MΦ occurs as a result of disease processes in metabolic diseases, allergic disorders (airway hyperactivity), autoimmune disease, cancer and various pathogen infections (bacterial, parasitic, fungal and viral) (Murray *et al*., 2014). MΦs can develop into different subsets depending on the activating stimuli. Whilst specialised tissue-resident macrophages (e.g. Kupffer cells in the liver, microglia in the brain, Langerhans cells in the skin) arise during embryonic development (Epelman *et al*., 2014), MΦs that arise from monocyte differentiation are recruited from the blood, and play essential roles in both disease and homeostasis throughout the body (Labonte *et al*., 2014). In the adult bone marrow, macrophage-colony forming units (M-CFU) differentiate into monoblasts, pro-monocytes and eventually mature circulating monocytes (macrophage precursors) (Das *et al*., 2015).

From the circulation, monocytes will migrate and extravasate through the endothelium, where finally, they differentiate into MΦs or dendritic cells (DCs) (Murray and Wynn, 2011a). Besides monocytes, MΦs and DCs, neutrophils and mast cells are also phagocytic cells. Although the phenotypic diversity of MΦs has mostly been experimentally determined with MΦs differentiated from mouse bone marrow cells (Price and Vance, 2014), such bone marrow-derived macrophages (BMDMΦs) are known to differ from tissue–resident MΦs in both mice and humans (Gautier *et al*., 2012; Epelman *et al*., 2014; Murray *et al*., 2014). These tissue-resident MΦs are present in tissues at steady state. They develop early in life and are maintained in adult tissues independently from the circulating monocyte pool (Gautier and Yvan-Charvet, 2014). MΦ can be categorised as classically activated/

type 1 macrophages (CAMΦs) and alternatively activated/ type 2 macrophages (AAMΦs).

As previously mentioned in Section 3.1, several MΦ models have been used to study the interactions between *F. hepatica* and *S. pneumoniae*. This chapter further discusses the consequences of co-exposure and investigates *F. hepatica* and *S. pneumoniae* interactions with murine BMDM. Differentiated MΦs from three different mouse strains (female CD1, BALB/c and C57BL/6) were infected with WT live D39 *S. pneumoniae*, followed by stimulation with FhES. Supernatants and cell lysates were assessed for NO and arginase production. Supernatants from BALB/c BMDMΦs were further assayed for inflammatory cytokine and chemokine levels. Finally, I also investigated the production of NO and arginase in BMDMΦs of older BALB/c mice to determine whether aging could alter MΦ activity in response to D39 infection and co-exposure to FhES products.

4.2 Results

4.2.1 Different patterns of BMDMΦ activation in response to FhES and live D39 pneumococcus co-exposure

To investigate the activation of BMDMΦs during FhES+D39-co-exposure, cell supernatants and lysates were analysed for CAMΦ and AAMΦ markers. BMDMΦs were stimulated with live D39 and FhES for 24 and 48 hours. Following incubation, the supernatants and lysates were analysed for NO and arginase production, respectively. Here, I observed different patterns of activation of BMDMΦs from different mouse strains after 24 and 48 hours. Figure 4.1a shows significantly increased NO levels in the co-exposed cultures of CD-1 mice compared to the PBS control, D39 and FhES cultures (p<0.0001) after 24 hours with low levels of NO detected in D39 cultures alone (0.07µM). After 48 hours of incubation, again NO in the co-exposed cultures were significantly increased, compared to the PBS cultures (p=0.0276), D39 and FhES cultures (p<0.0001), with lack of production of NO observed in D39 at this time point. BMDMΦs exposed to both D39 and FhES showed significantly up-modulated arginase compared to each stimulant alone (PBS and FhES; p<0.0001, D39; p=0.0029) (Figure 4.1b) after 24 hours, but not at

48 hours, suggesting mixed populations of CAMΦ and AAMΦ phenotypes at 24hours.

BMDMΦs from BALB/c mice infected with D39 alone showed significantly increased NO production compared to PBS stimulated cells (p=0.0003) after 24 hours (Figure 4.1c). NO levels were also significantly up-modulated in the co-exposed cultures compared to other tested cultures (p<0.0001), suggesting the modulation of BALB/c BMDMΦs towards a CAMΦ phenotype in *F. hepatica*-pneumococcus co-exposure cultures. However, no significant differences were observed in NO after 48 hours (Figure 4.1c) or in arginase productions at either time point in all tested cultures (Figure 4.1d). The same 24 hours supernatants from BALB/c BMDMΦs were also assayed for inflammatory cytokines and chemokine expression (discussed in Chapter 4.2.3).

Of all mouse strains tested, BMDMΦs from C57BL/6 mice infected with D39 alone demonstrated the highest levels of NO after 24 hours and were significantly higher compared to PBS control and FhES treated cultures (p<0.0001), but the levels dropped after 48 hours (Figure 4.1e). Co-exposed cultures produced significantly higher levels of NO compared to the PBS control (p=0.0030) but lower levels compared to cultures treated with D39 alone (p<0.0001) (Figure 4.1e), suggesting that co-exposure with FhES could prevent CAMΦ induction and modulate the cells towards the AAMΦ phenotype. However, arginase levels were not significantly different at either time point (Figure 4.1f).

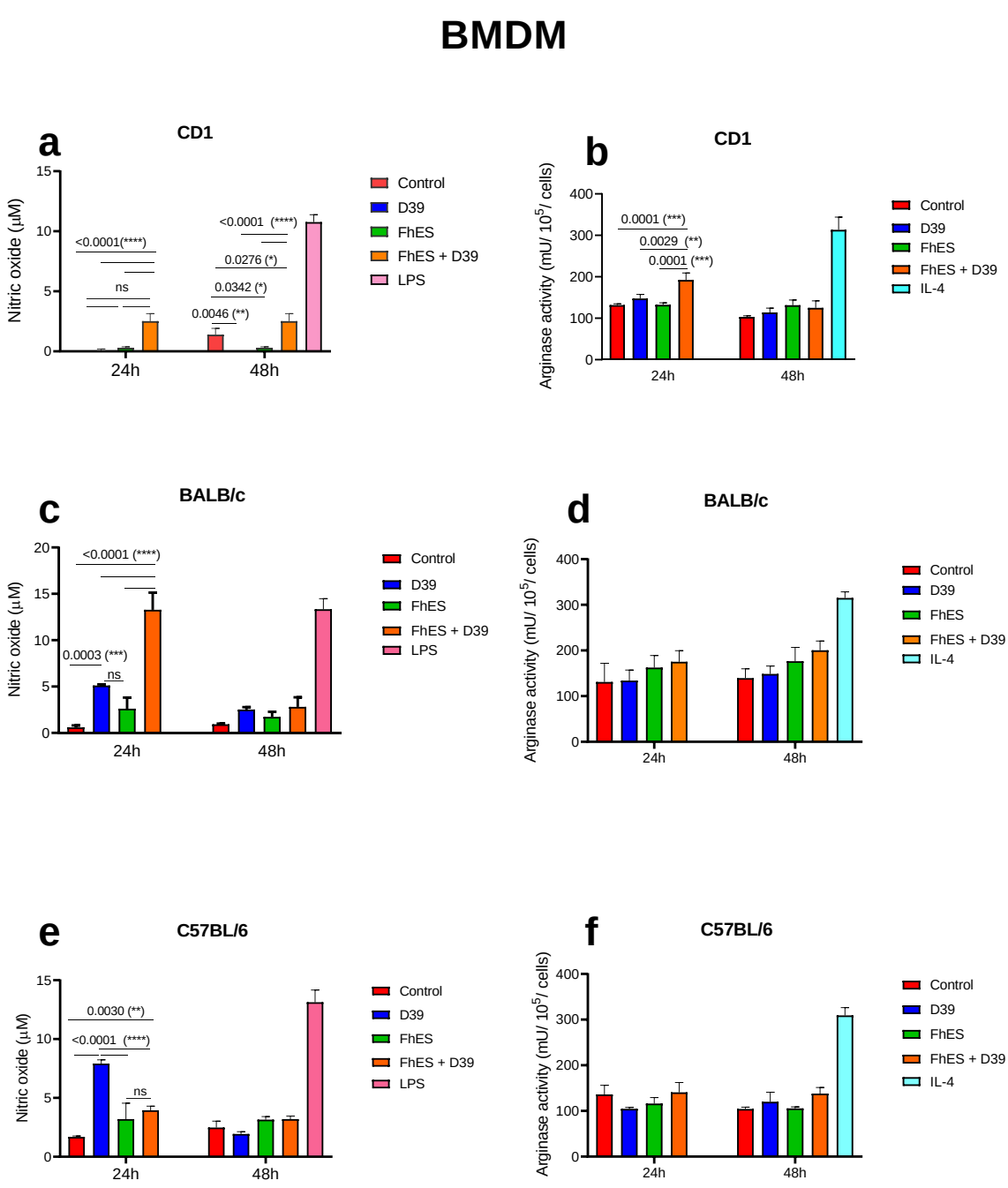

Figure 4.1: CD1, BALB/c and C57BL/6 BMDMΦs activation in *F. hepatica*-pneumococcus co-exposure. Left panels (a, c and e) showing production of nitric oxide (NO) and right panels (b, d, and f) showing arginase production in BMDM infected with live D39 and then co-exposed to FhES. Supernatants and lysates were analysed after 24 and 48h. The experiment was repeated three times and one representative experiment is shown. The levels shown are the mean of three cultures ±SEM. Asterisks indicate statistically significant differences analysed using one-way ANOVA followed by Tukey's multiple comparison post-test.

4.2.2 Older BALB/c mice show evidence of declining CAMΦ function during live D39 infection

I further investigated NO and arginase production in BMDMΦs from 15 week old BALB/c mice stimulated with both WT live D39 and FhES. Figure 4.2 shows NO and arginase levels in BMDMΦs isolated from BALB/c mice (Table 2.4) and infected with live D39 followed by FhES stimulation. Younger BALB/c BMDM (6-7 weeks) infected with D39 alone produced more NO than CD-1, but less than C57BL/6 mice (Figure 4.1a, c and e). In this part of the experiment, using older BALB/c mice, D39 infection induced much lower NO levels after 24 (older age mice; 0.48 µM, younger age mice; 5.11µM) and 48 (older age mice; 0.60 µM, younger age mice; 2.50µM) hours incubation (Figure 4.1c and 4.2a, respectively).

The levels were significantly lower than NO levels detected from FhES stimulated macrophages (p<0.0001; at 24 hours). Co-exposed cultures had significantly up-regulated levels of NO compared to D39 cultures (p=0.0004), as observed previously with younger age mice (Figure 4.1c) but the levels were again lower (older age mice; 1.34 µM, younger age mice; 13.27µM) after 24 hours. Although the overall levels of NO were lower in co-exposed BMDMΦs, they were significantly higher than in PBS (p<0.0001), D39 (p=0.0008) and FhES (p=0.0003) stimulated cultures after 48 hours (Figure 4.2a). NO levels were also reduced in older mice exposed to FhES at 24 (older age mice; 1.8 µM, younger age mice; 2.6 µM,) and 48 (older age mice; 0.5 µM, younger age mice; 1.7 µM) hours (Figure 4.1c and 4.2a, respectively).

Arginase levels of D39 infected BMDMΦs were lower in older mice compared with younger age mice after 24 (older age mice; 114 mU/ 10^5/ cells, younger age mice; 134 mU/ 10^5/ cells) and 48 (older age mice; 124 mU/ 10^5/ cells, younger age mice; 149 mU/ 10^5/ cells) hours (Figure 4.1d and 4.2b, respectively). Furthermore, arginase levels in the co-exposure cultures in older age mice were lower compared to the younger age mice after 24 (older age mice; 136 mU/ 10^5/ cells, younger age mice; 175 mU/ 10^5/ cells) and 48 (older age mice; 191 mU/ 10^5/ cells, younger age mice; 201 mU/ 10^5/ cells) hours.

Similar levels of arginase production were observed in FhES stimulated cultures in both age groups (older age mice; 173 mU and 137 mU (Figure 4.2b), younger age mice; 163 mU and 176 mU) (Figure 4.1d) at 24 and 48 hours. Nevertheless, no significant differences were observed in arginase levels at either time points for any of the tested cultures.

BMDM

BALB/c

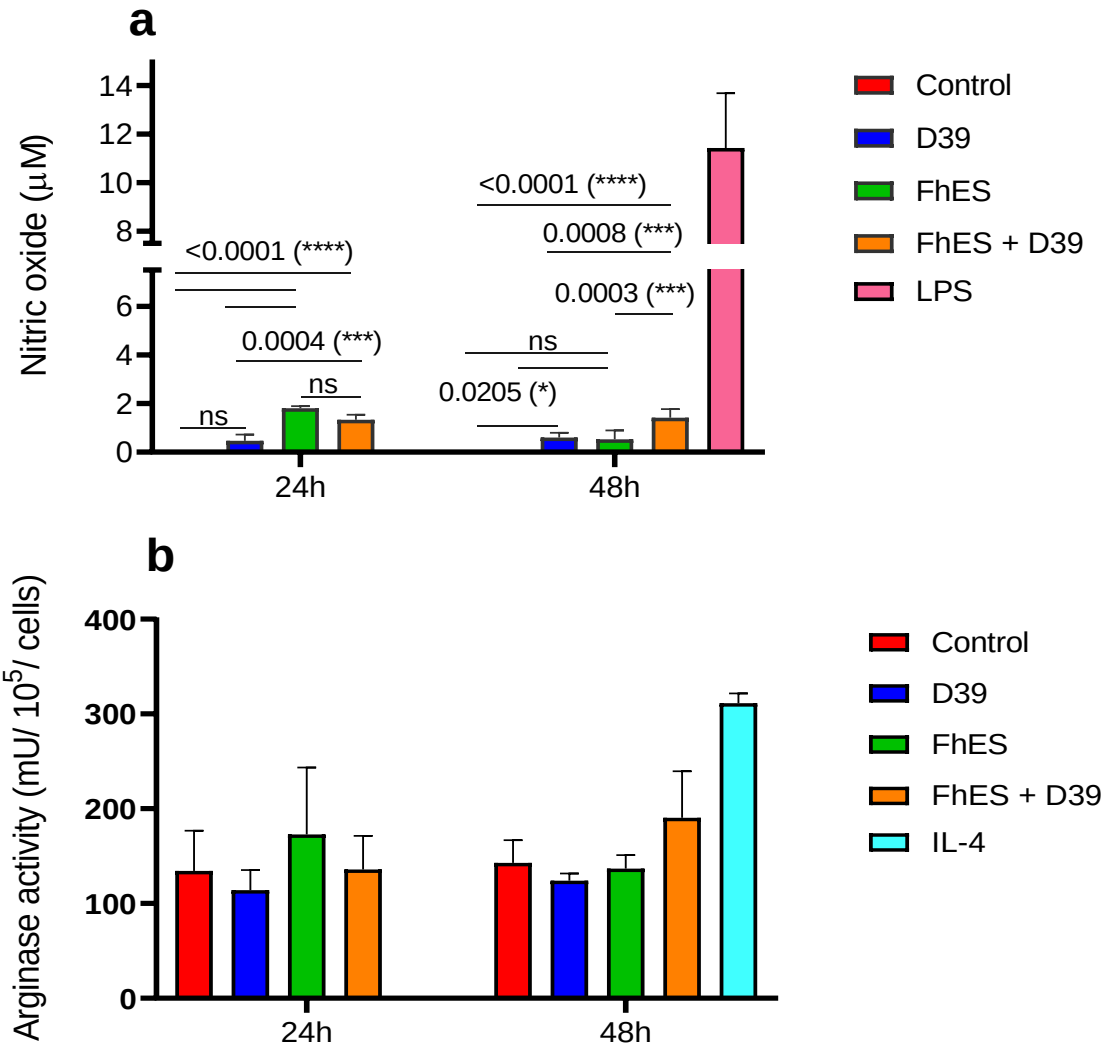

Figure 4.2: Reduced of NO and arginase activity in the activated BMDMΦs of 15 week old BALB/c mice in response to *F. hepatica*-pneumococcus exposure. Production of (a) nitric oxide (NO) and (b) arginase in BMDMΦs infected with live D39 and co-exposed with FhES. Supernatants and lysates were analysed after 24 and 48h. The experiment was repeated three times and one representative experiment is shown. The levels shown are the mean of three tested cultures ± SEM. Asterisks indicate statistically significant differences analysed using one-way ANOVA followed by Tukey's multiple comparison post-test.

4.2.3 Up-regulation of pro-inflammatory cytokines in FhES+D39 co-exposed BALB/c BMDM

Supernatants from the stimulated BMDMΦs cultures from 6-7 week old BALB/c mice, taken at 24 hours (Section 4.2.1) were assayed for cytokines and chemokines using the Multiplex MSD® U-PLEX. Figure 4.3 compares the means of different inflammatory proteins detected in each culture. For this part of the experiment, selection of a time point to be assayed for inflammatory proteins was decided based on the high NO production observed at 24 hours (Figure 4.1c; at 24 hours). Low levels of IFN-ɣ were detected in BMDMΦs, even when infected with live D39 (Figure 4.3a). IL-12p70 was detected, however, the levels in co-exposed cultures were not significantly up-regulated relative to D39 cultures (Figure 4.3b). This finding was contrary to the findings with J774.2 macrophages, where undetectable levels of IL-12p70 were observed in D39SN cultures (Table 3.2).

Pro-inflammatory cytokines TNF-α, IL-1β, IL-6 and the chemokine CXCL1/KC were up-regulated by D39 alone (Figure 4.3a, d, e and f). TNF-α, IL-6 and CXCL1/KC production was significantly increased in co-exposed cultures compared to FhES cultures (p=0.0202; Figure 4.3c, p=0.0054; Figure 4.3e, p=0.0057; Figure 4.3f, respectively), but the production of all these proteins was not significantly different from D39 alone. No significant difference between levels of IL-1β in cultures infected with D39 alone compared to those incubated with FhES (Figure 4.3d). FhES alone induced detectable TNF-α and CXCL1/KC (Figure 4.3c and f, respectively). Anti-inflammatory IL-10 production was significantly up-modulated in co-exposed cultures compared to the PBS control, D39 and FhES cultures (p<0.0001) (Figure 4.3g).

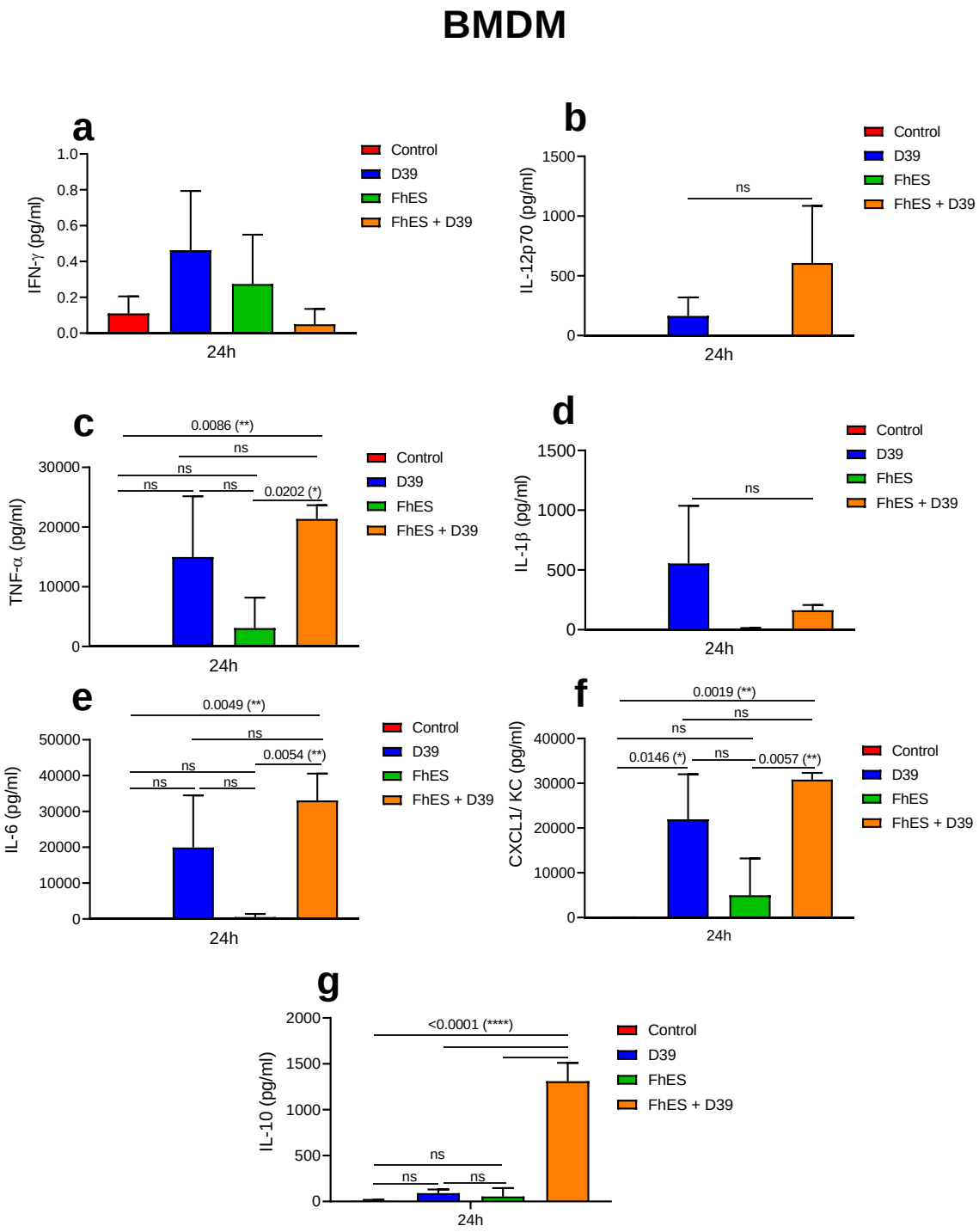

Figure 4.3: Cytokine and chemokine expression in BALB/c BMDMΦs 24 hours after exposure to live D39 and FhES. Supernatants were analysed using Multiplex MSD® U-PLEX after 24h for pro-inflammatory cytokines (a-g; IFN-ɣ, IL12p-70, TNF-α, IL-1β, IL-6, CXCL1/ KC and IL-10). The levels shown are the mean of three tested cultures ± SEM. Asterisks indicate statistically significant differences analysed using one-way ANOVA followed by Tukey's multiple comparison post-test.

4.3 Discussion

In this chapter, I investigated whether *F. hepatica* antigens are capable of modulating the immune response to *S. pneumoniae,* using bone marrow-derived macrophages from different strains of mice. In the previous chapter, I showed that J774.2 macrophages have the capacity to develop into AAMΦ when co-exposed to FhES and FhTEG antigens with MbSE but not to fluke antigens alone. J774.2 macrophages developed a CAMΦ phenotype when exposed to D39SN even in the presence of FhES, as shown by up-regulation of pro-inflammatory cytokines and down-regulation of anti-inflammatory IL-10.

In the first part of this chapter, I assessed the BMDMΦs isolated from the CD1, BALB/c and C57BL/6 mice on their capacity to produce NO and arginase in response to FhES and live D39 infection. After 24 hours incubation, significantly up-regulated levels of NO were detected in co-exposed cultures compared to D39, in BMDMΦs of CD1 and BALB/c mice. Among all three mouse strains, only co-exposed CD1 BMDMΦs showed significant up-regulation of arginase levels when exposed to D39/FhES co-treatment, suggesting that fluke and pneumococcus together induced a mixed CAMΦ and AAMΦ phenotype. Low (at 24 hours) or no (at 48 hours) NO was detected in CD1 BMDMΦs exposed to D39, suggesting CD1 mice may be susceptible to D39 pneumococcal infection, due to a muted ability to mount protective MΦ responses to infection. The susceptibility of CD1 mice is supported by previous findings where CD1 mice that were infected with D39 pneumococci showed an increasing number of bacteria inside splenic MΦs, and splenic clearance is less efficient with 100-fold higher blood counts observed at 24 hours of infection (Ercoli *et al*., 2018).

Differential activation of CAMΦ and AAMΦ mirrors the Th1/ Th2 polarisation of T cells (Wang *et al*., 2014). Tissues with a spectrum of activation sites may contain mixed populations of MΦ (Murray *et al*., 2014). Although bacteria-helminth co-infections have often been found to lead to a reduction in the protective Th1 cytokine response by developing a Th2 mediated response towards helminths and AAMΦ activation (Brady *et al*., 1999; O'Neill *et al*., 2000; Fox *et al*., 2000; Donnelly

et al., 2005; Chen *et al.*, 2006; Resende Co *et al*., 2007; Flynn *et al*., 2007a), several studies have documented mixed populations of MΦs and Th1/ Th2 phenotypes during infections. Severe respiratory syncytial virus (RSV) induced bronchiolitis is closely associated with mixed CAMΦ/ AAMΦ phenotypes (Shirey *et al*., 2010). The alternative activation marker, Arg-1 is also found to be up-regulated not only as expected in AAMΦ but also in CAMΦ spectrum MΦs in murine trypanosomiasis (Raes *et al*., 2002) and in *Toxoplasma*- and *Mycobacteria*–induced BMDMΦs (Kasmi *et al*., 2008). Mixed Th1/ Th2 phenotypes have also been observed in murine *Schistosoma mansoni* (Xu *et al*., 2010; Fahel *et al*., 2010) and *Trichuris muris* infections (Grencis, 2001). My findings that show the capacity of CD1 BMDMΦs to express mixed phenotypes of MΦs elicited by fluke-pneumococcus interaction, provides additional evidence for CAMΦ and AAMΦ mixed phenotypes during co-infection. Others have reported mixed MΦs profiles in atherosclerotic plaques (Kadl *et al*., 2010), murine tumours (Umemura *et al*., 2008) and adipose tissue MΦs from obese mice (Shaul *et al*., 2010). Outbred CD-1 mice reflect better the genetic diversity in human populations than inbred strains such as BALB/c and C57BL/6 (Hsieh *et al*., 2017). Since genetic variation was observed among outbred CD-1 mice (Aldinger *et al*., 2009), it is possible that this contributes to the heterogeneous CAMΦ and AAMΦ phenotypes observed in the presence of fluke and pneumococcus together.

High levels of NO were observed in C57BL/6 BMDMΦs following exposure to D39, indicating CAMΦ activation due to pneumococcus infection. Significantly lower levels of NO were detected in co-exposed cultures compared to D39 alone in the C57BL/6 BMDMΦs suggesting the FhES may have modulated this CAMΦ phenotype, although arginase production was not significantly up-regulated. Female C57BL/6 mice were reported to show resistance to *S. pneumoniae* serotype 3, marked by reduced bacterial survival in alveolar MΦs (Yang *et al*., 2014). This could further support the findings in the present study, where high levels of NO were produced in female C57BL/6 BMDMΦs exposed to serotype 2 D39. In contrast, NO levels in co-exposed cultures from BALB/c BMDMΦs were significantly higher than cultures incubated with D39 alone indicating CAMΦ

activation but with no modulation by FhES and there was no evidence of increased expression of arginase.

Mouse strains have been reported to have different susceptibilities to pneumococcal pneumonia, where BALB/c mice are highly resistant to respiratory challenge against a wide range of invasive pneumococci (Kerr *et al*., 2002; Denny *et al*., 2003; Kadioglu and Andrew, 2005; Jeong *et al*., 2011) that are confined to the lung without development of sepsis and then eliminated within 7 days (Neill *et al*., 2012) with only a transient bacteraemia, if any, observed (Gingles *et al*., 2001). Whilst some studies have shown that monocyte-derived MΦ and BMDMΦs from different strains of mice can differ in their response to IFN-ɣ, LPS and TNF-α (Weinberg, 1998; Tripathi, 2007), others have shown that differences in the rodent background can result in differences in MΦ gene expression (Mills *et al*., 2000; Mills, 2001; Murray and Wynn, 2011a). In the present study, both BALB/c and C57BL/6 strains, although resistant to pneumococci when infected with D39, have shown two different MΦ polarisations when co-exposed to FhES.

Murine strain variation provides a spectrum of disease phenotypes in parasite models. C57BL/6 and BALB/c mice are reported to be resistant to *T. muris*, where the parasite is quickly expelled from the host (deSchoolmeester *et al*., 2009; (Antignano *et al*., 2011; Klementowicz *et al*., 2012). BALB/c mice are also more resistant to the murine coccidian parasites *Eimeria papillata* and *Eimeria vermiformis* (Schito *et al*., 1996). In the context of the murine *F. hepatica* model, BALB/c and C57BL/6 mice have been used in several studies. The genes coding for Arg-1, Fizz1 and Ym1 but not iNOS were expressed in the peritoneal MΦ of BALB/c mice after oral infection with juvenile *F. hepatica* and intraperitoneal administration of PI (fraction of FhES which contains TPx (thiredoxin peroxidase)) (Donnelly *et al*., 2005). In another study, AAMΦ associated genes, but not iNOS, were expressed in the isolated peritoneal MΦ of BALB/c and C57BL/6 mice that were injected intraperitoneally with FhES and FhTEG (Adams *et al.*, 2014). Those findings were in contrast with the present study where NO production was detected in FhES cultures, including in CD1 BMDMΦ. However, these two types of MΦ were different in their functions, specialisation and development stage (Cassado *et al*.,

2015), which may result in different responses and biological marker expression during infection. Whilst BMDMΦs arise from their bone-marrow myeloid progenitors, the resident peritoneal MΦs are not derived from monocytes; instead they are derived from an embryonic precursor and maintained by self-renewal (Yona *et al*., 2013; Hashimoto *et al*., 2013). Future studies on MΦ activation outcomes from different progenitor/ precursor populations in response *to F. hepatica* products are therefore recommended.

The second aim of this chapter was to investigate the responses of BMDMΦ following exposure to FhES and D39 pneumococcus in older BALB/c mice, since age is associated with differences in TNF-α and NO production (Chorinchath *et al*.,1996). The levels of NO and arginase in the BMDMΦ from the older mice were lower compared to young mice, in the present study. The same findings but with different microbial stimuli have been demonstrated in several studies. Activity of iNOS and arginase, and cytokine production were altered in peritoneal MΦ of old BALB/c mice stimulated with LPS from *Escherichia coli* (Cecílio *et al*., 2011). Although 72 week old BALB/c mice were used in the previous study, my findings show that the reduced NO and arginase activities can be observed as early as 15 weeks of age in response to D39 pneumococci. Declining levels of NO production by MΦs were also observed in old BALB/c mice but pre-treating the mice with cholera toxin and Concanavalin A could enhance NO production (Kissin *et al*., 1996). Hypersecretion of NO in thiogycholate-elicited MΦs from senescent mice was observed compared to those obtained from young mice in response to LPS but the TNFα production was indistinguishable between MΦs from young and senescent mice (Chen *et al*., 1996). The present study has provided additional evidence that older mice could have a reduced efficiency of their innate immune cells to produce antimicrobial molecules for intracellular killing, such as NO, when infected with pneumococci.

The third aim of this chapter was to investigate the effect of exposure of BALB/c BMDMΦs to *F. hepatica* antigens and live D39 on cytokine and chemokine secretion. Whilst all the tested cultures produced low levels of IFN-ɣ, D39 and co-exposed BMDMΦs induced the production of IL-12p70; the levels in D39 cultures

were 500pg/ml less compared to the co-exposed cultures, although this was not statistically significant, given considerable variation in levels in the co-exposed cultures. As previously discussed in Section 3.3, the interrelationship between IFN-ɣ and IL-12p70 is particularly complex, where IL-12 activates IFN-ɣ secretion by Th1 cells to drive CAMΦ polarisation (Yun *et al*., 2002). IL-12 effects have been attributed to its ability to induce IFN-ɣ production *in vivo* (Trinchieri, 1995; Car *et al*., 1995; Trinchieri, 2003). In this experiment, IL-12p70 from D39 infected BMDMΦ was produced in higher levels than those previously observed in J774.2 cell line (derived from BALB/c mice) stimulated with D39SN. Here, I demonstrated two types of BALB/c MΦs (primary BMDMΦ and J774.2 cell line) that were infected with the same *F. hepatica* antigens but to different pneumococci preparations resulted in low (D39 infected BMDMΦ) to almost none (D39SN stimulated J774.2 cells) IFN-ɣ production. On the other hand, high (D39 infected BMDMΦ) to undetected (D39SN stimulated J774.2 cells) IL-12p70 production was also observed. This difference could be due to the different origin of the cells and of them being primary cells and a cell line. Primary BMDMΦs respond very strongly to *M. tuberculosis* infection whereas the response of J774 is delayed and more discreet in term of number of differentially expressed genes and magnitude of induction/ suppression (Andreu *et al*., 2017). It is suggested that the association of these cytokines in the context of fluke-pneumococcus infection is investigated in future studies. Although not statistically significant, the capacity of FhES to increase IL-12p70 production in co-exposed BALB/c BMDMΦs compared to D39 alone remains to be elucidated.

Infection of BMDMΦs of BALB/c mice with D39 induced the production of pro-inflammatory cytokines TNF-α, IL-1β, IL-6 and chemokine CXCL1/KC. IFN-ɣ, TNF-α, IL-6 and IL-12 are usually found in the circulation of patients with community acquired pneumonia (Glynn *et al*., 1999; Calbo *et al*., 2008) where IL-6, IL-12, IL-17 and IL-18 are important mediators in the innate response to pneumococcal infection (Endeman *et al*., 2011). In addition, TNF-α, IL-1β, IL-6 and IL-10 were involved and correlated with the clearance of pneumococcal cells from the lung and recovery from infection (Kerr *et al.*, 2002; Gingles *et al*., 2001). CXCL1/KC is one of the major chemoattractant factors for recruiting neutrophils in pneumococcal

infections (Paudel *et al*., 2019). Results, presented in this part of the chapter, provide additional evidence for involvement by pro-inflammatory cytokines in controlling D39 pneumococci infection. There was a higher expression of TNF-α and CXCL1/KC in FhES stimulated BMDMΦs compared to those observed in FhES stimulated J774.2 MΦs. Whilst TNF-α, IL-6 and CXCL1/KC production were not significantly up-modulated in co-exposed BALB/c BMDMΦs compared to D39, IL-1β was found to be down-modulated. The same findings were observed in co-exposed J774.2 cells except that IL-1β and CXCL1/KC were significantly up-modulated compared to D39SN. In summary, FhES had no statistically significant effect when added to culture of BMDMΦs with live D39, on TNF-α, IL-1β, IL-6 and CXCL1/KC secretion. Due to sample limitation, only three cultures were analysed for each cytokine/ chemokine in co-exposed BMDMΦs and J774.2 cells using Multiplex MSD® U-PLEX in the present study, thus more samples should be tested to increase power of the experiment.

Finally, anti-inflammatory IL-10 production was significantly up-regulated in BMDMΦ exposed to both D39 and FhES, compared to those incubated with D39 alone. The results presented here were different to those observed in the previous chapter with J774.2 cells, where there was no difference between IL-10 expression in the cells with these incubation protocols. The levels of IL-10 in D39 cultures were much lower in BMDMΦ than J774.2 cells. FhES stimulated BMDMΦ produced IL-10 production and these results are similar to those reported by others (Flynn and Mulcahy, 2008a, b; Walsh *et al*., 2009; Guasconi *et al*., 2011). Up regulation of IL-10 indicates an anti-inflammatory response which may be induced to prevent immunopathology during *F. hepatica*-D39 pneumococcus co-infection.

4.4 Conclusion

To the best of our knowledge, our results are the first to describe the response of murine BMDMΦ to *F. hepatica*-pneumococcus interaction. The results showed that CD1 BMDMΦs have the capacity to develop a mixed CAMΦ and AAMΦ phenotype when co-exposed to live D39 and *F. hepatica* antigen FhES. In contrast, BALB/c and C57BL/6 BMDMΦs developed CAMΦ and AAMΦ phenotypes respectively, when co-exposed to the same stimulants. The CAMΦ activation in BALB/c BMDMΦs is supported by detection of pro-inflammatory cytokines, although up-modulation of the regulatory cytokine IL-10 was also observed. Antimicrobial activities were reduced in older mice when infected with D39 which could reduce the efficiency of BMDMΦ to secrete NO for intracellular killing of pathogens.

Many of the co-infection studies despite being protozoan, viral or bacterial infection have focused on infections with helminth first due to their ability to down modulate immune responses (Ahmed *et al*., 2017). Here, we have applied a different approach where the BMDMΦs were exposed to D39 first before being stimulated with FhES. This could further explain our findings that show induction of potent pro-inflammatory Th1 cytokines in *F. hepatica*-D39 co-exposed cultures rather than Th1 cytokine suppression indicating Th2 immune responses. Thus, the timing of exposure of bacterial relative to helminth infection could have an important effect on the subsequent development of a polarised immune response.

Chapter 5

Investigating the effect of Fasciola hepatica antigens on Streptococcus pneumoniae nasopharyngeal carriage in a mouse model

CHAPTER 5

Investigating the effect of *Fasciola hepatica* antigens on *Streptococcus pneumoniae* nasopharyngeal carriage in a mouse model

5.1 Introduction

Co-infections between helminths and bacteria can alter mammalian host immune responses and shape the disease outcome. There is a growing body of evidence that helminth infected hosts may exhibit modulation of the immune response to bystander microbial infections. Chronic helminth infections increased susceptibility to pneumococcal pneumonia (Apiwattanakul *et al*., 2014a) and resulted in the outgrowth of bacteria in the lungs and blood (Apiwattanakul *et al*., 2014b). *Fasciola hepatica* infections have been reported to delay bacterial clearance in mice infected with *B. pertussis* (Brady *et al.*, 1999), increase the susceptibility of cattle to *Salmonella* Dublin (Aitken *et al*., 1976; Aitken *et al*., 1978; Hall *et al*., 1981) and alter the immune responses to bovine tuberculosis infection (Flynn *et al*., 2009). This chapter seeks to assess the impact of *F. hepatica*-pneumococcus interaction in a CD1 mouse model of pneumococcal nasopharyngeal carriage, assessing bacterial load, cytokine and chemokine production and host immune cell responses.

5.2 Results

5.2.1 FhES promotes increased colonisation of pneumococcus in the nasopharynx in co-exposed mice

Figure 5.1 shows the bacterial densities in CD-1 mice over 4 days post intranasal challenge with 10^5 CFU of *S. pneumoniae* D39 in 10µl of PBS. This dose and volume was chosen to establish asymptomatic nasopharyngeal carriage without dissemination to the lower respiratory tract (Neill *et al*., 2014), and FhES antigen was then administered intranasally to a sub-group of animals. An increase in pneumococcal densities was observed in FhES+D39 mice compared to D39 infected mice at 2 and 3 days post-challenge (Figure 5.1a). Viable bacterial counts from homogenates of nasopharyngeal (NP) tissues showed a significant increase (p=0.0380) in co-exposed mice compared to D39 infected mice at day 3 after the infection, indicating the potential of FhES to enhance D39 colonisation in the NP. However, I did not observe any difference in bacterial densities in the lungs over 4 days post-challenge (Figure 5.1b).

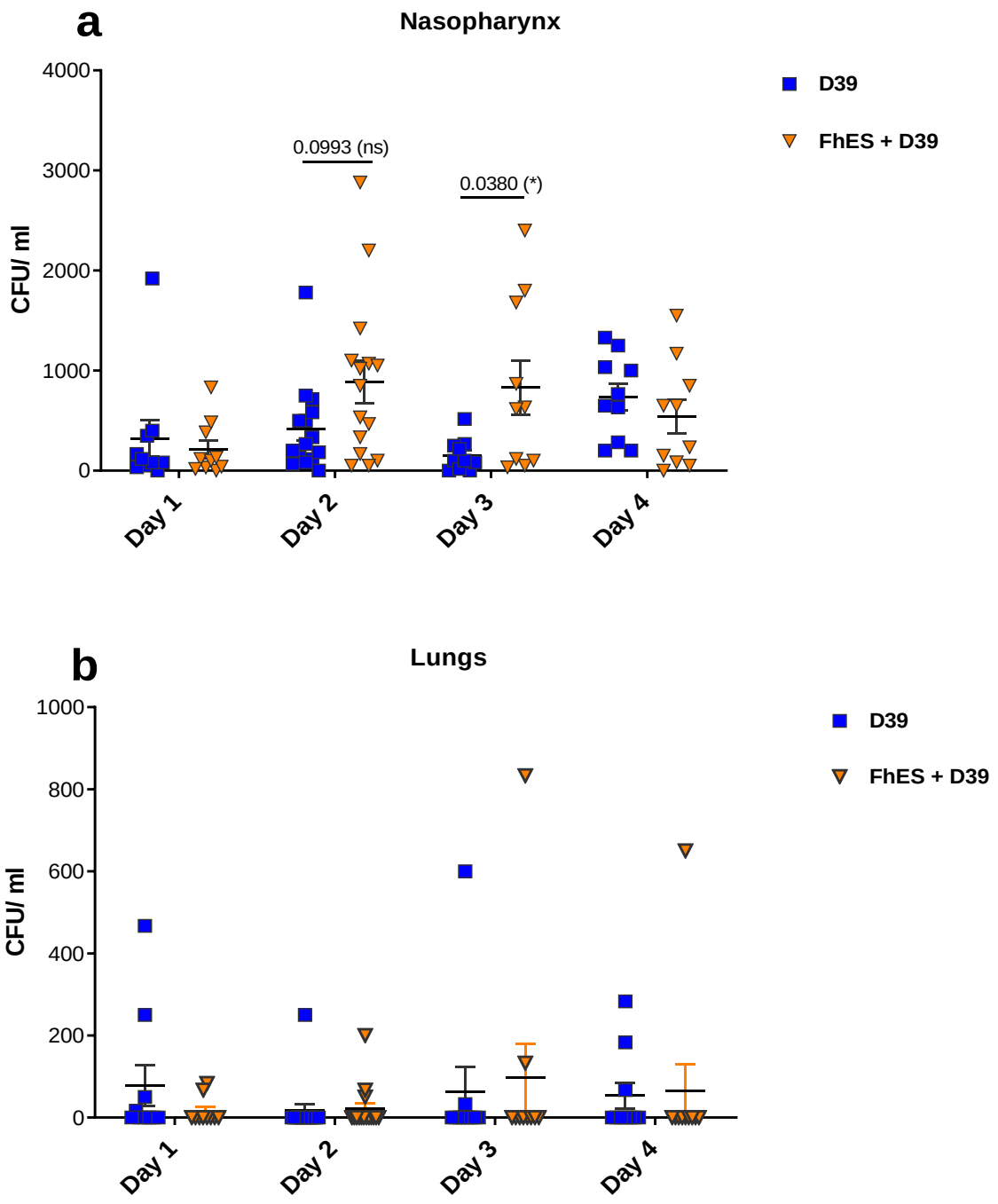

Figure 5.1: Bacterial densities determined by CFU from the nasopharynx (NP) and lungs of D39 and FhES+D39 mice. Female CD1 mice were infected with 10^5 CFU of D39 in a drop-wise fashion, divided between both nostrils, to establish carriage in the NP whilst FhES antigen was then exposed to co-exposed group. CFU per ml (CFU/ml) of tissue homogenate was counted in the (a) NP and (b) lungs over 4 days post intranasal challenge. The data shown are from two independent experiments for Day 1, 3 and 4 and three independent experiments for Day 2 (n=5 per experimental condition). Each symbol represents an individual mouse and error bars represented ±SEM. Asterisks indicate statistically significant differences analysed using two-way ANOVA followed by Sidak's multiple comparison post-test.

5.2.2 Cytokines and chemokine production during nasopharyngeal carriage

Based on the bacterial densities results in Figure 5.1, where no difference in viable bacterial count was seen in the lungs, only nasopharyngeal tissues were further analysed for cytokine and chemokine production. TGF-β1 levels in CD-1 nasopharyngeal supernatants were analysed using Mouse DuoSet ELISA kit. The NP supernatants were treated with 1N HCl to activate latent TGF-β1 to immunoreactive TGF-β1 and later neutralised with 1.2N NaOH/ 0.5M HEPES. Since *F. hepatica* infection induces TGF-β1 producing MΦs (Walsh *et al*., 2009) and TGF-β1 is associated with bovine fasciolosis (Haçariz *et al*., 2009), as expected, FhES treated mice produced significantly more TGF-β1 than the control mice at day 1 (p=0.0044) (Figure 5.2). The levels were reduced when co-exposed with D39. Other signalling proteins were analysed using Multiplex MSD® U-PLEX. Table 5.1 shows the cytokine and chemokine levels in CD-1 nasopharyngeal supernatants obtained from the spun homogenates over 3 days post intranasal challenge. The levels were found to be low in almost all of the tested signalling proteins. In contrast, I observed higher levels of these proteins in the previous experiments with J774.2 cells and BMDMΦs except for IFN-ɣ (Chapter 3 and 4, respectively).

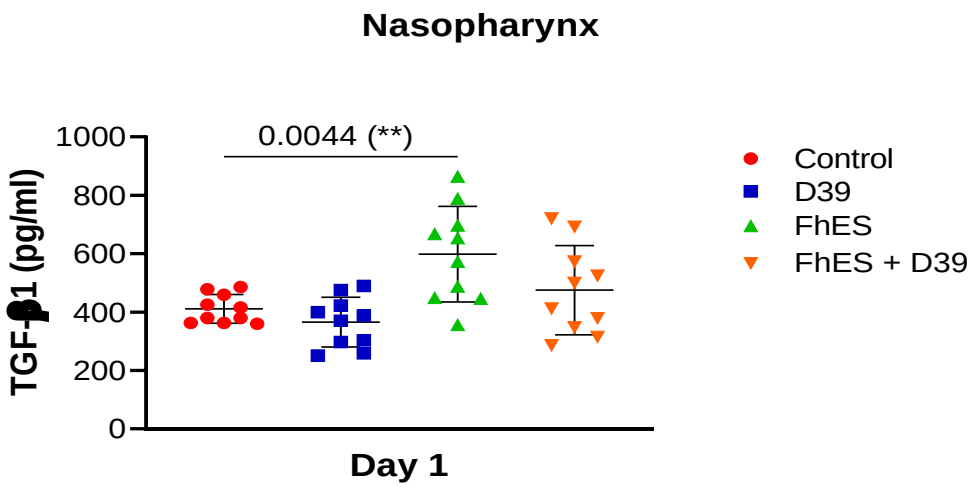

Figure 5.2: FhES induces production of TGF-β1 in CD-1 mice. Nasopharyngeal supernatants were analysed using Mouse DuoSet ELISA kit for TGF-β1 at day 1 post intranasal challenge. The levels are shown in symbols that represent an individual mouse and error bars represented as mean ±SEM. Asterisks indicate statistically significant differences analysed using one-way ANOVA followed by Dunnett's multiple comparison post-test.

Table 5. 1: Levels of inflammatory cytokines and chemokine from the mice nasopharynx in response to D39 and *F. hepatica* over 3 days of post intranasal challenge. The levels represent the mean of 5 mice per experimental condition per timepoint.

Group	Signalling protein (mean) (pg/ml)																				
	IFN-ɣ			IL-12p70			TNF-α			IL-1β			IL-6			CXCL1/KC			IL-10		
	Day 1	Day 2	Day 3	Day 1	Day 2	Day 3	Day 1	Day 2	Day 3	Day 1	Day 2	Day 3	Day 1	Day 2	Day 3	Day 1	Day 2	Day 3	Day 1	Day 2	Day 3
Control	0.00	0.00	0.00	0.00	0.00	0.00	0.00	0.00	0.00	0.00	0.00	0.00	0.00	0.00	0.00	0.00	0.00	0.00	0.00	0.00	0.00
D39	0.03	0.02	0.00	0.00	0.00	0.00	0.20	0.00	0.91	0.00	0.00	0.38	0.27	1.84	0.65	4.16	3.96	5.66	0.00	0.51	0.00
FhES	0.19	0.00	0.07	28.6	0.00	0.00	0.00	0.00	0.21	0.28	2.68	0.00	6.26	0.00	1.09	7.36	6.74	4.84	9.44	0.00	0.51
FhES+ D39	0.00	0.12	0.34	14.5	0.00	0.00	0.19	1.50	0.00	2.29	0.00	1.69	1.23	0.00	0.00	4.81	5.99	4.13	0.00	0.00	0.00

5.2.3 Host immune response in nasopharynx and lungs

The NP and lung cell pellets were stained with different leukocyte sub-population specific antibodies (Table 2.12), fixed in the dark and stored at 4^{o}C and the assay was performed the next day using flow cytometry. Figure 5.3 illustrates the gating strategy used in this part of the chapter. Cells were first gated using CD45 staining to identify leukocytes. CD45 positive cells that were also positive for markers of B cells (CD19), Natural Killer (NK) cells (NK1.1), Th cells (CD3 and CD4), neutrophils (Gr-1 and CD11b), macrophages (MΦs) (F4/80), monocytes (CD115) and mannose receptor (CD206) were gated next. Controls for isotype and fluorescence minus one (FMO) were used to assign limit to the gates.

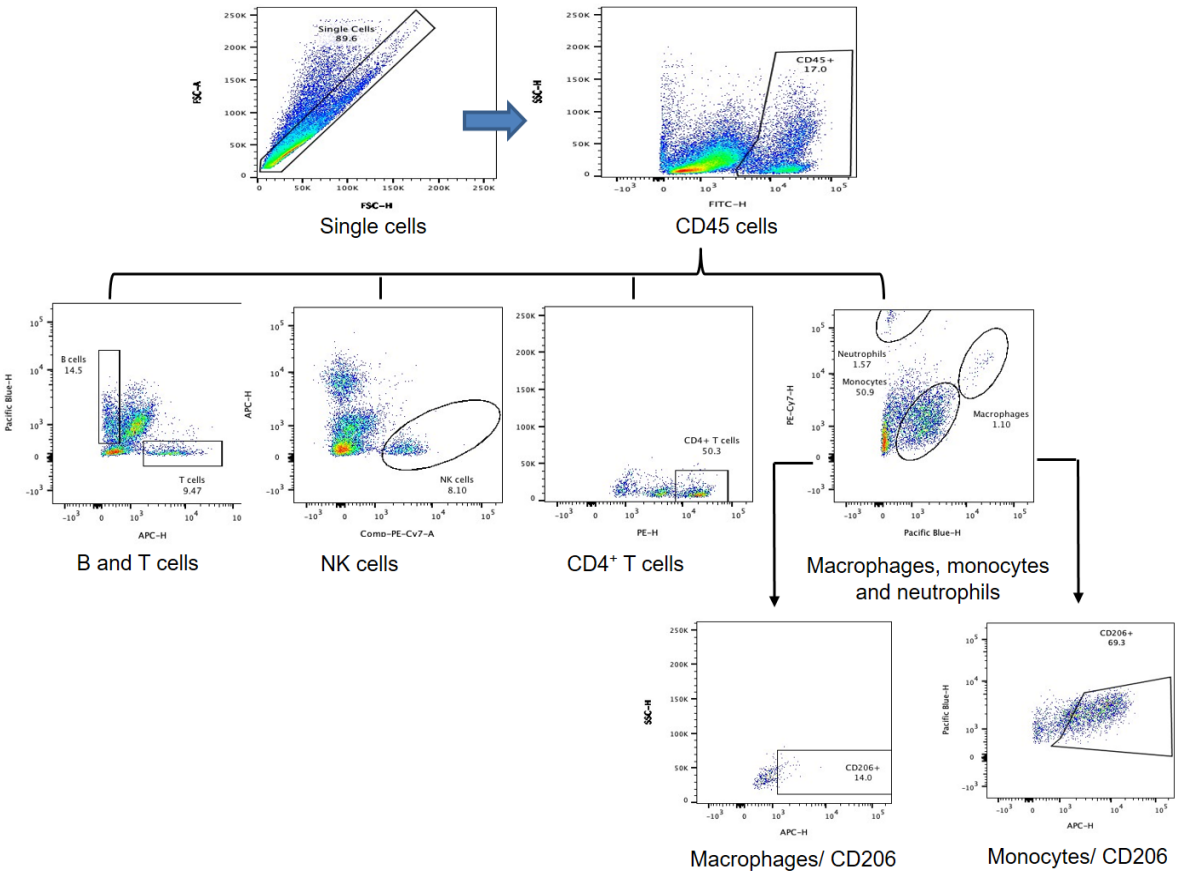

Figure 5.3: Gating strategy for isolation of CD45+, CD19+, NK1.1+, CD3+, CD4+ T, F4/80+, CD115 and CD206+ in NP and lungs. Fluorescence minus one (FM) and isotype controls provide the gating limits. Anti-CD45 FITC, Anti-CD19 Pacific Blue, Anti-CD3 APC, Anti-CD4 PE, Anti-NK PE Cyanine 7, Anti Gr-1 PE Cyanine 7, Anti-F4/80 Pacific Blue, Anti-CD115 PerCP/ Cyanine and Anti-CD206 APC.

Figure 5.4 shows macrophage (MΦ) numbers in the NP and lungs of CD-1 mice infected with D39 and exposed to FhES over the course of infection. Numbers of MΦs were found to be greater in the lungs compared to the NP, reflecting the large surface area of the organ and the tissue-resident alveolar macrophage (AMΦ) population that resides within the lung. The MΦ numbers in the NP of FhES exposed mice were significantly higher than the control (p=0.0074), D39 infected (p=0.0073) and co-exposed (p=0.0102) mice at day 3 after the infection (Figure 5.4a). The NP MΦ numbers were decreased in all experimental groups at day 4. The same findings were observed in macrophage mannose receptor (MR) (MR^+MΦ) numbers in the NP of FhES exposed mice at day 3. The numbers were significantly higher than the control (p=0.0048), D39 infected (p=0.0049) and co-exposed (p=0.0060) mice (Figure 5.5a). No significant differences were observed in the lung MΦ and MR^+MΦ in all experimental groups. The MΦ and MR^+MΦ cells present in the NP and lungs of the control mice (PBS-challenged) were higher than expected at day 2 (Figure 5.4 and 5.5). MΦ and MR^+MΦ cell numbers varied significantly over time in both the NP and lungs in ANOVA summary statistics (NP MΦ; p=0.0210, lungs MΦ; p=0.0244 and NP MR^+MΦ; p=0.0433, lungs MR^+MΦ; p=0.0060), but the differences between experimental treatment/infection groups were only significant for NP (MΦ and MR^+MΦ, both p=0.0006) but not for lungs.

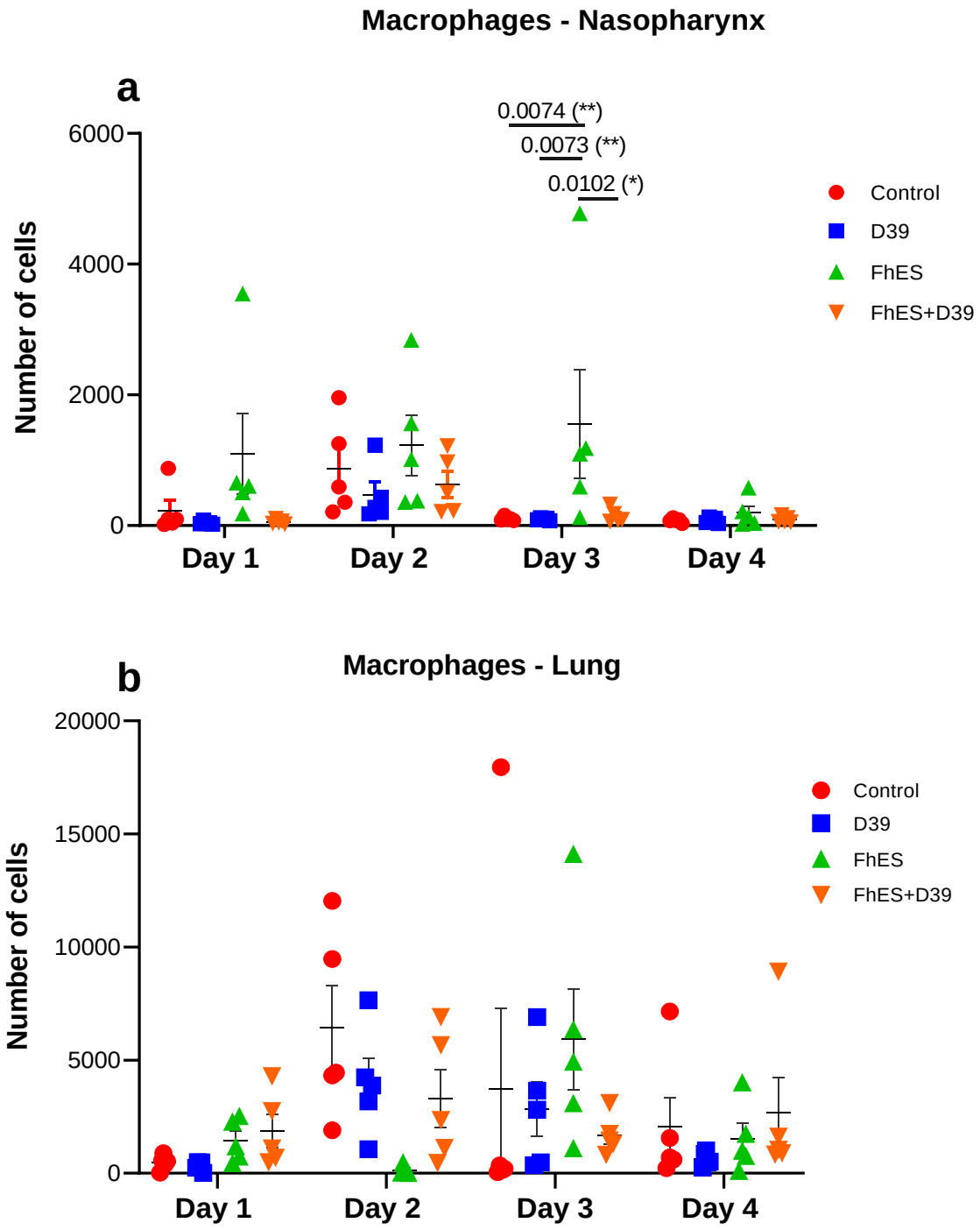

Figure 5.4: Number of macrophages (MΦ) in the nasopharynx and lungs over 4 days post intranasal challenge. (a) Nasopharyngeal and (b) lung cell pellets were stained with CD45 and F4/80 markers to identify macrophage populations. Each symbol represents a single mouse and error bars represented ±SEM. Asterisks indicate statistically significant differences analysed using two-way ANOVA followed by Tukey's multiple comparison post-test. The mean differences between variations (time and experimental groups) were analysed using two-way ANOVA summary statistic and α 0.05 was set for each comparison.

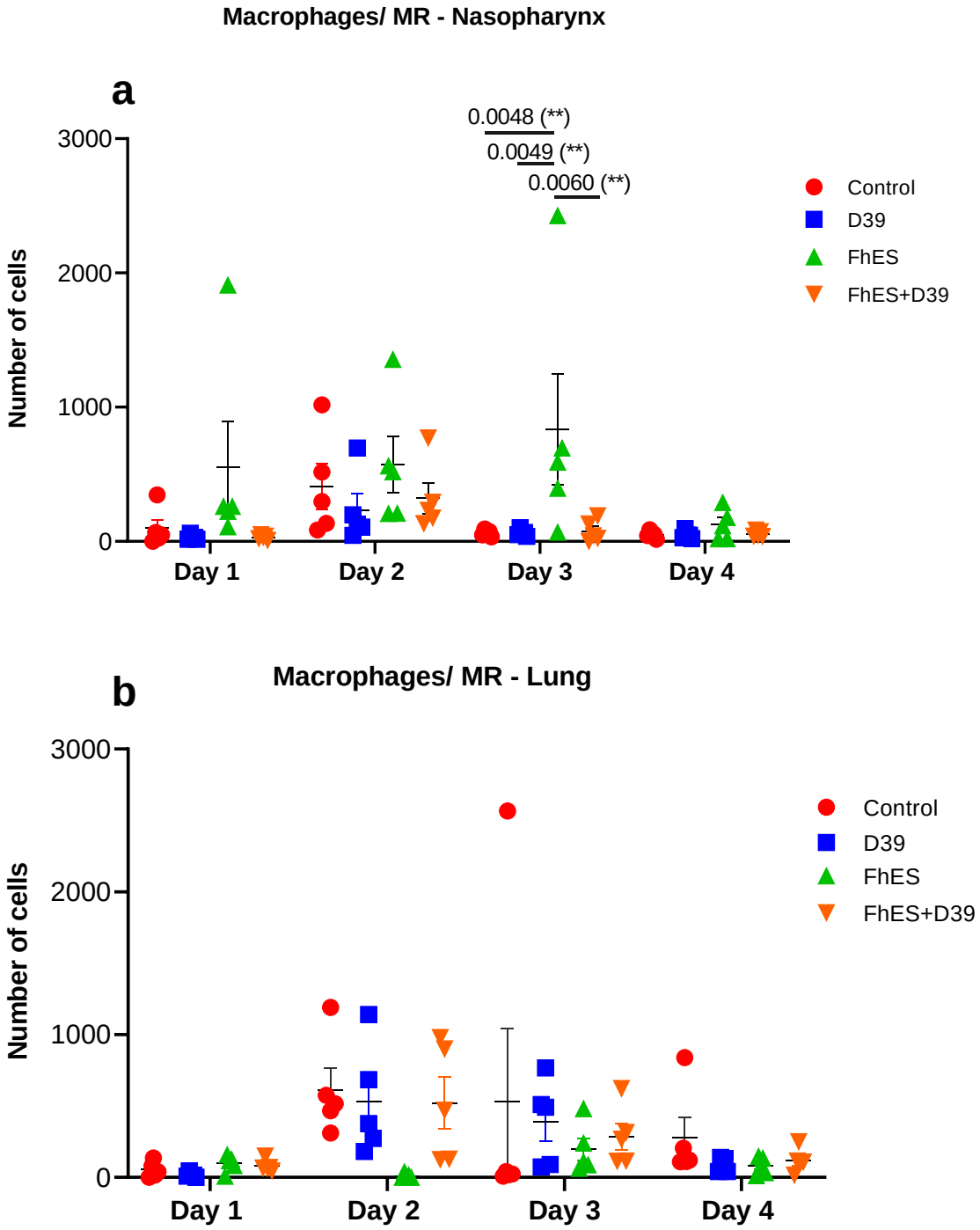

Figure 5.5: Number of MR^{+}MΦ in the nasopharynx and lungs over 4 days post intranasal challenge. (a) Nasopharyngeal and (b) lung cell pellets were stained with CD45, F4/80 and CD206 markers to identify mannose receptor populations. Each symbol represents a single mouse and error bars represented ±SEM. Asterisks indicate statistically significant differences analysed using two-way ANOVA. Asterisks indicate statistically significant differences analysed using one-way ANOVA followed by Tukey's multiple comparison post-test. The mean differences between variations (time and experimental groups) were analysed using two-way ANOVA summary statistic and α 0.05 was set for each comparison.

Monocyte numbers in the NP of FhES exposed mice were significantly higher than the control (p=0.0012), D39 infected (p=0.0016) and co-exposed (p=0.0015) mice at day 1 after the infection (Figure 5.6a). The lung monocytes in co-exposed mice were significantly higher than FhES mice at day 2 (p=0.0254; Figure 5.6b). The monocytes/ MR were more abundant in the lungs than NP. Monocytes/ MR cells in the NP of FhES mice were significantly higher than the control (p=0.0076), D39 infected (p=0.0155) and co-exposed (p=0.0099) mice at day 1 (Figure 5.7a). The expression of monocytes/ MR in the lungs of FhES mice were significantly lower from D39 infected (p=0.0482) and co-exposed mice (p=0.0042) (Figure 5.7b). Although control mice were only challenged with PBS, monocytes and monocytes/ MR in the NP and lungs from this group were identified to be higher than other treatment groups at day 2 (Figure 5.6 and 5.7). Nasopharyngeal monocyte cell numbers were significantly different between experimental groups (p=0.0021) whereas lung monocytes varied significantly only over time (p=0.0213) and not based on experimental group. Both NP and lung monocytes/ MR varied significantly both over time (NP monocytes/ MR; p=0.0066, lung monocytes/ MR; p=0.0407) and by experimental groups (NP monocytes/ MR; p=0.0005, lung monocytes/ MR; p=0.0204).

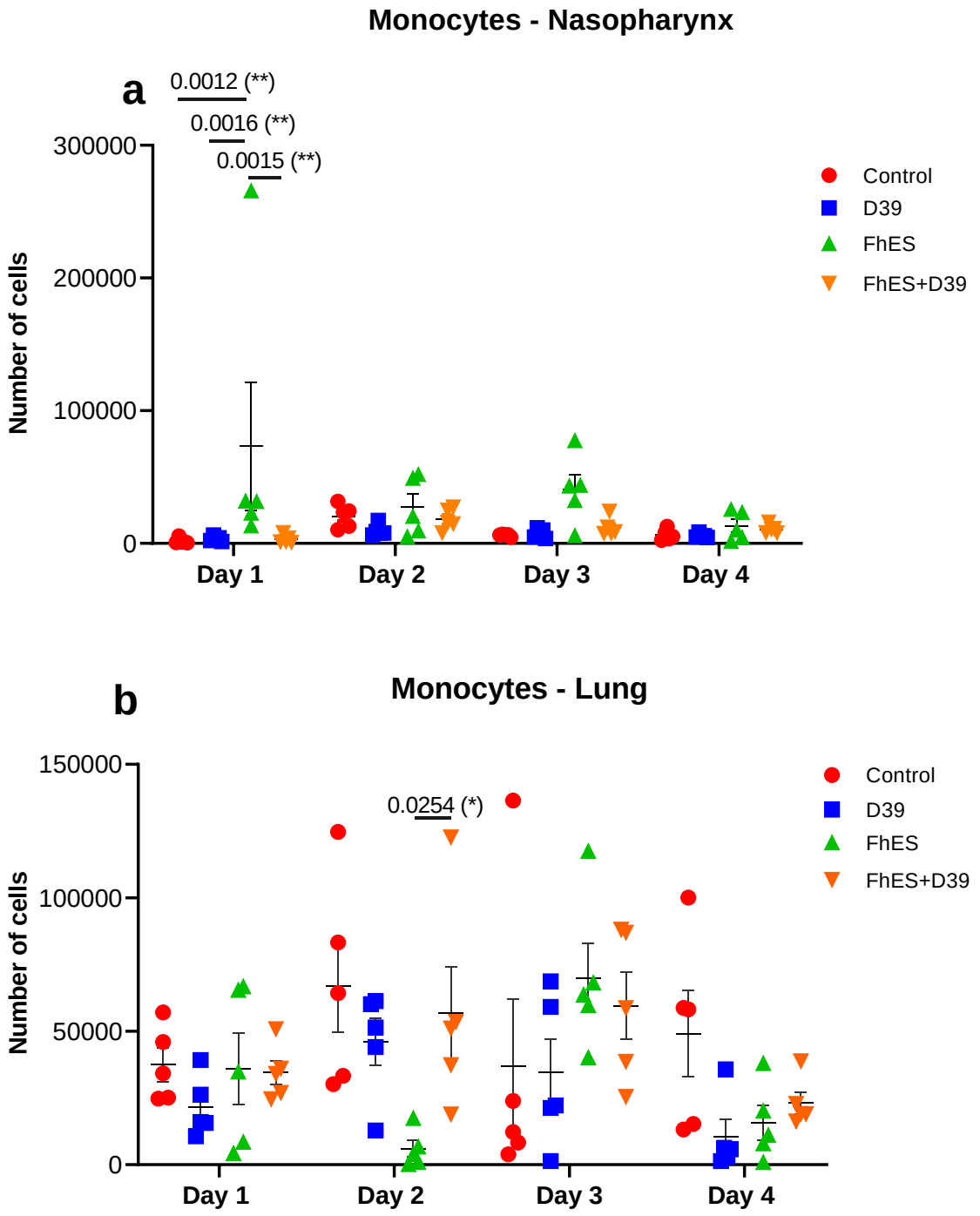

Figure 5.6: Number of monocytes in the nasopharynx and lungs over 4 days post intranasal challenge. (a) Nasopharyngeal and (b) lung cell pellets were stained with CD45 and CD115 markers to identify monocytes populations. Each symbol represents a single mouse and error bars represented ±SEM. Asterisks indicate statistically significant differences analysed using two-way ANOVA followed by Tukey's multiple comparison post-test. The mean differences between variations (time and experimental groups) were analysed using two-way ANOVA summary statistic and α 0.05 was set for each comparison.

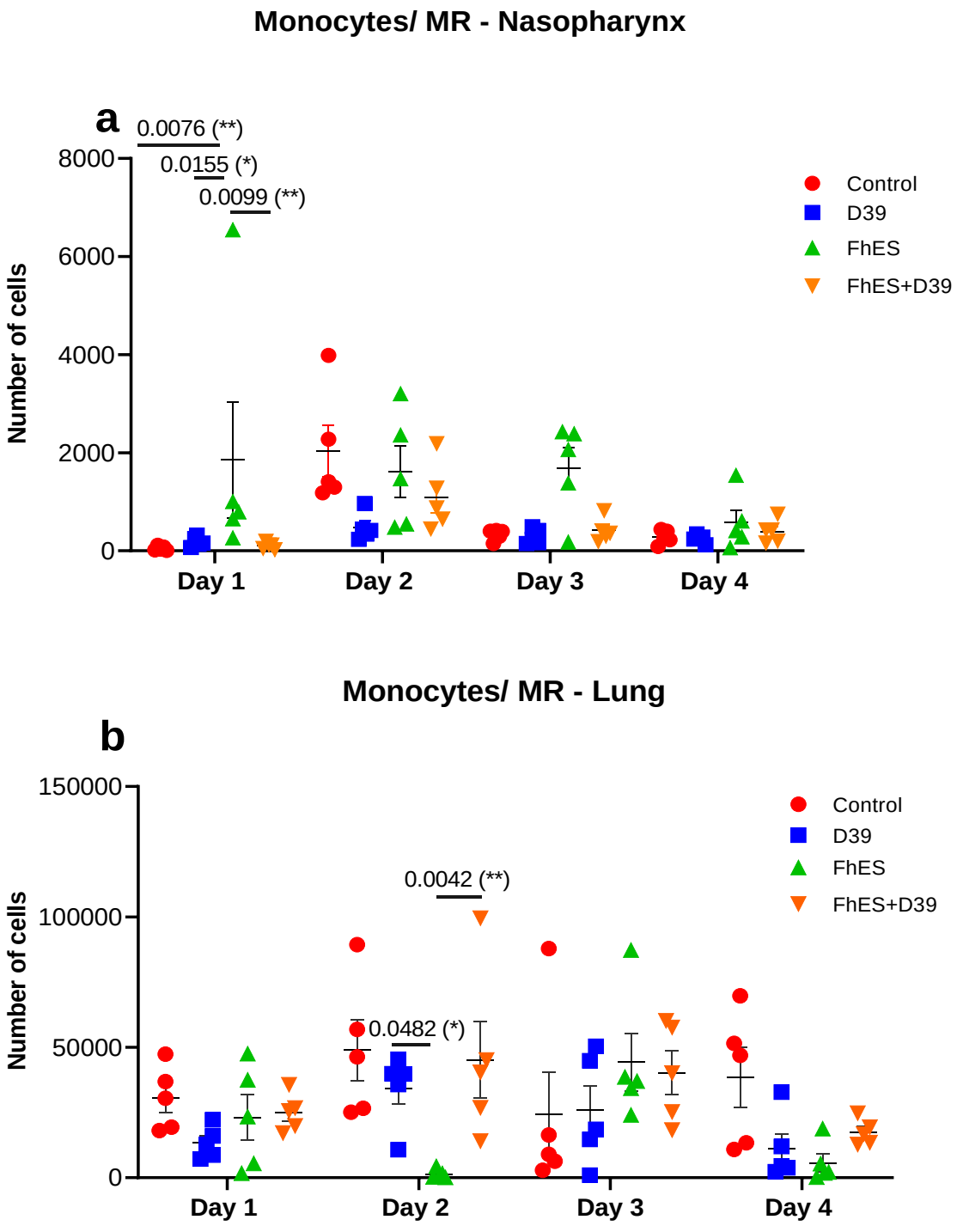

Figure 5.7: Number of monocytes/ MR in the nasopharynx and lungs over 4 days post intranasal challenge. (a) Nasopharyngeal and (b) lung cell pellets were stained with CD45, CD115 and CD206 markers to identify mannose receptor populations. Each symbol represents a single mouse and error bars represented ±SEM. Asterisks indicate statistically significant differences analysed using two-way ANOVA followed by Tukey's multiple comparison post-test. The mean differences between variations (time and experimental groups) were analysed using two-way ANOVA summary statistic and α 0.05 was set for each comparison.

Neutrophils were recruited in greater numbers to the NP than lungs. At day 1 after exposure, NP neutrophils in FhES mice were significantly higher than control mice (p=0.0489; Figure 5.8a) and lung neutrophils in FhES mice were significantly lower than co-exposed mice (p=0.0434; Figure 5.8b). Recruitment of lung neutrophils in FhES mice were significantly lower than D39 infected (p=0.0203) and co-exposed (p=0.0043) mice at days 2 post-challenge (Figure 5.8b). Infection time and experimental group variables were not significant in the NP but were significant in the lungs (duration of infections; p=0.0001 and experimental groups; p=0.0022).

B cell influx was apparent in the NP compared to the lungs. FhES mice were found to have significantly higher NP B cell numbers than D39 infected mice at day 2 (p=0.0035; Figure 5.9a). Lung B cells were significantly higher in FhES mice than D39 infected mice at day 4 (p=0.0147, Figure 5.9b). The NP B cell influx was significant across the course of infection (p<0.0001) and between experimental groups (p=0.0044). Neither variable was significant for the lungs.

At day 2 after infection, whilst NK cells recruited to the NP were significantly higher in FhES mice (p=0.0062; Figure 5.10a), NK cells recruited to the lungs of FhES mice were significantly lower than D39 infected mice (p=0.0333; Figure 5.10b). The time post-infection was a significant variable for NK cell numbers in both NP (p<0.0001) and lungs (p=0.0130) but only the NP experimental groups were significant for NK cells influx (p=0.0075).

T helper (Th) cells were found at higher numbers in the NP than in the lungs (Figure 5.11). The NP of the FhES mice demonstrated significantly higher Th cell recruitment than D39 infected mice at 2 days after infection (p=0.0202; Figure 5.11a) and time post-infection was a significant variable with respect to Th cell number (p<0.0001). No significant differences in the numbers of Th cells were observed in the lungs.

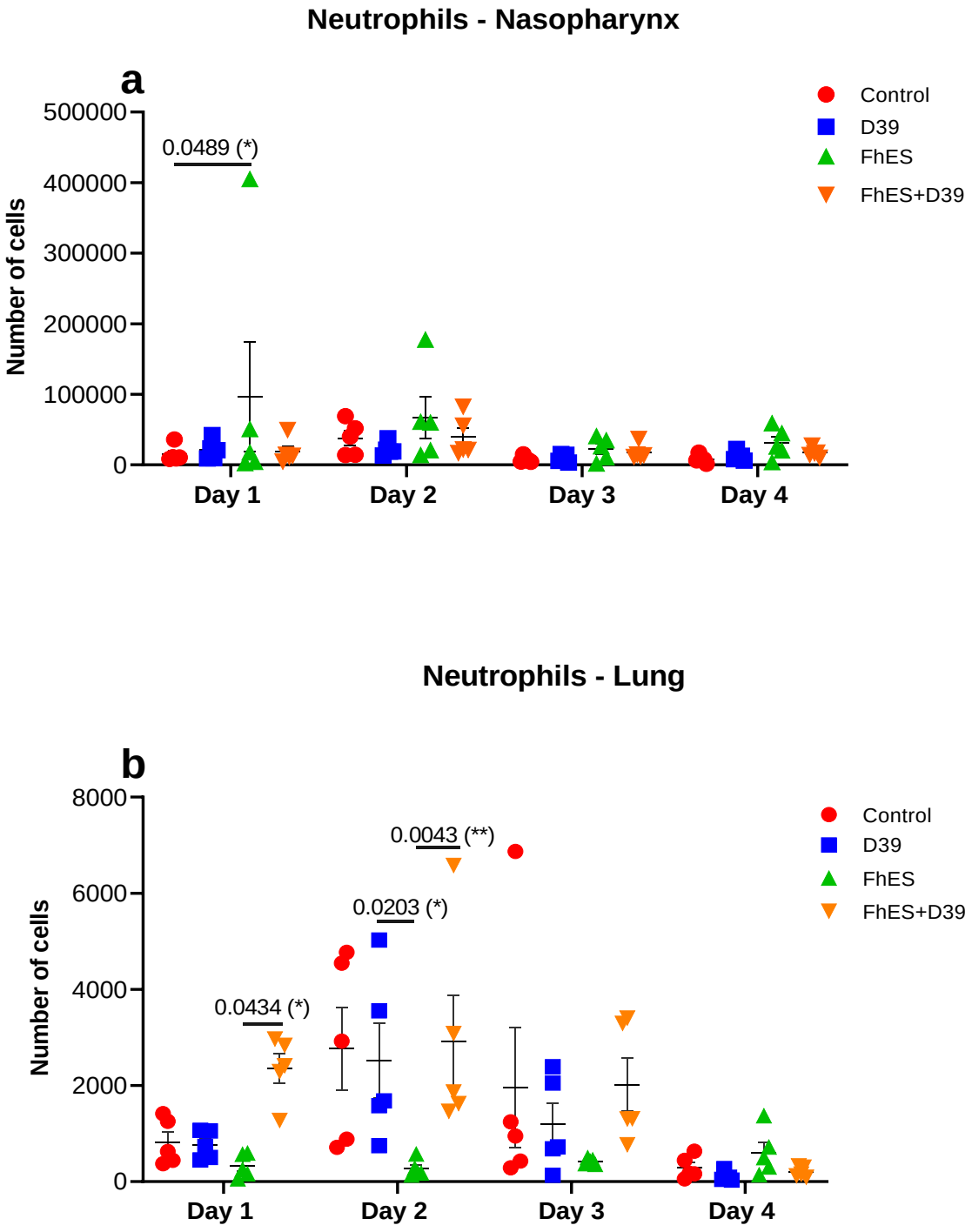

Figure 5.8: Number of neutrophils in the nasopharynx and lungs over 4 days post intranasal challenge. (a) Nasopharyngeal and (b) lung cell pellets were stained with CD45, Gr-1 and CD11b markers to identify neutrophil populations. Each symbol represents a single mouse and error bars represented ±SEM. Asterisks indicate statistically significant differences analysed using two-way ANOVA followed by Tukey's multiple comparison post-test. The mean differences between variations (time and experimental groups) were analysed using two-way ANOVA summary statistic and α 0.05 was set for each comparison.

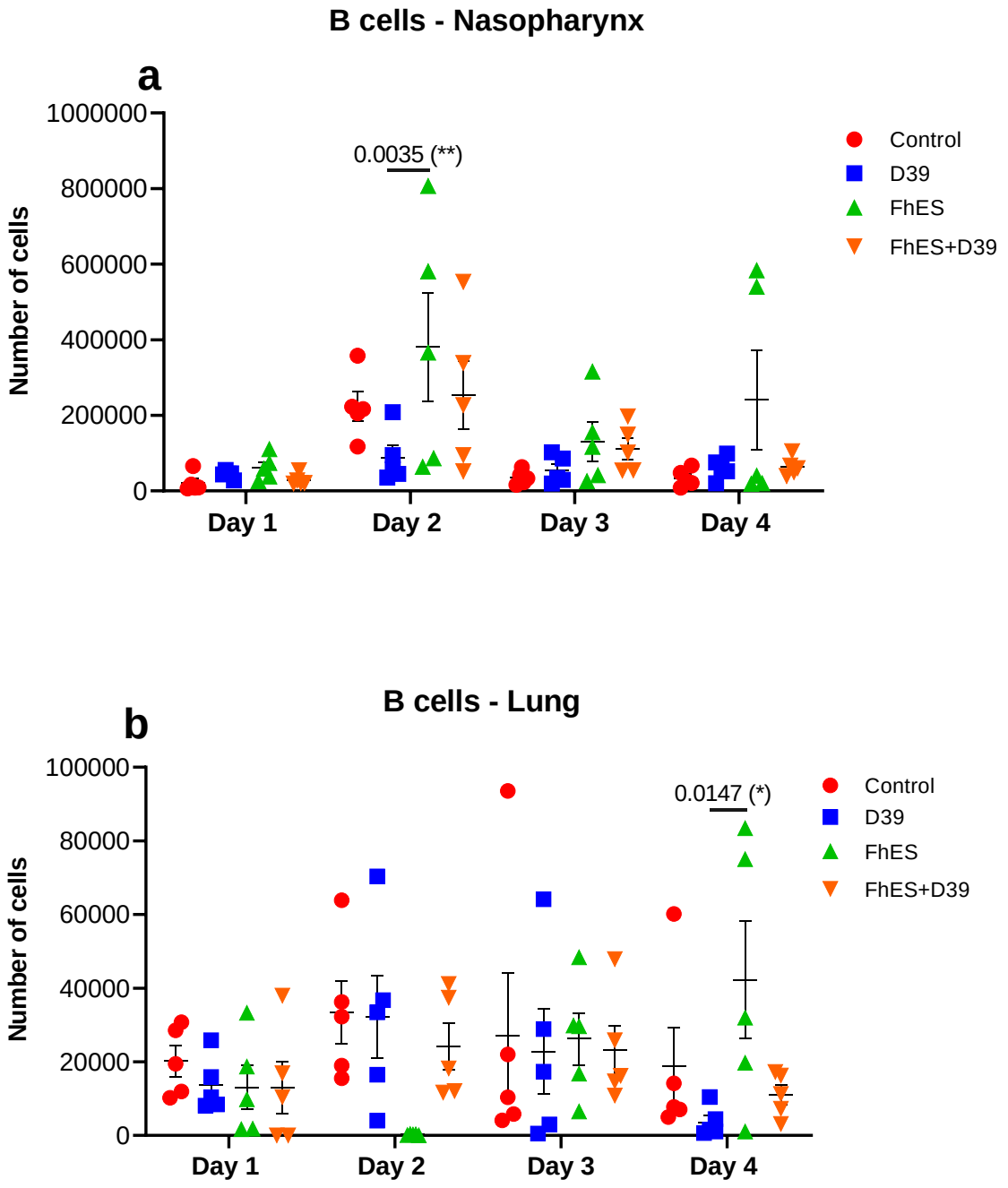

Figure 5.9: Number of B cells in the nasopharynx and lungs over 4 days post intranasal challenge. (a) Nasopharyngeal and (b) lung cell pellets were stained with CD45 and CD19 markers to identify B cell populations. Each symbol represents a single mouse and error bars represented ±SEM. Asterisks indicate statistically significant differences analysed using two-way ANOVA followed by Tukey's multiple comparison post-test. The mean differences between variations (time and experimental groups) were analysed using two-way ANOVA summary statistic and α 0.05 was set for each comparison.

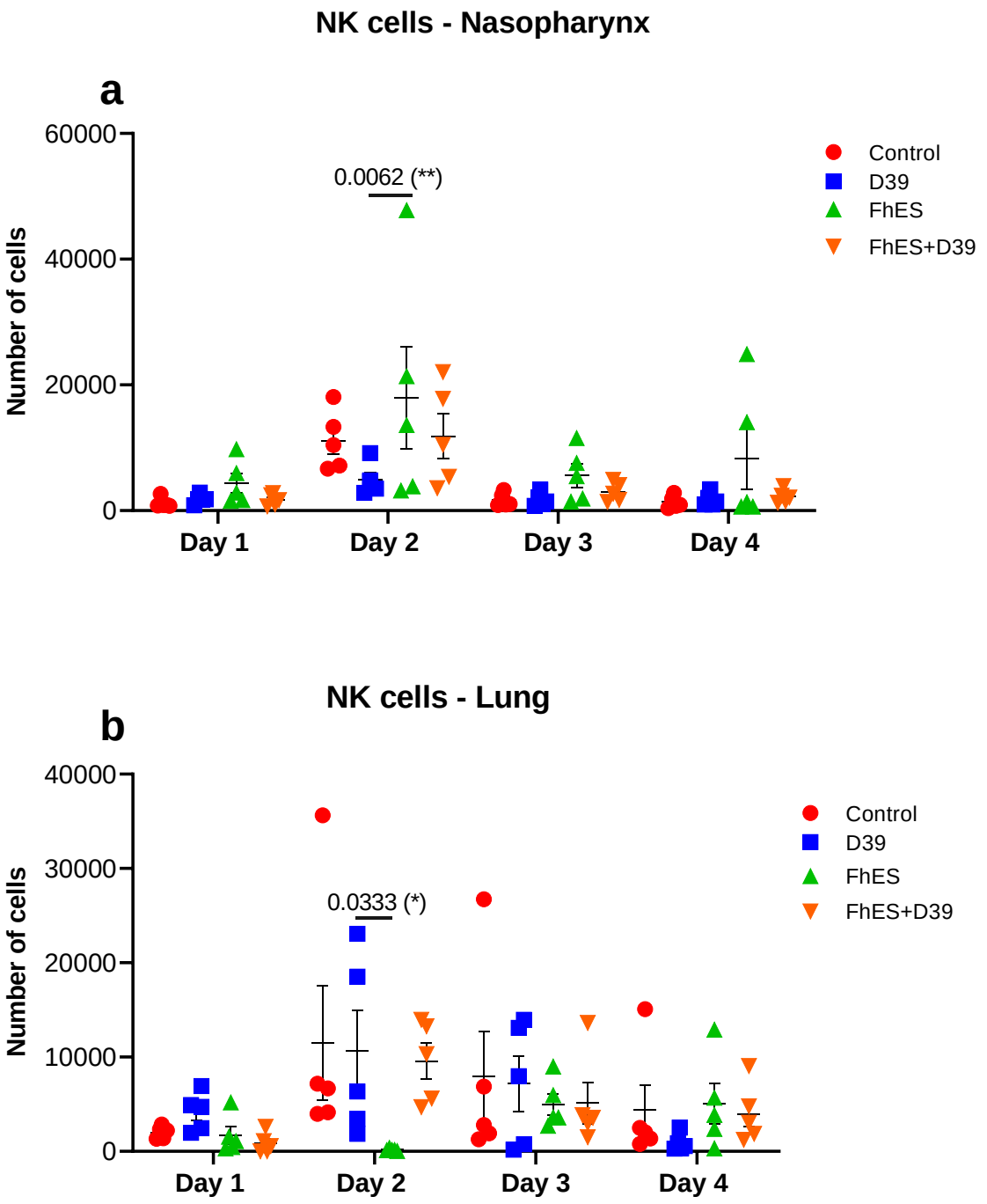

Figure 5.10: Number of Natural killer (NK) cells in the nasopharynx and lungs over 4 days post intranasal challenge. (a) Nasopharyngeal and (b) lung cell pellets were stained with CD45 and NK1.1 marker to identify NK cell populations. Each symbol represents a single mouse and error bars represented ±SEM. Asterisks indicate statistically significant differences analysed using two-way ANOVA followed by Tukey's multiple comparison post-test. The mean differences between variations (time and experimental groups) were analysed using two-way ANOVA summary statistic and α 0.05 was set for each comparison.

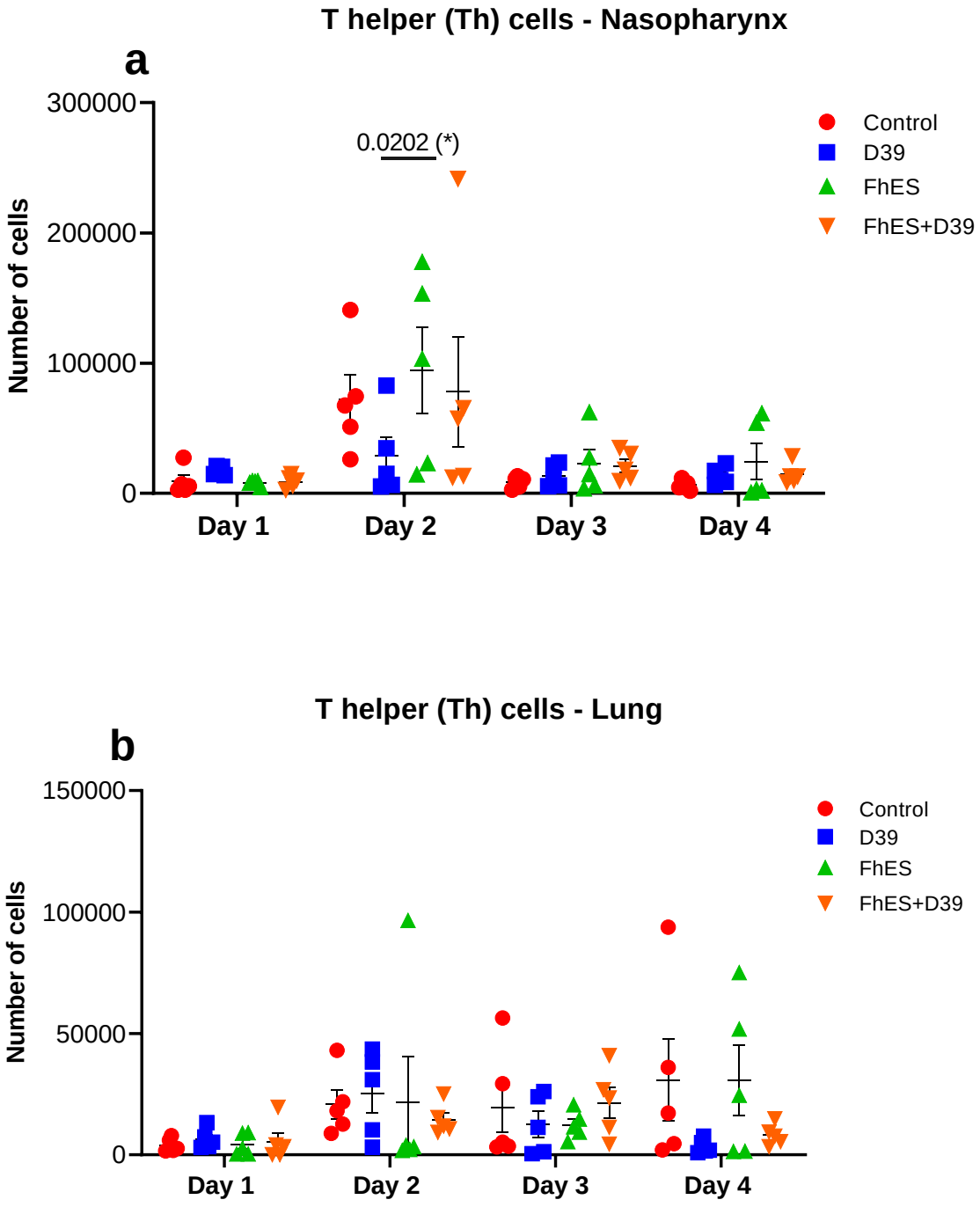

Figure 5.11: Number of T helper (Th) cells in the nasopharynx and lungs over 4 days post intranasal challenge. (a) Nasopharyngeal and (b) lung cell pellets were stained with CD45, CD3 and CD4 markers to identify Th cell populations. Each symbol represents a single mouse and error bars represented ±SEM. Asterisks indicate statistically significant differences analysed using two-way ANOVA followed by Tukey's multiple comparison post-test. The mean differences between variations (time and experimental groups) were analysed using two-way ANOVA summary statistic and α 0.05 was set for each comparison.

5.3 Discussion

S. pneumoniae, the pneumococcus, is a common commensal of the human nasopharynx. The bacteria are able to spread from the site of initial colonisation and carriage to cause a range of infections such as otitis media, pneumonia, bacteraemia and meningitis. Colonisation of the upper respiratory mucosal surface by *Streptococcus pneumoniae* is the first interaction with the human host and facilitates bacterial persistence as well as inducing host mechanisms that promote clearance. Although nasopharyngeal *S. pneumoniae* colonisation is asymptomatic, acquisition of bacterial carriage is a pre-requisite for invasive disease (Neill *et al*., 2014). *F. hepatica* is known to exert bystander suppression of Th1 responses to bacterial infection (Brady *et al.*, 1999) and has the ability to modulate the host immune system in ways which influence bovine tuberculosis diagnosis (Claridge *et al*., 2012). The present research explores, for the first time, the effects of *F. hepatica* antigens to modulate the immune response to pneumococcal infection.

The first part of this chapter demonstrates the potential of FhES antigens to enhance D39 pneumococcal nasopharynx colonisation in the NP of the co-exposed CD-1 mice. At 3 days post-challenge, bacterial densities were significantly higher in co-exposed mice than D39 infected mice. These findings were in line with those of previous studies where bacterial clearance were disturbed in the co-infected host. *F. hepatica-B. pertussis* co-infected mice recorded higher CFU count in the lungs than mice infected with bacteria alone, at 21 days after infection (Brady *et al.*, 1999). *Taenia crassiceps* and *Heligmosomoides polygyrus* infected mice challenged with serotype 2 D39 pneumococcus had an increased rate of pneumonia, decreased survival and an increased outgrowth of bacteria in the lungs and blood at 14 days after infection (Apiwattanakul *et al.*, 2014b). Although previous studies demonstrated the bacterial clearance in the lungs and blood at long duration, the results presented here shows that the bacterial clearance in the presence of FhES in the NP were disturbed at the early stages of nasopharyngeal carriage. This may relate to differences in the helminth used or in the character of the immune response induced in acute lung infection vs. asymptomatic nasopharyngeal carriage.

The impacts on host immunity of helminth-bacterial co-infection were also reported in previous studies. Innate immunity was impaired in *Heligmosomoides polygyrus*-*Salmonella enterica* serovar typhimurium co-infected mice with higher CFU counts in the faeces, mesenteric lymph nodes, spleen and liver compared to *Salmonella*-infected mice that were infected with 10^8 CFU of a SL1344 strain of *S. typhimurium* (Su *et al*., 2014). High bacterial loads in the lungs were observed in *Heligmosomoides polygyrus-Bordetella bronchisepta* lux^+ co-infected mice with significantly increased helminth egg production (Lass *et al*., 2013). In my study, whilst bacterial nasopharyngeal density at day 4 in D39 infected mice was increased, suggesting the continuity of bacterial proliferation, decreased bacterial density in co-exposed mice at this time point suggested FhES did not induce long term defects in bacterial clearance. With a low inoculum dose of 10^5 CFU D39 in 10µl PBS, I observed no significant differences when comparing lung bacterial densities over 4 days of infection. Seeding of bacteria from nasopharynx to lungs is not typical in this model, but when it does occur, it can indicate dysregulated immune responses (Shears *et al*., 2019) . Together, these results indicate that FhES may impact host regulation of nasopharyngeal carriage density, but that this does not markedly increase dissemination of bacteria to the lungs in CD-1 mice. Thus, a future study investigating the long-term effects of FhES exposure or using a higher bacterial dose (10^7 CFU) would be very interesting.

The second part of this chapter investigated cytokine and chemokine production during nasopharyngeal carriage. This part of the experiment did not detect high levels of IFN-ɣ, IL12p70, TNF-α, IL-1β, IL-6, CXCL1/KC or IL-10 production. These results were unexpected because I observed high levels of these signalling proteins in the previous chapters (except for IFN-ɣ). In the present study, all supernatants (J774.2, BMDM MΦs and NP) were assayed in the same Multiplex MSD® U-PLEX 96-well plate. There are several potential explanations that could describe low levels of these signalling proteins production. *In vitro* infection ensures that every MΦ gets exposed to the stimulants. The distribution of the stimulant's inoculum cannot be controlled in the *in vivo* setting, which probably explain the much weaker induction of MΦ responses. In addition, the dissected NP tissues were harvested in PBS that likely dilutes the cytokines quite considerably. Several cytokines, such as TNF-α, IFN-ɣ, IL-1β and IL-6 have been detected in lung homogenates at day 1, 4 and 7 after D39

infection using the same cytokine array (Shears *et al*., 2019). However, the present study only analysed the cytokines from the NP and this could explain the difference in cytokine detection production in the different types of homogenates. Whether the cytokines in the NP of the CD-1 mice during early infection are muted due to the low-density of infection or whether the method of dissection dilutes the protein too far for detection by multiplex assay requires further investigation.

Pneumococcal pneumonia in the context of influenza co-infection in a mouse model demonstrates elevated levels of both pro- and anti-inflammatory cytokines (Smith *et al*., 2007). TNF-α and IL-1β have long been known to mediate inflammation in Gram-positive bacterial infection and have been reported to be induced in pneumococcal meningitis (McAllister *et al*., 1975). Invasion by respiratory pathogens leads to the initial recognition of infection by lung epithelial cells and tissue-resident innate cells, including AMΦ and DCs. Clinical isolates of *S. pneumoniae* have been reported to induce pro-inflammatory TNF-α and IL-1β cytokines by A549 (human alveolar epithelial) and BEAS-2B (human bronchial epithelial) cells (Yoo *et al*., 2010) where Ply is responsible for the increase in TNF-α and IL-1β expression. IL-1β expression requires both Ply and TLR recognition of infection, leading to NLRP3 inflammasome activation (McNeela *et al*., 2010).

TGF-β1, an important immunosuppressive cytokine for parasite survival (Musah-Eroje and Flynn, 2018) was detected in FhES mice at day 1 after the infection by using Mouse DuoSet ELISA kit. Previous studies have reported TGF-β1 induction in *F. hepatica* infection. The TGF-β1 and IL-10 (both produced by Treg cells) induction was observed in chronic *F. hepatica* infection (Flynn and Mulcahy, 2008b; Dalton *et al.*, 2013). Neutralisation of IL-10 and TGF-β in peripheral blood mononuclear cells (PBMCs) isolated from *F. hepatica* infected cattle resulted in increased production of IFN-ɣ and IL-4 (Flynn and Mulcahy, 2008b).

S. pneumoniae is also capable of inducing TGF-β1 production, and NP Treg cell expansion *in vivo,* and this is crucial for prolonged carriage of pneumococci (Neill *et al*., 2014). BALB/c mice are known to be more resistant to pneumococcal pneumonia, demonstrated by bacterial clearance within 7 days (Gingles e*t al*., 2001; Denny *et al*.,

2003), however, blocking the TGF-β1 induction with an inhibitor impairs BALB/c resistance to infection and aids bacterial dissemination from lungs to blood (Neill *et al*., 2012). I observed lower levels of TGF-β1 production in D39 than FhES and co-exposed mice that could explain the susceptibility of CD-1 mice to D39 infection. These findings are consistent with the very low levels of NO in CD-1 BMDMΦ cultures infected with D39 compared to co-exposed cultures at 24 and 48 hours (discussed in Chapter 4). As a result of these investigations, suggestions were identified for future research. First, the use of Multiplex MSD® U-PLEX assay is not advisable to study the NP cytokine profiles in the early stages of *in vivo* nasopharyngeal carriage. Second, lung homogenates should be assayed for signalling protein production despite the bacterial densities outcome. Finally, different mouse strains, such as BALB/c, should be considered to elucidate the importance of TGF-β1 activity in the context of *F. hepatica*-pneumococcus interaction because different mouse strains are predisposed to different kinds of immune response.

The final section of this chapter describes the host immune cell responses in the NP and lungs of the CD-1 mice infected with D39 and co-exposed with FhES. As mentioned earlier, greater MΦ numbers were recorded in lung than NP, likely relating to the larger size of this organ and the presence of the tissue-resident AMΦ population. At 3 days post–exposure, FhES mice demonstrated significant increase of MΦs recruitment to the NP than other experimental groups. MΦs are involved in the elimination of intracellular pathogens such as *M. bovis* or *Listeria monocytogenes* (Gordon, 2003) and many extracellular pathogens including *F. hepatica* (Reyes and Terrazas, 2007). FhES antigens have been associated with the induction of immunomodulatory effects on MΦs (Guasconi *et al*., 2015) which lead to AAMΦ activation (Flynn *et al*., 2007a). Intra-peritoneal administration of FhES induced the recruitment of AAMΦ to the peritoneum of BALB/c mice (Donnelly *et al*., 2005). Others have reported that fatty acid binding protein (FABP) of *F. hepatica* induces the AAMΦ of human MΦs (Figueroa-Santiago and Espino, 2014).

In the context of *F. hepatica*-bacterial interactions, *F. hepatica* helminth defence molecules (FhHDM)-LPS binding impairs MΦ activation and induction of innate immune responses (Robinson *et al*., 2011). Infection with the extracellular bacteria *S.*

pneumoniae induces phagocytic activity of AMΦ (Knapp *et al*., 2003; Mina *et al*., 2015) to clear the bacteria from the lower airway (Aberdein *et al*., 2013), where MΦ phagocytosis is essential to the immune defence system against *S. pneumoniae.* AMΦ play an important role in the early hours of pneumococcal infection in murine models (Sun *et al*., 2011). Here, I observed high numbers of MΦ in the lungs of D39 mice at days 2 and 3 post-challenge, indicating the influx of these cells to the infected area from the NP or recruitment and differentiation of monocytes. NP MΦ numbers were reduced at days 3 and 4, perhaps suggesting the draining of MΦ that had taken up bacterial antigens to the local lymph nodes. Although the D39 infected mice were challenged with 10^5 CFU of D39 to establish nasopharyngeal carriage, the MΦ influx in the lungs suggest at least some dissemination of bacteria or bacterial products to the lower respiratory tract.

MR recognises mannose- and fucose- containing glycans in nematode and trematode parasites, and MR interaction with FhES induces immunoregulatory effects in MΦs (Guasconi *et al*., 2011). The binding of MR to Ply enhances pneumococcal survival by suppressing inflammatory responses (Subramanian *et al*., 2018). I observed significant expression of MR on NP MΦ in FhES mice compared to other experimental groups at day 3. The increase in MR-expressing MΦ in lungs of D39 infected mice at day 3 and 4 reflect the increases in total MΦ numbers in lungs in the same experimental group. The NP and lung MR^+/ MΦ in co-exposed mice were increased at day 2 but later decreased over time and these results are similar to those observed in the NP and lung MΦ populations in mice co-exposed to both pneumococci and FhES. To summarise, this experiment has demonstrated influx or expansion of MΦs in infected respiratory tissue following low dose D39 infection of CD-1 mice. D39 infection and FhES exposure in mice induces increased MΦ recruitment and increased expression of MR on MΦs in both NP and lungs, although this effect is transitory, with numbers reducing over time post-infection.

In animals, the circulating monocytes and their progeny, MΦ and DCs are derived from the bone marrow (Wynn *et al*., 2013). Blood monocytes are recruited into the nasal interstitial spaces, where they differentiate into MΦs that perform phagocytosis (Dorrington *et al*., 2013). Monocytes are essential in innate immune responses to

bacteria including *S. pneumoniae* (Webster *et al*., 2010) and contribute to T-cell recruitment at sites of infection (Serbina *et al*., 2008). $CD3^+$ T cell apoptosis in PBMC cultures required classical $CD4^+$ monocytes, which increased T cell activation (Daigneault *et al*., 2012). In the present study, monocytes and monocytes/ MR were recruited in significantly greater numbers to the NP of FhES mice compared to other experimental groups at day 1. FhES consists of many types of immunomodulatory proteins that possibly trigger the monocyte recruitment to the NP and lungs. NP monocytes and MR-expressing monocytes were steadily recruited up until day 3 and this may have helped maintain the differentiated MΦ populations in the NP. Co-exposed mice demonstrated a significant increase in lung monocytes and MR-expressing monocytes relative to FhES only mice at day 2. Whilst total lung monocytes did not differ significantly between D39 mice and FhES mice, the MR^+ lung monocytes population in D39 mice was significantly elevated as compared to FhES mice at day 2. Together, these results indicate that FhES induced monocyte recruitment and MR expression, and this pool of cells may help maintain and replenish MΦ populations in the NP. In the presence of D39, monocyte recruitment and MR expression was further enhanced in co-exposed animals.

The present study demonstrated elevated numbers of neutrophils in the NP compared to the lungs. These observations were not unexpected as neutrophils are the primary cells recruited to inflamed sites during an infection or tissue damage (Petri and Sanz, 2018). The initial immune response to pneumococcal colonisation is also characterised by a rapid neutrophil response (Zhang *et al*., 2009; Yamada *et al*., 2011). Neutrophil recruitment was significantly enhanced in D39 infected mice, as compared to FhES exposed mice at day 2 but the numbers decreased over time, which could be due to bacterial clearance, as neutrophils are known to be primary mediators of bacterial killing in the lungs (Tsai *et al*., 2000; Mizgerd, 2002). In pneumonia, cytokines and chemokines are released in order to attract neutrophils to the affected lung area when AMΦs fail to control the invading pathogens (Kolling *et al*., 2001; Nelson, 2001). Neutrophils were recruited into the lungs within 12 hours in response to cytokines and chemokines released from macrophages and epithelial cells (Kadioglu *et al*., 2000).

In the context of helminth infections, neutrophils are required for protective immunity to *Strongyloides stercoralis* in mice (O'Connell *et al.,* 2011). Besides neutrophils, eosinophils have been identified to be effector and immunomodulatory cells during helminth infections (Cadman and Lawrence, 2010). In *Nippostrongylus brasiliensis* infection, neutrophils 'train' lung MΦs to acquire long-term protective features against helminth larvae during secondary infection (Grainger and Grencis, 2014). *F. hepatica* secretes a factor that inhibits the superoxide output from activated neutrophils (Jefferies *et al*.,1997). Neutrophils, eosinophils, MΦ and mast cells were recruited into the peritoneal cavity of *F. hepatica* infected mice (Walsh *et al*.,2009) and rats (Jedlina *et al*., 2011). In the present study, FhES mice had significantly elevated neutrophil numbers in the NP than the control mice at day 1 but not in the lungs. However, in the presence of D39, lung neutrophils in the co-exposed mice were significantly higher from FhES mice at days 1 and 2 post-exposure. Although not significant, co-exposed mice demonstrated more neutrophils recruitment than D39 infected mice. Taken together, both stimulants, D39 and FhES activate neutrophil recruitment to the NP.

B cells, NK cells and T cells play an important role in both innate and adaptive immune response to *F. hepatica* (Fu *et al.*, 2016). FhES mice showed significantly higher B cell recruitment to the NP compared to the lungs. The cell numbers were significantly higher than D39 infected mice in the NP (day 2) and lung (day 4). B cells have been reported to promote and support Th2 immune responses during helminth infections (Hernandez *et al*., 1997; Blackwell and Else, 2001). IL-4 and IL-13 cytokines are secreted by Th2 cells and direct B cells to produce helminth-specific IgE antibody (Anthony *et al.*, 2007; Erb, 2007). B cells are responsible for producing antibodies, which are known to contribute towards immunity to *H. polygyrus* in mice (McCoy *et al*., 2008).

At day 2 post-exposure, whilst NK cells were significantly higher in the NP of the FhES mice, recruitment to the lung was significantly lower than in D39 infected mice. Sprague Dawley rats infected with *F. hepatica* demonstrated a significant increase of NK cells recruitment in the peritoneal cavity up until 4 days before decreasing at 7 days post-infection (Jedlina *et al.,* 2011). *Schistosoma mansoni* can activate NK cells to produce immunoregulatory cytokines *in vivo*, enabling them to influence the

adaptive immune response (Mallevaey *et al*., 2006). In the context of pneumococcal infection, NK cells are recruited to the lung in pneumococcal pneumonia within 6 hours of infection (Kawakami *et al*., 2003). NK cells are known to be the major source of IFN-ɣ in *S. pneumoniae* meningitis (Mitchell *et al*., 2012). NK cells are also responsible for rapidly inducing IFN-ɣ during acute infections caused by Group B *Streptococcus* and *Streptococcus suis* (Lemire *et al*., 2017).

$CD4^+$ T cells can be categorised into conventional Th cells and regulatory T (Treg) cells. Whilst Th cells regulate adaptive immunity against pathogens by activating other effector immune cells, Tregs suppress potentially deleterious activities of Th cells (Corthay, 2009). IL-17A secreting Th17 cells are essential for clearance of pneumococci from the NP in murine (Trzciński *et al*., 2008; Lu *et al*., 2008; Zhang *et al*., 2009) and human pneumococcal carriage (Wright *et al*., 2013). In contrast, a weak Th17 response was observed in infections caused by D39 and virulent serotype 4 (TIGR4) pneumococci compared to other frequently identified bacterial colonisers in the NP (Xu *et al*., 2020). Whilst live pneumococci elicited a Th1-biased response via production of IL-12p40, heat-killed pneumococci elicited a Th17 response through TLR2 in human monocytes (Olliver *et al*., 2011). *S. pneumoniae*-activated Tregs are known to be highly suppressive of T cell response (Zhang *et al*., 2011) and control the susceptibility to invasive pneumococcal pneumonia in mice (Neill *et al*., 2012). As previously described in Chapter 1, helminths are known to polarise CD4+ Th cells towards Th2 responses, induce AAMΦs and expand Treg cells. In the present study, Th cells were recruited to the NP of FhES exposed mice in significantly greater numbers than in D39 mice at day 2 post-exposure.

In summary, the findings presented in this part of the chapter show that live D39 and FhES antigens are able to trigger localised innate and adaptive immune responses. In this experiment, an increase in immune cell recruitment was observed in the control mice at day 2, limiting the ability to fully understand the true immune responses and the significance of the findings. Future work is required to establish the whole picture of immune profiles in FhES-pneumococcus interaction. The immunomodulatory phenotypes of Th cells subtypes (Th1, Th17, Treg) between these two pathogens in the host also remains to be elucidated.

C-type lectin receptors MR and Dectin-1 have been reported to modulate Arg-1 and programme-death ligand-1 (PDL-1) expressions, and TGF-β production by MΦs in response to *F. hepatica* excretory-secretory products (Guasconi *et al*., 2011; Guasconi *et al*., 2015). The elevation of immune-suppressive cytokine TGF-β1 driven by FhES may act as fluke strategy to extend their survival in the early stage of infection. FhES+D39 induced NP to maintain the TGF-β1 secretion for their survival, thus shaping the immune response of the co-exposed CD-1 mice by suppressing immune responses during infection. These results could serve as a disease model to extrapolate the outcome in the context of human co-infection. MR is an AAMΦ phenotype marker of cells involved in pathogen clearance and plays a role in innate and adaptive immune responses. The influx of MR expressing monocytes/ MΦs observed in the present study suggests the involvement of AAMΦs in the co-exposed mice that may influence the activation of the acquired immune system as the disease progresses.

The main limitation of this experiment is the use of FhES antigen rather than live fluke infection. Although the results presented here demonstrate the potential of FhES to promote pneumococcal colonisation and mediate immunomodulation in the co-exposed CD-1 mice, I believe, an active *F. hepatica* infection in the liver will enhance the impact on the pneumococcal survival and induce stronger MΦs responses. Thus, future studies should assess the impact of live fluke to further understand the real host immunity of *F. hepatica-S. pneumoniae* co-infection.

5.4 Conclusion

This part of the thesis discusses the impact of FhES exposure on D39 *S. pneumoniae* nasopharyngeal carriage in CD-1 mice. The results showed that FhES transiently promotes increased pneumococcal colonisation density that may affect host susceptibility to pneumococcal disease during the early stage of infection. The inflammatory cytokines and chemokine were only weakly induced in the NP, although immunomodulatory TGF-β1 was induced more strongly.

Innate and adaptive immune cells were recruited to the NP and lungs over the course of infection. Low dose colonisation of NP with D39 still allows for some dissemination of the bacteria to the lungs, indicated by the influx of immune cells to those tissues. Recruitment of MΦ and monocytes, including MR-expressing populations, was notable. Influx of neutrophils, B cells, NK cells and Th cells were apparent in the NP compared to the lungs, indicating this site as the focal point of immune responses to pneumococcal carriage.

Chapter 6

Macrophage gene expression in response to Fasciola hepatica-pneumococcus co-exposure

CHAPTER 6

Macrophage gene expression in response to *Fasciola hepatica*-pneumococcus co-exposure

6.1 Introduction

MΦs are involved in immune and homeostatic processes and can adopt a variety of activation phenotypes. Whilst bacterial infections typically induce classically activated MΦ (CAMΦ) that produce anti-microbial effector molecules such as NO and produce pro-inflammatory cytokines, helminth infections induce alternatively activated MΦ (AAMΦ) characterised by the up-regulation of arginase, Ym1 and Fizz1 and produce anti-inflammatory cytokines such as IL-10 and TGF-β. CAMΦ and AAMΦ have different roles that can destroy pathogens or repair the inflammation-associated injury, respectively (Shapouri-Moghaddam *et al*., 2018). Differentiation and activation of MΦs depends on various stimuli, signalling pathways and tightly regulated transcription (Schultze *et al*., 2015). In the present study, transcriptomic profiling of activated BMDMΦs was undertaken using Nanostring, a high throughput method for measuring multiple targets of gene expression in a single sample. The BMDMΦs were infected with 10^5 CFU of D39 and co-exposed to FhES for 6 hours, analysed for mRNA transcriptome using a Mouse Myeloid_v2 732-innate immunity gene panel and the plots were generated from the nCounter Advanced Analysis software (Section 2.11).

6.2 Results

6.2.1 Overview of principal component analysis (PCA) and heatmap of all data of innate immune gene expression

Figure 6.1 shows the summary of principal component analysis (PCA) of the normalised gene expression in BMDMΦs treated with different stimulants. PCA transforms multiple variable data into a linear set of principal components. Principal component 1 (PC1) captured the highest level of variance between samples, where a clear separation between treatments is observed. Replicates of the same treatment condition (represented the same colour) clustered most closely together in the PC1 plot. Each replicate from the same treatment group is highly correlated with each other.

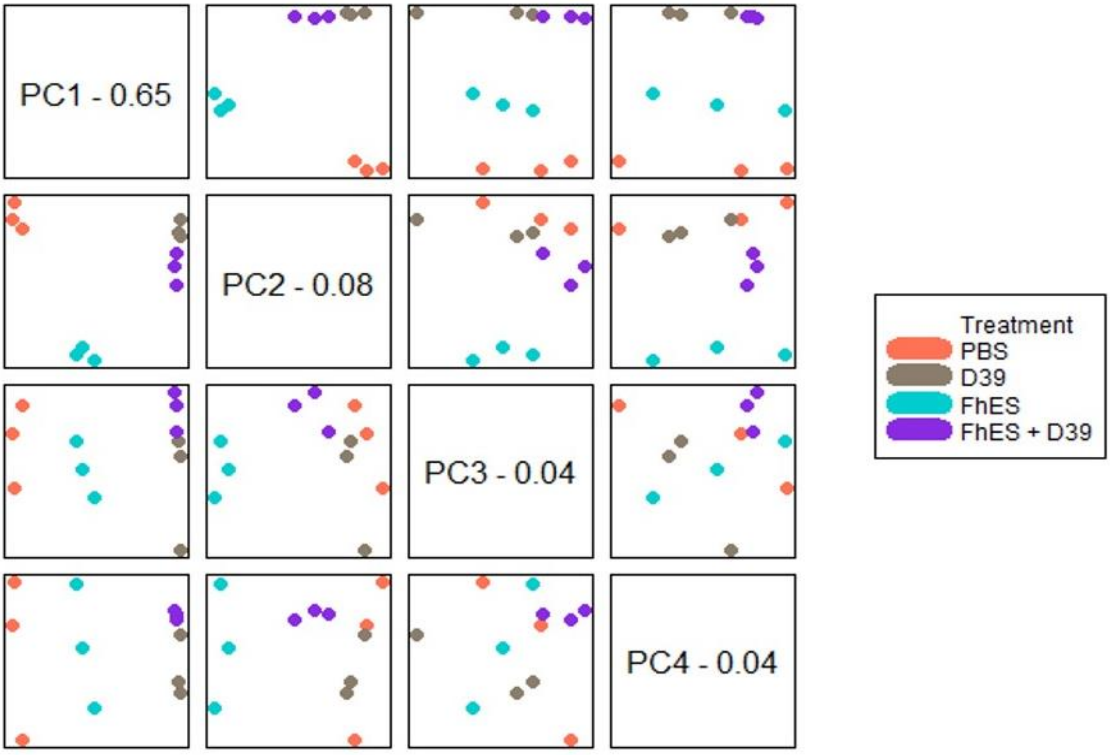

Figure 6.1: Principal component analysis (PCA) of the normalised genes for each treatment group after 6 hours of exposure to different stimulants. Each group is represented by three replicates and four principal components of the gene expression data are plotted against each other. The numbers represent positive coefficients for all variables.

Figure 6.2 displays the overview heatmap of the normalised data that is plotted by z-score, that measures the correlation distance from the mean of a normally distributed data set. All groups were clustered, based on shared patterns of gene expression, in a cluster dendrogram. A cluster dendrogram calculated from the expression level of all genes showed that BMDMΦs infected with D39 have a transcriptomic profile much more closely related to that of co-exposed cells than to PBS and FhES stimulated cells.

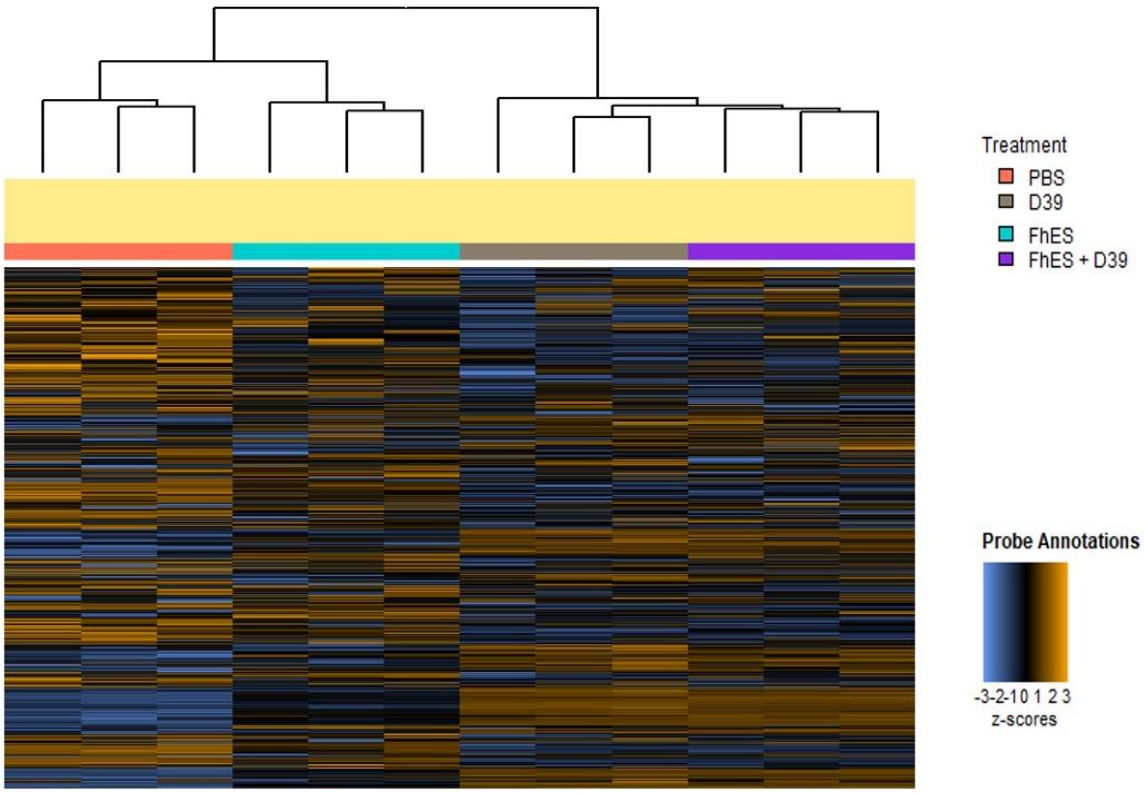

Figure 6.2: Overview of the heatmap of the normalised genes generated via unsupervised clustering. Each group is represented by three replicates and the normalised data was scaled to give all genes equal variance. Each row of the heatmap represents a single probe, and each column is a single sample. Orange indicates high expression; black indicates average expression; blue indicates low expression. Hierarchical clustering is used to generate dendrograms.

6.2.2 Differentially expressed genes (DEGs) in D39, FhES and co-exposed BMDMΦs

The genes of pro-inflammatory cytokines *TNF-α* and *IL-1β*, and chemokine ligands *CCL3*, *CCL4* and *CCL5* (or regulated upon activation normal T cell expressed and secreted; RANTES), were significantly up-regulated (p<0.01) in D39 infected BMDMΦs relative to PBS treated cells. The *IL-1β* gene represents the highest log2 fold change (log2 FC) (Figure 6.3). A member of the TNF receptor family, the *TRAF1* gene, and inflammasome *NLRP3* gene were also significantly up-regulated. The significantly up-regulated genes of FhES exposed BMDMΦs, compared to PBS treated cells, are shown in Figure 6.4. *TNF-α, IL-1β, CCL2* (monocyte chemoattractant protein 1 (MCP-1), *CCL3, CCL4, TRAF1* and toll-like receptor *(TLR) 2* genes were significantly up-regulated in response to FhES (p<0.01). Figure 6.5 displays the differentially expressed genes (DEGs) in co-exposed BMDMΦs, with *TNF-α, IL-1β, CCL3, CCL4, TRAF1, NLRP3* and *IL-10* genes all significantly up-regulated (p<0.01). *CXCL1* gene recorded the highest log2 FC in response to both stimulants. Table 6.1 represents the comparison of the most statistically significant DEGs in D39, FhES and in combination of both stimulants extracted from the nCounter Advanced Analysis table.

Table 6.1: Log2 fold changes between treatments of the most statistically significant DEGs after 6 hours of exposure vs. baseline of PBS control.

Gene	Treatment		
	D39	FhES	FhES + D39
	Log2 FC		
TNF-α	6.18	1.55	6.41
IL-1β	8.12	3.75	8.59
IL-10	3.65	1.91	5.04
CCL2	4.33	3.5	4.80
CCL3	5.54	1.46	5.78
CCL4	4.83	1.95	5.83
CCL5	5.77	1.66	6.47
TRAF1	6.28	3.75	6.78
NLRP3	4.94	2.37	5.11
TLR2	2.56	1.90	2.54
CXCL1	12.5	1.07	12.8

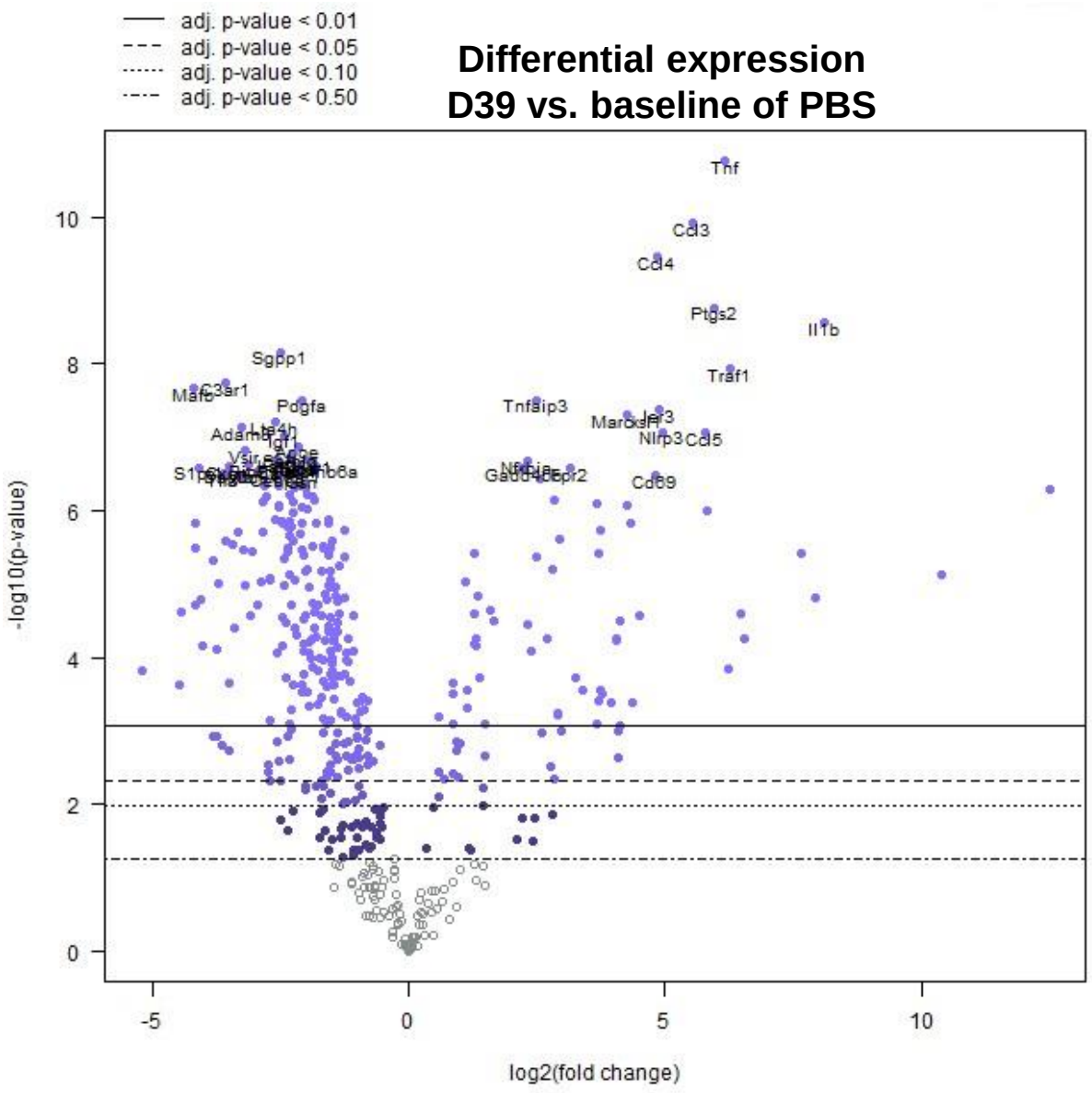

Figure 6.3: Volcano plot showing the extent of log_2 and –log10 adjusted p-value for the differentially expressed genes (DEGs) identified in D39 infected BMDMΦs vs. baseline of PBS (control). Highly statistically significant genes fall at the top of the plot above the horizontal lines and high fold changes fall to either side. Horizontal lines indicate various False Discovery Rate (FDR) thresholds or p-value thresholds. Coloured genes represent the p-value that is below the given FDR or p-value threshold. The statistically significant genes are labelled in the plot.

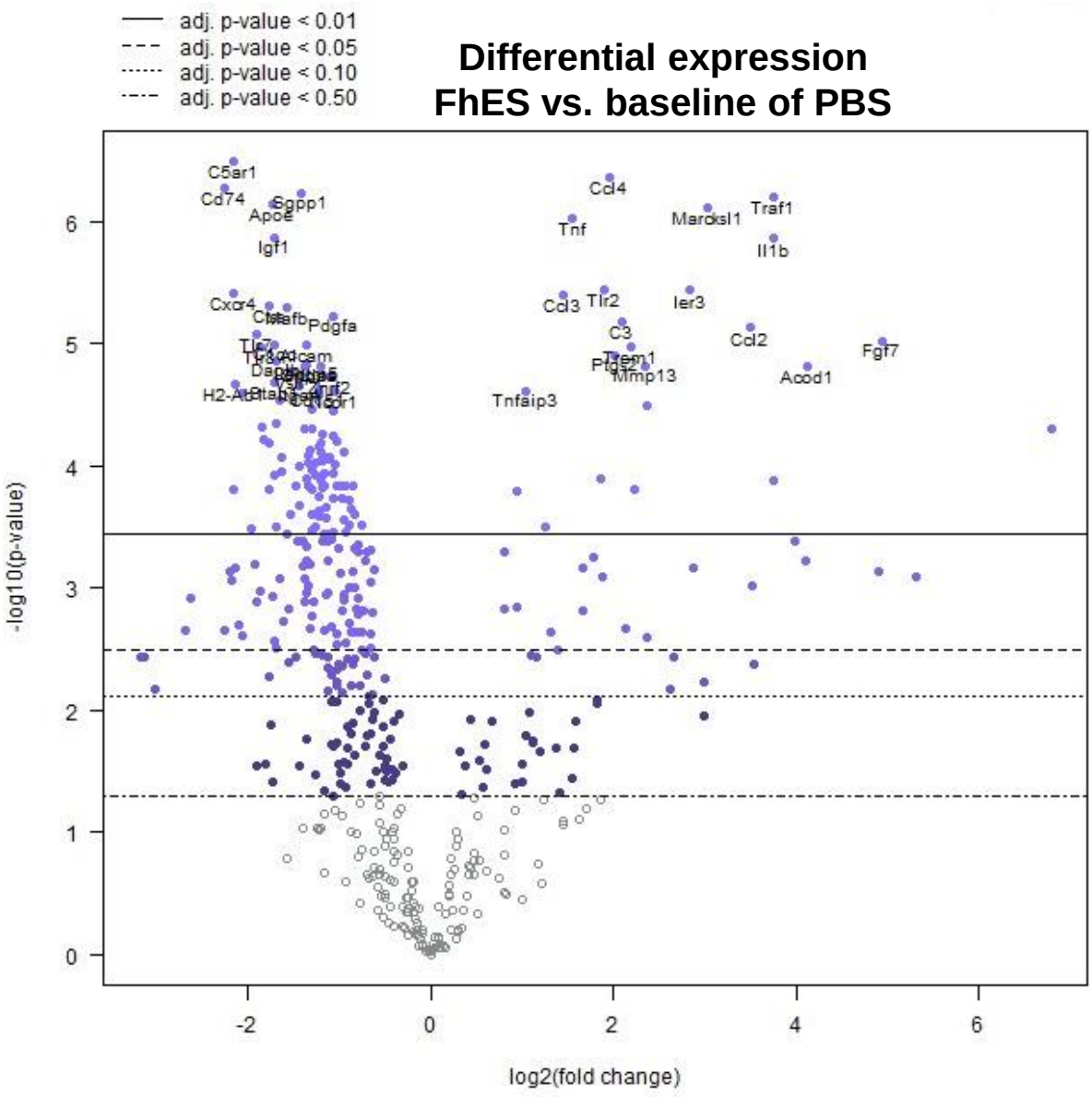

Figure 6.4: Volcano plot showing the extent of log_2 and –log10 adjusted p-value for the differentially expressed genes (DEGs) identified in FhES exposed BMDMΦs vs. baseline of PBS (control). Highly statistically significant genes fall at the top of the plot above the horizontal lines and high fold changes fall to either side. Horizontal lines indicate various False Discovery Rate (FDR) thresholds or p-value thresholds. Coloured genes represent the p-value that is below the given FDR or p-value threshold. The statistically significant genes are labelled in the plot.

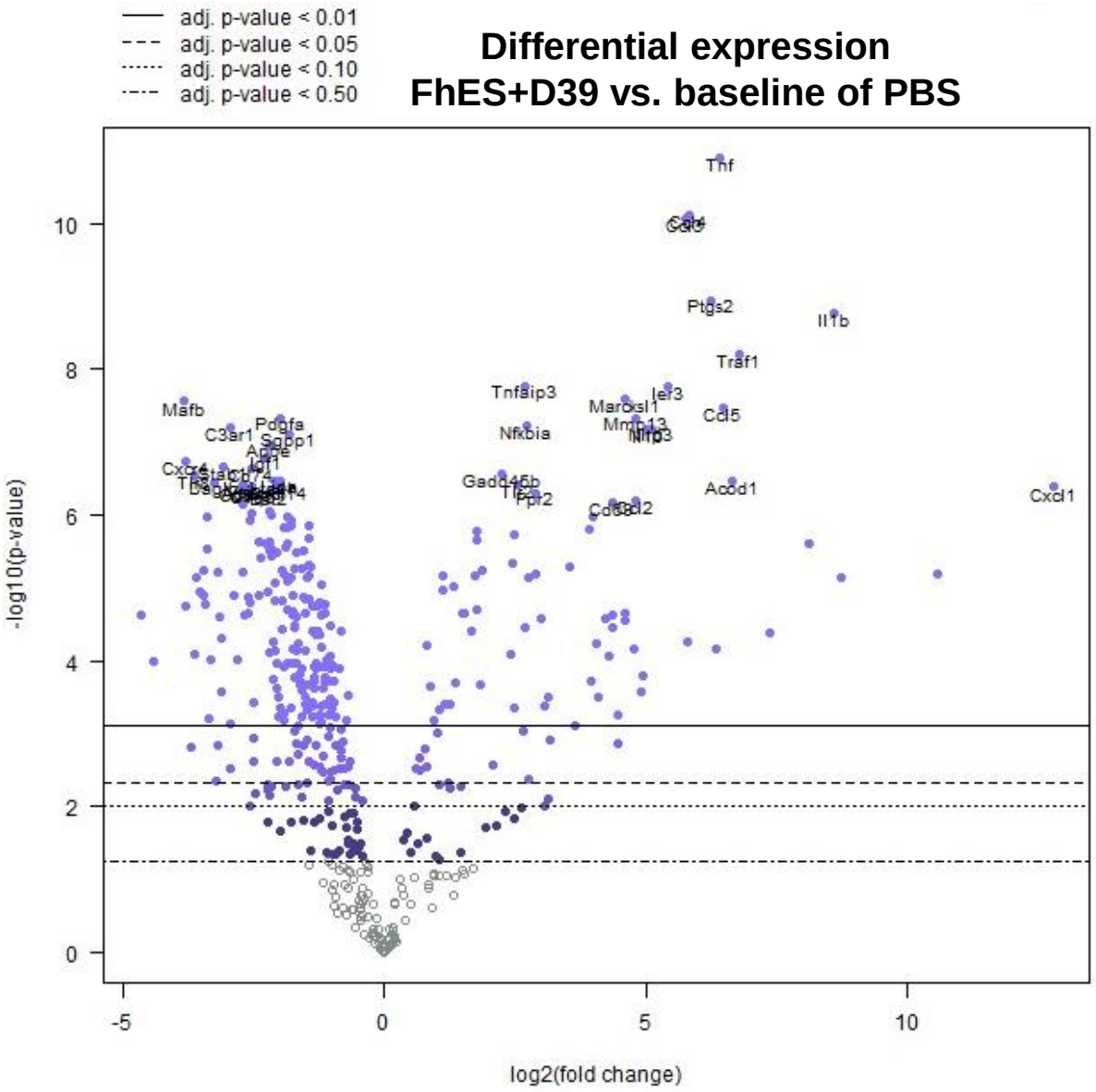

Figure 6.5 Volcano plot showing the extent of log_2 and –log10 adjusted p-value for the differentially expressed genes (DEGs) identified in FhES+D39 co-exposed BMDMΦs vs. baseline of PBS (control). Highly statistically significant genes fall at the top of the plot above the horizontal lines and high fold changes fall to either side. Horizontal lines indicate various False Discovery Rate (FDR) thresholds or p-value thresholds. Coloured genes represent the p-value that is below the given FDR or p-value threshold. The statistically significant genes are labelled in the plot.

6.2.3 Co-exposed BMDMΦs up-regulate Th1 associated genes

The heatmap depicted in Figure 6.6 represents the gene sets that are most differentially expressed. The extent of differential expression in each gene set is summarised using a global significance score. After 6 hours of exposure, D39 and co-exposed BMDMΦs show up-regulation of Th1 associated genes displayed by the red colour code indicating an extensive over-expression of the genes. However, FhES BMDMΦs display pale red in Th1 activation, chemokine signalling and pathogen response, indicating only weak up-regulation of members of these gene sets. On the other side, Th2 genes were down-regulated in all treatment groups, relative to PBS exposed cells. I next compared the differential expression of Th1 activation genes within the D39 and co-exposed groups showing most extensive evidence of up-regulation; D39 and co-exposed cultures. Th1 activation associated genes including pro-inflammatory *TNF-α* and *IL-12b*, and anti-inflammatory *IL-10* were significantly up-regulated in D39 infected cells (p<0.01) (Figure 6.7). *TNF-α* and *IL-10* were also found to be significantly more highly expressed in the co-exposed cells, vs. PBS controls (p<0.01) (Figure 6.8).

Co-exposed BMDMΦs were also seen to over-express genes in the chemokine signalling, pathogen response and TLR signalling functional groups, to a greater extent than D39 infected BMDMΦs, as indicated by the different intensity of the red colour on the heatmap (Figure 6.6). Chemokines *CCL2, CCL3, CCL4, CCL5, CCL7* and *CCL9*, and *CXCL1*, *CXCL2, CXCL3, CXCL5* and *CXCL10* were significant up-regulated (p<0.01) in the context of chemokine signalling (Figure 6.9). *TNF-α, IL-1β, IL-6, CCL5, CXCL1, CXCL10 (IP-10)* and *NLRP3* were significantly up-regulated in the pathogen response genes (p<0.01) (Figure 6.10). TLR signalling genes within significant up-regulation were *TNF-α, IL-1β, IL-6, CCL4, CCL5, CXCL10* and *TLR2* (p<0.01) (Figure 6.11).

Only four Th1 associated genes, *TNF-α, CCL3, CXCL1* and *CXCL2* differed significantly between D39 and co-exposed BMDMΦs suggesting that co-exposure with FhES only minimally alters the way in which BMDMΦ respond to pneumococcus. The raw mRNA counts of the most highly expressed genes were statistically analysed and summarised in Table 6.2.

Table 6.2: Comparison of the most highly differentially expressed genes between D39 and co-exposed BMDMΦs. The counts were analysed using two-way ANOVA followed by Sidak's multiple comparison post-test.

Gene	Significant	Adjusted *p* value
TNF-α	Yes	<0.0001
IL-1β	No	0.7191
IL-10	No	>0.9999
CCL2	No	>0.9999
CCL3	Yes	0.0006
CCL4	No	>0.9999
CCL5	No	>0.9999
CCL9	No	>0.9999
CXCL1	Yes	0.0016
CXCL2	Yes	0.0042
CXCL3	No	0.9919
TRAF1	No	>0.9999
NLRP3	No	>0.9999
TLR2	No	>0.9999
TGF-β1	No	>0.9999

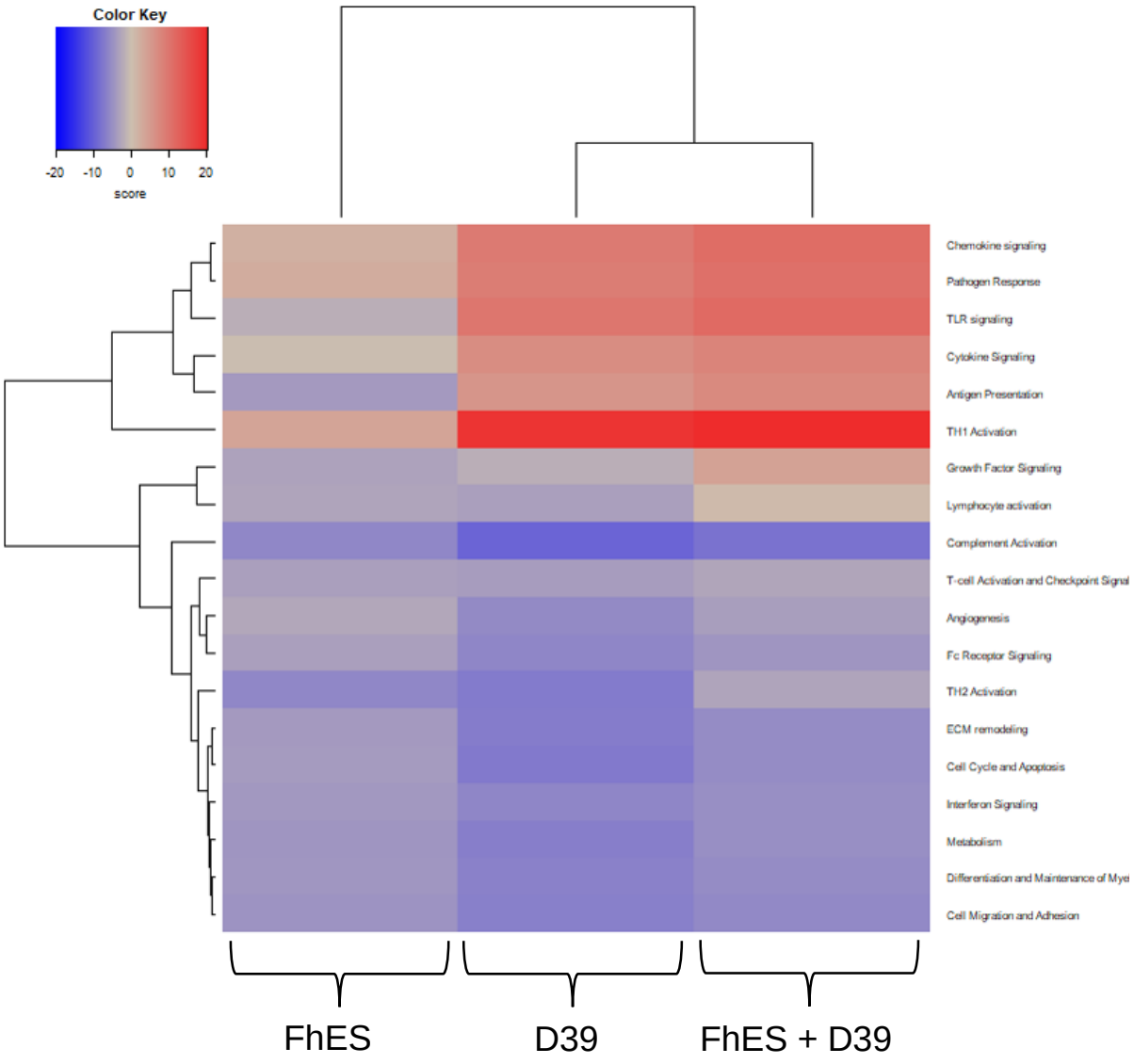

Figure 6.6: Gene set analysis (GSA) of differential gene expression is summarised at the gene set level using a global significance score. Heatmap displays each sample's directed global significance scores that measure the extent of up- or down-regulated genes. Red denotes extensive over-expression, blue denotes extensive under-expression.

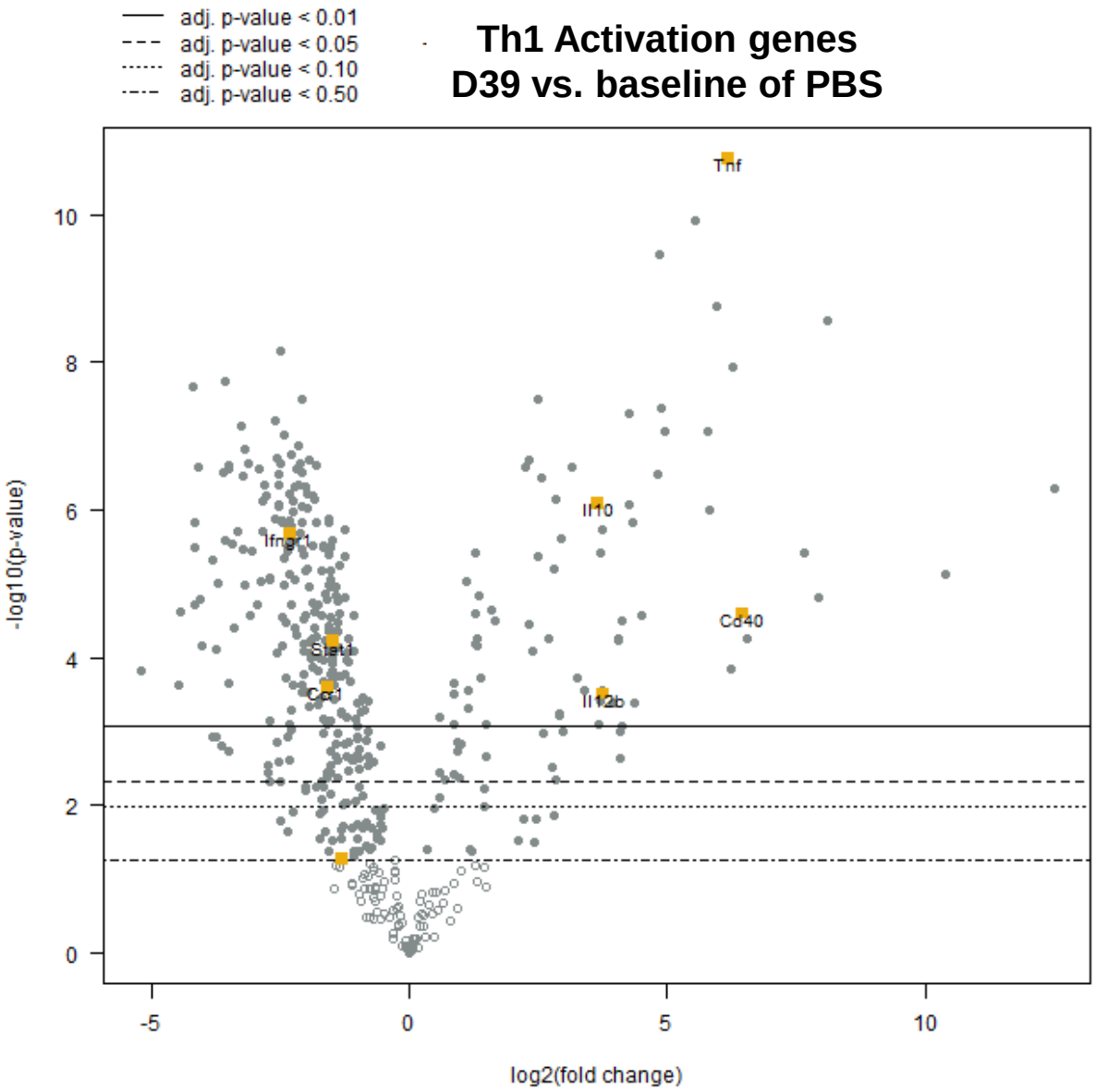

Figure 6.7: Volcano plot showing the extent of log_2 and –log10 adjusted p-value for the differentially expressed Th1 activation genes identified in D39 infected BMDMΦs vs. baseline of PBS (control). Highly statistically significant genes fall at the top of the plot above the horizontal lines and high fold changes fall to the sides. Horizontal lines indicate various False Discovery Rate (FDR) thresholds or p-value thresholds. Genes within the Th1 activation gene set are highlighted in orange. The statistically significant genes are labelled in the plot.

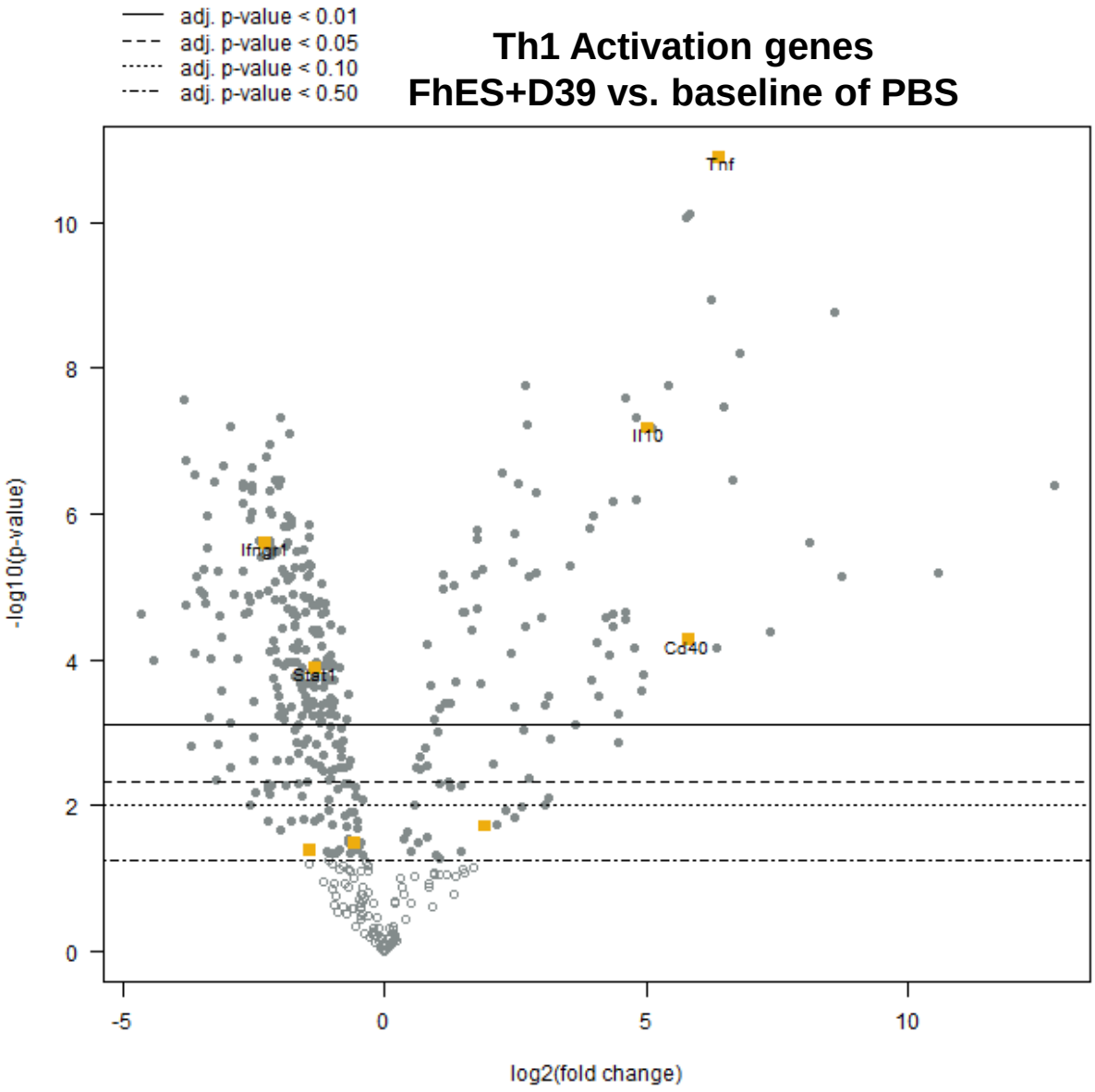

Figure 6.8: Volcano plot showing the extent of log_2 and –log10 adjusted p-value for the differentially expressed Th1 activation genes identified in FhES+D39 co-exposed BMDMΦs vs. baseline of PBS (control). Highly statistically significant genes fall at the top of the plot above the horizontal lines and high fold changes fall to the sides. Horizontal lines indicate various False Discovery Rate (FDR) thresholds or p-value thresholds. Genes within the Th1 activation gene set are highlighted in orange. The statistically significant genes are labelled in the plot.

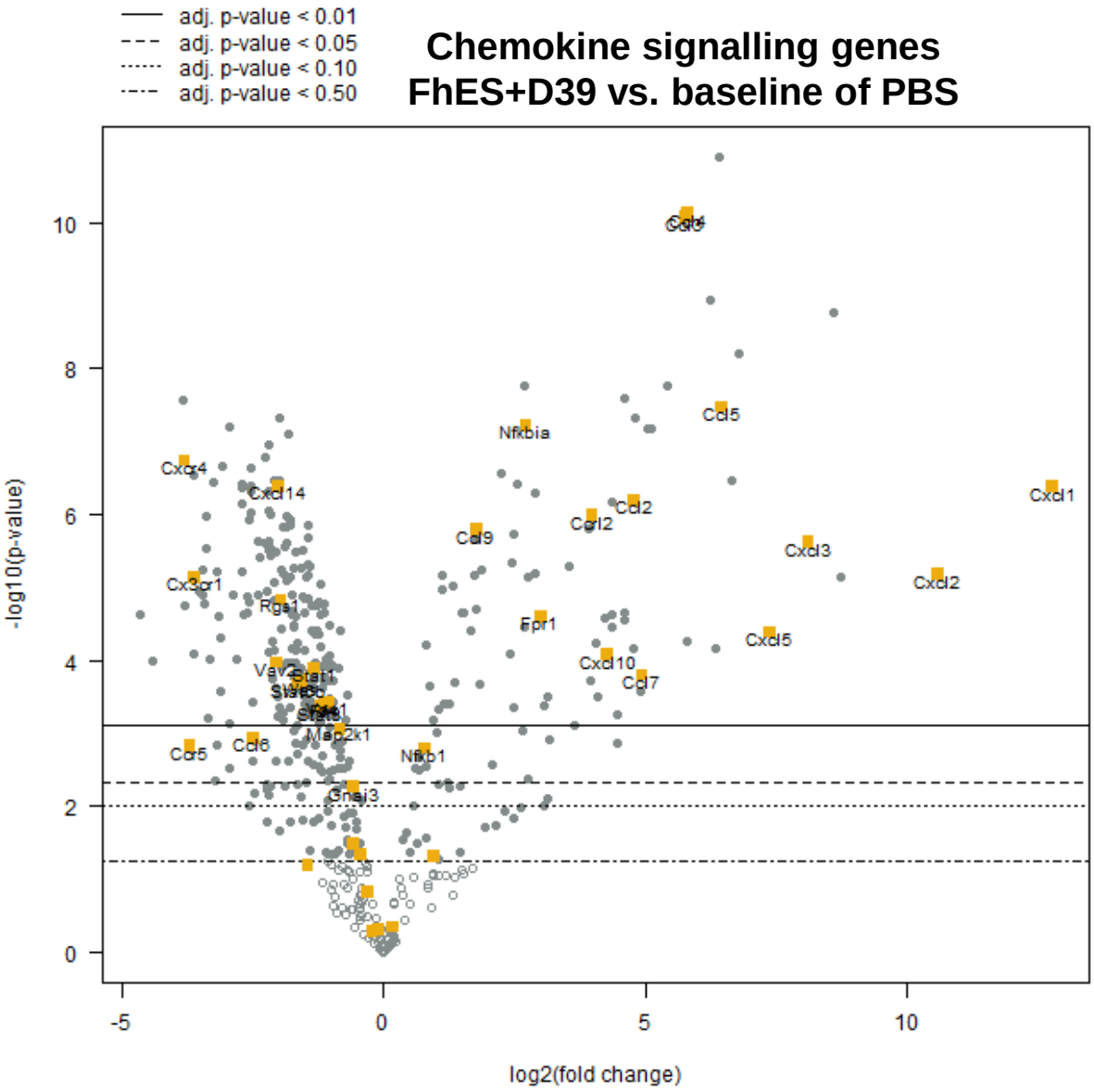

Figure 6.9: Volcano plot showing the extent of log_2 and –log10 adjusted p-value for the differentially expressed chemokine signalling genes identified in FhES+D39 co-exposed BMDMΦs vs. baseline of PBS (control). Highly statistically significant genes fall at the top of the plot above the horizontal lines and high fold changes fall to the sides. Horizontal lines indicate various False Discovery Rate (FDR) thresholds or p-value thresholds. Genes within the chemokine signalling gene set are highlighted in orange. The statistically significant genes are labelled in the plot.

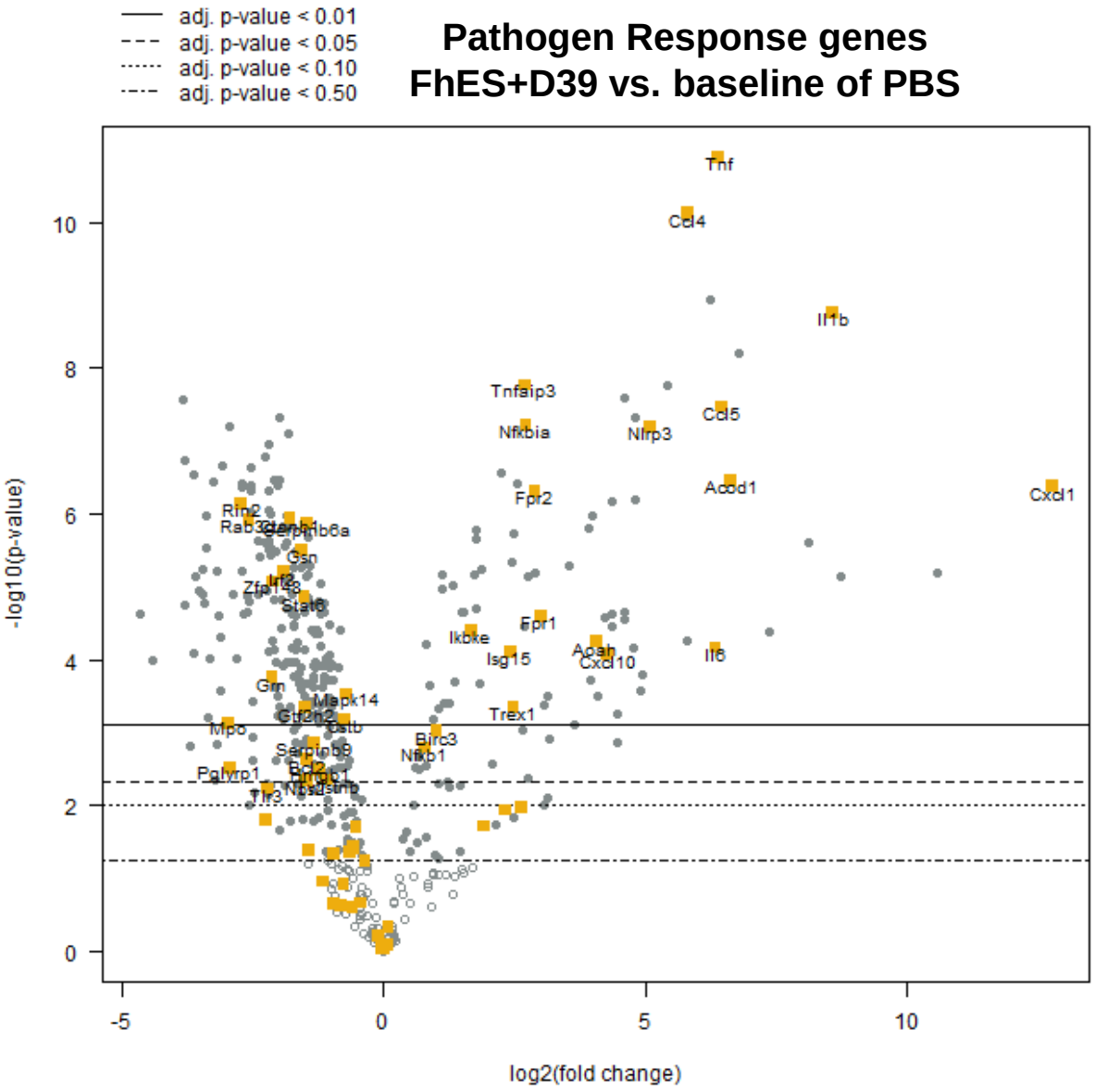

Figure 6.10: Volcano plot showing the extent of log_2 and –log10 adjusted p-value for the differentially expressed pathogen response genes identified in FhES+D39 co-exposed BMDMΦs vs. baseline of PBS (control). Highly statistically significant genes fall at the top of the plot above the horizontal lines and high fold changes fall to the sides. Horizontal lines indicate various False Discovery Rate (FDR) thresholds or p-value thresholds. Genes within the pathogen response gene set are highlighted in orange. The statistically significant genes are labelled in the plot.

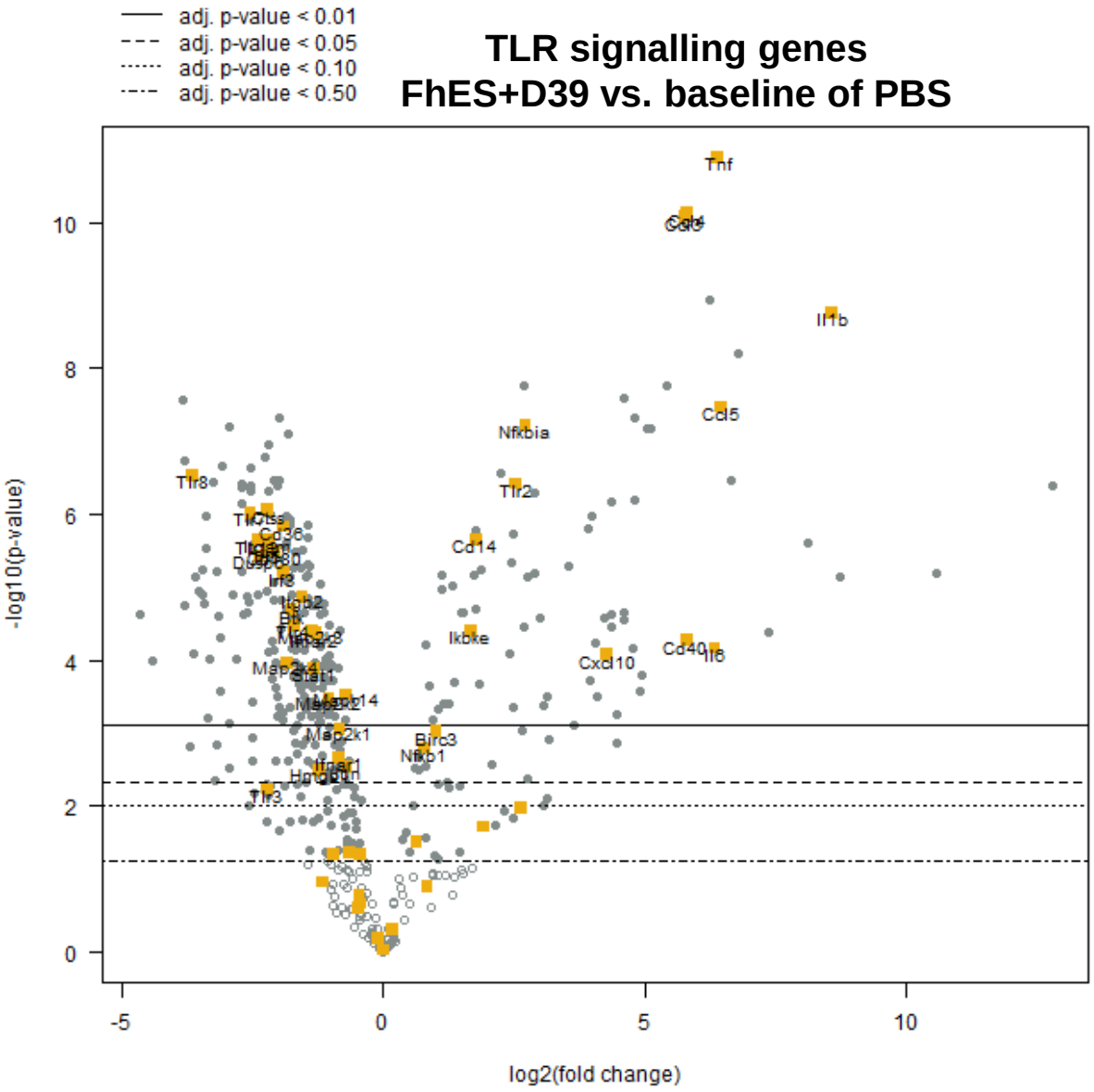

Figure 6.11: Volcano plot showing the extent of log_2 and –log10 adjusted p-value for the differentially expressed TLR signalling genes identified in FhES+D39 co-exposed BMDMΦs vs. baseline of PBS (control). Highly statistically significant genes fall at the top of the plot above the horizontal lines and high fold changes fall to the sides. Horizontal lines indicate various False Discovery Rate (FDR) thresholds or p-value thresholds. Genes within the TLR signalling gene set are highlighted in orange. The statistically significant genes are labelled in the plot.

6.2.4 D39 and co-exposed BMDMΦs exhibit Th1 activation pathway score profiles

From the global significance score in Figure 6.6 showing Th1 gene activation in D39 and co-exposed BMDMΦs, I further elucidated the Th1 activation pathway scores in both treatments. Pathway scores are calculated as the first principal component of the pathway genes' normalised expression. Figure 6.12 was generated to show the high level overview of how the pathway scores change across the samples. D39 and co-exposed BMDMΦs were clustered together in all pathway scores. Both treatments were colour coded with orange indicating high scores for Th1 activation where D39 cultures were more highly expressed than co-exposed cultures. On the other hand, PBS and FhES stimulated cells were represented in blue indicating low scores in almost all pathways.

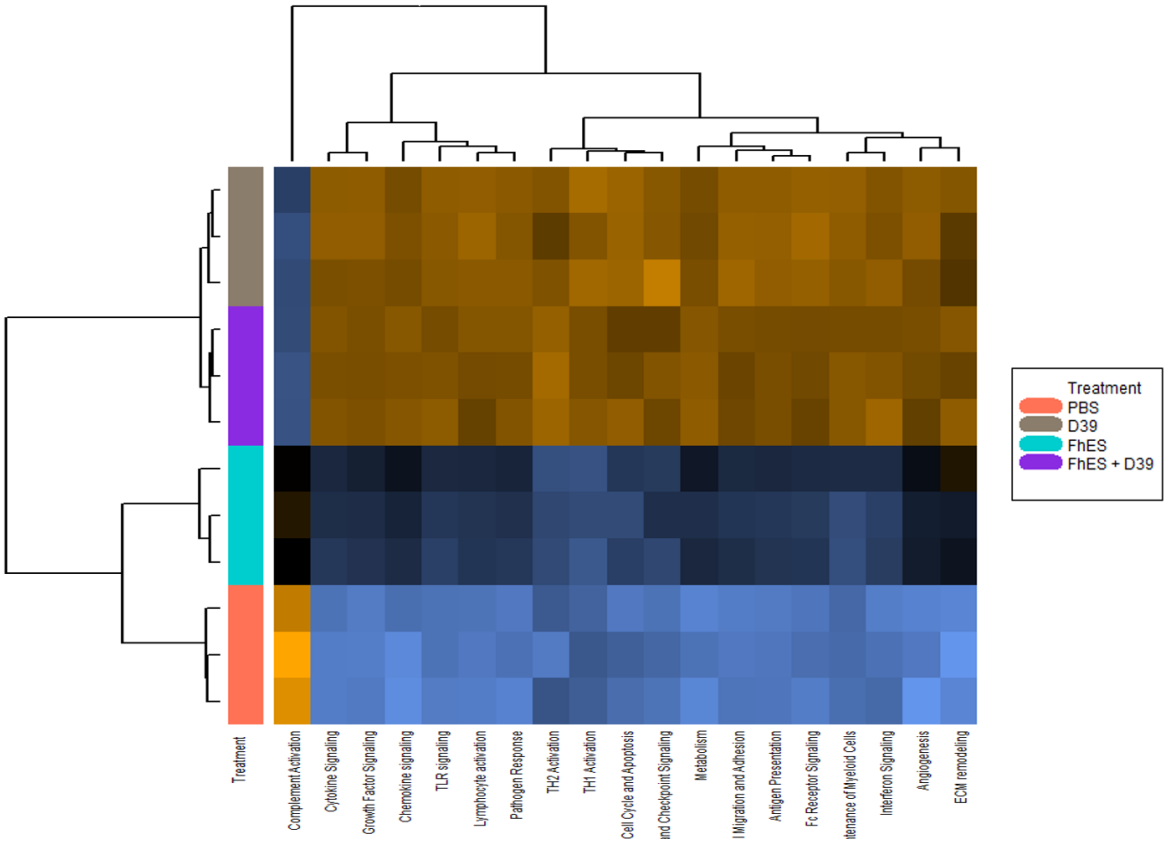

Figure 6.12: Pathway score profiles across all experimental groups. Heatmap of pathway score shows D39 infected and co-exposed BMDMΦs are clustered together. Orange indicates high scores; blue indicates low scores. Scores are displayed on the same scale via Z-transformation. Pathway scores are fit using the PC1 component of each gene set's data.

I then compared the pathway scores for Th1 activation, pathogen response and chemokine and TLR signalling in all treatment groups (Figure 6.13). D39 infected BMDMΦs represent the highest Th1 activation, pathogen response and TLR signalling scores, followed by co-exposed BMDMΦs indicating the up-regulation of the pathway (Figure 6.13a, c and d). Co-exposed BMDMΦs display a slightly higher chemokine signalling score than D39 infected cells (Figure 6.13b). FhES exposed BMDMΦs exhibit higher pathway scores in all gene sets than PBS control cells but the score levels were lower than zero indicating the down-regulation of the pathway.

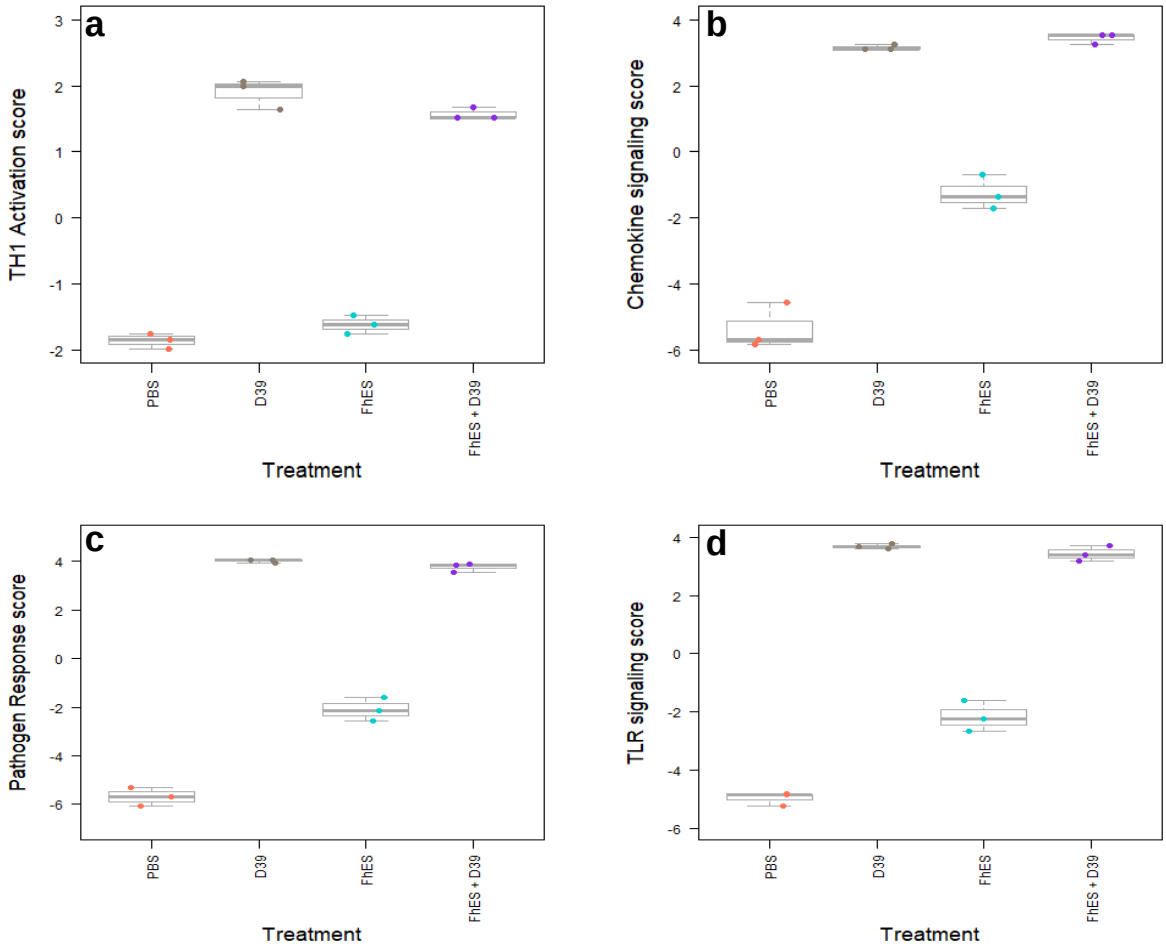

Figure 6.13: Plots of pathway scores against all treatment groups. (a) Th1 activation score, (b) chemokine signalling score, (c) pathogen response score and (d) TLR signalling score. D39 and co-exposed BMDMΦs demonstrate higher scores than FhES and PBS simulated cells in all selected pathway scores.

6.2.5 Pathway analysis in D39, FhES and co-exposed BMDMΦs

From the PathView tab generated from nCounter Advanced Analysis, I selected two pathways that are relevant to the present study. Cytokine-cytokine receptor interaction and TLR signalling pathways were compared between D39, FhES and in combination of both stimulants. Pathview displays different KEGG (Kyoto Encyclopaedia of Genes and Genomes) pathways that highlight pathway members most differentially expressed in the samples.

Chemokines *CCL2, CCL3, CCL4, CCL5, CCL7, CCL12 CXCL1, CXCL2, CXCL3, CXCL5, CXCL6* and *CXCL10*, pro-inflammatory cytokines *TNF-α, IL-6, IL-1α, IL-1β*, and *IL-12*, and anti-inflammatory *IL-10* were up-regulated in D39 and co-exposed BMDMΦs. On the other hand, *CCL6, CXCL4, CXCL4L1, CXCL14* and *TGF-β1* were found to be down-modulated, as indicated in blue (Figure 6.14a, c). FhES exposed BMDMΦs demonstrate the up-regulation of chemokines *CCL2, CCL4, CCL5, CCL7, CCL12, CXCL1, CXCL2, CXCL3, CXCL5* and *CXCL6*, and cytokines *TNF-α* and *IL-1β* but CCL6, CCL22, *CXCL4, CXCL4L1, CXCL14,* IL-15 and *TGF-β1* were down-regulated (Figure 6.14b). *IL-6, IL-12* and *IL-10* were not significantly differentially expressed in the FhES BMDMΦs. Whilst *IL-15* was significantly expressed only in D39 and FhES, *IL-18* was significantly expressed in co-exposed BMDMΦs.

D39 vs. baseline of PBS

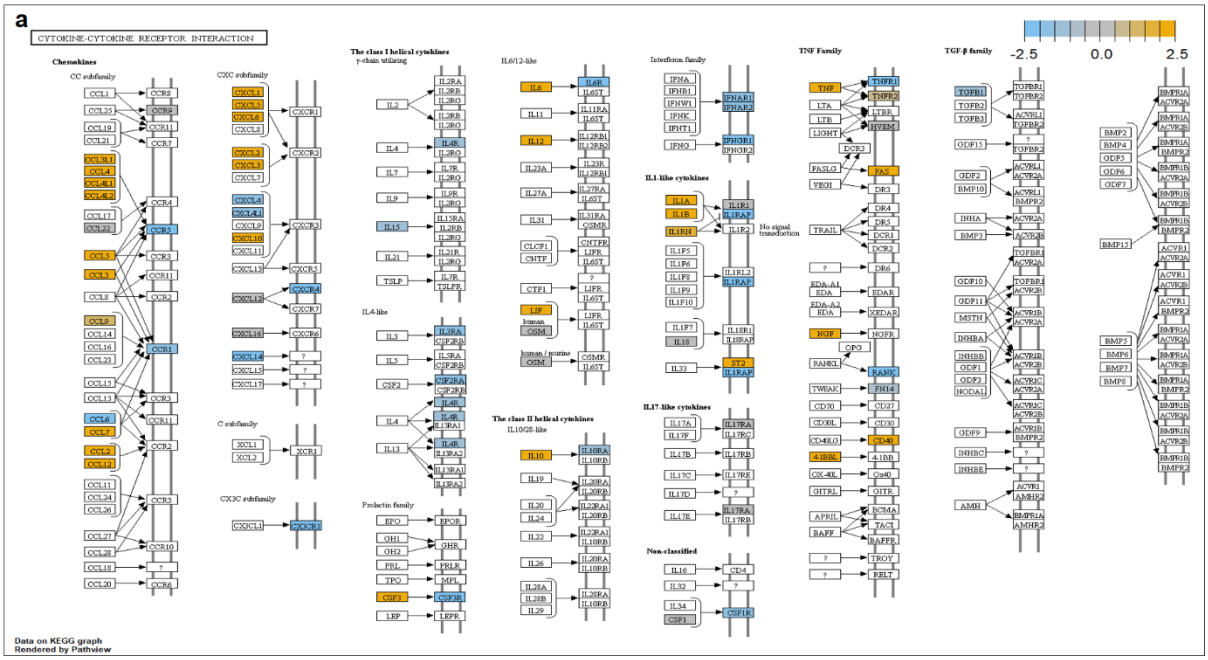

FhES vs. baseline of PBS

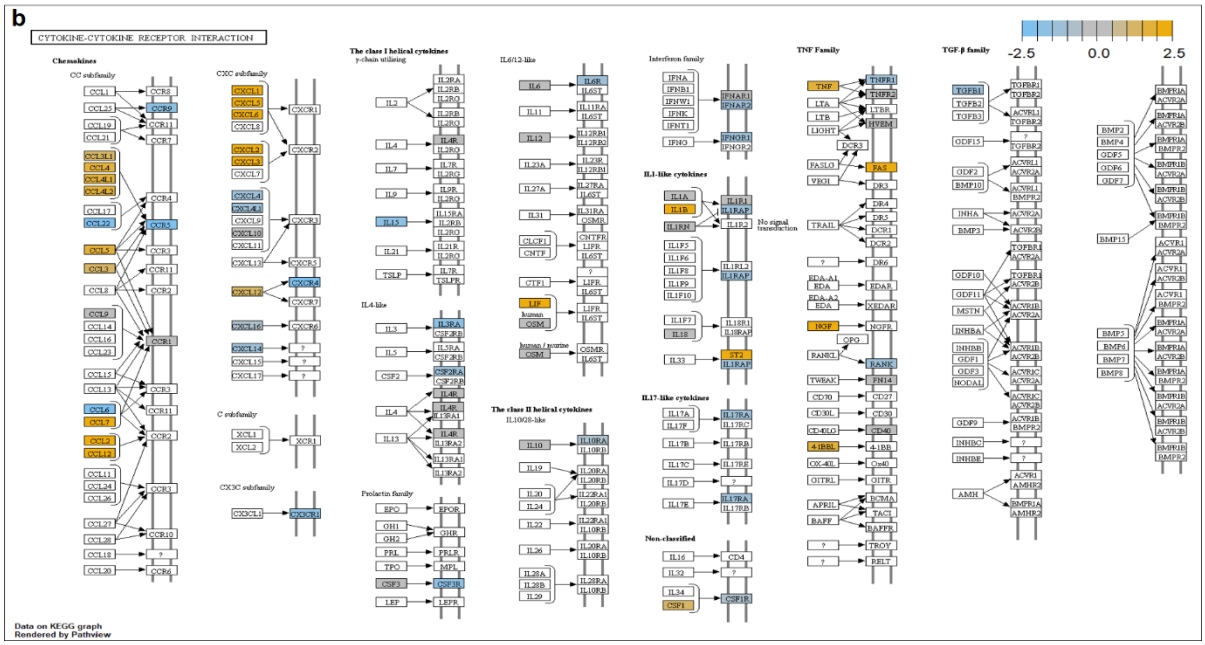

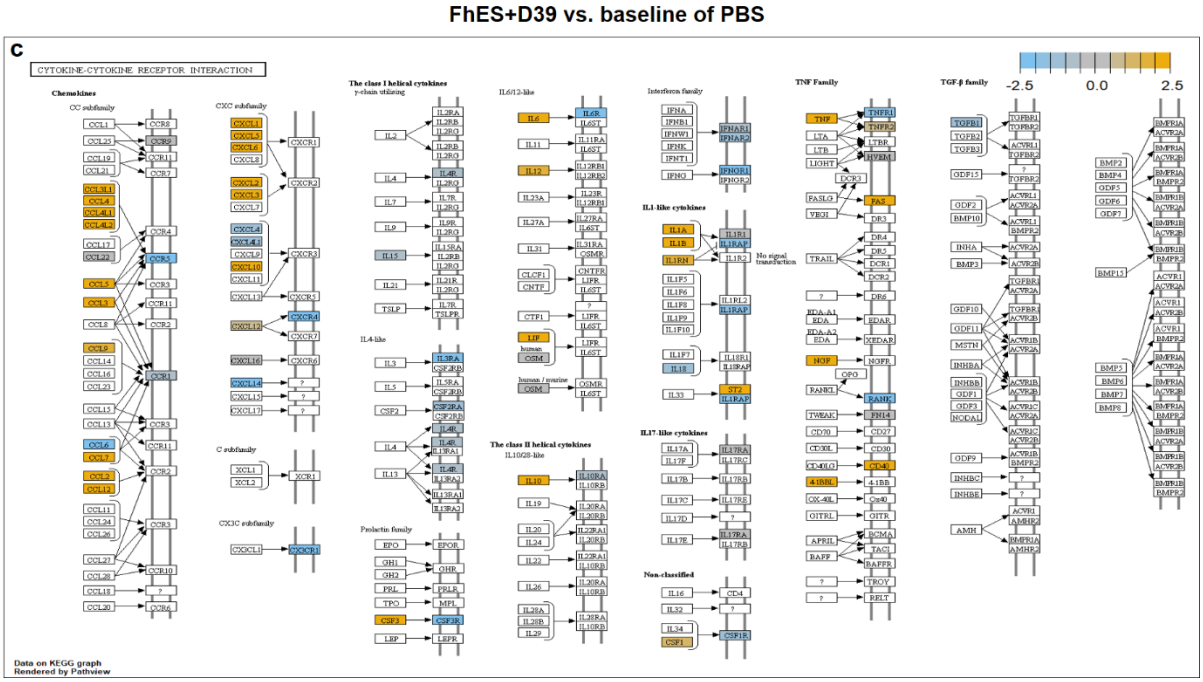

Figure 6.14: Pathview overlays the differential expression analysis of cytokine-cytokine receptor interaction on KEGG pathways. (a) D39, (b) FhES and (c) FhES+D39 vs. baseline of PBS. Genes within the panel are mapped to the pathway and differential expression is overlaid on the protein-based KEGG pathway image. Pathway nodes shown in white have no genes in the panel that map to them. Pathway nodes in grey have corresponding genes in the panel, however no significant differential expression is observed. Nodes in blue denote down-regulation relative to the selected baseline, whereas nodes in orange denote up-regulation relative to the selected baseline.

D39 and co-exposed BMDMΦs significantly expressed *TLR2* that activates and up-regulates the expression of inflammatory cytokines genes *TNF-α, IL-1β, IL-6* and *IL-12*, chemoattractants *CCL5*, macrophage inflammatory protein- *(MIP) 1α* and *1β*, *CD40* and *IP-10 (CXCL10)* (Figure 6.15a, c). TLR2 co-receptor, *CD-14* was also expressed but with less intensity in D39 compared to co-exposed BMDMΦs, indicated with pale orange. FhES exposed BMDMΦs significantly expressed *TLR2* but the intensity was decreased relative to D39 and co-exposed BMDMΦs. *TNF-α* and *IL-1β* were significantly expressed, however *IL-6, IL-12, CD14, CD40* and *IP-10 (CXCL10)* showed no significant differential expression (Figure 6.15b). *TLR4* and *TLR7* were down-regulated in all groups.

D39 vs. baseline of PBS

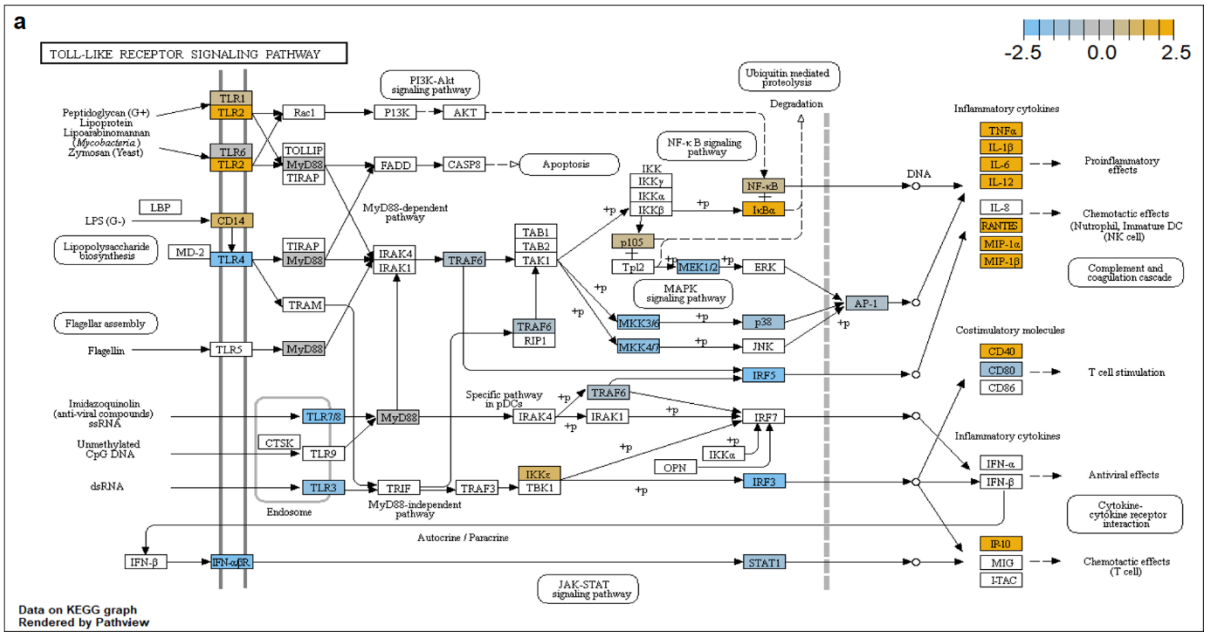

FhES vs. baseline of PBS

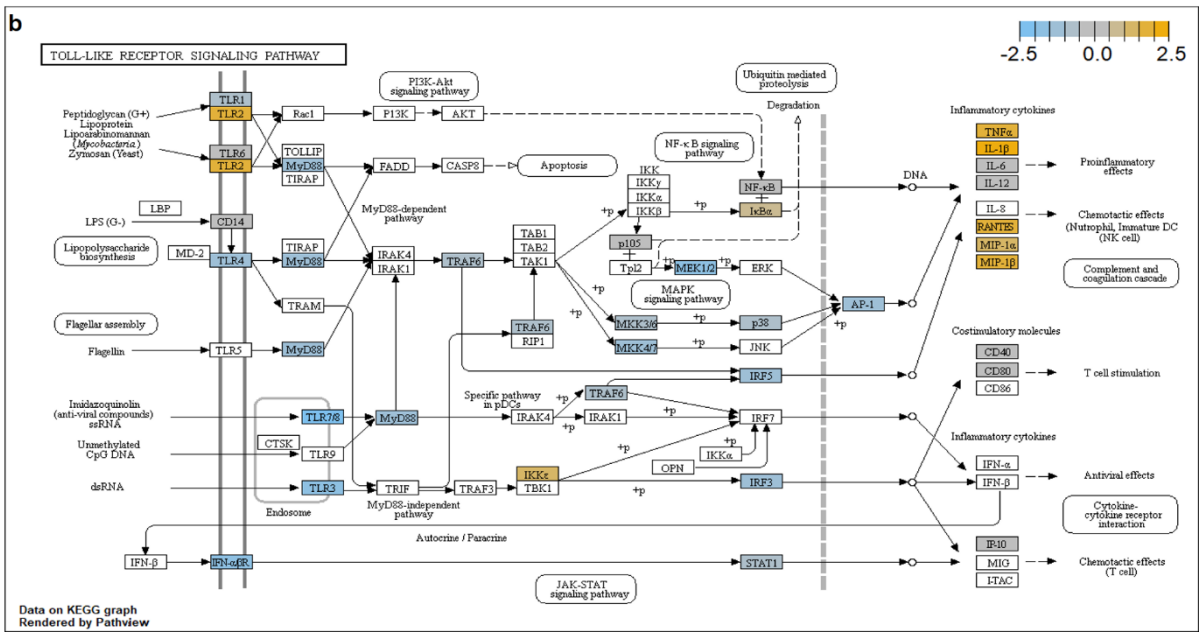

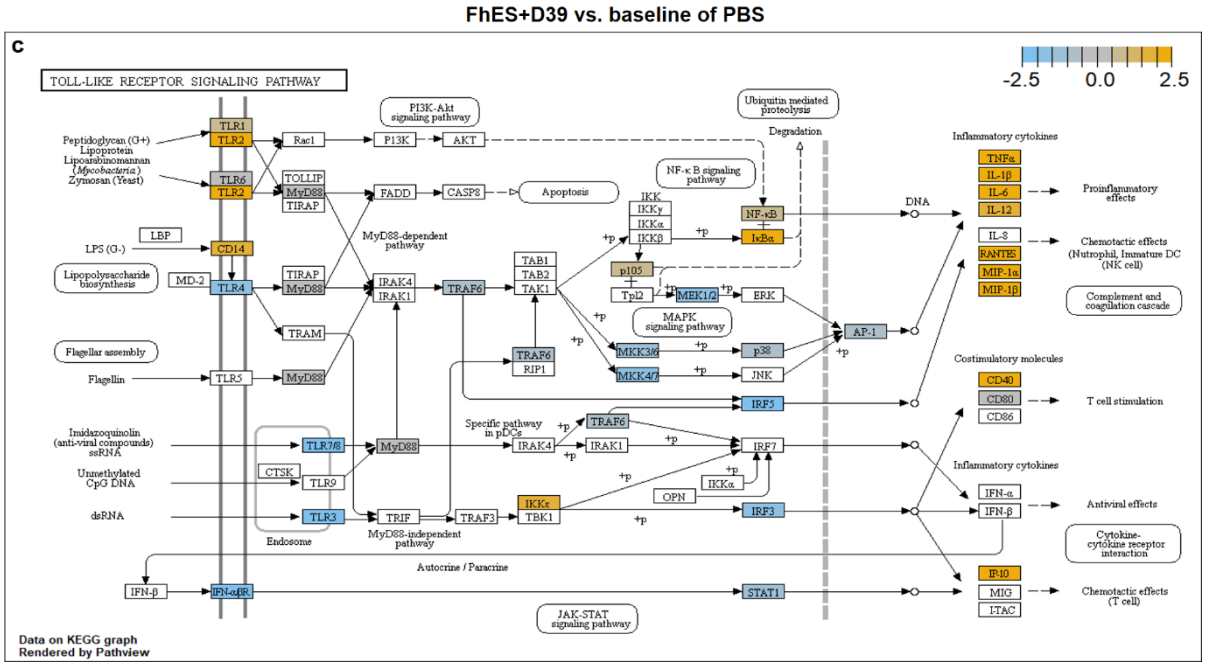

Figure 6.15: Pathview overlays the differential expression analysis of toll-like receptor interaction on KEGG pathways. (a) D39, (b) FhES and (c) FhES+D39 vs. baseline of PBS. Genes within the panel are mapped to the pathway and differential expression is overlaid on the protein-based KEGG pathway image. Pathway nodes in grey have corresponding genes in the panel, however no significant differential expression is observed. Nodes in blue denote down-regulation relative to the selected baseline, whereas nodes in orange denote up-regulation relative to the selected baseline.

6.3 Discussion

The purpose of this chapter was to investigate BMDMΦ gene expression in response to pneumococcus (D39) and if this was altered when cells were co-exposed to *F. hepatica* E/S antigen. In this chapter, the BMDMΦs of 6-7 weeks old female BALB/c mice were stimulated *ex vivo* with different conditions; PBS (control), live D39 pneumococcus, FhES and a combination of both stimulants. The expression of innate immune gene mRNAs was then analysed by employing the quantitative NanoString nCounter technique. The relative distance between different types of treatments was assessed using principal component analysis (PCA). Principal component 1 (PC1) of all genes expressed by the four sorted populations revealed a relative distance between the different treatments. The overview heatmaps of the normalised data were generated via unsupervised clustering. D39 and co-exposed BMDMΦs were clustered together in a dendrogram indicating closer relationship in both treatments. These results were somewhat expected because I had previously observed significantly higher NO production in co-exposed cultures than D39 infected cultures in BALB/c mice, indicating CAMΦ activation (discussed in Chapter 4). The potential of D39 to induce the classical activation of BALB/c BMDMΦs in the co-exposed cultures could further explain the closer gene expression relationship between those two treatments. D39 also drives much bigger changes in BMDMΦ gene expression than FhES.

After 6 hours of exposure, the differentially expressed genes (DEGs) in different treatment groups were analysed and a log2 FC of most significantly DEGs were tabulated. The genes of pro-inflammatory cytokines *TNF-α* and *IL-1β*, chemokine ligands *CCL3, CCL4* and *CCL5* were significantly expressed in D39 infected BMDMΦs. D39 infected BMDMΦs expressed the monocyte/ macrophage chemoattractant protein, *CCL2 (MCP-1)*, but the level was not higher than the co-exposed cultures. The induction of *CCL2* has been correlated with pneumococcal clearance in adult mice (Davis *et al*., 2011) but not in colonised infants (Siegel *et al*., 2015). In the present study, CCL2 expression was also observed in FhES exposed BMDMΦs. *CCL2* gene was reported to cause damage and liver necrosis in *F. hepatica* infected BALB/c mice (Rojas-Caraballo *et al*., 2015). Co-exposed BMDMΦs expressed the highest log2 FC of *TNF-α, IL-1β, IL-10, CCL3, CCL4, TRAF1, NLRP3*

and *CXCL1* compared to D39 and FhES cultures. CAMΦs are characterised by the ability to induce acute inflammatory responses marked by TNF-α, IL-1β, CCL2, CCL3, CCL4, CCL5 and CXCL1, which induce Th1 response activation (Atri *et al*., 2018). The combined effects of D39 and *F. hepatica* E/S on BMDMΦs could explain the highest log2 FC of *TNF-α, IL-1β, CCL2, CCL3, CCL4, CCL5* and *CXCL1* in co-exposed BMDMΦs in the present study, supporting CAMΦ activation induced by both stimulants. These findings were supported with the CAMΦ phenotypes of BALB/c BMDMΦs when co-exposed to the same stimulants discussed in Chapter 4.

From the global set analysis of DEGs, D39 and co-exposed BMDMΦs were denoted with red indicating extensive over-expression of Th1 genes. Pro-inflammatory genes of *TNF-α* and *IL-12b*, and anti-inflammatory *IL-10* were significantly expressed in D39 cultures, whereas co-exposed cultures demonstrated significantly overexpressed *TNF-α* and *IL-10*. Chemokine signalling, pathogen response and TLR signalling gene sets were further analysed for their DEGs.

In the present study, co-exposed BMDMΦs displayed significant up-regulation of *CCL2, CCL3, CCL4, CCL5, CCL7, CCL9, CXCL1, CXCL2, CXCL3, CXCL5* and *CXCL10* genes in the context of chemokine signalling. On the other hand, genes of *TNF-α, IL-1β, IL-6, CCL5, CXCL1, CXCL10* and *NLRP3* were significantly expressed in the pathogen response gene set. Significantly altered expression of *TNF-α, IL-1β, IL-6, CCL4, CCL5, CXCL10* and *TLR2* genes was observed in TLR signalling gene set. Monocytes and MΦs secrete cytokines and chemokines which are potent signalling molecules that mediate intercellular communication. Inflammatory stimuli induce MΦs to secrete a vastly different array of cytokines and chemokines that can either promote inflammation or wound healing. Whilst pro-inflammatory cytokines such as TNF-α, IL-1β, IL-6, IL-12 and IL-23, and chemokines CCL2, CCL3, CCL4, CCL5, CCL8, CCL9, CCL10 (IP-10) and CCL11 polarises the response towards a CAMΦ phenotype, anti-inflammatory cytokines IL-10 and TGF-β, and chemokines CCL17, CCL22 and CCL24 polarise AAMΦ phenotype (Duque and Descoteaux, 2014). Besides monocytes and MΦs, cytokines are also produced by activated lymphocytes, endothelial cells and fibroblasts. In concert with IL-17, TNF-α triggers the expression of neutrophil attracting chemokines CXCL1, CXCL2 and CXCL5 (Griffin *et al*., 2012).

The results presented here confirmed the CAMΦ activation in the co-exposed BALB/c BMDMΦs, which was associated with Th1 gene activation

Co-exposed BMDMΦs exhibit *NLRP3* inflammasome expression in the pathogen response gene set. NLRP3 inflammasome has a key function in peptidoglycan recognition and controls pneumococcal clearance (Kanneganti *et al*., 2007). NLRP3$^{-/-}$ mice are more susceptible to pneumococcal pneumonia than wild-type mice (Witzenrath *et al*., 2011). Ply has been identified as a novel NLRP3 activator and was required for immunity against *S. pneumoniae* (McNeela *et al*., 2010). The production of IL-1β is controlled by the NLRP3 inflammasome and influences the development of both innate and adaptive immune responses (Biswas and Mantovani, 2012). In the context of *F. hepatica* infection, cathepsin L3 (CL3) induces non-canonical NLRP3 inflammasome in murine DCs (Celias *et al*., 2019) and FhHDM-1 prevents NLRP3 inflammasome activation in MΦ, which prevents IL-1β production (Alvarado *et al*., 2017).

In the present study, *IL-1β* shows higher log2 FC than *NLRP3* inflammasome in the co-exposed BMDMΦs. *IL-1β* might induce CAMΦ activation in response to *NLRP3* inflammasome activation and this could be partially mediated by Ply. From the heatmap in the global significance analysis, although FhES cultures were not extensively expressed in the chemokine signalling and pathogen response gene sets, the presence of cathepsins in FhES may trigger the *NLRP3* inflammasome, which leads to the *IL-1β* gene expression. Whilst the *F. hepatica* CL3 is expressed mainly in the juvenile or invasive stage (Celias *et al*., 2019), FhES antigens in the present study were prepared from the adult flukes and contained CL1 and CL2, that could bring different activation of the *NLRP3* inflammasome and *IL-1β* expression in the BALB/c BMDMΦs. Additionally, in this part of the experiment, BMDMΦs were only exposed for 6 hours to look at gene expression in early infection. It is suggested that the association of *NLRP3* inflammasome *and IL-1β* using excretory/ secretory *F. hepatica* antigens from different stages, is investigated in future studies.

TLR2 gene was expressed in the TLR signalling gene set in the co-exposed BMDMΦs. Recognition of microbial products by TLRs initiates signal transduction pathways, which activates the expression of genes. These gene products regulate innate immune responses and subsequently instruct the development of antigen-specific acquired immunity (Takeda and Akira, 2005). TLR2 recognises lipoteichoic acid, peptidoglycan and lipopeptides of Gram positive bacteria (Lammers *et al*., 2012) and is known to play a role in the early inflammatory response to viable and heat-killed *S. pneumoniae* (Knapp *et al*., 2004; Mogensen *et al*., 2006). Alternatively, the LPS receptor, TLR4 recognises Gram negative bacteria (La Flamme *et al*., 2012; Malyshev and Malyshev, 2015). TLR4 works synergistically with TLR2 to activate MΦs and facilitate the clearance of low doses of *S. pneumoniae* from the murine lung (Malley *et al*., 2003; Branger *et al*., 2004). TLR2 but not TLR4 was found to be required for pneumococcal clearance in mice (van Rossum *et al*., 2005). Increased expression of TLR2 was observed in cattle blood monocyte-derived MΦs stimulated with FhES *in vitro* and in *F. hepatica*-infected animals (Garza-Cuartero *et al*., 2016).

However, the expression of TLR2 and its co-receptor CD14 were reduced in *F. hepatica-M. bovis* co-exposed animals, which resulted in lower *M. bovis* uptake by monocyte-derived MΦs (Garza-Cuartero *et al*., 2016). Enhancement of TLR2 expression following helminth infections was also reported in other studies (Correale and Farez, 2009; Correale and Farez, 2012). In the present study, the *TLR2* gene was expressed in D39 and FhES treatetd BMDMΦs with 2.56 and 1.90 log2 FC values, respectively. *TLR4* gene in D39 BMDMΦs recorded -2.23 log2 FC value indicating *TLR4* is less involved during pneumococcal infection. I also observed down-regulation of *TLR 4* (-1.23 log2 FC) and *TLR7* (-1.91 log2 FC) in FhES exposed BMDMΦs. Others have reported the up-regulation of TLR2 and TLR4 in *F. hepatica* chronically infected cattle, and TLR7 in the period of transition from acute to chronic fasciolosis in cattle (Garcia-Campos *et al*., 2019). TLR7 activation has also been reported in chronic *F. gigantica* infection in water buffalos (Zhang *et al*., 2018). The interaction of *F. hepatica* with the TLR system resulted in low IFN-ɣ secretion when incubated with a TLR2 antagonist (PPD-B, purified protein derivative from *M. bovis*) and reduction of NO production in MΦ stimulated with LPS and FhES (Flynn and Mulcahy, 2008a). I observed up-regulation of *TLR2* (2.54 log2 FC) and down-regulation of *TLR4* (-1.71

log 2 FC) and *TLR7* (-2.54 log2 FC) in the co-exposed BMDMΦs. These findings suggest the activation of *TLR2* but not *TLR4* and *TLR7* in the context of pneumococcus-*F. hepatica* infection. Nevertheless, these results were based upon the different types of MΦ origins and the duration of exposure compared to the previous studies. Further research should be undertaken to investigate the role of MΦs *TLR* genes in the presence of FhES alone and when co-exposed with pneumococcus.

Next, I sought to investigate the selected pathway scores in D39 and co-exposed BMDMΦs. The heatmap demonstrates the high level of the score in almost all pathways indicated with orange in D39 and co-exposed cultures and are clustered together. PBS and FhES demonstrate low scores indicated in blue. I have already demonstrated the activation of Th1 genes from the global set analysis of DEGs observed in D39 and co-exposed BMDMΦs. I then discussed the types of gene expression associated with Th1 activation; the cytokine signalling, pathogen response and TLR signalling gene sets. In this part of the analysis, as expected, D39 and co-exposed BMDMΦs exhibit higher scores than PBS and FhES BMDMΦs in all four selected pathways. In detail, whilst D39 BMDMΦs demonstrate the highest Th1 activation, pathogen response and TLR signalling scores, co-exposed BMDMΦs displayed slightly higher chemokine signalling score than D39 BMDMΦs demonstrated by significantly different expression of *TNF-α, CCL3, CXCL1* and *CXCL2* genes between D39 and co-exposed BMDMΦs. These results indicate that D39 alone induced expression of Th1 associated genes in BMDMΦs and continue to maintain the Th1 activation, even in the presence of FhES.

The last part of this chapter I discussed the pathway analysis in different treatments of BMDMΦs. Two different pathways which are cytokine-cytokine receptor and TLR signalling were selected to compare the differential expression between D39, FhES and in the combination of both treatments. The PathView module overlays the differential expression analysis results with various KEGG pathways. Elements that are over-expressed in this pathway are coloured orange, those that are under-expressed are coloured blue, and those that are unchanged are coloured grey. In the context of cytokine-cytokine receptor interaction, D39 and co-exposed BMDMΦs up-regulated the genes of *CCL2, CCL3, CCL4, CCL5, CCL7, CXCL1, CXCL2, CXCL3,*

CXCL5, CXCL6, CXCL10, TNF-α, IL-6, IL-1α, IL-1β, IL-12 and *IL-10* but down-regulated *CCL6, CXCL4, CXCL4L1, CXCL14* and *TGF-β1*. These findings were supported by many previous studies demonstrating the key role of the inflammatory response to containment of *S. pneumoniae* infection, evidenced by the induction of chemokines CCL2, CCL5, CCL7, CXCL1 and CXCL10, and cytokines IFN-ɣ, TNF-α, IL-1β, IL-6, IL-12, IL-17 and IL-10 (reviewed by Periselneris *et al*., 2015). In addition, pneumococcus also activates CAMΦ marked by those inflammatory chemokines and cytokines which associated to Th1 activation (Dorrington *et al*., 2013; Harvey *et al*., 2014; Coleman *et al*., 2017). However, I did not observe expression of IFN-ɣ in this part of the experiment and in D39 and co-exposed BMDMΦs using the Multiplex MSD® U-PLEX (discussed in Chapter 4). Chemokines *CCL2, CCL4, CCL5, CCL7, CXCL1, CXCL2, CXCL3, CXCL5* and *CXCL6*, and pro-inflammatory cytokines *TNF-α* and *IL-1β* were up-regulated, but *IL-6, IL-12 and IL-10* were not significantly expressed in FhES BMDMΦs. Although pneumococci and *F. hepatica* are able to drive TGF-β, the gene was found to be down-regulated in all treated groups where the BMDMΦs were exposed to the stimulants for only 6 hours. Gene expression and protein are not always mirrored. TGF-β is produced and the protein stored in a latent form intracellularly (Omer *et al*., 2000; Robertson *et al*., 2015; Nüchel *et al*., 2018). Thus, the stimuli used in the present study might lead to release of TGF-β protein without any change in gene expression. It is also suggested that the exposure time and the origin of MΦ used in this experiment may play a role in determining the TGF-β expression in the present study. Further studies, which take these variables into account, will need to be undertaken. Chemokines CCL6 and CXCL14 have intrinsic antibacterial properties (Moser *et al*., 2004; Kotarsky *et al*., 2009). Lower expression of CCL6 have been reported in pneumococcal infected IL-1r1$^{-/-}$ mice than wild-type mice due to the altered MΦ chemokine profile (Lemon *et al*., 2015). CXCL14 potentially killed *Pseudomonas aeruginosa, Streptococcus mitis* and *Streptococcus pneumoniae* (Dai *et al*., 2015). Chemokines CCL2 and CXCL4 have been reported to polarise MΦs to an AAMΦ phenotype (Roca *et al*., 2009; Gleissner *et al*., 2010). Down-regulation of *CCL6* and *CXCL14* genes observed when co-exposed with FhES would support further evidence for altered immunity in co-infection.

TLR2 was strongly expressed in D39 and co-exposed BMDMΦs compared to FhES cultures. These findings may explain the expression of *TNF-α, IL-1β, IL-6, IL-12, CCL5, MIP-1α and 1β, TLR2, CD40* and *IP-10 (CXCL10)* in both cultures that were infected with D39. Lower expression of *TLR2* in FhES cultures resulted in only *TNF-α* and *IL-1β* expression but not *IL-6, IL-12* and *CD14*. *S. pneumoniae* promotes TLR2 and TLR4 to activate MΦs to induce pro-inflammatory cytokines transcription (Malley *et al*., 2003; Tomlinson *et al*., 2014). *TLR4* and *TLR7* were found to be down-regulated in all treated groups indicating less involvement of these receptors in controlling *S. pneumoniae* and *F. hepatica* infections in the present study

6.4 Conclusion

This chapter has discussed the activated transcriptomic profiling of BALB/c BMDMΦs in response to D39 pneumococcus and FhES antigens. Co-exposed BMDMΦs polarised to CAMΦ phenotype indicated by significant expression of pro-inflammatory chemokines and cytokines genes. This is supported by the pathway score of Th1 gene activation, which is confirmed by chemokine signalling, pathogen response and TLR signalling gene set. Pathway analysis reveals pro-inflammatory cytokines and TLR2 pathways in the co-exposed BMDMΦs.

Chapter 7

General Discussion

CHAPTER 7

General Discussion

7.1 Background of thesis

This study was designed to advance our understanding of the impact of *Fasciola hepatica* mediated immunomodulation on the host's immune response to bacterial infection. The main aim of this thesis was to investigate the effect of *F. hepatica* antigen exposure on the subsequent response to *Streptococcus pneumoniae* infection. In brief, *F. hepatica* ES products (FhES) and tegumental antigens (FhTEG) have long been known to immunomodulate immune responses in infected hosts (Dalton *et al*., 2013; Ryan *et al.*, 2020).Whilst *M. bovis* is responsible for bovine tuberculosis and zoonoses in humans (Muller *et al*., 2013), *S. pneumoniae* is an obligate human pathogen and cause of community-acquired pneumonia, meningitis and otitis media (Coleman *et al*., 2017).

In the first part of the study, *in vitro* J774.2 cells were used to define the polarisation of MΦs exposed to either *F. hepatica* antigens (FhES and FhTEG), different pneumococcal preparations or *Mycobacterium bovis* sonicate extract. *M. bovis* was included as an additional comparator due to the well characterised effects of *F. hepatica-M. bovis* co-infection on macrophage phenotype. Secondly an *in vivo* mouse model was utilised to investigate the impact of FhES and live D39 pneumococcus co-exposure on the bacterial load, inflammatory protein production and host immune cell responses. *Ex vivo* models were used to understand further the consequences of co-exposure using transcriptomic profiling in the activated primary BMDMΦs. A summary of the main findings and suggestions which have arisen are provided in this discussion

7.2 Summary of findings

7.2.1 Modulation of macrophage phenotype following *Fasciola hepatica* and bacterial co-stimulation in the monocyte/ macrophage cell line J774.2

In Chapter 3, I investigated the modulation of J774.2 MΦ phenotype when exposed to *F. hepatica* antigens and different bacterial stimulants. In this thesis, I focussed on FhES products because of their highly immunogenic properties and ability to induce alternative MΦ activation (Flynn *et al*., 2007a; Flynn and Mulcahy, 2008a; Guasconi *et al*., 2011; Guasconi *et al*., 2012; Guasconi *et al*., 2015), whilst FhTEG was used only in MbSE co-exposure and IL-4 primed J774.2 MΦs. Cathepsin L proteases L1 and L2 were observed in the FhES preparation using SDS-PAGE. The immunomodulatory effects of the cathepsin Ls are thought to favour parasite longevity through the progression of non-protective Th2 responses by blocking the development of protective Th1 responses (O'Neill *et al*., 2000; O'Neill *et al*., 2001) and inhibiting CAMΦ activation (Donnelly *et al*., 2011). Both FhES+ and FhTEG+MbSE co-exposed cultures significantly down-modulated NO compared to MbSE alone, suggesting the prevention of CAMΦ induction and modulation of the J774.2 phenotype towards AAMΦ, with only FhES+MbSE showing significantly up-modulated arginase production. The augmentation of FhES further supports the evidence of AAMΦ polarisation caused by *F. hepatica* in our study. However, neither of the fluke antigens alone had an effect on arginase production in J774.2 MΦs. These findings were unexpected, knowing that *F. hepatica* alone is able to induce arginase (AAMΦ marker). From this chapter of work, the results indicated that J774.2 MΦs are capable of developing into AAMΦ when co-exposed to both *F. hepatica* antigens with MbSE, but not in the presence of fluke antigens alone.

Next, I investigated the responses of J774.2 MΦs following exposure to FhES and different preparations of pneumococci. At first, I investigated the ability of the Ply-deficient mutant D39Δply and WT D39 (Ply producing strain) to modulate NO production by J774.2 MΦs. Live, heat- and detergent-inactivated D39Δply failed to induce NO secretion, whilst low levels were detected in WT D39 cultures. The observations from D39Δply were in line with previous studies suggesting NO production was dependent on Ply (Braun *et al*., 1999; Bewley *et al*., 2014). The low level of NO observed in the WT D39 could be due to the absence of pre-activation with IFN-ɣ in the present study. Since, IFN-ɣ priming was essential to induce NO in WT D39 and NO secretion was dependent on Ply (Braun *et al*., 1999), future studies could explore the effects of IFN-ɣ priming on the production of NO following stimulation of J774.2 cells with WT D39.

Culture supernatant derived from D39 (D39SN) was used as an alternative to the different pneumococcal preparations. Significant up-modulation of NO was observed in FhES+D39SN co-exposed cultures compared to D39SN alone, whilst arginase levels were not significantly different in all treated cultures suggesting the modulation of CAMΦ phenotype. Two main findings were highlighted here. First, the FhES+D39SN co-exposed cultures promote CAMΦ phenotype, and second, the inability of FhES to induce AAMΦ. The first finding may be explained if Ply was released via autolysis of pneumococci during preparation of D39SN, with Ply inducing and maintaining CAMΦ instead of AAMΦ phenotype even in the presence of FhES. To further explore the second finding, I used *Trichuris muris* ES products (TmES) to know whether other types of helminth ES products are able to induce arginase from J774.2 MΦs. IL-4 stimulation confirmed that the cells were functionally capable of secreting arginase. Because TmES showed very similar results to those observed following stimulation with FhES, I next determined whether priming the cells with IL-4 could enhance the arginase production. To investigate this, the J774.2 MΦs were primed with IL-4 for 24 and 48 hours before adding the fluke antigens. A comparison was made between a low and high passage cell number (7 and 28, respectively). Surprisingly, the levels of arginase were significantly higher in IL-4 primed cells exposed to both fluke antigens compared to unprimed cells using a low passage number. The levels were observed higher in the 48 hours than 24 hours IL-4 primed

cells. To confirm the priming effect of IL-4 on low passage number of J774.2 cells, I further tested using TmES antigens. As expected, IL-4 primed cells exposed to TmES produced significantly higher arginase levels compared to unprimed cells and priming for 48 hours showed significantly higher level of arginase production compared to 24 hours priming. It is also suggested to use low cell passage number of J774.2 cells to avoid losing the capacity to secrete arginase in response to fluke antigens.

Next, the ability of J774.2 MΦs to express mannose receptor (MR) or CD206 (alternative marker of AAMΦ) after stimulation with IL-4 was investigated using flow cytometry. I observed low $CD206^{+}$ cell expression suggesting that absence of MR expression in the J774.2 clone even following priming with IL-4. Previous studies have reported high MR expression in J774E clone (Stahl *et al.*, 1980; Fiani *et al.*,1998). Although arginase and CD206 can be used as markers for AAMΦ, they result from activation of distinct pathways during AAMΦ polarisation. These findings could further explain the inability of J774.2 cells to induce arginase when exposed to fluke antigens alone. In future investigations, it might be possible to use a different clone of J774 cells to assess their ability to express MR following IL-4 stimulation.

In the context of cytokine-chemokine induction, elevated CAMΦ-associated cytokines are in line with the previous observation where D39SN alone up-regulates NO and increases the amount of NO produced when co-exposed with FhES. The interrelationship between IFN-γ and IL-12 is complex, where IFN-ɣ stimulation of MΦs is needed for the IL-12 production (de Groen *et al*., 2015) and Th1 cells drive CAMΦ activation via IFN-ɣ and IL-12 (Mège *et al*., 2011). In the present study, J774.2 MΦs were cultured without other immune cell types, perhaps explaining the lack of IFN-ɣ and IL-12p70 production induced by D39SN. In future investigations, it is suggested to consider appropriate stimulation (e.g. IL-12) on J774.2 cells for IFN-ɣ induction or *vice versa* depending on the cytokine of interest to be studied. Co-culture of FhES+D39SN showed no effect on pro-inflammatory cytokines TNF-α, IL-6 or anti-inflammatory IL-10 secretion and induced modest but significant increases in IL-1β and chemokine CXCL1/ KC in J774.2 MΦs. Increased levels of IL-1β in FhES+D39SN stimulated cells could potentially cause tissue damage, inflammatory responses and enhance immunity against *S. pneumoniae* in co-infected hosts. Up-modulation of

CXCL1/ KC in the co-exposed cultures may also improve host survival by recruiting leukocytes to infection sites. This is an important issue for future research work, determining whether continuous fluke exposure may augment the IL-1β and CXCL1/ KC induction. IL-10 was observed in D39SN and co-exposed cultures but not in FhES alone. The lack of production of IL-10 in FhES raised a question as this immunosuppressive cytokine was reported to increase after stimulation with *F. hepatica* ES products (Guasconi *et al*., 2011). From the discussion in Section 3.3, our results suggest that the concentration of ES used may play a role in IL-10 induction. In this experiment, I stimulated J774.2 MΦ with 5 µg/ml FhES based on the optimal NO and arginase production in our titration studies. Further investigation and experimentation using higher concentration of FhES is strongly recommended to induce IL-10 in J774.2 MΦs.

7.2.2 *Fasciola hepatica* and *Streptococcus pneumoniae* interactions with murine bone marrow-derived macrophages

In Chapter 4, I investigated the ability of *F. hepatica* ES products to modulate the immune response to live *S. pneumoniae* using BMDMΦs from different strains of mice. Outbred CD1 mice may be susceptible to D39 infection, demonstrated by low NO production. The presence of CAMΦ and AAMΦ phenotypes in the co-stimulated CD1 BMDMΦs provides additional evidence for CAMΦ and AAMΦ mixed phenotypes during co-exposure. CAMΦ activation was observed in both C57BL/6 and BALB/c BMDMΦs following exposure to D39. There was evidence that FhES may have modulated the response towards a AAMΦ phenotype in C57BL/6 BMDMΦs co-exposed cultures. In contrast, BALB/c co-stimulated BMDMΦs produced significantly higher levels of NO than those infection with D39 alone, indicating enhanced CAMΦ activation by FhES. Thus, BALB/c and C57BL/6 strains showed two different MΦ polarisation phenotypes when co-exposed to FhES. Those two mouse strains also showed NO production when stimulated with FhES in the present study. The results presented here were in contrast with previous studies where only AAMΦ associated genes, but not CAMΦs, were expressed in isolated peritoneal MΦ of BALB/c and C57BL/6 mice that were injected with fluke products (Donnelly *et al*., 2005; Adams *et al*., 2014). MΦ activation outcomes from different progenitor/ precursor populations in response *to F. hepatica* products are therefore recommended for future studies.

The second part of this chapter investigated the impact of age on the response and showed a reduction of NO and arginase activity in BALB/c mice as early as 15 weeks of age in response to D39 pneumococci. These findings provide additional evidence of declining CAMΦ function in response to live D39 infection in older BALB/c mice, demonstrated by reduction of NO secretion. The final part of the chapter investigated inflammatory protein secretion in response to both stimulants, using BALB/c mice. One of the main findings observed was the detection of IL-12p70 in the D39 infected BALB/c BMDMΦs and the capacity of FhES to increase this cytokine in co-exposed BALB/c BMDMΦs compared to D39 alone. IL-12p70 was not detected in the previous chapter investigating J774.2 MΦ (BALB/c monocyte/ macrophage cell line) exposed to D39SN. Different origin of the cells could explain the different IL-12p70 secretion. I observed not significantly up-modulated of TNF-α, IL-6 and CXCL1/ KC production in co-exposed BALB/c BMDMΦs compared to D39 from three replicate cultures. Thus, more samples should be tested to increase confidence in these findings. With an FhES concentration of 5µg/ml, BALB/c BMDMΦs produced IL-10 when exposed to FhES alone where the same FhES concentration failed to induce IL-10 in J774.2 MΦs. The experimental design, whereby I introduced D39 first, before stimulation with FhES, could further explain the induction of a CAMΦ rather than AAMΦ phenotype in chapters 3 and 4. Thus, it would be interesting to alternate the exposure approach by introducing the fluke products first followed by bacterial stimulation in future studies.

Overall, these results suggest that cell passage number, mouse age, mouse strain and the order in which cells are stimulated with D39, i.e. before treatment with FhES, are critical in determining the subsequent responses observed in these studies.

7.2.3 Investigating the effect of *Fasciola hepatica* antigens on *Streptococcus pneumoniae* nasopharyngeal carriage in a mouse model

In Chapter 5, the ability of FhES to modulate the immune responses to pneumococcal infection was investigated. Our study showed that FhES may have a short-term impact via promotion of increased nasopharyngeal colonisation of D39 at day 3 in the co-exposed CD1 mice. In this model, with a low inoculum dose of 10^5 CFU D39 in 10µl PBS, seeding of bacteria from nasopharynx to lungs is not typical, although it can occur and can be indicative of an elevated risk of pneumonia. The use of antigens

rather than a live fluke infection may have limited the duration of effects in the co-infected host. Thus, for the future it would be interesting to investigate the long-term effects using live *F. hepatica* infection and using a higher bacterial dose (10^7 CFU). Analysis of nasopharynx samples did not detect high levels of cytokine and chemokine production. The weaker induction of MΦ activation could be due to the uncontrolled distribution of the stimulant inoculum in the *in vivo* setting compared to the *in vitro* setting. Low-density of infection or dilution of proteins due to the dissection methods may also have made detection by the multiplex assay challenging and requires further investigation. Lung homogenates could also be assayed for production of signalling proteins. This is important because recruitment of some immune cells was observed in the lungs and could be associated with cytokine or chemokine responses in the exposed tissues. D39 mice demonstrated lower TGF-β1 production than FhES and co-exposed mice and this could partially explain the susceptibility of CD-1 mice to D39 infection. These results are supported by the very low levels of in NO CD-1 BMDMΦ cultures infected with D39 compared to co-exposed cultures (discussed in Chapter 4). The final part of this chapter described the immune cell recruitment over the course of infection. An influx of innate and adaptive immune cells to the lungs from the NP was observed, despite the low dose of D39 inoculum utilised in the present study. NP appears to act as a focal point of immune responses to pneumococcal carriage, as compared to the lungs and evidenced by the relative levels of neutrophils, B cell, NK cell and Th cell influx to the tissues. However, future work is still needed to establish the whole picture of immune profiles in FhES-pneumococcus interaction. The future investigation of immunomodulatory phenotypes of Th cells subtypes (Th1, Th17, Treg) between these two pathogens in the co-infected host would be very interesting. TGF-β1 that was maintained in the NP of the co-exposed mice shaping the pathogen survival by suppressing the immune response during infection. Recruitment of MR expressing populations of MΦ and monocytes, suggest the involvement of AAMΦ in the co-exposed mice that influence the activation of the acquired immune response. Perhaps, the use of live fluke suggested for future studies will also induce stronger MΦs responses.

Overall these results have shown that CD1 mice infected with low dose of D39 and treated with FhES have higher bacterial loads in the nasopharynx, an increase expression of TGF-β1 and low levels of NO production, suggesting that FhES treatment moderated the murine response to D39 infection.

7.2.4 Macrophage gene expression in response to *Fasciola hepatica*-pneumococcus co-exposure

In Chapter 6, BALB/c BMDMΦ gene expression following exposure to both stimulants was investigated using Nanostring. D39 and co-exposed cultures were clustered together, indicating a closer relationship in both cultures than to FhES alone or uninfected cultures. The genes of pro-inflammatory cytokines and chemokine ligands were significantly expressed in D39 infected BMDMΦs. The most obvious findings in this part of analysis is the expression of *CCL2* gene that was also observed in FhES exposed BMDMΦs. Combined effects of both fluke and D39 stimulants demonstrated the highest log2 FC of CAMΦ associated genes. Co-exposed BMDMΦs up-regulate the expression of type 1 immunity associated genes, confirming the CAMΦ activation in the co-exposed BALB/c BMDMΦs. *IL-1β* induced CAMΦ activation in the co-exposed BALB/c BMDMΦs is likely in response to *NLRP3* inflammasome activation, mediated by Ply released by D39 and cathepsins in FhES. *F. hepatica* cathepsin L3 is expressed mainly in the juvenile fluke and also known to induce non-canonical NLRP3 inflammasome in murine DCs (Celias *et al*., 2019). In the present study, FhES antigens were prepared from the adult fluke that could differently activate the *NLRP3* inflammasome and *IL-1β* expression in the co-exposed BALB/c BMDMΦs. Thus, the association of *NLRP3* inflammasome and *IL-1β* using different stages of excretory/ secretory *F. hepatica* antigens is recommended for future investigation. At 6 hours of exposure, *TLR2* but not *TLR4* and *TLR7* genes were activated in the co-exposed BALB/c BMDMΦs. However, whilst, *TL2* and *TLR4* were also expressed in D39, *TLR4* and *TLR7* were down-regulated in FhES exposed BMDMΦs in the present study. The pathway score revealed that D39 expressed Th1 associated genes and maintain the Th1 activation, although in the presence of FhES. Pathway analysis indicated pro-inflammatory cytokines and TLR2 pathways in the co-exposed BMDMΦs. *CCL6, CXCL4, CXCL4L1, CXCL14* and *TGF-β1* genes were down-regulated in co-exposed BMDMΦs. Although CCL6 and *CXCL14* genes are known to have antibacterial

properties, the down-regulation of these genes in co-exposed BMDMΦs could alter the immunity in co-infection. In the present study, the stimuli used might lead to the activation of TGF-β protein without any change in gene expression that resulted in the down-regulation of *TGF-β1* in D39 and co-exposed cultures.

In conclusion, the results presented in this thesis highlight the complexity of the immune response in co-infection. Co-exposure of FhES consistently enhanced CAMΦ phenotype in D39SN exposed J774.2 and in D39-infected BALB/C BMDMΦ supported by the detection of pro-inflammatory cytokines. Th1 gene activation was also observed in FhES+D39 co-exposed BALB/C BMDMΦ cultures. Use of *in vitro* and *in vivo* murine model systems can help elucidate some of these interactions although the outcomes then need exploring in real life situations such as in human populations exposed to both liver fluke and pneumococcal disease. The results I have presented in this thesis show that immune responses are affected by the passage number of immortalised cell lines, the age and strain of mice used in each study and the order in which the animals/cells are exposed to each pathogen. However, overall, these results suggest that *F. hepatica* can modulate the macrophage response to *Streptococcus pneumoniae* infection, potentially exacerbating the establishment and dissemination of the bacterium.

REFERENCES

Abdullahi, O., Karani, A., Tigoi, C. C., Mugo, D., Kungu, S., Wanjiru, E., Jomo, J., Musyimi, R., Lipsitch, M., Scott, J. A. G. (2012). Rates of acquisition and clearance of pneumococcal serotypes in the nasopharynges of children in Kilifi District, Kenya. *Journal of Infectious Diseases*, *206*(7), 1020–1029. https://doi.org/10.1093/infdis/jis447

Aberdein, J. D., Cole, J., Bewley, M. A., Marriott, H. M., Dockrell, D. H. (2013). Alveolar macrophages in pulmonary host defence-the unrecognized role of apoptosis as a mechanism of intracellular bacterial killing. *Clinical and Experimental Immunology*, *174*(2), 193–202. https://doi.org/10.1111/cei.12170

Adams, P. N., Aldridge, A., Vukman, K. V., Donnelly, S., Oneill, S. M. (2014). *Fasciola hepatica* tegumental antigens indirectly induce an M2 macrophage-like phenotype *in vivo*. *Parasite Immunology*, *36*(10), 531–539. https://doi.org/10.1111/pim.12127

Afshan, K., Fortes-Lima, C. A., Artigas, P., Valero, A. M., Qayyum, M., Mas-Coma, S. (2014). Impact of climate change and man-made irrigation systems on the transmission risk, long-term trend and seasonality of human and animal fascioliasis in Pakistan. *Geospatial Health*, *8*(2), 317–334. https://doi.org/10.4081/gh.2014.22

Ahmed, N., French, T., Rausch, S., Kühl, A., Hemminger, K., Dunay, I. R., Steinfelder, S., Hartmann, S. (2017). Toxoplasma co-infection prevents Th2 differentiation and leads to a helminth-specific Th1 response. *Frontiers in Cellular and Infection Microbiology*, *7*(July), 1–12. https://doi.org/10.3389/fcimb.2017.00341

Aitken, M. M., Jones, P. W., Hall, G. A., Hughes, D. L. (1976). The effect of fascioliasis on susceptibility of cattle to *Salmonella Dublin. The British Veterinary Journal*, *132*(1), 119–120. https://doi.org/10.1016/S0007-1935(17)34799-1

Aitken, Maureen M., Hughes, D. L., Jones, P. W., Hall, G. A., Collis, K. A. (1978). Effects of intravenous *Salmonella Dublin* on cattle at different stages of *Fasciola hepatica* infection. *Journal of Comparative Pathology*, *88*(3), 433–442. https://doi.org/10.1016/0021-9975(78)90048-8

Aldinger, K. A., Sokoloff, G., Rosenberg, D. M., Palmer, A. A., Millen, K. J. (2009). Genetic variation and population substructure in outbred CD-1 mice: Implications for genome-wide association studies. *PLoS ONE*, *4*(3), 2–11. https://doi.org/10.1371/journal.pone.0004729

Aldridge, A., O'Neill, S. M. (2016). *Fasciola hepatica* tegumental antigens induce anergic-like T cells via dendritic cells in a mannose receptor-dependent manner. *European Journal of Immunology*, *46*(5), 1180–1192. https://doi.org/10.1002/eji.201545905

Alhamdi, Y., Neill, D. R., Abrams, S. T., Malak, H. A., Yahya, R., Barrett-Jolley, R.,Wang, G., Kadioglu, A., Toh, C. H. (2015). Circulating pneumolysin is a potent inducer of cardiac injury during pneumococcal infection. *PLoS Pathogens*, *11*(5), 1–29. https://doi.org/10.1371/journal.ppat.1004836

Almirall, J., González, C. A., Balanzó, X., Bolíbar, I. (1999). Proportion of community-acquired pneumonia cases attributable to tobacco smoking. *Chest*, *116*(2), 375–379. https://doi.org/10.1378/chest.116.2.375

Alvarado, R., To, J., Lund, M. E., Pinar, A., Mansell, A., Robinson, M. W., O'Brien, B. A., Dalton, J. P., Donnelly, S. (2017). The immune modulatory peptide FhHDM-1 secreted by the helminth *Fasciola hepatica* prevents NLRP3 inflammasome activation by inhibiting endolysosomal acidification in macrophages. *FASEB Journal*, *31*(1), 85–95. https://doi.org/10.1096/fj.201500093R

Andreu, N., Phelan, J., de Sessions, P. F., Cliff, J. M., Clark, T. G., Hibberd, M. L. (2017). Primary macrophages and J774 cells respond differently to infection with *Mycobacterium tuberculosis*. *Scientific Reports*, *7*(October 2016), 42225. https://doi.org/10.1038/srep42225

Andrews, S. J. (1999). The Life Cycle of *Fasciola hepatica*, in: Dalton, J.P. (Ed.), Fasciolosis. CABI Publishing, New York, pp.1-29

Anthony, R. M., Rutitzky, L. I., Urban Jr., J. F., Stadecker, M. J., Gause, W. C. (2007). Protective immune mechanisms in helminth infection. *Nature Reviews Immonulogy*, *7*(12), 975–987. https://doi.org/10.1038/nri2199

Antignano, F., Mullaly, S. C., Burrows, K., Zaph, C. (2011). *Trichuris muris* infection: A model of type 2 immunity and inflammation in the gut. *Journal of Visualized Experiments*, (51), 1–5. https://doi.org/10.3791/2774

Anuracpreeda, P., Songkoomkrong, S., Sethadavit, M., Chotwiwatthanakun, C., Tinikul, Y., Sobhon, P. (2011). *Fasciola gigantica*: Production and characterization of a monoclonal antibody against recombinant cathepsin B3. *Experimental Parasitology*, *127*(2), 340–345. https://doi.org/10.1016/j.exppara.2010.08.012

Apiwattanakul, N., Thomas, P. G., Iverson, A. R., McCullers, J. A. (2014a). Chronic helminth infections impair pneumococcal vaccine responses. *Vaccine*, *32*(42), 5405–5410. https://doi.org/10.1016/j.vaccine.2014.07.107

Apiwattanakul, N., Thomas, P. G., Kuhn, R. E., Herbert, D. R., McCullers, J. A. (2014b). Helminth infections predispose mice to pneumococcal pneumonia but not to other pneumonic pathogens. *Medical Microbiology and Immunology*, *203*(5), 357–364. https://doi.org/10.1007/s00430-014-0344-3

Ashrafi, K., Bargues, M. D., O'Neill, S., Mas-Coma, S. (2014). Fascioliasis: A worldwide parasitic disease of importance in travel medicine. *Travel Medicine and Infectious Disease*, *12*(6), 636–649. https://doi.org/10.1016/j.tmaid.2014.09.006

Atri, C., Guerfali, F. Z., Laouini, D. (2018). Role of human macrophage polarization in inflammation during infectious diseases. *International Journal of Molecular Sciences*, *19*(6). https://doi.org/10.3390/ijms19061801

Auranen, K., Mehtälä, J., Tanskanen, A., Kaltoft, M. S. (2010). Between-strain competition in acquisition and clearance of pneumococcal carriage epidemiologic evidence from a longitudinal study of day-care children. *American Journal of Epidemiology*, *171*(2), 169–176. https://doi.org/10.1093/aje/kwp351

Balachandran, P., Hollingshead, S. K., Paton, J. C., Briles, D. E. (2001). The autolytic enzyme lytA of *Streptococcus pneumoniae* is not responsible for releasing pneumolysin. *Journal of Bacteriology*, *183*(10), 3108–3116. https://doi.org/10.1128/JB.183.10.3108-3116.2001

Bashi, T., Bizzaro, G., Ben-Ami Shor, D., Blank, M., Shoenfeld, Y. (2015). The mechanisms behind helminth's immunomodulation in autoimmunity. *Autoimmunity Reviews*, *14*(2), 98–104. https://doi.org/10.1016/j.autrev.2014.10.004

Bąska, P., Norbury, L. J., Zawistowska-Deniziak, A., Wiśniewski, M., Januszkiewicz, K. (2017). Excretory/secretory products from two *Fasciola hepatica* isolates induce different transcriptional changes and IL-10 release in LPS-activated bovine "BOMA" macrophages. *Parasitology Research*, *116*(10), 2775–2782. https://doi.org/10.1007/s00436-017-5588-6

Bąska, P., Zawistowska-Deniziak, A., Norbury, L. J., Wiśniewski, M., Januszkiewicz, K. (2019). *Fasciola hepatica* isolates induce different immune responses in unmaturated bovine macrophages. *Journal of Veterinary Research (Poland)*, *63*(1), 63–70. https://doi.org/10.2478/jvetres-2019-0011

Beesley, N. J., Caminade, C., Charlier, J., Flynn, R. J., Hodgkinson, J. E., Martinez-Moreno, A., Martinez-Valladares, M., Perez, J., Rinaldi, L., Williams, D. J. L. (2017a). Fasciola and fasciolosis in ruminants in Europe: Identifying research needs. *Transboundary and Emerging Diseases*, (April), 1–18. https://doi.org/10.1111/tbed.12682

Beesley, Nicola J., Williams, D. J. L., Paterson, S., Hodgkinson, J. (2017b). *Fasciola hepatica* demonstrates high levels of genetic diversity, a lack of population structure and high gene flow: possible implications for drug resistance. *International Journal for Parasitology*, *47*(1), 11–20. https://doi.org/10.1016/j.ijpara.2016.09.007

Bennett, J. M., Reeves, G., Billman, G. E., Sturmberg, J. P. (2018). Inflammation-nature's way to efficiently respond to all types of challenges: Implications for understanding and managing "the epidemic" of chronic diseases. *Frontiers in Medicine*, *5*(NOV), 1–30. https://doi.org/10.3389/fmed.2018.00316

Benoit, M., Desnues, B., Mege, J.-L. (2008). Macrophage polarization in bacterial infections. *The Journal of Immunology*, *181*(6), 3733–3739. https://doi.org/10.4049/jimmunol.181.6.3733

Benton, K. A., Paton, J. C., Briles, D. E. (1997). Differences in virulence for mice among *Streptococcus pneumoniae* strains of capsular types 2, 3, 4, 5, and 6 are not attributable to differences in pneumolysin production. *Infection and Immunity*, *65*(4), 1237–1244.

Bewley, M. A., Marriott, H. M., Tulone, C., Francis, S. E., Mitchell, T. J., Read, R. C.,Chain, B., Kroemer, G., Whyte, M.K.B, Dockrell, D. H. (2011). A cardinal role for cathepsin D in co-ordinating the host-mediated apoptosis of macrophages and killing of pneumococci. *PLoS Pathogens*, *7*(1). https://doi.org/10.1371/journal.ppat.1001262

Bewley, M. A., Naughton, M., Preston, J., Mitchell, A., Holmes, A., Marriott, H. M., Read, R. C., Miytchell, T. J., Whyte, M. K. B., Dockrell, D. H. (2014). Pneumolysin activates macrophage lysosomal membrane permeabilization and executes apoptosis by distinct mechanisms without membrane pore formation. *MBio*, *5*(5), 1–13. https://doi.org/10.1128/mBio.01710-14

Biswas, S. K., Mantovani, A. (2012). Orchestration of metabolism by macrophages. *Cell Metabolism*, *15*(4), 432–437. https://doi.org/10.1016/j.cmet.2011.11.013

Blackwell, N. M., Else, K. J. (2001). B cells and antibodies are required for resistance to the parasitic gastrointestinal nematode *Trichuris muris*. *Infection and Immunity*, *69*(6), 3860–3868. https://doi.org/10.1128/IAI.69.6.3860-3868.2001

Bogaert, D., De Groot, R., Hermans, P. W. M. (2004). *Streptococcus pneumoniae* colonisation: The key to pneumococcal disease. *Lancet Infectious Diseases*, *4*(3), 144–154. https://doi.org/10.1016/S1473-3099(04)00938-7

Brady, M., O'Neil, S., Dalton, J., Mills, K. (1999). *Fasciola hepatica* suppresses a protective Th1 response against *Bordetella pertussis*. *Infect Immun*, *67*(10), 5372–5378.

Branger, J., Knapp, S., Weijer, S., Leemans, J. C., Pater, J. M., Speelman, P., Florquin, S., van Der Poll, T. (2004). Role of toll-like receptor 4 in gram-positive and gram-negative pneumonia in mice. *Infection and Immunity*, *72*(2), 788–794. https://doi.org/10.1128/IAI.72.2.788-794.2004

Braun, J. S., Novak, R., Gao, G., Murray, P. J., Shenep, J. L. (1999). Pneumolysin, a protein toxin of *Streptococcus pneumoniae*, induces nitric oxide production from macrophages. *Infection and Immunity*, *67*(8), 3750–3756.

Briken, V., Mosser, D. M. (2011). Editorial: switching on arginase in M2 macrophages. *Journal of Leukocyte Biology*, *90*(5), 839–841. https://doi.org/10.1189/jlb.0411203

Bronte, V., Serafini, P., De Santo, C., Marigo, I., Tosello, V., Mazzoni, A., Segal, D. M., Staib, C., Lowel, M., Sutter, G., Colombo, M. P., Zanovello, P. (2003). IL-4-induced arginase 1 suppresses alloreactive T cells in tumor-bearing mice. *The Journal of Immunology*, *170*(1), 270–278. https://doi.org/10.4049/jimmunol.170.1.270

Brown, J. S., Hussell, T., Gilliland, S. M., Holden, D. W., Paton, J. C., Ehrenstein, M. R., Walport, M. J., Botto, M., Botto, M. (2002). The classical pathway is the dominant complement pathway required for innate immunity to *Streptococcus pneumoniae* infection in mice. *Proceedings of the National Academy of Sciences of the United States of America*, *99*(26), 16969–16974. https://doi.org/10.1073/pnas.012669199

Cadman, E. T., Lawrence, R. A. (2010). Granulocytes: Effector cells or immunomodulators in the immune response to helminth infection? *Parasite Immunology*, *32*(1), 1–19. https://doi.org/10.1111/j.1365-3024.2009.01147.x

Calbo, E., Alsina, M., Rodríguez-Carballeira, M., Lite, J., Garau, J. (2008). Systemic expression of cytokine production in patients with severe pneumococcal pneumonia: Effects of treatment with a β-lactam versus a fluoroquinolone. *Antimicrobial Agents and Chemotherapy*, *52*(7), 2395–2402. https://doi.org/10.1128/AAC.00658-07

Cancela, M., Acosta, D., Rinaldi, G., Silva, E., Durán, R., Roche, L., Zaha, A., carmona, C., Tort, J. F. (2008). A distinctive repertoire of cathepsins is expressed by juvenile invasive *Fasciola hepatica*. *Biochimie*, *90*(10), 1461–1475. https://doi.org/10.1016/j.biochi.2008.04.020

Cancela, M., Ruétalo, N., Dell'Oca, N., da Silva, E., Smircich, P., Rinaldi, G., Roche, L., Carmona, C., Alvarez-Valin, F., Zaha, A., Tort, J. F. (2010). Survey of transcripts expressed by the invasive juvenile stage of the liver fluke *Fasciola hepatica*. *BMC Genomics*, *11*(1). https://doi.org/10.1186/1471-2164-11-227

Canvin, J. R., Marvin, A. P., Sivakumaran, M., Paton, J. C., Boulnois, G. J., Andrew, P. W., Mitchell, T. J. (1995). The role of pneumolysin and autolysin in the pathology of pneumonia and septicemia in mice infected with a type 2 pneumococcus. *Journal of Infectious Diseases*, *172*(1), 119–123. https://doi.org/10.1093/infdis/172.1.119

Car, B. D., Eng, V. M., Schnyder, B., LeHir, M., Shakhov, A. N., Woerly, G., Huang, S., Aguet, M., Anderson, T. D., Ryffel, B. (1995). Role of interferon-γ in interleukin 12-induced pathology in mice. *American Journal of Pathology*, *147*(6), 1693–1707

Carmona, C., Dowd, A. J., Smith, A. M., Dalton, J. P. (1993). Cathepsin L proteinase secreted by *Fasciola hepatica in vitro* prevents antibody-mediated eosinophil attachment to newly excysted juveniles. *Molecular and Biochemical Parasitology*, *62*(1), 9–17. https://doi.org/10.1016/0166-6851(93)90172-T

Cassado, A. A., D'Império Lima, M. R., Bortoluci, K. R. (2015). Revisiting mouse peritoneal macrophages: Heterogeneity, development, and function. *Frontiers in Immunology*, *6*(MAY), 1–9. https://doi.org/10.3389/fimmu.2015.00225

Cecílio, C. A., Costa, E. H., Simioni, P. U., Gabriel, D. L., Tamashiro, W. M. S. C. (2011). Aging alters the production of iNOS, arginase and cytokines in murine macrophages. *Brazilian Journal of Medical and Biological Research*, *44*(7), 671–681. https://doi.org/10.1590/S0100-879X2011000700010

Celias, D. P., Corvo, I., Silvane, L., Tort, J. F., Chiapello, L. S., Fresno, M., Arranz, A., Motran, C. C., Cervi, L. (2019). Cathepsin L3 from *Fasciola hepatica* induces NLRP3 inflammasome alternative activation in murine dendritic cells. *Frontiers in Immunology*, *10*(MAR), 1–15. https://doi.org/10.3389/fimmu.2019.00552

Cervi, L., Serradell, M. C., Guasconi, L., Masih, D. T. (2009). New insights into the modulation of immune response by *Fasciola hepatica* excretory-secretory products. *Current Immunology Reviews*, *5*(4), 277–284. https://doi.org/10.2174/157339509789503961

Charlier, J., Duchateau, L., Claerebout, E., Williams, D., Vercruysse, J. (2007). Associations between anti-*Fasciola hepatica* antibody levels in bulk-tank milk samples and production parameters in dairy herds. *Preventive Veterinary Medicine*, *78*(1), 57–66. https://doi.org/10.1016/j.prevetmed.2006.09.010

Charlier, J., Hostens, M., Jacobs, J., van Ranst, B., Duchateau, L., Vercruysse, J. (2012). Integrating fasciolosis control in the dry cow management: The effect of closantel treatment on milk production. *PLoS ONE*, *7*(8), 1–7. https://doi.org/10.1371/journal.pone.0043216

Chen, C.-C., Louie, S., McCormick, B. A., Walker, W. A., Shi, H. N. (2006). Helminth-primed dendritic cells alter the host response to enteric bacterial infection. *The Journal of Immunology*, *176*(1), 472–483. https://doi.org/10.4049/jimmunol.176.1.472

Chen, L. C., Pace, J. L., Russell, S. W., Morrison, D. C. (1996). Altered regulation of inducible nitric oxide synthase expression in macrophages from senescent mice. *Infection and Immunity*, *64*(10), 4288–4298.

Chen, L., Deng, H., Cui, H., Fang, J., Zuo, Z., Deng, J., Li, Y., Wang, X., Zhao, L. (2018). Inflammatory responses and inflammation-associated diseases in organs. *Oncotarget*, *9*(6), 7204–7218. Retrieved from www.impactjournals.com/oncotarget/

Chorinchath, B. B., Kong, L.-Y., Mao, L., McCallum, R. E. (1996). Age-associated differences in TNF-α and nitric oxide production in endotoxic mice. *Journal of Immunology*, *156*(4), 1525–1530.

Claridge, J., Diggle, P., McCann, C. M., Mulcahy, G., Flynn, R., McNair, J.,Strain, S., Welsh, M., Baylis, M., Williams, D. J. L. (2012). *Fasciola hepatica* is associated with the failure to detect bovine tuberculosis in dairy cattle. *Nature Communications*, *3*(May), 853. https://doi.org/10.1038/ncomms1840

Clery, D. G., Mulcahy, G. (1998). Lymphocyte and cytokine responses of young cattle during primary infection with *Fasciola hepatica*. *Research in Veterinary Science*, *65*(2), 169–171. https://doi.org/10.1016/S0034-5288(98)90171-0

Clery, D., Torgerson, P., Mulcahy, G. (1996). Immune responses of chronically infected adult cattle to *Fasciola hepatica*. *Veterinary Parasitology*, *62*(1–2), 71–82. https://doi.org/10.1016/0304-4017(95)00858-6

Coleman, F. T., Blahna, M. T., Kamata, H., Yamamoto, K., Zabinski, M. C., Kramnik, I., Wilson, A. A., Kotton, D. , N., Quinton, L. J., Jones, M. R., Pelton, S. I, Mizgerd, J. P. (2017). Capacity of pneumococci to activate macrophage nuclear factor κB: Influence on necroptosis and pneumonia severity. *Journal of Infectious Diseases*, *216*(4), 425–435. https://doi.org/10.1093/infdis/jix159

Collins, P. R., Stack, C. M., O'Neill, S. M., Doyle, S., Ryan, T., Brennan, G. P., Moueley, A., Stewart, M., Maule, A. G., Dalton, J. P., Donnelly, S. (2004). Cathepsin L1, the major protease involved in liver fluke (*Fasciola hepatica*) virulence: Propeptide cleavage sites and autoactivation of the zymogen secreted from gastrodermal cells. *Journal of Biological Chemistry*, *279*(17), 17038–17046. https://doi.org/10.1074/jbc.M308831200

Correale, J., Farez, M. (2009). Helminth antigens modulate immune responses in cells from multiple sclerosis patients through TLR2-dependent mechanisms. *The Journal of Immunology*, *183*(9), 5999–6012. https://doi.org/10.4049/jimmunol.0900897

Correale, J., Farez, M. F. (2012). Does helminth activation of toll-like receptors modulate immune response in multiple sclerosis patients? *Frontiers in Cellular and Infection Microbiology*, *2*(August), 1–14. https://doi.org/10.3389/fcimb.2012.00112

Corthay, A. (2009). How do regulatory t cells work? *Scandinavian Journal of Immunology*, *70*(4), 326–336. https://doi.org/10.1111/j.1365-3083.2009.02308.x

Cosivi, O., Grange, J. M., Daborn, C. J., Raviglione, M. C., Fujikura, T., D, C., Cousins, D., Robinsons, R. A., Huchzermeyer, H. F. A. K., de Kantor, I., Meslin, F.-X. (2016). Zoonotic tuberculosis due to *Mycobacterium bovis* in developing countries. *Emerging Infectious Diseases*, *4*(1), 1–8. https://doi.org/10.1214/10-STS330

Couper, K. N., Blount, D. G., Riley, E. M. (2008). IL-10: The master regulator of immunity to infection. *The Journal of Immunology*, *180*(9), 5771–5777. https://doi.org/10.4049/jimmunol.180.9.5771

Cwiklinski, K., O'Neill, S. M., Donnelly, S., Dalton, J. P. (2016). A prospective view of animal and human Fasciolosis. *Parasite Immunology*, *38*(9), 558–568. https://doi.org/10.1111/pim.12343

Cwiklinski, Krystyna, Jewhurst, H., McVeigh, P., Barbour, T., Maule, A. G., Tort, J., O'Neill, S. M., Robinson, M. W., Donnelly, S., Dalton, J. P. (2018). Infection by the helminth parasite *Fasciola hepatica* requires rapid regulation of metabolic, virulence, and invasive factors to adjust to its mammalian host. *Molecular and Cellular Proteomics*, *17*(4), 792–809. https://doi.org/10.1074/mcp.RA117.000445

Dai, C., Basilico, P., Cremona, T. P., Collins, P., Moser, B., Benarafa, C., Wolf, M. (2015). CXCL14 displays antimicrobial activity against respiratory tract bacteria and contributes to clearance of *Streptococcus pneumoniae* pulmonary infection . *The Journal of Immunology*, *194*(12), 5980–5989. https://doi.org/10.4049/jimmunol.1402634

Daigneault, M., de Silva, T. I., Bewley, M. A., Preston, J. A., Marriott, H. M., Mitchell, A. M., Mitchel, T. J., Read, R. C., Whyte, M. K. B., Dockrell, D. H. (2012). Monocytes regulate the mechanism of T-cell death by inducing Fas-mediated apoptosis during bacterial infection. *PLoS Pathogens*, *8*(7), 30. https://doi.org/10.1371/journal.ppat.1002814

Dalton, J. P., Mulcahy, G. (2001). Parasite vaccines - A reality? *Veterinary Parasitology*, *98*(1–3), 149–167. https://doi.org/10.1016/S0304-4017(01)00430-7

Dalton, J. P., McGonigle, S., Rolph, T. P., Andrews, S. J. (1996). Induction of protective immunity in cattle against infection with *Fasciola hepatica* by vaccination with cathepsin L proteinases and with hemoglobin. *Infection and Immunity*, *64*(12), 5066–5074. https://doi.org/10.1128/iai.64.12.5066-5074.1996

Dalton, J. P., Robinson, M. W., Mulcahy, G., O'Neill, S. M., Donnelly, S. (2013). Immunomodulatory molecules of *Fasciola hepatica*: Candidates for both vaccine and immunotherapeutic development. *Veterinary Parasitology*, *195*(3–4), 272–285. https://doi.org/10.1016/j.vetpar.2013.04.008

Das, A., Sinha, M., Datta, S., Abas, M., Chaffee, S., Sen, C. K., Roy, S. (2015). Monocyte and macrophage plasticity in tissue repair and regeneration. *American Journal of Pathology*, *185*(10), 2596–2606. https://doi.org/10.1016/j.ajpath.2015.06.001

Davis, K. M., Nakamura, S., Weiser, J. N. (2011). Nod2 sensing of lysozyme-digested peptidoglycan promotes macrophage recruitment and clearance of *S. pneumoniae* colonization in mice. *Journal of Clinical Investigation*, *121*(9), 3666–3676. https://doi.org/10.1172/JCI57761

de Groen, R. A., Boltjes, A., Hou, J., Liu, B. S., Mcphee, F., Friborg, J., Janssen, H. L. A., Boonstra, A. (2015). IFN-λ-mediated IL-12 production in macrophages induces IFN-γ production in human NK cells. *European Journal of Immunology*, *45*(1), 250–259. https://doi.org/10.1002/eji.201444903

de La Rua-Domenech, R. (2006). Human *Mycobacterium bovis* infection in the United Kingdom: Incidence, risks, control measures and review of the zoonotic aspects of bovine tuberculosis. *Tuberculosis*, *86*, 77–109. https://doi.org/10.1016/j.tube.2005.05.002

del Mar García-Suárez, M., Cima-Cabal, M. D., Flórez, N., García, P., Cernuda-Cernuda, R., Astudillo, A., Vazquez, F., Toyos, J, R. D., L., Méndez, F. J. (2004). Protection against pneumococcal pneumonia in mice by monoclonal antibodies to pneumolysin. *Infection and Immunity*, *72*(8), 4534–4540. https://doi.org/10.1128/IAI.72.8.4534-4540.2004

Denny, P., Hopes, E., Gingles, N., Broman, K. W., McPheat, W., Morten, J., Alexander, J., Andrew, P. W, Brown, S. D. M. (2003). A major locus conferring susceptibility to infection by *Streptococcus pneumoniae* in mice. *Mammalian Genome*, *14*(7), 448–453. https://doi.org/10.1007/s00335-002-2261-9

deSchoolmeester, M. L., Martinez-Pomares, L., Gordon, S., Else, K. J. (2009). The mannose receptor binds *Trichuris muris* excretory/secretory proteins but is not essential for protective immunity. *Immunology*, *126*(2), 246–255. https://doi.org/10.1111/j.1365-2567.2008.02893.x

Dietrich, C. F., Kabaalioglu, A., Brunetti, E., Richter, J. (2015). Fasciolosis. *Z Gastroenterology*, *53*,285–290. http://dx.doi.org/ 10.1055/s-0034-1385728

Diment, S., Leech, M. S., Stahl, P. D. (1987). Generation of macrophage variants with 5-Azacytidine: Selection for mannose receptor expression. *Journal of Leukocyte Biology*, *42*(5), 485–490. https://doi.org/10.1002/jlb.42.5.485

Dockrell, D. H., Lee, M., Lynch, D. H., Read, R. C. (2001). Immune-mediated phagocytosis and killing of *Streptococcus pneumoniae* are associated with direct and bystander macrophage apoptosis. *Journal of Infectious Diseases*, *184*(6), 713–722. https://doi.org/10.1086/323084

Dockrell, D. H., Marriott, H. M., Prince, L. R., Ridger, V. C., Ince, P. G., Hellewell, P. G., Whyte, M. K. B. (2003). Alveolar macrophage apoptosis contributes to pneumococcal clearance in a resolving model of pulmonary infection. *The Journal of Immunology*, *171*(10), 5380–5388. https://doi.org/10.4049/jimmunol.171.10.5380

Domon, H., Oda, M., Maekawa, T., Nagai, K., Takeda, W., Terao, Y. (2016). *Streptococcus pneumoniae* disrupts pulmonary immune defence via elastase release following pneumolysin-dependent neutrophil lysis. *Scientific Reports*, *6*(June), 1–13. https://doi.org/10.1038/srep38013

Donnelly, S, Dalton, J. P., Robinson, M. (2011). How pathogen-derived cysteine proteases modulate host immune responses, in: Robinson, M. W. and Dalton, J. P. (Ed.), Cysteine Proteases of Pathogenic Organisms. Landes Biosciences and Springer Science+Business Media, pp. 192-207

Donnelly, S., O'Neill, S. M., Sekiya, M., Mulcahy, G., Dalton, J. P. (2005). Thioredoxin Peroxidase Secreted by *Fasciola hepatica* induces the alternative activation of macrophages. *Infection and Immunity*, *73*(1), 166–173. https://doi.org/10.1128/IAI.73.1.166

Donnelly, S., O'Neill, S. M., Stack, C. M., Robinson, M. W., Turnbull, L., Whitchurch, C., Dalton, J. P. (2010). Helminth cysteine proteases inhibit TRIF-dependent activation of macrophages via degradation of TLR3. *Journal of Biological Chemistry*, *285*(5), 3383–3392. https://doi.org/10.1074/jbc.M109.060368

Donnelly, Sheila, Stack, C. M., O'Neill, S. M., Sayed, A. A, Williams, D. L., Dalton, J. P. (2008). Helminth 2-Cys peroxiredoxin drives Th2 responses through a mechanism involving alternatively activated macrophages. *The FASEB*, *22*(11), 4022–4032. https://doi.org/10.1096/fj.08-106278

Dornand, J., Gross, A., Lafont, V., Liautard, J., Oliaro, J., Liautard, J. P. (2002). The innate immune response against *Brucella* in humans. *Veterinary Microbiology*, *90*(1–4), 383–394. https://doi.org/10.1016/S0378-1135(02)00223-7

Dorrington, M. G., Roche, A. M., Chauvin, S. E., Tu, Z., Mossman, K. L., Weiser, J. N., Bowdish, D. M. E. (2013). MARCO is required for TLR2- and Nod2-mediated responses to *Streptococcus pneumoniae* and clearance of pneumococcal colonization in the murine nasopharynx . *The Journal of Immunology*, *190*(1), 250–258. https://doi.org/10.4049/jimmunol.1202113

Dowling, D. J., Hamilton, C. M., Donnelly, S., La Course, J., Brophy, P. M., Dalton, J., O'Neill, S. M. (2010). Major secretory antigens of the helminth *Fasciola hepatica* activate a suppressive dendritic cell phenotype that attenuates Th17 cells but fails to activate Th2 immune responses. *Infection and Immunity*, *78*(2), 793–801. https://doi.org/10.1128/IAI.00573-09

Drickamer, K. (1992). Engineering galactose-binding activity into a C-type mannose-binding protein. *Nature*, *360*(6400), 183–186.

Duque, G. A., Descoteaux, A. (2014). Macrophage cytokines: Involvement in immunity and infectious diseases. *Frontiers in Immunology*, *5*(OCT), 1–12. https://doi.org/10.3389/fimmu.2014.00491

Endeman, H., Meijvis, S. C. A., Rijkers, G. T., Van Velzen-Blad, H., Van Moorsel, C. H. M., Grutters, J. C., Biesma, D. H. (2011). Systemic cytokine response in patients with community-acquired pneumonia. *European Respiratory Journal*, *37*(6), 1431–1438. https://doi.org/10.1183/09031936.00074410

Epelman, S., Lavine, K. J., Randolph, G. J. (2014). Origin and functions of tissue macrophages. *Immunity*, *41*(1), 21–35. https://doi.org/10.1016/j.immuni.2014.06.013

Erb, K. J. (2007). Helminths, allergic disorders and IgE-mediated immune responses: Where do we stand? *European Journal of Immunology*, *37*(5), 1170–1173. https://doi.org/10.1002/eji.200737135

Ercoli, G., Fernandes, V. E., Chung, W. Y., Wanford, J. J., Thomson, S., Bayliss, C. D., Straatman, K., Crocker, P.R., Dennison, A., Martinez-Pomares, L., Andrew, P. W., Moxon, E. R., Oggioni, M. R. (2018). Intracellular replication of *Streptococcus pneumoniae* inside splenic macrophages serves as a reservoir for septicaemia. *Nature Microbiology*, *3*(5), 600–610. https://doi.org/10.1038/s41564-018-0147-1

Everts, B., Hussaarts, L., Driessen, N. N., Meevissen, M. H. J., Schramm, G., van der Ham, A. J., van der Hoeven, B., Scholzen, T., Burgdorf, S., Mohrs, M. Pearce, E. J, Hokke, C. H, Haas, H, Smits, H. H., Yazdanbakhsh, M. (2012). Schistosome-derived omega-1 drives Th2 polarization by suppressing protein synthesis following internalization by the mannose receptor. *Journal of Experimental Medicine*, *209*(10), 1753–1767. https://doi.org/10.1084/jem.20111381

Fahel, J. S., MacEdo, G. C., Pinheiro, C. S., Caliari, M. V., Oliveira, S. C. (2010). IPSE/alpha-1 of *Schistosoma mansoni* egg induces enlargement of granuloma but does not alter Th2 balance after infection. *Parasite Immunology*, *32*(5), 345–353. https://doi.org/10.1111/j.1365-3024.2009.01192.x

Falcón, C. R., Masih, D., Gatti, G., Sanchez, M. C., Motrán, C. C., Cervi, L. (2014). *Fasciola hepatica* Kunitz type molecule decreases dendritic cell activation and their ability to induce inflammatory responses. *PLoS ONE*, *9*(12), 1–18. https://doi.org/10.1371/journal.pone.0114505

Fang, R., Tsuchiya, K., Kawamura, I., Shen, Y., Hara, H., Sakai, S., Yamamoto, T., Fernandes-Alnemri, T., Yang, R., Hernandez-Cueller, E., Dewamitta, S. R., Xu, Y., Qu, H., Alnemri, E. S., Mitsuyama, M. (2011). Critical roles of ASC inflammasomes in caspase-1 activation and host innate resistance to *Streptococcus pneumoniae* infection. *The Journal of Immunology*, *187*(9), 4890–4899. https://doi.org/10.4049/jimmunol.1100381

Fiani, M. L., Beitz, J., Turvy, D., Blum, J. S., Stahl, P. D. (1998). Regulation of mannose receptor synthesis and turnover in mouse J774 macrophages. *Journal of Leukocyte Biology*, *64*(1), 85–91. Retrieved from http://www.ncbi.nlm.nih.gov/pubmed/9665280

Figueroa-Santiago, O., Espino, A. M. (2014). *Fasciola hepatica* fatty acid binding protein induces the alternative activation of human macrophages. *Infection and Immunity*, *82*(12), 5005–5012. https://doi.org/10.1128/IAI.02541-14

Figueroa-Santiago, O., Espino, A. M. (2017). *Fasciola hepatica* ESPs could indistinctly activate or block multiple toll-like receptors in a human monocyte cell line. *Annals Clinical Pathology*, *5*(3),1-7.

Flynn, R. J., Irwin, J. A., Olivier, M., Sekiya, M., Dalton, J. P., Mulcahy, G. (2007a). Alternative activation of ruminant macrophages by *Fasciola hepatica*. *Veterinary Immunology and Immunopathology*, *120*(1–2), 31–40. https://doi.org/10.1016/j.vetimm.2007.07.003

Flynn, R. J., Mulcahy, G., Welsh, M., Cassidy, J. P., Corbett, D., Milligan, C., Andersen, P., Strain, S., McNair, J. (2009). Co-Infection of cattle with *Fasciola hepatica* and *Mycobacterium bovis* - Immunological consequences. *Transboundary and Emerging Diseases*, *56*(6–7), 269–274. https://doi.org/10.1111/j.1865-1682.2009.01075.x

Flynn, R. J., Mannion, C., Golden, O., Hacariz, O., Mulcahy, G. (2007b). Experimental *Fasciola hepatica* infection alters responses to tests used for diagnosis of bovine tuberculosis. *Infection and Immunity*, *75*(3), 1373–1381. https://doi.org/10.1128/IAI.01445-06

Flynn, R. J., Mulcahy, G. (2008a). Possible role for toll-like receptors in interaction of *Fasciola hepatica* excretory/secretory products with bovine macrophages. *Infection and Immunity*, *76*(2), 678–684. https://doi.org/10.1128/IAI.00732-07

Flynn, R. J., Mulcahy, G. (2008b). The roles of IL-10 and TGF-β in controlling IL-4 and IFN-γ production during experimental *Fasciola hepatica* infection. *International Journal for Parasitology*, *38*(14), 1673–1680. https://doi.org/10.1016/j.ijpara.2008.05.008

Flynn, R. J., Mulcahy, G., Elsheikha, H. M. (2010). Coordinating innate and adaptive immunity in *Fasciola hepatica* infection: Implications for control. *Veterinary Parasitology*, *169*(3–4), 235–240. https://doi.org/10.1016/j.vetpar.2010.02.015

Fox, J. G., Beck, P., Dangler, C. A., Whary, M. T., Wang, T. C., Shi, H. N., Nagler-Anderson, C. (2000). Concurrent enteric helminth infection modulates inflammation and gastric immune responses and reduces helicobacter-induced gastric atrophy. *Nature Medicine*, *6*(5), 536–542. https://doi.org/10.1038/75015

Fu, Y., Chryssafidis, A. L., Browne, J. A., Sullivan, J. O., Mcgettigan, A., Mulcahy, G. (2016). Transcriptomic study on ovine immune responses to *Fasciola hepatica* infection. *PloS Neglected Tropical Diseases*,*10*(9), 1–27. https://doi.org/10.1371/journal.pntd.0005015

Fürst, T., Keiser, J., Utzinger, J. (2012). Global burden of human food-borne trematodiasis: A systematic review and meta-analysis. *The Lancet Infectious Diseases*, *12*(3), 210–221. https://doi.org/10.1016/S1473-3099(11)70294-8

Ganaie, F., Saad, J. S., McGee, L., van Tonder, A. J., Bentley, S. D., Lo, S. W., Gladstone, R. A., Turner, P., Keenan, J. D., Breiman, R. F., Nahm, M. H. (2020). A new pneumococcal capsule type, 10D, is the 100th serotype and has a large cps fragment from an oral Streptococcus. *MBio*, *11*(3), 1–15. https://doi.org/10.1128/mBio.00937-20

Gandhi, P., Schmitt, E. K., Chen, C. W., Samantray, S., Venishetty, V. K., Hughes, D. (2019). Triclabendazole in the treatment of human fascioliasis: A review. *Transactions of the Royal Society of Tropical Medicine and Hygiene*, *113*(12), 797–804. https://doi.org/10.1093/trstmh/trz093

Garcia-Campos, A., Correia, C. N., Naranjo-Lucena, A., Garza-Cuartero, L., Farries, G., Browne, J. A., MacHugh, D. E, Mulcahy, G. (2019). *Fasciola hepatica* infection in cattle: Analyzing responses of peripheral blood mononuclear cells (PBMC) using a transcriptomics approach. *Frontiers in Immunology*, *10*(August), 1–16. https://doi.org/10.3389/fimmu.2019.02081

Garza-Cuartero, L., O'Sullivan, J., Blanco, A., McNair, J., Welsh, M., Flynn, R. J., Williams, D., Diggle, P., Cassidy, J., Mulcahy, G. (2016). *Fasciola hepatica* infection reduces *Mycobacterium bovis* burden and mycobacterial uptake and suppresses the pro-inflammatory response. *Parasite Immunology*, *38*(7), 387–402. https://doi.org/10.1111/pim.12326

Gautier, E.L., Shay, T., Miller, J., Greter, M., Jakubzick, C., Ivanov, S., Helft, J., Chow, A., Elpek, K.G., Gordonov, S., Mazloom, A. R., Ma'ayan, A., Chua, W.-J., Hansen, T. H., Turley, S. J., Merad, M., Randolph, G. J. (2012). Gene expression profiles and transcriptional regulatory pathways underlying mouse tissue macrophage identity and diversity. *Nature Immunology*, *13*(11), 1118–1128. https://doi.org/10.1038/ni.2419.

Gautier, E. L., Yvan-Charvet, L. (2014). Understanding macrophage diversity at the ontogenic and transcriptomic levels. *Immunological Reviews*, *262*(1), 85–95. https://doi.org/10.1111/imr.12231

Gazi, U., Martinez-Pomares, L. (2009). Influence of the mannose receptor in host immune responses. *Immunobiology*, *214*(7), 554–561. https://doi.org/10.1016/j.imbio.2008.11.004

Gazzinelli-Guimaraes, P. H., Nutman, T. B. (2018). Helminth parasites and immune regulation. *F1000Research*, *7*(0), 1685. https://doi.org/10.12688/f1000research.15596.1

Gee, K., Guzzo, C., Mat, N. F. C., Ma, W., Kumar, A. (2009). The IL-12 family of cytokines in infection, inflammation and autoimmune disorders. *Inflammation and Allergy - Drug Targets*, *8*(1), 40–52. https://doi.org/10.2174/187152809787582507

Geno, K. A., Gilbert, G. L., Song, J. Y., Skovsted, I. C., Klugman, K. P., Jones, C., Konradsen, H. B., Nahm, M. H. (2015). Pneumococcal capsules and their types: Past, present, and future. *Clinical Microbiology Reviews*, *28*(3), 871–899. https://doi.org/10.1128/CMR.00024-15

Geno, K. A., Saad, J. S., Nahm, H. (2017). *Discovery of Novel Pneumococcal Serotype 35D, a Natural WciG-Deficient Variant of Serotype 35B*. *Journal Clincal of Microbiology, 55*(5), 1416–1425.

Gerlini, A., Colomba, L., Furi, L., Braccini, T., Manso, A. S., Pammolli, A., Wang, B., Vivi, A., Tassni, M., van Rooijen, N., Pozzi, G., Ricci, S., Andrew, P. W., Koedel, U., Moxon, E.R., Oggioni, M. R. (2014). The role of host and microbial factors in the pathogenesis of pneumococcal bacteraemia arising from a single bacterial cell bottleneck. *PLoS Pathogens*, *10*(3). https://doi.org/10.1371/journal.ppat.1004026

Gilbert, R. J. C., Jiménez, J. L., Chen, S., Tickle, I. J., Rossjohn, J., Parker, M., Andrew, P. W., Saibil, H. R. (1999). Two structural transitions in membrane pore formation by pneumolysin, the pore-forming toxin of *Streptococcus pneumoniae*. *Cell*, *97*(5), 647–655. https://doi.org/10.1016/S0092-8674(00)80775-8

Gingles, N. A., Alexander, J. E., Kadioglu, A., Andrew, P. W., Kerr, A., Mitchell, T. J., Hopea, E., Denny, P., Brown, S., Jones, H. B., Little, S., Booth, G. C., Mcpheat, W. L. (2001). Role of genetic resistance in invasive pneumococcal infection : identification and study of susceptibility and resistance in inbred mouse strains. *Infect Immun*, *69*(1), 426–434. https://doi.org/10.1128/IAI.69.1.426

Gleissner, C.A., Shaked, I., Little, K.M. Ley, K. (2010). CXCL4 induces a unique transcriptome in monocyte-derived macrophages. *J Immunol.*, *184*(9), 4810–4818. https://doi.org/10.4049/jimmunol.0901368.CXCL4

Glynn, P., Coakley, R., Kilgallen, I., Murphy, N., O'Neill, S. (1999). Circulating interleukin 6 and interleukin 10 in community acquired pneumonia. *Thorax*, *54*(1), 51–55. https://doi.org/10.1136/thx.54.1.51

Golden, O., Flynn, R. J., Read, C., Sekiya, M., Donnelly, S. M., Stack, C., Dalton, J. P., Mulcahy, G. (2010). Protection of cattle against a natural infection of *Fasciola hepatica* by vaccination with recombinant cathepsin L1 (rFhCL1). *Vaccine*, *28*(34), 5551–5557. https://doi.org/10.1016/j.vaccine.2010.06.039

Gondorf, F., Berbudi, A., Buerfent, B. C., Ajendra, J., Bloemker, D., Specht, S., Schmidt, D., Neumann, A.-L., Layland, L.E., Hoerauf, A., Hübner, M. P. (2015). Chronic filarial infection provides protection against bacterial sepsis by functionally reprogramming macrophages. *PLoS Pathogens*, *11*(1), 1–27. https://doi.org/10.1371/journal.ppat.1004616

Goodrum, K. J., McCormick, L. L., Schneider, B. (1994). Group B streptococcus-induced nitric oxide production in murine macrophages is CR3 (CD11b/CD18) dependent. *Infection and Immunity*, *62*(8), 3102–3107.

Gordon, S. (2003). Alternative activation of Macrophages. *Nat Rev Immunol 2003; 3: 23-35*, *3*, 23–35. https://doi.org/10.1017/CBO9781107415324.004

Gordon, S., Martinez-Pomares, L. (2017). Physiological roles of macrophages. *Pflugers Archiv European Journal of Physiology*, *469*(3–4), 365–374. https://doi.org/10.1007/s00424-017-1945-7

Graczyk, T., Fried, B. (1999). Development of *Fasciola hepatica* in the intermediate host, in: Dalton, J. P. (Ed.), Fasciolosis. CABI Publishing, New York, pp. 31-45

Grainger, J. R., Grencis, R. K. (2014). Neutrophils worm their way into macrophage long-term memory. *Nature Immunology*, *15*(10), 902–904. https://doi.org/10.1038/ni.2990

Grencis, R. K. (2001). Cytokine regulation of resistance and susceptibility to intestinal nematode infection - From host to parasite. *Veterinary Parasitology*, *100*(1–2), 45–50. https://doi.org/10.1016/S0304-4017(01)00482-4

Griffin, G.K., Newton, G., Tarrio, M.L., Bu, D-X, Maganto-Garcia, E., Azcutia, V., Alcaide, P., Grabie, N., Luscinskas, F. W., Croce, K. J., Lichtman, A. H. (2012). IL-17 and TNF-α sustain neutrophil recruitment during inflammation through synergistic effects on endothelial activation. *The Journal of Immunology*, *188*(12), 6287-6299. doi:10.4049/jimmunol.1200385

Grohmann, U., Belladonna, M. L., Vacca, C., Bianchi, R., Fallarino, F., Orabona, C., Fioretti, M. C., Puccetti, P. (2001). Positive regulatory role of IL-12 in macrophages and modulation by IFN-γ. *The Journal of Immunology*, *167*(1), 221–227. https://doi.org/10.4049/jimmunol.167.1.221

Guasconi, L., Chiapello, L. S., Masih, D. T. (2015). *Fasciola hepatica* excretory-secretory products induce CD4+T cell anergy via selective up-regulation of PD-L2 expression on macrophages in a Dectin-1 dependent way. *Immunobiology*, *220*(7), 934–939. https://doi.org/10.1016/j.imbio.2015.02.001

Guasconi, L., Serradell, M. C., Garro, A. P., Iacobelli, L., Masih, D. T. (2011). C-type lectins on macrophages participate in the immunomodulatory response to *Fasciola hepatica* products. *Immunology*, *133*(3), 386–396. https://doi.org/10.1111/j.1365-2567.2011.03449.x

Guasconi, L., Serradell, M. C., Masih, D. T. (2012). *Fasciola hepatica* products induce apoptosis of peritoneal macrophages. *Veterinary Immunology and Immunopathology*, *148*(3–4), 359–363. https://doi.org/10.1016/j.vetimm.2012.06.022

Haçariz, O., Sayers, G., Flynn, R. J., Lejeune, A., Mulcahy, G. (2009). IL-10 and TGF-β1 are associated with variations in fluke burdens following experimental fasciolosis in sheep. *Parasite Immunology*, *31*(10), 613–622. https://doi.org/10.1111/j.1365-3024.2009.01135.x

Haçariz, O., Sayers, G., Mulcahy, G. (2011). A preliminary study to understand the effect of *Fasciola hepatica* tegument on naive macrophages and humoral responses in an ovine model. *Veterinary Immunology and Immunopathology*, *139*(2–4), 245–249. https://doi.org/10.1016/j.vetimm.2010.08.007

Hall, G. A., Jones, P. W., Aitken, M. M., Parsons, R., Brown, G. T. H. (1981). Experimental oral *Salmonella Dublin* infection in cattle: Effects on concurrent infection with *Fasciola hepatica*. *J. Comp. Path*.,91,227-233

Hamilton, C. M., Dowling, D. J., Loscher, C. E., Morphew, R. M., Brophy, P. M., O'Neill, S. M., Neill, S. M. O. (2009). The *Fasciola hepatica* tegumental antigen suppresses dendritic cell maturation and function. *Infection and Immunity*, *77*(6), 2488–2498. https://doi.org/10.1128/IAI.00919-08

Harnett, W. (2014). Secretory products of helminth parasites as immunomodulators. *Molecular and Biochemical Parasitology*, *195*(2), 130–136. https://doi.org/10.1016/j.molbiopara.2014.03.007

Harvey, R. M., Hughes, C. E., Paton, A. W., Trappetti, C., Tweten, R. K., Paton, J. C. (2014). The impact of pneumolysin on the macrophage response to *Streptococcus pneumoniae* is strain-dependent. *PLoS ONE*, *9*(8), 1-9. https://doi.org/10.1371/journal.pone.0103625

Hashimoto, D., Chow, A., Noizat, C., Teo, P., Beasley, M. B., Leboeuf, M., Becker, C. D., See, P., Price, J., Lucas, D., Greter, M., Mortha, A., Boyer, S. W., Forsberg, E. C., Tanaka, M., van Rooijen, N., Garcia-Sastre, A., Stanleyn E. R., Ginhoux, F., Frenette, P. S., Merad, M. (2013). Tissue-resident macrophages self-maintain locally throughout adult life with minimal contribution from circulating monocytes. *Immunity*, *38*(4), 792–804. https://doi.org/10.1016/j.immuni.2013.04.004

Henriques-Normark, B., Tuomanen, E. I. (2013). The pneumococcus: Epidemiology, microbiology, and pathogenesis. *Cold Spring Harbor Perspectives in Medicine*, *3*(7). https://doi.org/10.1101/cshperspect.a010215

Hernandez, H. J., Wang, Y., Stadecker, M. J. (1997). In infection with *Schistosoma mansoni*, B cells are required for T helper type 2 cell responses but not for granuloma formation. *The Journal of Immunology*, *158*(10), 4832–4837.

Hewitson, J. P., Grainger, J. R., Maizels, R. M. (2009). Helminth immunoregulation: The role of parasite secreted proteins in modulating host immunity. *Molecular and Biochemical Parasitology*, *167*(1), 1–11. https://doi.org/10.1016/j.molbiopara.2009.04.008

Hill, P. C., Townend, J., Antonio, M., Akisanya, B., Ebruke, C., Lahai, G., Greenwood, B. M., Adegbola, R. A. (2010). Transmission of *Streptococcus pneumoniae* in rural gambian villages: A longitudinal study. *Clinical Infectious Diseases*, *50*(11), 1468–1476. https://doi.org/10.1086/652443

Hirahara, K., Vahedi, G., Ghoreschi, K., Yang, X. P., Nakayamada, S., Kanno, Y., O'shea, J. J., Laurence, A. (2011). Helper T-cell differentiation and plasticity: Insights from epigenetics. *Immunology*, *134*(3), 235–245. https://doi.org/10.1111/j.1365-2567.2011.03483.x

Hirst, R. A., Kadioglu, A., O'Callaghan, C., Andrew, P. W. (2004). The role of pneumolysin in pneumococcal pneumonia and meningitis. *Clinical and Experimental Immunology*, *138*(2), 195–201. https://doi.org/10.1111/j.1365-2249.2004.02611.x

Hodgkinson, J. W., Fibke, C., Belosevic, M. (2017). Recombinant IL-4/13A and IL-4/13B induce arginase activity and down-regulate nitric oxide response of primary goldfish (*Carassius auratus L*.) macrophages. *Developmental and Comparative Immunology*, *67*, 377–384. https://doi.org/10.1016/j.dci.2016.08.014

Högberg, L., Geli, P., Ringberg, H., Melander, E., Lipsitch, M., Ekdahl, K. (2007). Age- and serogroup-related differences in observed durations of nasopharyngeal carriage of penicillin-resistant pneumococci. *Journal of Clinical Microbiology*, *45*(3), 948–952. https://doi.org/10.1128/JCM.01913-06

Houldsworth, S., Andrew, P. W., Mitchell, T. J. (1994). Pneumolysin stimulates production of tumor necrosis factor alpha and interleukin-1β by human mononuclear phagocytes. *Infection and Immunity*, *62*(4), 1501–1503.

Howell, A., Baylis, M., Smith, R., Pinchbeck, G., Williams, D. (2015). Epidemiology and impact of *Fasciola hepatica* exposure in high-yielding dairy herds. *Preventive Veterinary Medicine*, *121*(1–2), 41–48. https://doi.org/10.1016/j.prevetmed.2015.05.013

Howell, A. K., Malalana, F., Beesley, N. J., Hodgkinson, J. E., Rhodes, H., Sekiya, M., Archer, D., Clough, H. E., Gilmore, P., Williams, D. J. L. (2019b). *Fasciola hepatica* in UK horses . *Equine Veterinary Journal*, *0*(December 2017), 1–6. https://doi.org/10.1111/evj.13149

Howell, Alison K., McCann, C. M., Wickstead, F., Williams, D. J. L. (2019a). Co-infection of cattle with *Fasciola hepatica* or *F. gigantica* and *Mycobacterium bovis*: A systematic review. *PLoS ONE*, *14*(12), 1–21. https://doi.org/10.1371/journal.pone.0226300

Howell, Alison K., Tongue, S. C., Currie, C., Evans, J., Williams, D. J. L., McNeilly, T. N. (2017). Co-infection with *Fasciola hepatica* may increase the risk of *Escherichia coli* O157 shedding in British cattle destined for the food chain. *Preventive Veterinary Medicine*, *150*(October 2017), 70–76. https://doi.org/10.1016/j.prevetmed.2017.12.007

Hsieh, L. S., Wen, J. H., Miyares, L., Lombroso, P. J., Bordey, A. (2017). Outbred CD1 mice are as suitable as inbred C57BL/6J mice in performing social tasks. *Neuroscience Letters*, *637*, 142–147. https://doi.org/10.1016/j.neulet.2016.11.035

Hume, D. A. (2006). The mononuclear phagocyte system. *Current Opinion in Immunology*, *18*(1), 49–53. https://doi.org/10.1016/j.coi.2005.11.008

Hung, I. F. N., Tantawichien, T., Tsai, Y. H., Patil, S., Zotomayor, R. (2013). Regional epidemiology of invasive pneumococcal disease in Asian adults: Epidemiology, disease burden, serotype distribution, and antimicrobial resistance patterns and prevention. *International Journal of Infectious Diseases*, *17*(6), e364–e373. https://doi.org/10.1016/j.ijid.2013.01.004

Inclan-Rico, J. M., Siracusa, M. C. (2018). First responders: Innate immunity to helminths. *Trends in Parasitology*, *34*(10), 861–880. https://doi.org/10.1016/j.pt.2018.08.007

Jacques, L. C., Panagiotou, S., Baltazar, M., Senghore, M., Khandaker, S., Xu, R., Bricio-Moreno, L., Yang, M., Dowson, C. G., Everett, D. B., Neill, D. R., Kadioglu, A. (2020). Increased pathogenicity of pneumococcal serotype 1 is driven by rapid autolysis and release of pneumolysin. *Nature Communications*, (2020), 1–13. https://doi.org/10.1038/s41467-020-15751-6

Jedlina, L., Kozak-Ljunggren, M., Wedrychowicz, H. (2011). *In vivo* studies of the early, peritoneal, cellular and free radical response in rats infected with *Fasciola hepatica* by flow cytometric analysis. *Experimental Parasitology*, *128*(3), 291–297. https://doi.org/10.1016/j.exppara.2011.02.004

Jefferies, J. R., Turner, R. J., Barrett, J. (1997). Effect of *Fasciola hepatica* excretory-secretory products on the metabolic burst of sheep and human neutrophils. *International Journal for Parasitology*, *27*(9), 1025–1029. https://doi.org/10.1016/S0020-7519(97)00067-2

Jeong, D.-G., Jeong, E.-S., Seo, J.-H., Heo, S.-H., Choi, Y.-K. (2011). Difference in resistance to *Streptococcus pneumoniae* infection in mice . *Laboratory Animal Research*, *27*(2), 91. https://doi.org/10.5625/lar.2011.27.2.91

Jeong, D.-G., Seo, J.-H., Heo, S.-H., Choi, Y.-K., Jeong, E.-S. (2015). Tumor necrosis factor-alpha deficiency impairs host defense against *Streptococcus pneumoniae*. *Laboratory Animal Research*, *31*(2), 78. https://doi.org/10.5625/lar.2015.31.2.78

Jones, K. J., Perris, A. D., Vernallis, A. B., Worthington, T., Lambert, P. A., Elliott, T. S. J. J. (2005). Induction of inflammatory cytokines and nitric oxide in J774.2 cells and murine macrophages by lipoteichoic acid and related cell wall antigens from Staphylococcus epidermidis. *Journal of Medical Microbiology*, *54*(4), 315–321. https://doi.org/10.1099/jmm.0.45872-0

Jonsson, S., Musher, D.M., Chapman, A., Goree, A., Lawrence, E. C. (1985). Phagocytosis and killing of common bacterial pathogens of the lung by human alveolar macrophages. *The Journal of Infectious Diseases*, *152*(1), 4–13. https://doi.org/https://doi.org/10.1093/infdis/152.1.4

Jusot, J. F., Neill, D. R., Waters, E. M., Bangert, M., Collins, M., Bricio Moreno, L., Lawan, K. G., Moussa, M. M., Dearing, E., Everett, D. B., Collard, J.-M., Kadioglu, A. (2017). Airborne dust and high temperatures are risk factors for invasive bacterial disease. *Journal of Allergy and Clinical Immunology*, *139*(3), 977-986.e2. https://doi.org/10.1016/j.jaci.2016.04.062

Kadioglu, A, Gingles, N. A., Grattan, K., Kerr, A., Mitchell, T. J., Andrew, P. W. (2000). Host cellular immune response to pneumococcal lung infection in mice. *Infection and Immunity*, *68*(2), 492–501. https://doi.org/10.1128/IAI.68.2.492-501.2000

Kadioglu, A., Andrew, P. W. (2005). Susceptibility and resistance to pneumococcal disease in mice. *Briefings in Functional Genomics and Proteomics*, *4*(3), 241–247. https://doi.org/10.1093/bfgp/4.3.241

Kadioglu, A., Taylor, S., Iannelli, F., Pozzi, G., Mitchell, T. J., Andrew, P. W. (2002). Upper and lower respiratory tract infection by *Streptococcus pneumoniae* is affected by pneumolysin deficiency and differences in capsule type. *Infection and Immunity*, *70*(6), 2886–2890. https://doi.org/10.1128/IAI.70.6.2886-2890.2002

Kadioglu, A., Weiser, J. N., Paton, J. C., Andrew, P. W. (2008). The role of *Streptococcus pneumoniae* virulence factors in host respiratory colonization and disease. *Nature Reviews Microbiology*, *6*(4), 288–301. https://doi.org/10.1038/nrmicro1871

Kadl, A., Meher, A. K., Sharma, P. R., Lee, M. Y., Doran, A. C., Johnstone, S. R., Elliot, M. R., Gruber, F., Han, J., Chen, W., Kensler, T., Ravichandran, K. S., Isakson, B. E., Wamhoff, B. R., Leitinger, N. (2010). Identification of a novel macrophage phenotype that develops in response to atherogenic phospholipids via Nrf2. *Circulation Research*, *107*(6), 737–746. https://doi.org/10.1161/CIRCRESAHA.109.215715

Kafka, D., Ling, E., Feldman, G., Benharroch, D., Voronov, E., Givon-Lavi, N., Iwakura, Y., Dagan, R., Apte, R. N., Mizrachi-Nebenzahl, Y. (2008). Contribution of IL-1 to resistance to *Streptococcus pneumoniae* infection. *International Immunology*, *20*(9), 1139–1146. https://doi.org/10.1093/intimm/dxn071

Kaiko, G. E., Horvat, J. C., Beagley, K. W., Hansbro, P. M. (2008). Immunological decision-making: How does the immune system decide to mount a helper T-cell response? *Immunology*, *123*(3), 326–338. https://doi.org/10.1111/j.1365-2567.2007.02719.x

Kalata, N. L., Nyazika, T. K., Swarthout, T. D., Everett, D., French, N., Heyderman, R. S., Gordon, S. B., Jambo, K. C. (2019). Pneumococcal pneumonia and carriage in Africa before and after introduction of pneumococcal conjugate vaccines, 2000-2019: Protocol for systematic review. *BMJ Open*, *9*(11), 1–5. https://doi.org/10.1136/bmjopen-2019-030981

Kang, P. B., Azad, A. K., Torrelles, J. B., Kaufman, T. M., Beharka, A., Tibesar, E., Desjardin, L. E, Schlesinger, L. S. (2005). The human macrophage mannose receptor directs *Mycobacterium tuberculosis* lipoarabinomannan-mediated phagosome biogenesis. *Journal of Experimental Medicine*, *202*(7), 987–999. https://doi.org/10.1084/jem.20051239

Kanneganti, T. D., Lamkanfi, M., Kim, Y. G., Chen, G., Park, J. H., Franchi, L., Vandenabeele, P., Núñez, G. (2007). Pannexin-1-mediated recognition of bacterial molecules activates the cryopyrin inflammasome independent of toll-like receptor signaling. *Immunity*, *26*(4), 433–443. https://doi.org/10.1016/j.immuni.2007.03.008

Kaplan, R. M. (2001). *Fasciola hepatica* : A review of the economic impact in cattle and considerations for control. *Veterinary Therapeutics*, *2*(1), 40–50.

Karlström, Å., Boyd, K. L., English, B. K., McCullers, J. A. (2009). Treatment with protein synthesis inhibitors improves outcomes of secondary bacterial pneumonia after influenza. *The Journal of Infectious Diseases*, *199*(3), 311–319. https://doi.org/10.1086/596051

Kasmi, K. C. El, Qualls, J. E., Pesce, J. T., Smith, A. M., Robert, W., Henao-Tamayo, M., Basaraba, R. J., Konig, T., Schleicher, U., Koo, M.-S., Kaplan, G., Fitzgerald, K. A., Tuomanen, E. I., Orme, I. M., Kanneganti, T.-D., Bogdan, C., Wynn, T. A., Murray, P. J. (2008). Toll-like receptor–induced arginase 1 in macrophages thwarts effective immunity against intracellular pathogens. *Nature Immunology, 9*(12), 1399–1406. https://doi.org/10.1038/ni.1671.

Kawakami, K., Yamamoto, N., Kinjo, Y., Miyagi, K., Nakasone, C., Uezu, K., Kinjo, T., Nakayama, T., Taniguchi, M., Saito, A. (2003). Critical role of Vα14+ natural killer T cells in the innate phase of host protection against *Streptococcus pneumoniae* infection. *European Journal of Immunology*, *33*(12), 3322–3330. https://doi.org/10.1002/eji.200324254

Kerr, A. R., Irvine, J. J., Search, J. J., Gingles, N. A., Kadioglu, A., Andrew, P. W., McPheat, W. L., Booth, C. G., Mitchell, T. J. (2002). Role of inflammatory mediators in resistance and susceptibility to pneumococcal infection. *Infection and Immunity*, *70*(3), 1547–1557. https://doi.org/10.1128/IAI.70.3.1547-1557.2002

Kessler, B., Rinchai, D., Kewcharoenwong, C., Nithichanon, A., Biggart, R., Hawrylowicz, C. M., Bancroft, G. J., Lertmemongkolchai, G. (2017). Interleukin 10 inhibits pro-inflammatory cytokine responses and killing of *Burkholderia pseudomallei*. *Scientific Reports*, *7*(February), 1–11. https://doi.org/10.1038/srep42791

Khan, M. K., Sajid, M. S., Riaz, H., Ahmad, N. E., He, L., Shahzad, M., Hussain, A., Khan, M. N.,Iqbal, Z., Zhao, J. (2013). The global burden of fasciolosis in domestic animals with an outlook on the contribution of new approaches for diagnosis and control. *Parasitology Research*, *112*(7), 2421–2430. https://doi.org/10.1007/s00436-013-3464-6

Kidd, P. (2003). Th1/Th2 balance: The hypothesis, its limitations, and implications for health and disease. *Alternative Medicine Review*, *8*(3), 223–246.

Kissin, E., Tomasi, M., McCartney-Francis, N., Gibbs, C. L., Smith, P. D. (1996). Age-related decline in murine macrophage production of nitric oxide. *The Journal of Infectious Diseases*, *175*(4), 1004–1007. https://doi.org/10.1086/513959

Klaver, E. J., Kuijk, L. M., Laan, L. C., Kringel, H., van Vliet, S. J., Bouma, G., Cummings, R. D, Kraal, G., Van Die, I. (2013). *Trichuris suis*-induced modulation of human dendritic cell function is glycan-mediated. *International Journal for Parasitology*, *43*(3–4), 191–200. https://doi.org/10.1016/j.ijpara.2012.10.021

Klementowicz, J. E., Travis, M. A., Grencis, R. K. (2012). *Trichuris muris*: A model of gastrointestinal parasite infection. *Seminars in Immunopathology*, *34*(6), 815–828. https://doi.org/10.1007/s00281-012-0348-2

Knapp, S., Leemans, J. C., Florquin, S., Branger, J., Maris, N. A., Pater, J., van Rooijen, N., van der Poll, T. (2003). Alveolar macrophages have a protective antiinflammatory role during murine pneumococcal pneumonia. *American Journal of Respiratory and Critical Care Medicine*, *167*(2), 171–179. https://doi.org/10.1164/rccm.200207-698OC

Knapp, S., Wieland, C. W., van 't Veer, C., Takeuchi, O., Akira, S., Florquin, S., van der Poll, T. (2004). Toll-Like receptor 2 plays a role in the early inflammatory response to murine pneumococcal pneumonia but does not contribute to antibacterial defense. *The Journal of Immunology*, *172*(5), 3132–3138. https://doi.org/10.4049/jimmunol.172.5.3132

Knubben-Schweizer, G., Torgerson, P. R. (2015). Bovine fasciolosis: Control strategies based on the location of *Galba truncatula* habitats on farms. *Veterinary Parasitology*, *208*(1–2), 77–83. https://doi.org/10.1016/j.vetpar.2014.12.019

Kolling, U. K., Hansen, F., Braun, J., Rink, L., Katus, H. A., Dalhoff, K. (2001). Leucocyte response and anti-inflammatory cytokines in community acquired pneumonia. *Thorax*, *56*(2), 121–125. https://doi.org/10.1136/thorax.56.2.121

Koppe, U., Suttorp, N., Opitz, B. (2012). Recognition of *Streptococcus pneumoniae* by the innate immune system. *Cellular Microbiology*, *14*(4), 460–466. https://doi.org/10.1111/j.1462-5822.2011.01746.x

Köstenberger, K., Tichy, A., Bauer, K., Pless, P., Wittek, T. (2017). Associations between fasciolosis and milk production, and the impact of anthelmintic treatment in dairy herds. *Parasitology Research*, *116*(7), 1981–1987. https://doi.org/10.1007/s00436-017-5481-3

Kotarsky, K., Sitnik, K. M., Stenstad, H., Kotarsky, H., Schmidtchen, A., Koslowski, M., Wehkamp, J., Agace, W. W. (2009). A novel role for constitutively expressed epithelial-derived chemokines as antibacterial peptides in the intestinal mucosa. *Mucosal Immunology*, *3*(1), 40–48. https://doi.org/10.1038/mi.2009.115

Kurt, A. N. C., Aygun, A. D., Godekmerdan, A., Kurt, A., Dogan, Y., Yilmaz, E. (2007). Serum IL-1beta, IL-6, IL-8, and TNF-alpha levels in early diagnosis and management of neonatal sepsis. *Mediators of Inflammation*, *2007*, 31397. https://doi.org/10.1155/2007/31397

Kwist, K., Bridges, W. C., Burg, K. J. L. (2016). The effect of cell passage number on osteogenic and adipogenic characteristics of D1 cells. *Cytotechnology*, *68*(4), 1661–1667. https://doi.org/10.1007/s10616-015-9883-8

La Flamme, A. C., Kharkrang, M., Stone, S., Mirmoeini, S., Chuluundorj, D., Kyle, R. (2012). Type II-activated murine macrophages produce IL-4. *PLoS ONE*, *7*(10), 1–9. https://doi.org/10.1371/journal.pone.0046989

Labonte, A. C., Tosello-Trampont, A.-C., Hahn, Y. S. (2014). The role of macrophage polarization in infectious and inflammatory diseases. *Molecules and Cells*, *37*(4), 275–285. https://doi.org/10.14348/molcells.2014.2374

LaCourse, E. J., Perally, S., Morphew, R. M., Moxon, J. V., Prescott, M., Dowling, D. J., O'Neill, S. M., Kipar, A., hetzel, U, Hoey, E., Zafra, R., Buffoni, L., Arevalo, J.P., Brophy, P. M. (2012). The Sigma class glutathione transferase from the liver fluke *Fasciola hepatica*. *PLoS Neglected Tropical Diseases*, *6*(5). https://doi.org/10.1371/journal.pntd.0001666

Laemelli, U. K. (1970). Cleavage of structural proteins during the assembly of the head of bacteriophage T4. *Nature*, *227*(5259), 680–685. https://doi.org/10.1038/227680a0

Lammers, A. J. J., de Porto, A. P. N. A., de Boer, O. J., Florquin, S., van der Poll, T. (2012). The role of TLR2 in the host response to pneumococcal pneumonia in absence of the spleen. *BMC Infectious Diseases*, *12*. https://doi.org/10.1186/1471-2334-12-139

LaRock, C. N., Nizet, V. (2015). Inflammasome/IL-1β responses to streptococcal pathogens. *Frontiers in Immunology*, *6*(OCT*)*,1-11. https://doi.org/10.3389/fimmu.2015.00518

Lass, S., Hudson, P. J., Thakar, J., Saric, J., Harvill, E., Albert, R., Perkins, S. E. (2013). Generating super-shedders: co-infection increases bacterial load and egg production of a gastrointestinal helminth. *Journal of the Royal Society, Interface*, *10*(80), 20120588. https://doi.org/10.1098/rsif.2012.0588

Lechner, C. J., Komander, K., Hegewald, J., Huang, X., Gantin, R. G., Soboslay, P. T., Agossou, A., Banla, M., Köhler, C. (2013). Cytokine and chemokine responses to helminth and protozoan parasites and to fungus and mite allergens in neonates, children, adults, and the elderly. *Immunity and Ageing*, *10*(1), 1–10. https://doi.org/10.1186/1742-4933-10-29

Lees, J. A., Croucher, N. J., Goldblatt, D., Nosten, F., Parkhill, J., Turner, C., Turner, P., Bentley, S. D. (2017). Genome-wide identification of lineage and locus specific variation associated with pneumococcal carriage duration. *ELife*, *6*, 1–25. https://doi.org/10.7554/eLife.26255

LeMessurier, K. S., Häcker, H., Chi, L., Tuomanen, E., Redecke, V. (2013). Type I interferon protects against pneumococcal invasive disease by inhibiting bacterial transmigration across the lung. *PLoS Pathogens*, *9*(11), 1-12. https://doi.org/10.1371/journal.ppat.1003727

Lemire, P., Galbas, T., Thibodeau, J., Segura, M. (2017). Natural killer cell functions during the innate immune response to pathogenic streptococci. *Frontiers in Microbiology*, *8*(JUN), 1–17. https://doi.org/10.3389/fmicb.2017.01196

Lemon, J. K., Miller, M. R., Weiser, J. N. (2015). Sensing of interleukin-1 cytokines during *Streptococcus pneumoniae* colonization contributes to macrophage recruitment and bacterial clearance. *Infection and Immunity*, *83*(8), 3204–3212. https://doi.org/10.1128/IAI.00224-15

Lu, Y. J., Gross, J., Bogaert, D., Finn, A., Bagrade, L., Zhang, Q., Kolls, J. K., Srivastava, A., Lundgren, A., Forte, S., Thompson, C.M, Harney, K. F., Anderson, P. W., Lipsitch, M., Malley, R. (2008). Interleukin-17A mediates acquired immunity to pneumococcal colonization. *PLoS Pathogens*, *4*(9). https://doi.org/10.1371/journal.ppat.1000159

Lucena, A.N., Garza Cuartero, L., Mulcahy, G., Zintl, A. (2017). The immunoregulatory effects of co-infection with *Fasciola hepatica*: From bovine tuberculosis to Johne's disease. *Veterinary Journal*, *222*, 9–16. https://doi.org/10.1016/j.tvjl.2017.02.007

Lund, M. E., O'Brien, B. A., Hutchinson, A. T., Robinson, M. W., Simpson, A. M., Dalton, J. P., Donnelly, S. (2014). Secreted proteins from the helminth *Fasciola hepatica* inhibit the initiation of autoreactive T cell responses and prevent diabetes in the NOD mouse. *PLoS ONE*, *9*(1), 1–10. https://doi.org/10.1371/journal.pone.0086289

Modolell, M., Corraliza, I. M., Link, F., Soler, G., Eichman, K. (1995). Reciprocal regulation of the nitric oxide synthase/arginase balance in mouse bone marrow-derived macrophages by TH 1 and TH 2 cytokines. *Eur. J. Immunol*, *25*(4), 1101–1104. https://doi.org/10.1159/000276761

Ma, X., Yan, W., Zheng, H., Du, Q., Zhang, L., Ban, Y., Li, N., Wei, F. (2015). Regulation of IL-10 and IL-12 production and function in macrophages and dendritic cells. *F1000Research*, *4*(0), 1–13. https://doi.org/10.12688/f1000research.7010.1

Mabbott, N. A. (2018). The influence of parasite infections on host immunity to co-infection with other pathogens. *Frontiers in Immunology*, *9*(November), 1–14. https://doi.org/10.3389/fimmu.2018.02579

Macdonald, A. S., Araujo, M. I., Edward, J., Pearce, E. J. (2002). Immunology of parasitic helminth infections immunology of parasitic helminth infections. *Infection and Immunity*, *70*(2), 427–433. https://doi.org/10.1128/IAI.70.2.427

MacMicking, J., Xie, Q. W., Nathan, C. (1997). Nitric oxide and macrophage function. *Annual Review of Immunology*, *15*(1), 323–350. https://doi.org/10.1146/annurev.immunol.15.1.323

Maizels, R. M. (2016). Parasitic helminth infections and the control of human allergic and autoimmune disorders. *Clinical Microbiology and Infection*, *22*(6), 481–486. https://doi.org/10.1016/j.cmi.2016.04.024

Maizels, R. M., Balic, A., Gomez-Escobar, N., Nair, M., Taylor, M. D., Allen, J. E. (2004). Helminth parasites - Masters of regulation. *Immunological Reviews*, *201*, 89–116. https://doi.org/10.1111/j.0105-2896.2004.00191.x

Maizels, R. M., McSorley, H. J. (2016). Regulation of the host immune system by helminth parasites. *Journal of Allergy and Clinical Immunology*, *138*(3), 666–675. https://doi.org/10.1016/j.jaci.2016.07.007

Maizels, R. M., Smits, H. H., McSorley, H. J. (2018). Modulation of host immunity by helminths: The expanding repertoire of parasite effector molecules. *Immunity*, *49*(5), 801–818. https://doi.org/10.1016/j.immuni.2018.10.016

Makepeace, B. L., Martin, C., Turner, J. D., Specht, S. (2012). Granulocytes in helminth infection - who is calling the shots? *Current Medicinal Chemistry*, *19*(10), 1567–1586. https://doi.org/10.2174/092986712799828337

Mallevaey, T., Zanetta, J. P., Faveeuw, C., Fontaine, J., Maes, E., Platt, F., Capron, M., Leite-de-Moraes, L., Trottein, F. (2006). Activation of invariant NKT cells by the helminth parasite *Schistosoma mansoni. The Journal of Immunology*, *176*(4), 2476–2485. https://doi.org/10.4049/jimmunol.176.4.2476

Malley, R., Henneke, P., Morse, S. C., Cieslewicz, M. J., Lipsitch, M., Thompson, C. M., Kurt-Jones, E., Paton, J. C., Wessels,M. R., Golenbock, D. T. (2003). Recognition of pneumolysin by Toll-like receptor 4 confers resistance to pneumococcal infection. *Proceedings of the National Academy of Sciences of the United States of America*, *100*(4), 1966–1971. https://doi.org/10.1073/pnas.0435928100

Malyshev, I., Malyshev, Y. (2015). Current concept and update of the macrophage plasticity concept: Intracellular mechanisms of reprogramming and M3 macrophage "switch" phenotype. *BioMed Research International*, *2015*, 341308. https://doi.org/10.1155/2015/341308

Marriott, H. M., Ali, F., Read, R. C., Mitchell, T. J., Whyte, M. K. B., Dockrell, D. H. (2004). Nitric oxide levels regulate macrophage commitment to apoptosis or necrosis during pneumococcal infection. *The FASEB Journal*, *18*(10), 1126–1128. https://doi.org/10.1096/fj.03-1450fje

Marriott, H. M., Hellewell, P. G., Cross, S. S., Ince, P. G., Whyte, M. K. B., Dockrell, D. H. (2006). Decreased alveolar macrophage apoptosis is associated with increased pulmonary inflammation in a murine model of pneumococcal pneumonia. *The Journal of Immunology*, *177*(9), 6480–6488. https://doi.org/10.4049/jimmunol.177.9.6480

Marriott, H. M., Hellewell, P. G., Whyte, M. K. B., Dockrell, D. H. (2007). Contrasting roles for reactive oxygen species and nitric oxide in the innate response to pulmonary infection with *Streptococcus pneumoniae. Vaccine*, *25*(13), 2485–2490. https://doi.org/10.1016/j.vaccine.2006.09.024

Martin, I., Cabán-hernández, K., Espino, A. M., Figueroa-Santiago, O., Martin, I., Caba, K., Espino, A. M. (2016). *Fasciola hepatica* fatty acid binding protein inhibits TLR4 activation and suppresses the inflammatory cytokines induced by lipopolysaccharide *in vitro* and *in vivo. Journal of Immunology, 194*(8), 3924–3936. https://doi.org/10.4049/jimmunol.1401182

Martinez-Pomares, L. (2012). The mannose receptor. *Journal of Leukocyte Biology*, *92*(6), 1177–1186. https://doi.org/10.1189/jlb.0512231

Martinez, F. O., Gordon, S. (2014). The M1 and M2 paradigm of macrophage activation: time for reassessment. *F1000prime Reports*, *6*(March), 13. https://doi.org/10.12703/P6-13

Martner, A., Dahlgren, C., Paton, J. C., Wold, A. E. (2008). Pneumolysin released during *Streptococcus pneumoniae* autolysis is a potent activator of intracellular oxygen radical production in neutrophils. *Infection and Immunity*, *76*(9), 4079–4087. https://doi.org/10.1128/IAI.01747-07

Martner, A., Skovbjerg, S., Paton, J. C., Wold, A. E. (2009). *Streptococcus pneumoniae* autolysis prevents phagocytosis and production of phagocyte-activating cytokines. *Infection and Immunity*, *77*(9), 3826–3837. https://doi.org/10.1128/IAI.00290-09

Mas-Coma, S. (2005). Epidemiology of fascioliasis in human endemic areas. *Journal of Helminthology*, *79*, 207–216. https://doi.org/https://doi.org.10.1079/joh2005296

Mas-Coma, S., Bargues, M. D., Valero, M. A. (2018). Human fascioliasis infection sources, their diversity, incidence factors, analytical methods and prevention measures. *Parasitology*, *145*, 1665–1699. https://doi.org/https://doi.org/10.1017/S0031182018000914

Mazeri, S., Rydevik, G., Handel, I., Bronsvoort, B. M. D., Sargison, N. (2017). Estimation of the impact of *Fasciola hepatica* infection on time taken for UK beef cattle to reach slaughter weight. *Scientific Reports*, *7*(1), 1–15. https://doi.org/10.1038/s41598-017-07396-1

McAllister, C. K., O'Donoghue, J. M., Beaty, H. N. (1975). Experimental pneumococcal meningitis. II. Characterisation and quantitation of the inflammatory process. *The Journal of Infectious Diseasestious Disease*, *132*(4), 355–360.

McCool, T. L., Cate, T. R., Moy, G., Weiser, J. N. (2002). The immune response to pneumococcal proteins during experimental human carriage. *Journal of Experimental Medicine*, *195*(3), 359–365. https://doi.org/10.1084/jem.20011576

McCool, T. L., Weiser, J. N. (2004). Limited role of antibody in clearance of *Streptococcus pneumoniae* in a murine model of colonization. *Infection and Immunity*, *72*(10), 5807–5813. https://doi.org/10.1128/IAI.72.10.5807-5813.2004

McCoy, K. D., Stoel, M., Stettler, R., Merky, P., Fink, K., Senn, B. M., Schaer, C., Massacand, J., Odermatt, B., Oetttgen, H. C., Zinkernagel, R. M., Bos, N. A., Hengartner, H., Macpherson, A. J., Harris, N. L. (2008). Polyclonal and specific antibodies mediate protective immunity against enteric helminth infection. *Cell Host and Microbe*, *4*(4), 362–373. https://doi.org/10.1016/j.chom.2008.08.014

McNeela, E. A., Burke, Á., Neill, D. R., Baxter, C., Fernandes, V. E., Ferreira, D., Smeaton, S., El-rachkidy, R., McLoughlin, R. M., Mori, A., Moran, B., Fitzgerald, K. A., Tschopp, J., Petrilli, V., Andrew, P. W., Kadioglu, A., Lavelle, E. C. (2010). Pneumolysin activates the NLRP3 inflammasome and promotes proinflammatory cytokines independently of TLR4. *PLoS Pathogens*, *6*(11). https://doi.org/10.1371/journal.ppat.1001191

McNeilly, T. N., Nisbet, A. J. (2014). Immune modulation by helminth parasites of ruminants: implications for vaccine development and host immune competence. *Parasite (Paris, France)*, *21*, 51. https://doi.org/10.1051/parasite/2014051

McSorley, H. J., Hewitson, J. P., Maizels, R. M. (2013). Immunomodulation by helminth parasites: Defining mechanisms and mediators. *International Journal for Parasitology*, *43*(3–4), 301–310. https://doi.org/10.1016/j.ijpara.2012.11.011

McSorley, H. J., Maizels, R. M. (2012). Helminth infections and host immune regulation. *Clinical Microbiology Reviews*, *25*(4), 585–608. https://doi.org/10.1128/CMR.05040-11

Mège, J.-L., Mehraj, V., Capo, C. (2011). Macrophage polarization and bacterial infections. *Current Opinion in Infectious Diseases*, *24*(3), 230–234. https://doi.org/10.1097/QCO.0b013e328344b73e

Mezo, M., González-Warleta, M., Castro-Hermida, J. A., Muiño, L., Ubeira, F. M. (2011). Association between anti-*F. hepatica* antibody levels in milk and production losses in dairy cows. *Veterinary Parasitology*, *180*(3–4), 237–242. https://doi.org/10.1016/j.vetpar.2011.03.009

Miller, B. H., Fratti, R. A., Poschet, J. F., Timmins, G. S., Master, S. S., Burgos, M., Marletta, M. A., Deretic, V. (2004). Mycobacteria inhibit nitric oxide synthase recruitment to phagosomes during macrophage infection. *Infection and Immunity*, *72*(5), 2872–2878. https://doi.org/10.1128/IAI.72.5.2872-2878.2004

Miller, C. M. D., Smith, N. C., Ikin, R. J., Boulter, N. R., Dalton, J. P., Donnelly, S. (2009). Immunological interactions between 2 common pathogens, Th1-inducing protozoan *Toxoplasma gondii* and the Th2-inducing helminth *Fasciola hepatica*. *PLoS ONE*, *4*(5), 1–10. https://doi.org/10.1371/journal.pone.0005692

Mills, C. D., Kincaid, K., Alt, J. M., Heilman, M. J., Hill, A. M. (2000). M-1/M-2 macrophages and the Th1/Th2 paradigm. *The Journal of Immunology*, *164*(12), 6166–6173. https://doi.org/10.4049/jimmunol.164.12.6166

Mills, C D. (2001). Macrophage arginine metabolism to ornithine/urea or nitric oxide/citrulline: a life or death issue. *Critical Reviews in Immunology*, *21*(4), 399–425. https://doi.org/10.1615/CritRevImmunol.v21.i5.10

Mills, C. D., Ley, K. (2014). M1 and M2 macrophages: The chicken and the egg of immunity. *Journal of Innate Immunity*, *6*(6), 716–726. https://doi.org/10.1159/000364945

Mills, C. D. (2012). M1 and M2 Macrophages: Oracles of health and disease. *Critical Reviews in Immunology*, *32*(6), 463–488. https://doi.org/DOI: 10.1615/critrevimmunol.v32.i6.10

Mills, C. D. (2015). Anatomy of a discovery: M1 and M2 macrophages. *Frontiers in Immunology*, *6*(May), 212. https://doi.org/10.3389/fimmu.2015.00212

Mina, M. J., Brown, L. A. S., Klugman, K. P. (2015). Dynamics of increasing IFN-γ exposure on murine MH-S cell-line alveolar macrophage phagocytosis of *Streptococcus pneumoniae. Journal of Interferon and Cytokine Research*, *35*(6), 474–479. https://doi.org/10.1089/jir.2014.0087

Mishra, P. K., Palma, M., Bleich, D., Loke, P., Gause, W. C. (2014). Systemic impact of intestinal helminth infections. *Mucosal Immunology*, *7*(4), 753–762. https://doi.org/10.1038/mi.2014.23.

Mitchell, A. J., Yau, B., McQuillan, J. A., Ball, H. J., Too, L. K., Abtin, A., Hertzog, P., Leib, S. L., Jones, C. A, Gerega, S. K., Weninger, W., Hunt, N. H. (2012). Inflammasome-dependent IFN-γ drives pathogenesis in *Streptococcus pneumoniae* meningitis. *The Journal of Immunology*, *189*(10), 4970–4980. https://doi.org/10.4049/jimmunol.1201687

Mitchell, A. M., Mitchell, T. J. (2010). *Streptococcus pneumoniae*: Virulence factors and variation. *Clinical Microbiology and Infection*, *16*(5), 411–418. https://doi.org/10.1111/j.1469-0691.2010.03183.x

Mitchell, G. (2002). Update on fasciolosis in cattle and sheep. *In Practice*, *24*, 378–385.

Miyashita, L., Suri, R., Dearing, E., Mudway, I., Dove, R. E., Neill, D. R., Zyl-Smit, R. V., Kadioglu, A., Grigg, J. (2018). E-cigarette vapour enhances pneumococcal adherence to airway epithelial cells. *European Respiratory Journal*, *51*(2). https://doi.org/10.1183/13993003.01592-2017

Mizgerd, J. P. (2002). Molecular mechanisms of neutrophil recruitment elicited by bacteria in the lungs. *Seminars in Immunology*, *14*(2), 123–132. https://doi.org/10.1006/smim.2001.0349

Mogensen, T. H., Paludan, S. R., Kilian, M., Ostegaard, L. (2006). Live S*treptococcus pneumoniae*, *Haemophilus influenzae*, and *Neisseria meningitidis* activate the inflammatory response through toll-like receptors 2, 4, and 9 in species-specific patterns. *Journal of Leukocyte Biology*, *80*(2), 267–277. https://doi.org/10.1189/jlb.1105626

Mogensen, T. H. (2009). Pathogen recognition and inflammatory signaling in innate immune defenses. *Clinical Microbiology Reviews*, *22*(2), 240–273. https://doi.org/10.1128/CMR.00046-08

Molina-Hernández, V., Mulcahy, G., Pérez, J., Martínez-Moreno, Á., Donnelly, S., O'Neill, S. M., Dalton, J. P., Cwiklinski, K. (2015). *Fasciola hepatica* vaccine: We may not be there yet but we're on the right road. *Veterinary Parasitology*, *208*(1–2), 101–111. https://doi.org/10.1016/j.vetpar.2015.01.004

Moreau, E., Chauvin, A. (2010). Immunity against helminths: Interactions with the host and the intercurrent infections. *Journal of Biomedicine and Biotechnology*, *2010*. https://doi.org/10.1155/2010/428593

Morita, H., He, F., Fuse, T., Ouwehand, A. C., Hashimoto, H., Hosoda, M., Mizumachi, K., Kurisaki, J. I. (2002). Cytokine production by the murine macrophage cell line J774.1 after exposure to lactobacilli. *Bioscience, Biotechnology and Biochemistry*, *66*(9), 1963–1966. https://doi.org/10.1271/bbb.66.1963

Mortimer, K., Gordon, S. B., Jindal, S. K., Accinelli, R. A., Balmes, J., Martin, W. J. (2012). Household air pollution is a major avoidable risk factor for cardiorespiratory disease. *Chest*, *142*(5), 1308–1315. https://doi.org/10.1378/chest.12-1596

Mosser, D. M., Zhang, X. (2008). Interleukin-10: New perspectives on an old cytokine. *Immunological Reviews*, *226*(1), 205–218. https://doi.org/10.1111/j.1600-065X.2008.00706.x

Motran, C. C., Silvane, L., Chiapello, L. S., Theumer, M. G., Ambrosio, L. F., Volpini, X., Celias, D. P., Cervi, L. (2018). Helminth infections: Recognition and modulation of the immune response by innate immune cells. *Frontiers in Immunology*, *9*(APR), 1–12. https://doi.org/10.3389/fimmu.2018.00664

Mouriaux, F., Zaniolo, K., Bergeron, M. A., Weidmann, C., De La Fouchardière, A., Fournier, F., Droit, A., Morcos, M. W., Landreville, S., Guérin, S. L. (2016). Effects of long-term serial passaging on the characteristics and properties of cell lines derived from uveal melanoma primary tumors. *Investigative Ophthalmology and Visual Science*, *57*(13), 5288–5301. https://doi.org/10.1167/iovs.16-19317

Moxon, J. V., LaCourse, E. J., Wright, H. A., Perally, S., Prescott, M. C., Gillard, J. L., Barret, J., Hamilton, J. V., Brophy, P. M. (2010). Proteomic analysis of embryonic *Fasciola hepatica*: Characterization and antigenic potential of a developmentally regulated heat shock protein. *Veterinary Parasitology*, *169*(1–2), 62–75. https://doi.org/10.1016/j.vetpar.2009.12.031

Mulcahy, G., Dalton, J. P. (2001). Cathepsin L proteinases as vaccines against infection with *Fasciola hepatica* (liver fluke) in ruminants. *Research in Veterinary Science*, *70*(1), 83–86. https://doi.org/10.1053/rvsc.2000.0425

Mulcahy, G., O'Connor, F., Clery, D., Hogan, S. F., Dowd, A. J., Andrews, S. J., Dalton, J. P. (1999). Immune responses of cattle to experimental anti-*Fasciola hepatica* vaccines. *Research in Veterinary Science*, *67*(1), 27–33. https://doi.org/10.1053/rvsc.1998.0270

Mulcahy, G., O'Connor, F., McGonigle, S., Dowd, A., Clery, D. G., Andrews, S. J., Dalton, J. P. (1998). Correlation of specific antibody titre and avidity with protection in cattle immunized against *Fasciola hepatica. Vaccine*, *16*(9–10), 932–939. https://doi.org/10.1016/S0264-410X(97)00289-2

Muller, B., Durr, S., Hattendorf, J., Laisse, C. J. M., Parsons, S. D. C., van Helden, P. D., Zinsstag, J. (2013). Zoonotic *Mycobacterium bovis*-induced tuberculosis in humans. *Emerging Infectious Diseases*, *19*(6), 899–908. https://doi.org/https://doi.org/10.3201/eid1906.120543

Munder, M. (2009). Arginase: An emerging key player in the mammalian immune system: REVIEW. *British Journal of Pharmacology*, *158*(3), 638–651. https://doi.org/10.1111/j.1476-5381.2009.00291.x

Munder, M., Eichmann, K., Modolell, M. (1988). Alternative metabolic states in murine macrophages reflected by the nitric oxide regulation by CD4 + T cells correlates with Th1/Th2 phenotype. *The Journal of Immunology*, *160*, 5347–5354.

Munder, M., Mallo, M., Eichmann, K., Modolell, M. (1998). A novel pathway of autocrine macrophage activation. *Journal of Experimental Medicine*, *187*(12), 2103–2108

Muraille, E., Leo, O., Moser, M. (2014). Th1/Th2 paradigm extended: Macrophage polarization as an unappreciated pathogen-driven escape mechanism? *Frontiers in Immunology*, *5*(NOV), 1–12. https://doi.org/10.3389/fimmu.2014.00603

Mureithi, M. W., Finn, A., Ota, M. O., Zhang, Q., Davenport, V., Mitchell, T. J., Williams, N. A., Adegbola, R. A., Heyderman, R. S. (2009). T cell memory response to pneumococcal protein antigens in an area of high pneumococcal carriage and disease. *Journal of Infectious Diseases*, *200*(5), 783–793. https://doi.org/10.1086/605023

Murray, P. J., Allen, J. E., Biswas, S. K., Fisher, E. A., Gilroy, D. W., Goerdt, S., Gordon, S., Hamilton, J.A, Ivashkiv, L.B., Lawerence, T., Locati, M.,Mantonavi, Alberto, Martinez, F. O, Mege, J.-L., Mosser, D. M., Natoli, G, Saeji, J. P, Schultze, J. L, Shirey, K.A, Sica, A., Suttles, J, Udalova, I., van Ginderachter, J.-A., Vogel, S.,N, Wynn, T. A. (2014). Macrophage activation and polarization: Nomenclature and experimental guidelines. *Immunity*, *41*(1), 14–20. https://doi.org/10.1016/j.immuni.2014.06.008

Murray, P. J., Wynn, T. A. (2011a). Protective and pathogenic functions of macrophage subsets. *Nature Reviews Immunology*, *11*(11), 723–737. https://doi.org/Doi 10.1038/Nri3073

Murray, P. J., Wynn, T. A. (2011b). Obstacles and opportunities for understanding macrophage polarization. *Journal of Leukocyte Biology*, *89*(4), 557–563. https://doi.org/10.1189/jlb.0710409

Musah-Eroje, M., Flynn, R. J. (2018). *Fasciola hepatica*, TGF-β and host mimicry: the enemy within. *Current Opinion in Microbiology*, *46*, 80–85. https://doi.org/10.1016/j.mib.2018.09.002

Nair, M. G., Gallagher, I. J., Taylor, M. D., Loke, P., Coulson, P. S., Wilson, R. A., Maizels, R. M, Allen, J. E. (2005). Chitinase and Fizz family members are a generalized feature of nematode infection with selective upregulation of Ym1 and Fizz1 by antigen-presenting cells. *Infection and Immunity*, *73*(1), 385–394. https://doi.org/10.1128/IAI.73.1.385-394.2005

Neill, D. R., Coward, W. R., Gritzfeld, J. F., Richards, L., Garcia-Garcia, F. J., Dotor, J., Gordon, S. B., Kadioglu, A. (2014). Density and duration of pneumococcal carriage is maintained by transforming growth factor β1 and T regulatory cells. *American Journal of Respiratory and Critical Care Medicine*, *189*(10), 1250–1259. https://doi.org/10.1164/rccm.201401-0128OC

Neill, D. R., Fernandes, V. E., Wisby, L., Haynes, A. R., Ferreira, D. M., Laher, A., Strickland, N., Gordon, S. B., Denny, P., Kadioglu, A., Andrew, P. W. (2012). T regulatory cells control susceptibility to invasive pneumococcal pneumonia in mice. *PLoS Pathogens*, *8*(4). https://doi.org/10.1371/journal.ppat.1002660

Nelson, S. (2001). Novel nonantibiotic therapies for pneumonia: Cytokines and host defense. *Chest*, *119*(2 SUPPL.), 419S-425S. https://doi.org/10.1378/chest.119.2_suppl.419S

Nüchel, J., Ghatak, S., Zuk, A. V., Illerhaus, A., Mörgelin, M., Schönborn, K., Blumbach, K., Wicktrom, S. A., Krieg, T., Sengle, G., Plomann, M., Eckes, B. (2018). TGFβ1 is secreted through an unconventional pathway dependent on the autophagic machinery and cytoskeletal regulators. *Autophagy*, *14*(3), 465–486. https://doi.org/10.1080/15548627.2017.1422850

Nutman, T. B. (2015). Looking beyond the induction of Th2 responses to explain immunomodulation by helminths. *Parasite Immunology*, *37*(6), 304–313. https://doi.org/10.1111/pim.12194

Nyindo, M., Lukambagire, A. H. (2015). Fascioliasis: An ongoing zoonotic trematode infection. *BioMed Research International*, *2015*. https://doi.org/10.1155/2015/786195

O'Connell, A. E., Hess, J. A., Santiago, G. A., Nolan, T. J., Lok, J. B., Lee, J. J., Abraham, D. (2011). Major basic protein from eosinophils and myeloperoxidase from neutrophils are required for protective immunity to *Strongyloides stercoralis* in mice. *Infection and Immunity*, *79*(7), 2770–2778. https://doi.org/10.1128/IAI.00931-10

O'Neill, S M, Mills, K. H., Dalton, J. P. (2001). *Fasciola hepatica* cathepsin L cysteine proteinase suppresses *Bordetella pertussis*-specific interferon-gamma production *in vivo*. *Parasite Immunology*, *23*(10), 541–547. https://doi.org/10.1046/j.1365-3024.2001.00411.x

O'Neill, Sandra M., Brady, M. T., Callanan, J. J., Mulcahy, G., Joyce, P., Mills, K. H. G., Dalton, J. P. (2000). *Fasciola hepatica* infection downregulates Th1 responses in mice. *Parasite Immunology*, *22*(3), 147–155. https://doi.org/10.1046/j.1365-3024.2000.00290.x

O'Neill, Sandra M., Parkinson, M., Strauss, W., Angles, R., Dalton, J. P. (1998). Immunodiagnosis of *Fasciola hepatica* infection (Fascioliasis) in a human population in the Bolivian Altiplano using purified cathepsin L cysteine proteinase. *American Journal of Tropical Medicine and Hygiene*, *58*(4), 417–423. https://doi.org/10.4269/ajtmh.1998.58.417

Olliver, M., Hiew, J., Mellroth, P., Henriques-Normark, B., Bergman, P. (2011). Human monocytes promote Th1 and Th17 responses to *Streptococcus pneumoniae*. *Infection and Immunity*, *79*(10), 4210–4217. https://doi.org/10.1128/IAI.05286-11

Omer, F. M., Kurtzhals, J. A. L., Riley, E. M. (2000). Maintaining the immunological balance in parasitic infections: A role for TGF-β? *Parasitology Today*, *16*(1), 18–23. https://doi.org/10.1016/S0169-4758(99)01562-8

Orecchioni, M., Ghosheh, Y., Pramod, A. B., Ley, K. (2019). Macrophage polarization: Different gene signatures in M1(Lps+) vs. classically and M2(LPS-) vs. alternatively activated macrophages. *Frontiers in Immunology*, *10*(MAY), 1–14. https://doi.org/10.3389/fimmu.2019.01084

Panagiotou, S., Chaguza, C., Yahya, R., Audshasai, T., Baltazar, M., Ressel, L., Khandaker, S., Alsahag, M., Mitchell, T. J., Prudhomme, M., Kadioglu, A., (2020). Hypervirulent pneumococcal serotype 1 harbours two pneumolysin variants with differential haemolytic activity. *Scientific Reports*, 1–15. https://doi.org/10.1038/s41598-020-73454-w

Passos, L. S. A., Gazzinelli-Guimarães, P. H., de Oliveira Mendes, T. A., Guimarães, A. C. G., da Silveira Lemos, D., Ricci, N. D., Goncalves, R., Bartholomeu, D. C., Fujiwara, R. T., Bueno, L. L. (2017). Regulatory monocytes in helminth infections: Insights from the modulation during human hookworm infection. *BMC Infectious Diseases*, *17*(1), 1–9. https://doi.org/10.1186/s12879-017-2366-0

Paterson, G. K., Orihuela, C. J. (2010). Pneumococci: Immunology of the innate host response. *Respirology*, *15*(7), 1057–1063. https://doi.org/10.1111/j.1440-1843.2010.01814.x

Pathak, A. K., Pelensky, C., Boag, B., Cattadori, I. M. (2012). Immuno-epidemiology of chronic bacterial and helminth co-infections: Observations from the field and evidence from the laboratory. *International Journal for Parasitology*, *42*(7), 647–655. https://doi.org/10.1016/j.ijpara.2012.04.011

Paudel, S., Baral, P., Ghimire, L., Bergeron, S., Jin, L., DeCorte, J. A., le, J. T., cai, S., Jeyaseelan, S. (2019). CXCL1 regulates neutrophil homeostasis in pneumonia-derived sepsis caused by *Streptococcus pneumoniae* serotype 3. *Blood*, *133*(12), 1335–1345. https://doi.org/10.1182/blood-2018-10-878082

Paveley, R. A., Aynsley, S. A., Turner, J. D., Bourke, C. D., Jenkins, S. J., Cook, P. C., martinez-pomares, L., Mountford, A. P. (2011). The mannose receptor (CD206) is an important pattern recognition receptor (PRR) in the detection of the infective stage of the helminth *Schistosoma mansoni* and modulates IFNγ production. *International Journal for Parasitology*, *41*(13–14), 1335–1345. https://doi.org/10.1016/j.ijpara.2011.08.005

Pérez-Lago, L., Navarro, Y., García-de-Viedma, D. (2014). Current knowledge and pending challenges in zoonosis caused by *Mycobacterium bovis*: A review. *Research in Veterinary Science*, *97*, 94–100. https://doi.org/10.1016/j.rvsc.2013.11.008

Periselneris, J., José, R. J., Brown, J. (2015). Targeting inflammatory responses to *Streptococcus pneumoniae*. *New Horizons in Translational Medicine*, *2*(6–7), 167–174. https://doi.org/10.1016/j.nhtm.2015.09.002

Pesce, J. T., Ramalingam, T. R., Mentink-Kane, M. M., Wilson, M. S., Kasmi, K. C. E., Smith, A. M., Thompson, R. W., Cheever, A. W., Murray, P. J., Wynn, T. A. (2009). Arginase-1-expressing macrophages suppress Th2 cytokine-driven inflammation and fibrosis. *PLoS Pathogens*, *5*(4). https://doi.org/10.1371/journal.ppat.1000371

Petri, B., Sanz, M.-J. (2018). Neutrophil chemotaxis. *Cell and Tissue Research*, *371*(3), 425–436. https://doi.org/10.1007/s00441-017-2776-8

Piccioli, P., Rubartelli, A. (2013). The secretion of IL-1β and options for release. *Seminars in Immunology*, *25*(6), 425–429. https://doi.org/10.1016/j.smim.2013.10.007

Piedrafita, D., Spithill, T. W., Smith, R. E., Raadsma, H. W. (2010). Improving animal and human health through understanding liver fluke immunology. *Parasite Immunology*, *32*(8), 572–581. https://doi.org/10.1111/j.1365-3024.2010.01223.x

Pollock, J. M., Neill, S. D. (2002). *Mycobacterium bovis* infection and tuberculosis in cattle. *Veterinary Journal*, *163*(2), 115–127. https://doi.org/10.1053/tvjl.2001.0655

Preston, J. A., Bewley, M. A., Marriott, H. M., Houghton, A. M. G., Mohasin, M., Jubrail, J., Morris. L, Stephenson, Y. L., Cross, S., Greaves, D. R., Craig, R. W., van Rooijen, N., Bingle, C. D., Read, R. C., Mitchell, T. J., Whyte, M. K. B, Shapiro, S. D., Dockrell, D. H. (2019). Alveolar macrophage apoptosis-associated bacterial killing helps prevent murine pneumonia. *American Journal of Respiratory and Critical Care Medicine*, *200*(1), 84–97. https://doi.org/10.1164/rccm.201804-0646OC

Préveraud-Sindou, M., Rondelaud, D. (1995). Localization and outcome of *Fasciola hepatica* sporocysts in *Lymnaea truncatula* subjected to mono- or plurimiracidial exposure. *Parasitology Research*, *81*, 265–267. https://doi.org/10.1007/BF00937121

Preza, O., Klapa, I., Tsiakalos, A., Cokkinos, D. D., Chatziioannou, A. (2019). Fascioliasis: A challenging differential diagnosis for radiologists. *Journal of Radiology Case Reports*, *13*(1), 11–16. https://doi.org/10.3941/jrcr.v13i1.3451

Price, J. V., Vance, R. E. (2014). The macrophage paradox. *Immunity*, *41*(5), 685–693. https://doi.org/10.1016/j.immuni.2014.10.015

Quigley, A., Sekiya, M., Garcia-Campos, A., Paz-Silva, A., Howell, A., Williams, D. J. L., Mulcahy, G. (2020). Horses are susceptible to natural, but resistant to experimental, infection with the liver fluke, F*asciola hepatica*. *Veterinary Parasitology*, *281*(March), 109094. https://doi.org/10.1016/j.vetpar.2020.109094

Rath, M., Müller, I., Kropf, P., Closs, E. I., Munder, M. (2014). Metabolism via arginase or nitric oxide synthase: Two competing arginine pathways in macrophages. *Frontiers in Immunology*, *5*(OCT), 1–10. https://doi.org/10.3389/fimmu.2014.00532

Ravida, A., Cwiklinski, K., Aldridge, A. M., Clarke, P., Thompson, R., Gerlach, J. Q., Kilcoyne, M., Hokke, C. H., Dalton, J. P., O'Neill, S. M. (2016). *Fasciola hepatica* surface tegument: glycoproteins at the interface of parasite and host. *Molecular and Cellular Proteomics : MCP*, (8), 1–48. https://doi.org/10.1074/mcp.M116.059774

Rayner, C. F. J., Jackson, A. D., Rutman, A., Dewar, A., Mitchell, T. J., Andrew, P. W., Cole, P. J., Wilson, R. (1995). Interaction of pneumolysin-sufficient and -deficient isogenic variants of *Streptococcus pneumoniae* with human respiratory mucosa. *Infection and Immunity*, *63*(2), 442–447. https://doi.org/10.1128/iai.63.2.442-447.1995

Reading, P. C., Miller, J. L., Anders, E. M. (2000). Involvement of the mannose receptor in infection of macrophages by influenza virus. *Journal of Virology*, *74*(11), 5190–5197. https://doi.org/10.1128/JVI.74.11.5190-5197.2000

Resende Co, T., Hirsch, C. S., Toossi, Z., Dietze, R., Ribeiro-Rodrigues, R. (2007). Intestinal helminth co-infection has a negative impact on both anti-*Mycobacterium tuberculosis* immunity and clinical response to tuberculosis therapy. *Clinical and Experimental Immunology*, *147*(1), 45–52. https://doi.org/10.1111/j.1365-2249.2006.03247.x

Reyes, J. L., Terrazas, L. I. (2007). The divergent roles of alternatively activated macrophages in helminthic infections. *Parasite Immunology*, *29*(12), 609–619. https://doi.org/10.1111/j.1365-3024.2007.00973.x

Ritchie, N. D., Mitchell, T. J., Evans, T. J. (2012). What is different about serotype 1 pneumococci? *Future Microbiology*, *7*(1), 33–46. https://doi.org/10.2217/fmb.11.146

Robertson, I. B., Horiguchi, M., Zilberberg, L., Dabovic, B., Hadjiolova, K., Daniel B. Rifkin. (2015). Latent TGF-β-binding protein. *Matrix Biol.*, *47*, 44–53. https://doi.org/doi:10.1016/j.matbio.2015.05.005

Robinson, M. W., Dalton, J. P. (2009). Zoonotic helminth infections with particular emphasis on fasciolosis and other trematodiases. *Philosophical Transactions of the Royal Society B: Biological Sciences*, *364*(1530), 2763–2776. https://doi.org/10.1098/rstb.2009.0089

Robinson, M. W., Dalton, J. P., O'Brien, B. A., Donnelly, S. (2013). *Fasciola hepatica*: The therapeutic potential of a worm secretome. *International Journal for Parasitology*, *43*(3–4), 283–291. https://doi.org/10.1016/j.ijpara.2012.11.004

Robinson, M. W., Donnelly, S., Hutchinson, A. T., To, J., Taylor, N. L., Norton, R. S., Perugini, M. A., Dalton, J. P. (2011). A family of helminth molecules that modulate innate cell responses via molecular mimicry of host antimicrobial peptides. *PLoS Pathogens*, *7*(5). https://doi.org/10.1371/journal.ppat.1002042

Robinson, M. W., Menon, R., Donnelly, S. M., Dalton, J. P., Ranganathan, S. (2009). An integrated transcriptomics and proteomics analysis of the secretome of the helminth pathogen *Fasciola hepatica:* Proteins associated with invasion and infection of the mammalian host. *Molecular and Cellular Proteomics*, *8*(8), 1891–1907. https://doi.org/10.1074/mcp.M900045-MCP200

Roca, H., Varcos, Z. S., Sud, S., Craig, M. J., Pienta, K. J. (2009). CCL2 and interleukin-6 promote survival of human CD11b+ peripheral blood mononuclear cells and induce M2-type macrophage polarization. *Journal of Biological Chemistry*, *284*(49), 34342–34354. https://doi.org/10.1074/jbc.M109.042671

Rodríguez, E., Kalay, H., Noya, V., Brossard, N., Giacomini, C., van Kooyk, Y., Garcia-Valejo. J.J., Freire, T. (2017). *Fasciola hepatica* glycoconjugates immuneregulate dendritic cells through the dendritic cell-specific intercellular adhesion molecule-3-grabbing non-integrin inducing T cell anergy. *Scientific Reports*, *7*(March), 46748. https://doi.org/10.1038/srep46748

Rodríguez, E., Noya, V., Cervi, L., Chiribao, M. L., Brossard, N., Chiale, C., Carmona, C., Giacomini, C., Freire, T. (2015). Glycans from *Fasciola hepatica* modulate the host immune response and TLR-induced maturation of dendritic cells. *PLoS Neglected Tropical Diseases*, *9*(12), 1–26. https://doi.org/10.1371/journal.pntd.0004234

Rojas-Caraballo, J., López-Abán, J., Fernández-Soto, P., Vicente, B., Collía, F., Muro, A. (2015). Gene expression profile in the liver of BALB/c mice infected with *Fasciola hepatica*. *PLoS ONE*, *10*(8), 1–20. https://doi.org/10.1371/journal.pone.0134910

Rolot, M., Dewals, B. G. (2018). Macrophage activation and functions during helminth infection: Recent advances from the laboratory mouse. *Journal of Immunology Research*, *2018*, 1–17. https://doi.org/10.1155/2018/2790627

Romagnani, S. (2000). T-cell subsets (Th1 versus Th2). *Annals of Allergy, Asthma and Immunology*, *85*(1), 9–18. https://doi.org/10.1016/S1081-1206(10)62426-X

Rose, M. A., Christopoulou, D., Myint, T. T. H., De Schutter, I. (2014). The burden of invasive pneumococcal disease in children with underlying risk factors in North America and Europe. *International Journal of Clinical Practice*, *68*(1), 8–19. https://doi.org/10.1111/ijcp.12234

Rosenberg, H. F., Dyer, K. D., Foster, P. S. (2013). Eosinophils: Changing perspectives in health and disease. *Nature Reviews Immunology*, *13*(1), 9–22. https://doi.org/10.1038/nri3341

Roszer, T. (2015). Understanding the mysterious M2 macrophage through activation markers and effector mechanisms. *Mediators of Inflammation, 2015*, 1-16. https://doi.org/http://dx.doi.org/10.1155/2015/816460

Rubins, J. B., Paddock, A. H., Charboneau, D., Berry, A. M., Paton, J. C., Janoff, E. N. (1998). Pneumolysin in pneumococcal adherence and colonization. *Microbial Pathogenesis*, *25*(6), 337–342. https://doi.org/10.1006/mpat.1998.0239

Ryan, S., Shiels, J., Taggart, C. C., Dalton, J. P., Weldon, S. (2020). *Fasciola hepatica*-derived molecules as regulators of the host immune response. *Frontiers in Immunology*, *11*(September), 1–9. https://doi.org/10.3389/fimmu.2020.02182

Sabourin, E., Alda, P., Vázquez, A., Hurtrez-Boussès, S., Vittecoq, M. (2018). Impact of human activities on fasciolosis transmission. *Trends in Parasitology*, *34*(10), 891–903. https://doi.org/10.1016/j.pt.2018.08.004

Sarazin, A., Poulain, D., Jouault, T. (2010). *In vitro* pro-and anti-inflammatory responses to viable *Candida albicans* yeasts by a murine macrophage cell line. *Medical Mycology*, *48*(7), 912–921. https://doi.org/10.3109/13693781003767592

Sargison, N. D., Scott, P. R. (2011). Diagnosis and economic consequences of triclabendazole resistance in *Fasciola hepatica* in a sheep flock in south-east Scotland. *Veterinary Record*, *168*(6), 159. https://doi.org/10.1136/vr.c5332

Savage, J., Meaney, M., Brennan, G. P., Hoey, E., Trudgett, A., Fairweather, I. (2013). Increased action of triclabendazole (TCBZ) *in vitro* against a TCBZ-resistant isolate of *Fasciola hepatica* following its co-incubation with the P-glycoprotein inhibitor, R(+)-verapamil. *Experimental Parasitology*, *135*(3), 642–653. https://doi.org/10.1016/j.exppara.2013.09.015

Schito, M. L., Barta, J. R., Chobotar, B. (1996). Comparison of four murine *Eimeria* species in immunocompetent and immunodeficient mice. *Journal of Parasitology*, *82*(2), 255–262. https://doi.org/10.2307/3284157

Schlesinger, P. H., Doebber, T. W., Mandell, B. F., White, R., DeSchryver, C., Rodman, J. S., Miller, M. J., Stahl, P. (1978). Plasma clearance of glycoproteins with terminal mannose and N-acetylglucosamine by liver non-parenchymal cells. Studies with β-glucuronidase, N-acetyl-β-D-glucosaminidase, ribonuclease B and agalacto-orosomucoid. *Biochemical Journal*, *176*(1), 103–109. https://doi.org/10.1042/bj1760103

Schultze, J. L., Freeman, T., Hume, D. A., Latz, E. (2015). A transcriptional perspective on human macrophage biology. *Seminars in Immunology*, *27*(1), 44–50. https://doi.org/10.1016/j.smim.2015.02.001

Serbina, N. V., Jia, T., Hohl, T. M., Pamer, E. G. (2008). Monocyte-mediated defense against microbial pathogens. *Annual Review of Immunology*, *26*, 421–452. https://doi.org/10.1146/annurev.immunol.26.021607.090326

Shapouri-Moghaddam, A., Mohammadian, S., Vazini, H., Taghadosi, M., Esmaeili, S. A., Mardani, F., Seifi, B., Mohammadi, A., Afshari, J. T., Sahebkar, A. (2018). Macrophage plasticity, polarization, and function in health and disease. *Journal of Cellular Physiology*, *233*(9), 6425–6440. https://doi.org/10.1002/jcp.26429

Shaul, M. E., Bennett, G., Strissel, K. J., Greenberg, A. S., Obin, M. S. (2010). Dynamic, M2-like remodeling phenotypes of CD11c+ adipose tissue macrophages during high-fat diet - Induced obesity in mice. *Diabetes*, *59*(5), 1171–1181. https://doi.org/10.2337/db09-1402

Shears, R. K., Jacques, L. C., Naylor, G., Miyashita, L., Khandaker, S., Lebre, F., Lavelle, E. C., Grigg, J., French, N., Neill, D. R., Kadioglu, A. (2019). Exposure to diesel exhaust particles increases susceptibility to invasive pneumococcal disease. *Journal of Allergy and Clinical Immunology*, 1-19. https://doi.org/10.1016/j.jaci.2019.11.039

Shenoy, A. T., Brissac, T., Gilley, R. P., Kumar, N., Wang, Y., Gonzalez-Juarbe, N., Hinkle, W. S., Daugherty, S. C.,Shetty, A. C., Ott, S., Tallon, l. J., Deshane, J., Tettelin, H., Orihuela, C. J. (2017). *Streptococcus pneumoniae* in the heart subvert the host response through biofilm-mediated resident macrophage killing. In *PLoS Pathogens, 13*(8), 1-31. https://doi.org/10.1371/journal.ppat.1006582

Shepherd, C., Navarro, S., Wangchuk, P., Wilson, D., Daly, N. L., Loukas, A. (2015). Identifying the immunomodulatory components of helminths. *Parasite Immunology*, *37*(6), 293–303. https://doi.org/10.1111/pim.12192

Shirey, K. A., Pletneva, L. M., Puche, A. C., Keegan, A. D., Prince, G. A., Blanco, J. C. G., Vogel, S. N. (2010). Control of RSV-induced lung injury by alternatively activated macrophages is IL-4Rα-, TLR4-, and IFN-B-dependent. *Mucosal Immunology*, *3*(3), 291–300. https://doi.org/10.1038/mi.2010.6

Siegel, S. J., Tamashiro, E., Weiser, J. N. (2015). Clearance of pneumococcal colonization in infants is delayed through altered macrophage trafficking. *PLoS Pathogens*, *11*(6), 1–17. https://doi.org/10.1371/journal.ppat.1005004

Singer, M. N., Heath, C., Muinde, J., Gildengorin, V., Mutuku, F. M., Vu, D., Mukoko, D., King, C. L., Malhotra, L. J., King, C. H., LaBeaud, A. D. (2017). Pneumococcal vaccine response after exposure to parasites in utero, in Infancy, or mid-childhood. *Pediatrics*, *139*(4), e20162781. https://doi.org/10.1542/peds.2016-2781

Skuce, P. J., Zadoks, R. N. (2013). Liver fluke - A growing threat to UK livestock production. *Cattle Practice*, *21*, 138–149.

Sleeman, K. L., Griffiths, D., Shackley, F., Diggle, L., Gupta, S., Maiden, M. C., Moxon, E. R., Crook, D. W., Peto, T. E. A. (2006). Capsular serotype-specific attack rates and duration of carriage of *Streptococcus pneumoniae* in a population of children. *Journal of Infectious Diseases*, *194*(5), 682–688. https://doi.org/10.1086/505710

Smallwood, T. B., Giacomin, P. R., Loukas, A., Mulvenna, J. P., Clark, R. J., Miles, J. J. (2017). Helminth immunomodulation in autoimmune disease. *Frontiers in Immunology*, *8*(APR). https://doi.org/10.3389/fimmu.2017.00453

Smith, A. M., Dowd, A. J., McGonigle, S., Keegan, P. S., Brennan, G., Trudgett, A., Dalton, J. P. (1993). Purification of a cathepsin L-like proteinase secreted by adult *Fasciola hepatica*. *Molecular and Biochemical Parasitology*, *62*(1), 1–8. https://doi.org/10.1016/0166-6851(93)90171-S

Smith, M. W., Schmidt, J. E., Rehg, J. E., Orihuela, C. J., McCullers, J. A. (2007). Induction of pro- and anti-inflammatory molecules in a mouse model of pneumococcal pneumonia after influenza. *Comparative Medicine*, *57*(1), 82–89.

Stahl, P., Schlesinger, P. H., Sigardson, E., Rodman, J. S., Lee, Y. C. (1980). Receptor-mediated pinocytosis of mannose glycoconjugates by macrophages: Characterization and evidence for receptor recycling. *Cell*, *19*(1), 207–215. https://doi.org/10.1016/0092-8674(80)90402-X

Standish, A. J., Weiser, J. N. (2009). Human neutrophils kill *Streptococcus pneumoniae* via rerine proteases. *The Journal of Immunology*, *183*(4), 2602–2609. https://doi.org/10.4049/jimmunol.0900688

Stempin, C. C., Dulgerian, L. R., Garrido, V. V., Cerban, F. M. (2010). Arginase in parasitic infections: Macrophage activation, immunosuppression, and intracellular signals. *Journal of Biomedicine and Biotechnology*, *2010*. https://doi.org/10.1155/2010/683485

Su, L., Su, C. W., Qi, Y., Yang, G., Zhang, M., Cherayil, B. J., Zhang, X., Shi, H. N. (2014). Coinfection with an intestinal helminth impairs host innate immunity against *Salmonella enterica* serovar typhimurium and exacerbates intestinal inflammation in mice. *Infection and Immunity*, *82*(9), 3855–3866. https://doi.org/10.1128/IAI.02023-14

Subramanian, K., Neill, D. R., Malak, H. A., Spelmink, L., Khandaker, S., Marchiori, G. D. L., Dearing, E., Kirby, A., Yang, M., Achour, A., Nilvebrant, J., Nygren, P.-A., Plant, L., Kadioglu, A., Henriques-Normark, B. (2018). Pneumolysin binds to the mannose receptor C type 1 (MRC-1) leading to anti-inflammatory responses and enhanced pneumococcal survival. *Nature Microbiology*, *1*. https://doi.org/10.1038/s41564-018-0280-x

Sun, K., Gan, Y., Metzger, D. W. (2011). Analysis of murine genetic predisposition to pneumococcal infection reveals a critical role of alveolar macrophages in maintaining the sterility of the lower respiratory tract. *Infection and Immunity*, *79*(5), 1842–1847. https://doi.org/10.1128/IAI.01143-10

Supali, T., Verweij, J. J., Wiria, A. E., Djuardi, Y., Hamid, F., Kaisar, M. M. M., Wammes, L. J, van Lieshout, L., Luty, A. J. F., Sartono, E., Yazdanbakhsh, M. (2010). Polyparasitism and its impact on the immune system. *International Journal for Parasitology*, *40*(10), 1171–1176. https://doi.org/10.1016/j.ijpara.2010.05.003

Taciak, B., Białasek, M., Braniewska, A., Sas, Z., Sawicka, P., Kiraga, Ł., Rygiel, T., Król, M. (2018). Evaluation of phenotypic and functional stability of RAW 264.7 cell line through serial passages. *PLoS ONE*, *13*(6), 1–13. https://doi.org/10.1371/journal.pone.0198943

Takeda, K., Akira, S. (2005). Toll-like receptors in innate immunity. *International Immunology*, *17*(1), 1–14. https://doi.org/10.1093/intimm/dxh186

Talaue, M. T., Venketaraman, V., Hazbón, M. H., Peteroy-Kelly, M., Seth, A., Colangeli, R., Alland, D., Connell, N. D. (2006). Arginine homeostasis in J774.1 macrophages in the context of *Mycobacterium bovis* BCG infection. *Journal of Bacteriology*, *188*(13), 4830–4840. https://doi.org/10.1128/JB.01687-05

Taylor, M. A., Coop, R. L., Wall, R. L. (2016). Veterinary parasitology (4th Ed.). Wiley Blackwell, UK, pp. 480-486

Taylor, P. R., Brown, G. D., Reid, D. M., Willment, J. A., Martinez-Pomares, L., Gordon, S., Wong, S. Y. C. (2002). The β-glucan receptor, dectin-1, is predominantly expressed on the surface of cells of the monocyte/macrophage and neutrophil lineages. *The Journal of Immunology*, *169*(7), 3876–3882. https://doi.org/10.4049/jimmunol.169.7.3876

Taylor, P. R., Gordon, S., Martinez-Pomares, L. (2005). The mannose receptor: Linking homeostasis and immunity through sugar recognition. *Trends in Immunology*, *26*(2), 104–110. https://doi.org/10.1016/j.it.2004.12.001

Terrazas, L. I., Montero, D., Terrazas, C. A., Reyes, J. L., Rodríguez-Sosa, M. (2005). Role of the programmed death-1 pathway in the suppressive activity of alternatively activated macrophages in experimental cysticercosis. *International Journal for Parasitology*, *35*(13), 1349–1358. https://doi.org/10.1016/j.ijpara.2005.06.003

Tilley, S. J., Orlova, E. V., Gilbert, R. J. C., Andrew, P. W., Saibil, H. R. (2005). Structural basis of pore formation by the bacterial toxin pneumolysin. *Cell*, *121*(2), 247–256. https://doi.org/10.1016/j.cell.2005.02.033

Toet, H., Piedrafita, D. M., Spithill, T. W. (2014). Liver fluke vaccines in ruminants: Strategies, progress and future opportunities. *International Journal for Parasitology*, *44*(12), 915–927. https://doi.org/10.1016/j.ijpara.2014.07.011

Tomlinson, G., Chimalapati, S., Pollard, T., Lapp, T., Cohen, J., Camberlein, E., Stafford, S., Periselneris, J., Aldridge, C., Vollmer, W., Picard, C., Casanova, J.-L., Noursadeghi, M., Brown, J. (2014). TLR-mediated inflammatory responses to *Streptococcus pneumoniae* are highly dependent on surface expression of bacterial lipoproteins. *The Journal of Immunology*, *193*(7), 3736–3745. https://doi.org/10.4049/jimmunol.1401413

Trinchieri, G. (1995). Interleukin-12 and interferon-gamma. Do they always go together? *The American Journal of Pathology*, *147*(6), 1534–1538.

Trinchieri, G. (2003). Interleukin-12 and the regulation of innate resistance and adaptive immunity. *Nature Reviews Immunology*, *3*(2), 133–146. https://doi.org/10.1038/nri1001

Tripathi, P. (2007). Nitric oxide and immune response. *Indian Journal of Biochemistry and Biophysics*, *44*(5), 310–319.

Trivedi, N. H., Yu, J. J., Hung, C. Y., Doelger, R. P., Navara, C. S., Armitige, L. Y., Seshu, J., Sinai, A. P., Chambers, J. P., Guentzel, M. Neal, Arulanandam, B. P. (2018). Microbial co-infection alters macrophage polarization, phagosomal escape, and microbial killing. *Innate Immunity*, *24*(3), 152–162. https://doi.org/10.1177/1753425918760180

Trzciński, K., Thompson, C. M., Srivastava, A., Basset, A., Malley, R., Lipsitch, M. (2008). Protection against nasopharyngeal colonization by *Streptococcus pneumoniae* is mediated by antigen-specific CD4+ T cells. *Infection and Immunity*, *76*(6), 2678–2684. https://doi.org/10.1128/IAI.00141-08

Tsai, W. C., Strieter, R. M., Mehrad, B., Newstead, M. W., Zeng, X., Standiford, T. J. (2000). CXC chemokine receptor CXCR2 is essential for protective-innate host response in murine *Pseudomonas aeruginosa* pneumonia. *Infection and Immunity*, *68*(7), 4289–4296. https://doi.org/10.1128/IAI.68.7.4289-4296.2000

Turner, M. D., Nedjai, B., Hurst, T., Pennington, D. J. (2014). Cytokines and chemokines: At the crossroads of cell signalling and inflammatory disease. *Biochimica et Biophysica Acta - Molecular Cell Research*, *1843*(11), 2563–2582. https://doi.org/10.1016/j.bbamcr.2014.05.014

Umemura, N., Saio, M., Suwa, T., Kitoh, Y., Bai, J., Nonaka, K., Ouyang, G.-F., Okada, M., Balazs, M., Adany, R., Shibata, T., Takami, T. (2008). Tumor-infiltrating myeloid-derived suppressor cells are pleiotropic-inflamed monocytes/macrophages that bear M1- and M2-type characteristics. *Journal of Leukocyte Biology*, *83*(5), 1136–1144. https://doi.org/10.1189/jlb.0907611

van Die, I., Cummings, R. D. (2017). The mannose receptor in regulation of helminth-mediated host immunity. *Frontiers in Immunology*, *8*(NOV), 1–9. https://doi.org/10.3389/fimmu.2017.01677

van Panhuys, N., Prout, M., Forbes, E., Min, B., Paul, W. E., Le Gros, G. (2011). Basophils are the major producers of IL-4 during primary helminth infection. *The Journal of Immunology*, *186*(5), 2719–2728. https://doi.org/10.4049/jimmunol.1000940

van Rossum, A. M. C., Lysenko, E. S., Weiser, J. N. (2005). Host and bacterial factors contributing to the clearance of colonization by *Streptococcus pneumoniae* in a murine model. *Infection and Immunity*, *73*(11), 7718–7726. https://doi.org/10.1128/IAI.73.11.7718-7726.2005

Vaumourin, E., Vourc'h, G., Gasqui, P., Vayssier-Taussat, M. (2015). The importance of multiparasitism: examining the consequences of co-infections for human and animal health. *Parasites and Vectors*, *8*(1), 1–13. https://doi.org/10.1186/s13071-015-1167-9

Vayr, F., Martin-Blondel, G., Savall, F., Soulat, J. M., Deffontaines, G., Herin, F. (2018). Occupational exposure to human *Mycobacterium bovis* infection: A systematic review. *PLoS Neglected Tropical Diseases*, *12*(1), 1–14. https://doi.org/10.1371/journal.pntd.0006208

Viola, A., Munari, F., Sánchez-Rodríguez, R., Scolaro, T., Castegna, A. (2019). The metabolic signature of macrophage responses. *Frontiers in Immunology*, *10*(July), 1–16. https://doi.org/10.3389/fimmu.2019.01462

Vukman, K. V., Adams, P. N., O'Neill, S. M. (2013b). *Fasciola hepatica* tegumental coat antigen suppresses MAPK signalling in dendritic cells and up-regulates the expression of SOCS3. *Parasite Immunology*, *35*(7–8), 234–238. https://doi.org/10.1111/pim.12033

Vukman, K. V., Adams, P. N., Dowling, D., Metz, M., Maurer, M., O'Neill, S. M. (2013c). The effects of *Fasciola hepatica* tegumental antigens on mast cell function. *International Journal for Parasitology*, *43*(7), 531–539. https://doi.org/10.1016/j.ijpara.2013.01.011

Vukman, K. V, Adams, P. N., Metz, M., Maurer, M., O'Neill, S. M. (2013a). *Fasciola hepatica* Tegumental Coat Impairs Mast Cells' Ability To Drive Th1 Immune Responses. *The Journal of Immunology*, *190*(6), 2873–2879. https://doi.org/10.4049/jimmunol.1203011

Walsh, K. P., Brady, M. T., Finlay, C. M., Boon, L., Mills, K. H. G. (2009). Infection with a helminth parasite attenuates autoimmunity through TGF-beta-mediated suppression of Th17 and Th1 responses. *Journal of Immunology*, *183*, 1577–1586. https://doi.org/10.4049/jimmunol.0803803

Wang, N., Liang, H., Zen, K. (2014). Molecular mechanisms that influence the macrophage M1-M2 polarization balance. *Frontiers in Immunology*, *5*(NOV), 1–9. https://doi.org/10.3389/fimmu.2014.00614

Watson, D. A., Musher, D. M., Jacobson, J. W., Verhoef, J. (1993). A brief history of the pneumococcus in biomedical research: A panoply of scientific discovery. *Clinical Infectious Diseases*, *17*(5), 913–924. https://doi.org/10.1093/clinids/17.5.913

Webster, S. J., Daigneault, M., Bewley, M. A., Preston, J. A., Marriott, H. M., Walmsley, S. R., read, R. C., Whyte, M. K.. B., Dockrell, D. H. (2010). Distinct cell death programs in monocytes regulate innate responses following challenge with common causes of invasive bacterial disease. *The Journal of Immunology*, *185*(5), 2968–2979. https://doi.org/10.4049/jimmunol.1000805

Weinberg, J. B. (1998). Nitric oxide production and nitric oxide synthase type 2 expression by human mononuclear phagocytes: A review. *Molecular Medicine*, *4*(9), 557–591. https://doi.org/10.1007/bf03401758

Weinberger, D. M., Dagan, R., Givon-Lavi, N., Regev-Yochay, G., Malley, R., Lipsitch, M. (2008). Epidemiologic evidence for serotype-specific acquired immunity to pneumococcal carriage. *Journal of Infectious Diseases*, *197*(11), 1511–1518. https://doi.org/10.1086/587941

Weis, W. I., Taylor, M. E., Drickamer, K. (1998). The C-type lectin superfamily in the immune system. *Immunological Reviews*, *163*, 19–34. https://doi.org/10.1111/j.1600-065X.1998.tb01185.x

Weiser, J. N., Ferreira, D. M., Paton, J. C. (2018). *Streptococcus pneumoniae*: Transmission, colonization and invasion. *Nature Reviews Microbiology*, *16*(6), 355–367. https://doi.org/10.1038/s41579-018-0001-8

WHO - World Health Organisation (2020). Foodborne Trematode Infection. [website] https://www.who.int/foodborne_trematode_infections/fascioliasis/en/ [Acessed 14th May 2020]

Williams, D. J. L., Hodgkinson, J. E. (2017). Fasciolosis in horses: A neglected, re-emerging disease. *Equine Veterinary Education*, *29*(4), 202–204. https://doi.org/10.1111/eve.12521

Wills-Karp, M., Finkelman, F. D. (2011). Innate lymphoid cells wield a double-edged sword. *Nature Immunology*, *12*(11), 1025–1027. https://doi.org/10.1038/ni.2142

Witzenrath, M., Pache, F., Lorenz, D., Koppe, U., Gutbier, B., Tabeling, C., reppe, K., Meixenberger, K., Dorhoi, A., Ma, J., Holmes, A., Tredelenburg, G., Heimesaat, M. M., Bereswill, S., van der linden, M., Tschopp, J., Mitchell, T. J, Suttorp, N., Opitz, B. (2011). The NLRP3 inflammasome is differentially activated by pneumolysin variants and contributes to host defense in pneumococcal pneumonia. *The Journal of Immunology*, *187*(1), 434–440. https://doi.org/10.4049/jimmunol.1003143

Wright, A. K. A., Bangert, M., Gritzfeld, J. F., Ferreira, D. M., Jambo, K. C., Wright, A. D., Collins, A. M., Gordon, S. B. (2013). Experimental human pneumococcal carriage augments IL-17A-dependent T-cell defence of the lung. *PLoS Pathogens*, *9*(3). https://doi.org/10.1371/journal.ppat.1003274

Wright, A. K. A., Ferreira, D. M., Gritzfeld, J. F., Wright, A. D., Armitage, K., Jambo, K. C., bate, E., Batrawy, S. E., Collins, A., Gordon, S. B. (2012). Human nasal challenge with *Streptococcus pneumoniae* is immunising in the absence of carriage. *PLoS Pathogens*, *8*(4), 16–19. https://doi.org/10.1371/journal.ppat.1002622

Wynn, T. A., Chawla, A., Pollard, J. W. (2013). Macrophage biology in development, homeostasis and disease. *Nature*, *496*(7446), 445–455. https://doi.org/10.1038/nature12034

Xu, R., Shears, R. K., Sharma, R., Krishna, M., Webb, C., Ali, R., Wei, Z., Kadioglu, A., Zhang, Q. (2020). IL-35 is critical in suppressing superantigenic *Staphylococcus aureus*-driven inflammatory Th17 responses in human nasopharynx-associated lymphoid tissue. *Mucosal Immunology*, (December 2019), 1–11. https://doi.org/10.1038/s41385-019-0246-1

Xu, X., Wen, X., Chi, Y., He, L., Zhou, S., Wang, X., Zhao, J., Liu, F., Su, C. (2010). Activation-induced T helper cell death contributes to Th1/Th2 polarization following murine *Schistosoma japonicum* infection. *Journal of Biomedicine and Biotechnology*, *2010*(1), 1-12. https://doi.org/10.1155/2010/202397

Yamada, M., Gomez, J. C., Chugh, P. E., Lowell, C. A., Dinauer, M. C., Dittmer, D. P., Doerschuk, C. M. (2011). Interferon-γ production by neutrophils during bacterial pneumonia in mice. *American Journal of Respiratory and Critical Care Medicine*, *183*(10), 1391–1401. https://doi.org/10.1164/rccm.201004-0592OC

Yang, Z., Ming, X. F. (2014). Functions of arginase isoforms in macrophage inflammatory responses: Impact on cardiovascular diseases and metabolic disorders. *Frontiers in Immunology*, *5*(OCT), 1–10. https://doi.org/10.3389/fimmu.2014.00533

Yang, Zhiping, Huang, Y. C. T., Koziel, H., de Crom, R., Ruetten, H., Wohlfart, P., Thomsen, R. W., Kahlert, J. A., Sorensen, H. T., Jozefowski, S., Colby, A., Kobzik, L. (2014). Female resistance to pneumonia identifies lung macrophage nitric oxide synthase-3 as a therapeutic target. *ELife*, *3*, 1–17. https://doi.org/10.7554/eLife.03711

Yona, S., Kim, K. W., Wolf, Y., Mildner, A., Varol, D., Breker, M., Strauss-Ayali, D., Viukov, S., Guilliams, M., Misharin, A., Hume, D. A, Perlman, H., Malissen, B., Zelzer, E., Jung, S. (2013). Fate mapping reveals origins and dynamics of monocytes and tissue macrophages under homeostasis. *Immunity*, *38*(1), 79–91. https://doi.org/10.1016/j.immuni.2012.12.001

Yoo, I. H., Shin, H. S., Kim, Y. J., Kim, H. B., Jin, S., Ha, U. H. (2010). Role of pneumococcal pneumolysin in the induction of an inflammatory response in human epithelial cells. *FEMS Immunology and Medical Microbiology*, *60*(1), 28–35. https://doi.org/10.1111/j.1574-695X.2010.00699.x

Yun, P. L. W., DeCarlo, A. A., Collyer, C., Hunter, N. (2002). Modulation of an interleukin-12 and gamma interferon synergistic feedback regulatory cycle of T-cell and monocyte cocultures by *Porphyromonas gingivalis* lipopolysaccharide in the absence or presence of cysteine proteinases. *Infection and Immunity*, *70*(10), 5695–5705. https://doi.org/10.1128/IAI.70.10.5695-5705.2002

Zakeri, A., Hansen, E. P., Andersen, S. D., Williams, A. R., Nejsum, P. (2018). Immunomodulation by helminths: Intracellular pathways and extracellular vesicles. *Frontiers in Immunology*, *9*(OCT). https://doi.org/10.3389/fimmu.2018.02349

Zamze, S., Martinez-Pomares, L., Jones, H., Taylor, P. R., Stillion, R. J., Gordon, S., Wong, S. Y. C. (2002). Recognition of bacterial capsular polysaccharides and lipopolysaccharides by the macrophage mannose receptor. *Journal of Biological Chemistry*, *277*(44), 41613–41623. https://doi.org/10.1074/jbc.M207057200

Zhang, F. K., Hou, J. L., Guo, A. J., Tian, A. L., Sheng, Z. A., Zheng, W. B., Huang, W.-I., Elsheinka, H. M, Zhu, X. Q. (2018). Expression profiles of genes involved in TLRs and NLRs signaling pathways of water buffaloes infected with *Fasciola gigantica*. *Molecular Immunology*, *94*(April 2017), 18–26. https://doi.org/10.1016/j.molimm.2017.12.007

Zhang, J.-M., An, J. (2007). Cytokines, Inflammation and Pain. *Int. Anesthesiol. Clin.*, *45*(2), 27–37. https://doi.org/10.1097/AIA.0b013e318034194e.

Zhang, Q., Bernatoniene, J., Bagrade, L., Paton, J. C., Mitchell, T. J., Hammerschmidt, S., Nunez, D. A., Finn, A. (2006a). Regulation of production of mucosal antibody to pneumococcal protein antigens by T-cell-derived gamma interferon and interleukin-10 in children. *Infection and Immunity*, *74*(8), 4735–4743. https://doi.org/10.1128/IAI.00165-06

Zhang, Q., Bernatoniene, J., Bagrade, L., Pollard, A. J., Mitchell, T. J., Paton, J. C., Finn, A. (2006b). Serum and mucosal antibody responses to pneumococcal protein antigens in children: Relationships with carriage status. *European Journal of Immunology*, *36*(1), 46–57. https://doi.org/10.1002/eji.200535101

Zhang, Q., Leong, S. C., McNamara, P. S., Mubarak, A., Malley, R., Finn, A. (2011). Characterisation of regulatory T cells in nasal associated lymphoid tissue in children: Relationships with pneumococcal colonization. *PLoS Pathogens*, *7*(8). https://doi.org/10.1371/journal.ppat.1002175

Zhang, Z., Clarke, T. B., Weiser, J. N. (2009). Cellular effectors mediating Th17-dependent clearance of pneumococcal colonization in mice. *Journal of Clinical Investigation*, *119*(7), 1899–1909. https://doi.org/10.1172/jci36731

APPENDIX

1) Appendix A1: Dilution scheme for micro test tube or microplate protocols (working range = 1-25µg/ml)

Vial	Volume of Diluent (µl)	Volume and Source of BSA	Final BSA concentration (µl/ml)
A	3555	45µl of stock	25
B	6435	65µl of stock	20
C	3970	30µl of stock	15
D	3000	3000µl of vial B dilution	10
E	2500	2500µl of vial D dilution	5
F	1700	3000µl of vial E dilution	2.5
G	4000	0	0 (Blank)

2) Appendix A2: Dilutions and procedures for preparing endotoxin standard stock solutions

Vial	Volume of Endotoxin Standard Stock	Volume of vial A (ml)	Endotoxin free-water (ml)	Final endotoxin concentration (EU/ml)
A	0.05	-	(X-1)/ 20*	1.0
B	-	0.25	0.25	0.50
C	-	0.25	0.75	0.25
D	-	0.1	0.9	0.1

*X = endotoxin concentration of *E. coli* Endotoxin Standard supplied with the kit; refer to the Certificate of Analysis to get the lot-specific concentration.

3) Appendix A3: Nitrite ($NO2^-$) standard reference curve used in NO assay

Well (in triplicate)	Matrix/ Buffer (DMEM media) (µl)	100µM nitrite solution	NO2- concentration (µM)
A	0	100	100
B	50	50	50
C	50	50	25
D	50	50	12.5
E	50	50	6.25
F	50	50	3.13
G	50	50	1.56
H	50	0	0

Prepare 1ml of a 100µM nitrite solution by diluting the provided 0.1M Nitrite Standard 1:1000 in the matrix/ buffer used for the experimental samples

4) Appendix A4: Urea standard reference curve (mM) used in arginase assay

Vial	Water (µl)	Urea 10mM stock (µl)	Concentration (mM)
A	800	200	2mM
B	850	150	1.5mM
C	875	125	1.25mM
D	900	100	1mM
E	925	75	0.75mM
F	950	50	0.5mM
G	975	25	0.25mM
H	987.5	12.0	0.125mM
I	1000	0	0mM

Dissolve 0.06g urea powder in 100ml dH_2O

5) Appendix A5: MSD-U-PLEX Calibrator standard reference curve

Tube	Calibrator Standard	Source of calibrator	Volume of Reconstituted Calibrator (µl)	Assay Diluent (µl)	Total volume (µl)
1	1	Calibrator Standard 1 (top of curve)	50	200	250
2	2	From Tube 1	75	225	300
3	3	From Tube 2	75	225	300
4	4	From Tube 3	75	225	300
5	5	From Tube 4	75	225	300
6	6	From Tube 5	75	225	300
7	7	From Tube 6	75	225	300
8	8 (zero Calibrator)	-	0	225	300

6) Appendix A6: TGF-β1 standard reference curve

Vial	Volume of Standard (µl)	Volume of Reagent Diluent (µl)	Concentration (pg/ml)
A	16.67	1000	2000
B	500µl of vial A dilution	500	1000
C	500µl of vial B dilution	500	500
D	500µl of vial C dilution	500	250
E	500µl of vial D dilution	500	125
F	500µl of vial E dilution	500	62.5
G	500µl of vial F dilution	500	31.3